ÉCOLE DE TECHNOLOGIE SUPÉRIEURE
UNIVERSITÉ DU QUÉBEC

THESIS PRESENTED TO
ÉCOLE DE TECHNOLOGIE SUPÉRIEURE

IN PARTIAL FULFILLMENT OF THE REQUIREMENTS FOR
THE DEGREE OF DOCTOR OF PHILOSOPHY
Ph.D.

BY
Alireza JAVADI

DESIGN AND IMPLEMENTATION OF HYBRID SERIES COMPENSATORS FOR SMART GRID APPLICATIONS

MONTREAL, 3 MARCH 2016

BOARD OF EXAMINERS (THESIS PH.D.)

THIS THESIS HAS BEEN EVALUATED

BY THE FOLLOWING BOARD OF EXAMINERS

Prof. Kamal Al-Haddad, Thesis Supervisor
Department of Electrical Engineering, École de technologie supérieure

Prof. Stéphane Hallé, President of the Board of Examiners
Department of Mechanical Engineering, École de technologie supérieure

Prof. Ambrish Chandra, Member of the Jury
Department of Electrical Engineering, École de technologie supérieure

Prof. Pierre Jean Lagacé, Member of the Jury
Department of Electrical Engineering, École de technologie supérieure

Prof. Sheldon Williamson, Independent External Evaluator
Department of Electrical Engineering, University of Ontario Institute of Technology

THIS THESIS WAS PRESENTED AND DEFENDED

IN THE PRESENCE OF A BOARD OF EXAMINERS AND THE PUBLIC

FEBRUARY 24, 2016

AT ÉCOLE DE TECHNOLOGIE SUPÉRIEURE

ACKNOWLEDGMENTS

I would like to express my sincere gratitude to my thesis director, Professor Kamal Al-Haddad, for the opportunity he has given me to work in the GREPCI. Without his thrust, excellent technical guidance, patience, and moral support, my research would not have been successful. Undoubtedly, he was the most influential person during my doctoral studies and I hope the tie that we established during the time that this research project has being carried out will continue for many years to come.

My immense appreciation extends to Prof. Stéphane Hallé, Prof. Ambrish Chandra, Prof. Pierre Jean Lagacé, Prof. Sheldon Williamson, and Prof. Kamal-Al-Haddad for serving as members of jury of my PhD defense committee and for providing valuable comments.

I would like to acknowledge the École de technologie supérieure for providing me the opportunity to pursue my PhD studies and recommending me for scholarships and awards offered by the Ministry of Education. I would like to acknowledge the Canada Research Chair in Electrical Energy Conversion and Power Electronics (CRC-EECPE), and the Fonds de Recherche du Québec – Nature et Technologies (FRQNT) for their financial support.

Special thanks go to my parents, and friends that my success in carrying out and completion of this project would certainly not have been possible without their generous support.

Thanks to my lovely son who gives me the will and power to go beyond difficulties and without whom this work would have been completed years earlier. I dedicate this thesis to my dear Sobhan.

Finally, I wish to give my wholehearted thanks to my beloved wife for her support, encouragements, and patience while lifting much of the burden of life during the final stages of this thesis.

DESIGN AND IMPLEMENTATION OF HYBRID SERIES COMPENSATORS FOR SMART GRID APPLICATIONS

Alireza JAVADI

SUMMARY

The vision of future modern grids goes through the increase of renewable energies penetration while providing an efficient, reliable and sustainable power supply to consumers. According to the recent report on climate challenging the way electrical energy is produced and because of the rapid emerging of power electronics based equipment; some serious actions should be engaged. In order to achieve such promoting visions, all power grids are required to become smarter especially at the distribution level. Increasing the application of renewable energy sources and distributed generations assist these vision in the development of a modern power grid where modern equipment are becoming highly sensitive to the supplied voltage quality. Moreover, in this paradigm of design, the traditional power systems based on large concentrated power plants should be able to deal with these unpredictable sources of energy at distribution level. Under these circumstances, considerable activities were carried out aiming to render the grid more flexible and intelligent while taking the power efficiency and its environmental impacts into account. In this way, the power quality issues should be considered for the development of new type of smart grids which are more efficient and sustainable with regards to environmental constraints.

Available active and passive compensators are widely involved to improve major power quality issues. Recent trends towards realization of multitasking devices which can solve several power quality issues simultaneously, propose Hybrid active filters or Unified power quality conditioners. These versatile devices should threaten both voltage and current related issues in one place for compensation. They can significantly improve power quality issues, such as voltage distortions, voltage sags, voltage swells, voltage unbalances, and ensure a constant and reliable voltage supply to the load. On the other hand, they compensate for current problems of linear and non-linear loads, such as current harmonics, unbalances, neutral current, and load reactive power. The Hybrid series active filter (HSeAF) is among the most versatile and efficient power electronics based active power compensators. Without the shunt passive filter, the active part could operate solely to rectify for voltage problems and is commonly known as Dynamic voltage restorer.

A conventional HSeAF, targeting three-phase system, consists of a three separate series isolation transformer connected to a three-phase converter sharing a common DC link bus. The device is controlled as a variable voltage source in similar but duality manner as of Shunt active power filter. A shunt passive filter tuned for harmonic frequencies is installed to produce an alternative path for load current harmonics and reducing voltage distortions at the load terminals. The existing literature suggests utilizing the hybrid active power filters to compensate for load current related issues only, while due to the complexity and implementation outlays of such devices, it shows a significant drawback of under usage of series compensation to address such power quality problems.

The present doctoral research is based on the philosophy of optimal utilization of the available resources in the most efficient way to enhance the product efficiency and to reduce the overall cost. This work proposes a novel control approach for three-phase system in which both the grid's voltage and load current issues are treated in a co-ordination between the series active and the shunt passive filters without affecting the basic voltage or current compensation capabilities. This eventually results in a better utilization of the series active filter, reduction of the shunt passive filter rating to some extent, and ultimately in the reduction of the overall cost for a unified compensator.

Moreover, this thesis also introduces a novel transformerless topology in which the three-phase configuration is split into separate devices. It is then possible to extent the Series active power compensation based for three-phase systems with three or four wires to single-phase or bi-phase systems. This newly transformerless hybrid series active filter (THSeAF) is first hosted for single-phase system where appropriate developed controllers ensure adequate operation under low profile power quality systems. The developed single-phase THSeAF concept is successfully validated through digital simulations as well as real-time extensive experimental investigations. The experimental results show that for a given laboratory test conditions with highly polluted nonlinear loads, the active compensator ride of the bulky transformer is capable of compensating load current and correcting the power factor. Moreover, the performance of the THSeAF under polluted grid supply with voltage harmonics, sags, and swells, demonstrates regulated and reduced voltage distortions at the load's terminals.

Following this successful transformerless configuration, and to integrate the series compensation concepts dedicated for power quality improvement of distribution network, the three-phase configuration is anticipated. Three-phase control strategies developed previously for the HSeAF are applied to the proposed topology to make the point of common coupling (PCC) smarter and to decentralize the control of the distribution network. This affordable solution increases the efficiency and sustainability of modern smart power systems and help higher penetration of renewable fluctuating power into the network. The off-line simulations demonstrate that the three-phase THSeAF is capable of healing voltage problems and load current issues simultaneously. The real-time experimental results, carried out on a laboratory prototype, validate successfully the proposed configuration.

Keywords: Active power filter, power quality, current harmonic compensation, voltage restoration, reactive power correction, transformerless series active filtering, instantaneous power compensation.

LA CONCEPTION ET MISE EN ŒUVRE D'UN COMPENSATEUR SÉRIE POUR APPLICATION AU RÉSEAU INTELLIGENT

Alireza JAVADI

RÉSUMÉ

La vision des futurs réseaux modernes passe par l'augmentation des énergies renouvelables tout en fournissant une alimentation efficace, fiable et durable pour les consommateurs. Selon les récents défis climatiques pour changer la façon dont l'énergie électrique est produite et l'émergence très rapide des équipements à base d'électronique de puissance, force l'industrie a changé sa perception des réseaux électriques. Afin de réaliser ces visions prometteuses, les réseaux électriques doivent inévitablement devenir plus intelligents à tous les niveaux, spécialement au niveau des réseaux de distribution. L'augmentation de la demande de sources d'énergies renouvelables et les générations distribuées ont contribué à cette vision dans le développement durable d'un réseau électrique moderne qui tient compte des nouvelles technologies très sensibles à la qualité de la tension fournie. En outre, dans ce paradigme de conception, les systèmes d'alimentation traditionnels basés sur les grandes centrales concentrées devraient être en mesure de faire face à ces sources d'énergie imprévisibles au niveau de la distribution. Dans ces circonstances, des activités considérables ont été réalisées en vue de rendre le réseau plus perspicace et intelligent, tout en tenant compte de l'efficacité énergétique et ses impacts environnementaux. Par ailleurs, les problèmes liés à la qualité de l'énergie devraient être considérés pour le développement de ce nouveau type de réseaux intelligents plus efficaces et plus sains.

En ce qui concerne les questions sur la qualité de l'énergie, des solutions actives et passives ont été proposées dont certaines font déjà face à une large propagation dans l'industrie. Les récents développements de dispositifs multitâches qui peuvent résoudre plusieurs questions de la qualité d'énergie simultanément, sont axés sur des filtres actifs hybrides ou des UPQC. Ces appareils polyvalents règlent à la fois les problèmes liés à la qualité de la tension ainsi que ceux liés à la qualité du courant tiré par les charges linéaires et non-linéaires. Et donc, ils améliorent de manière significative les problèmes de qualité de l'alimentation, tels que les distorsions, les creux, les surtensions, et le déséquilibre de la tension et ainsi assurent une alimentation constante et fiable à la charge. D'autre part, elles peuvent compenser les problèmes actuels des charges linéaires et non linéaires, tels que les harmoniques de courant, les déséquilibres, le courant de neutre, et la puissance réactive. Parmi ces différentes solutions, le filtre hybride actif série (HSeAF) est parmi les compensateurs polyvalents les plus robustes et efficaces. Sans sa partie passive, la partie active pourrait fonctionner pour corriger les problèmes de tension (appelée DVR).

Un HSeAF conventionnelle dédié pour le système triphasé est composé de trois transformateurs d'isolation reliés à un convertisseur triphasé qui partage un bus DC commun. L'appareil opère comme une source de tension variable et de manière similaire mais duale à un filtre actif parallèle. Un filtre passif parallèle ajusté aux fréquences des harmoniques est installé pour produire un chemin alternatif pour les harmoniques du courant de la charge et

ainsi permet une réduction considérable des distorsions de la tension aux bornes de la charge. En raison de la complexité et de la mise en œuvre des filtres séries, ces derniers n'ont pas reçu le succès que leurs confrères parallèles dans l'industrie. Donc, la présente thèse de doctorat est basée sur la philosophie de l'utilisation optimale des ressources disponibles de manière la plus efficace pour améliorer l'efficacité du filtrage série. Ce travail de recherche propose une stratégie de commande pour les systèmes triphasés dans lesquels la tension aux bornes de la charge et le courant tiré du réseau sont considérés pour compensation. Ceci, résulte à une meilleure utilisation de ressources physiques disponibles pour la réalisation du filtre actif série, la réduction du dimensionnement du filtre passif parallèle et finalement la réduction du coût de production.

Cette thèse introduit également une nouvelle topologie sans transformateur, dans laquelle la configuration à trois phases est divisée en trois modules séparés. Cette nouvelle technologie permet d'aborder la qualité de l'énergie des systèmes monophasés, biphasés, et triphasés avec trois ou quatre fils. Ce filtre hybride sans transformateur (THSeAF) est d'abord implanté pour un système monophasé où une commande appropriée a été développée en conséquence pour assurer un fonctionnement adéquat dans un système avec un faible profil de qualité. La notion THSeAF-monophasée est validée avec succès par des simulations numériques ainsi que des implémentations temps-réel en laboratoire. Les résultats expérimentaux démontrent pour les essais en laboratoire avec des charges non linéaires très polluées, les formes d'ondes du courant tiré du réseau sont sinusoïdales avec un facteur de puissance unitaire. Par ailleurs, la performance du THSeAF a également été évaluée quand la tension du réseau est polluée avec des harmoniques ou quand ce dernier subit des sous- ou surtensions.

Suite au succès de cette configuration sans transformateur, le concept a été intégré pour l'amélioration de la qualité de l'alimentation d'un réseau de distribution triphasée. La commande développée précédemment pour application dans le HSeAF a été modifiée pour être compatible avec le THSeAF triphasée pour rendre le point de raccordement (PCC) plus intelligent et décentraliser le contrôle du réseau de distribution. Cette solution abordable accroît l'efficacité et la stabilité des systèmes d'énergie modernes et aide à une plus forte pénétration des énergies renouvelables. Les simulations démontrent que le THSeAF triphasé est capable de résoudre les problèmes liés à la tension ainsi que ceux liés au courant de la charge simultanément et ainsi améliorer la qualité de l'énergie. Les résultats expérimentaux effectués sur un prototype temps-réel en laboratoire ont validé avec succès la configuration proposée.

Mots-clés : Filtrage actif, qualité de l'énergie, la compensation des courants harmoniques, restauration de la tension, correction de la puissance réactive, compensateur série sans transformateur de couplage, compensation de la puissance instantanée.

TABLE OF CONTENTS

Page

LIST OF TABLES

Page

LIST OF FIGURES

Page

LIST OF ABREVIATIONS

3P3W	Three-phase with three-wire system
3P4W	Three-phase with four-wire system
AC	Alternating current
AF	Active filter
APF	Active power filter
CSC	Current source converter
CSI	Current source inverter
CPU	Central processing unit
DBR	Diode bridge rectifier
DC	Direct current
Discr.	Discrete
DVR	Dynamic voltage restorer
DSP	Digital signal processor
Eqn.	Equation
FACTS	Flexible AC transmission systems
FFT	Fast Fourier transforms
FPGA	Field-programmable gate array
Fund.	Fundamental component
GREPCI	Groupe de recherche en électronique de puissance et commande industrielle
HIL	Hardware-In-the-Loop
HPF	High pass filter
HSeAF	Hybrid series active filter
IGBT	Insulated gate bipolar transistor
IREQ	Institute de recherche d'Hydro-Québec
KCL	Kirchhoff’s current law
KVL	Kirchhoff’s voltage law
LPF	Low pass filter
MIMO	Multiple-input and multiple-output system

NPC	Neutral point clamped converter
PCB	Printed circuit board
PCC	Point of common coupling
PF	Power factor
PI	Proportional integral
PLL	Phase-locked loop
PR	Proportional plus Resonant control
PWM	Pulse width modulation
PV	Photovoltaic source
RCP	Rapid control prototyping
rms	Root mean square
RPM	Revolution per minute
SeAF	Series active filter
SPS	SimPowerSystems
SSC	Static series compensator
STATCOM	Static var compensator
THD	Total harmonic distortion
THSeAF	Transformerless hybrid series active filter
UPQC	Unified power quality conditioner
VA	Volt-ampere
vai	Volt-ampere imaginary
var	Volt-ampere reactive
VSC	Voltage source converter
VSI	Voltage source inverter
w.r.t.	With respect to

LIST OF SYMBOLS AND UNITS OF MEASUREMENTS

ω	Angular frequency
δ	Power angle between source and load voltages
φ	Phase angle between source current w.r.t. to source voltage
C_{dc}	DC link capacitor
C_f	Ripple filter capacitor
D	Distorted power
eff	Effective value
f	System frequency
F_h	Respective harmonic's order shunt passive filter
f_{PWM}	Switching frequency
G	Gain proportional to current harmonics
h	Harmonic order
Hz	Hertz
HP	Horse power
i_S	Source current
i_L	Load current
I_{Sh}	Source harmonic current
K_P	Proportional gain
K_i	Integral gain
L	Inductance
N	Non-active power
Ω	Ohm
P	Active power
p.u.	Per unit
Q	Reactive power
r or R	Resistance
s	Second
S	Apparent power

XXX

T_S	Discrete sampling time
V	Voltage
W	Watt
Z	Impedance

Multiple and sub-multiple of SI unities

M:	$10^6 = 1\ 000\ 000$	mega
k:	$10^3 = 1\ 000$	kilo
m:	0.001	mili
μ:	$10^{-6} = 0.000\ 001$	micro

Mathematical symbols

Bold ($\boldsymbol{V}$ or $\boldsymbol{v}$)	Matrix
Asterisk (V*)	Reference signal
Hat ($\hat{v}$)	Measured value
Dote ($\dot{v}$)	Derivative
V	rms value
v	Instantaneous value
$\vec{V}$	Vector in frequency domain
$\vec{v}$	Instantaneous vector in time domain
$\lvert V \rvert$	Absolute value
$\lvert\vec{V}\rvert$ or $\lvert\vec{v}\rvert$	Generalized rms value of the vector $\vec{V}$ or $\vec{v}$

INTRODUCTION

In the early nineteenth century, commercial electric power observed different mutations. Transmission of electric power from the generating plant to consumers was first with direct current (DC) in 1882, which was not possible to increase in voltage for long-distance transmission at that time. To overcome this problem engineers introduced the alternating current (AC) transmission systems and later the three-phase power systems were developed. These traditional power systems were designed assuming ideal component with insignificant non-linearity behavior and that the power flows from the grid to consumers and not vice versa.

In the twentieth century with the special approbation followed by massive investment of governments, the generation of power from renewable energies had observed a significant increase. The decision of investment on sustainable sources was essentially founded on the desire to reduce usage of natural resources and decrease the pollutant emissions. Renewable energies, commonly called “green energies”, include natural energetic processes that can be harnessed with slight environmental pollutions. However, to extract electric power from these alternative resources the industry faced considerable dilemmas. At first, these sources are not able to produce a constant power due to their energy characteristic and unpredictable behavior. They have low commercial efficiency. Furthermore, they require sophisticated, advanced, and expensive components and controllers. Meanwhile, due to important worries for the future of our green planet and future generation’s concerns, the governments followed by energy industries have chosen this shift toward producing electric power from less harmful resources.

The existing power system faced to the employment of such distributed generations, contrary to the traditional system, should be able to manage power flow from multiple sources instantaneously, control energy management, and have flexibility. This handicap of existing power system leads to the creation of the Smart Grid concept. Consequently, the power system’s infrastructures should be updated or modified to deal with the additional power

coming from the distributed sources in the system. To achieve such pragmatic visions, the grid and consumers should act ingeniously, and their components should also change to smart devices in order to recognize various scenarios and adapt themselves to operate instinctively.

The forecast of Smart Grids associated with the massive increase of switch-mode power converters, drives, and both domestic and industrial nonlinear loads has created a serious concern on the power quality of the future power systems as shown in the following figure.

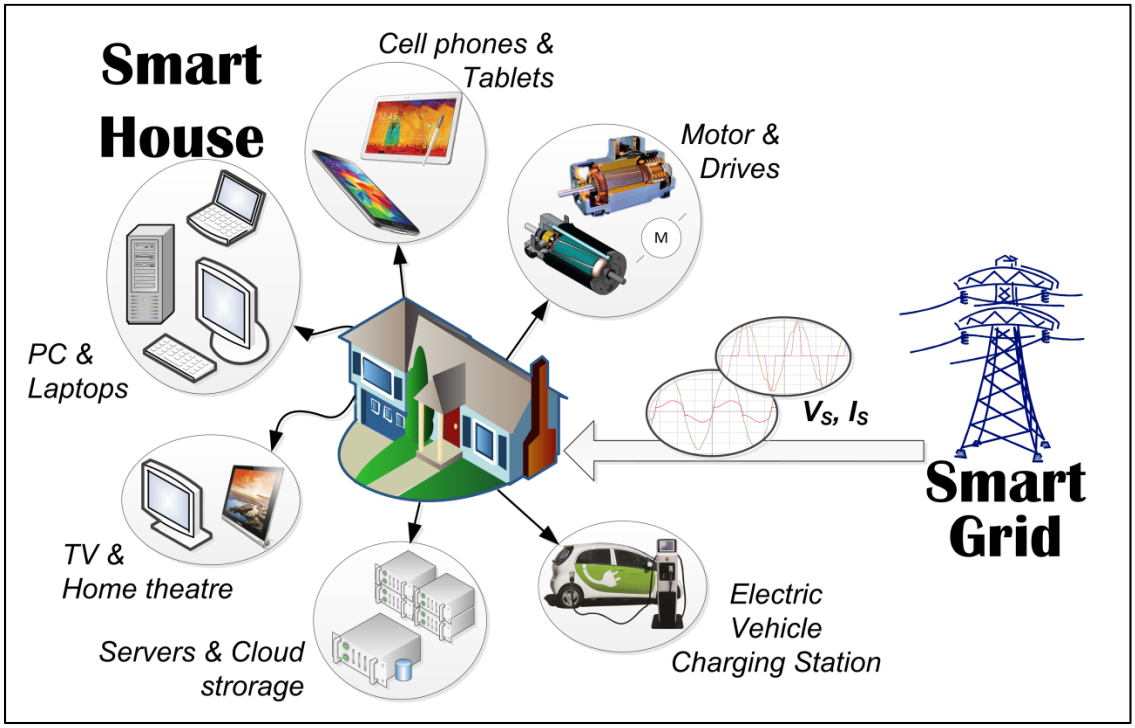

Figure 0.1 Pictogram of a Smart residential consumer with common non-linear electronic loads

This growing concern in power quality can be explained in the following contexts:

- The current harmonic pollution fed from nonlinear loads has also deteriorated the power quality of current power systems and has created a major concern for the power networks. Together the current source converters (CSC) and voltage source converters

(VSC) are contributing in deteriorating current quality. They inject undesired harmonics causing increase of the current magnitude, which indeed increases the losses and overall heating. A low efficiency of the system and failure of the electrical equipment are some of multiple problems that current distortions may create if they are not appropriately compensated (Singh et al., 2005; Singh, Chandra et Al-Haddad, 2015; Zobaa, 2014);

- The upsurge of more aware and stringent consumers, forced the power suppliers to find solution in order to deliver a more reliable and high quality electric power. This means that, they are required to supply a clean, distortion-free, and stable voltage at the consumer's terminals. In case of a three-phase system, the voltage should be balanced without harmonic components;

- Along with the current and voltage issues, the authorities are exposed to the aforementioned trend of increasing implication of renewable sources in the electric power system. The integration of renewable energies in terms of power quality and power flow management is often complex and require sophisticated elaborations.

In this context the increase of Electric Vehicle market creates significant concerns for engineers and researchers in terms of their impacts on the power quality of the system. Figure 0.2 demonstrates the measured voltage and highly distorted current waveforms of an electric car plugged for example into the École de technologie supérieure charging station level 2 (220V, 30A). The development of smart grids requires assessment on the power quality of the system. Where, the major related problems which requires assessment of current and future grids at distribution level, mentioned hereafter.

Current Harmonics: Current harmonics are components with frequencies other than the systems nominal frequency (e.g. 50 or 60 Hz). These components with various amplitudes are sources of multiple disorders in the electrical systems; excessive losses in lines and electrical components, when passing through an inductance or transformer create voltage distortions, acoustic noises in electro-magnetic devices, reducing efficiency, producing

neutral current. The growth of harmonic pollution fed from nonlinear loads, which could have a detrimental impact on the power system and affect equipment in the polluting plant should also be considered. To limit current disturbance, maximum allowable distortion was defined in IEEE standard 519 and 1459 (IEEE Recommended Practices and Requirements for Harmonic Control in Electrical Power Systems, 1993; IEEE Standard Definitions for the Measurement of Electric Power Quantities Under Sinusoidal, Nonsinusoidal, Balanced, or Unbalanced Conditions, 2010). Furthermore, the International Electrotechnical Commission (IEC) has issued technical reports (International Electrotechnical Commission (IEC), 2009-04), to assess the connection of non-linear loads to the power plant.

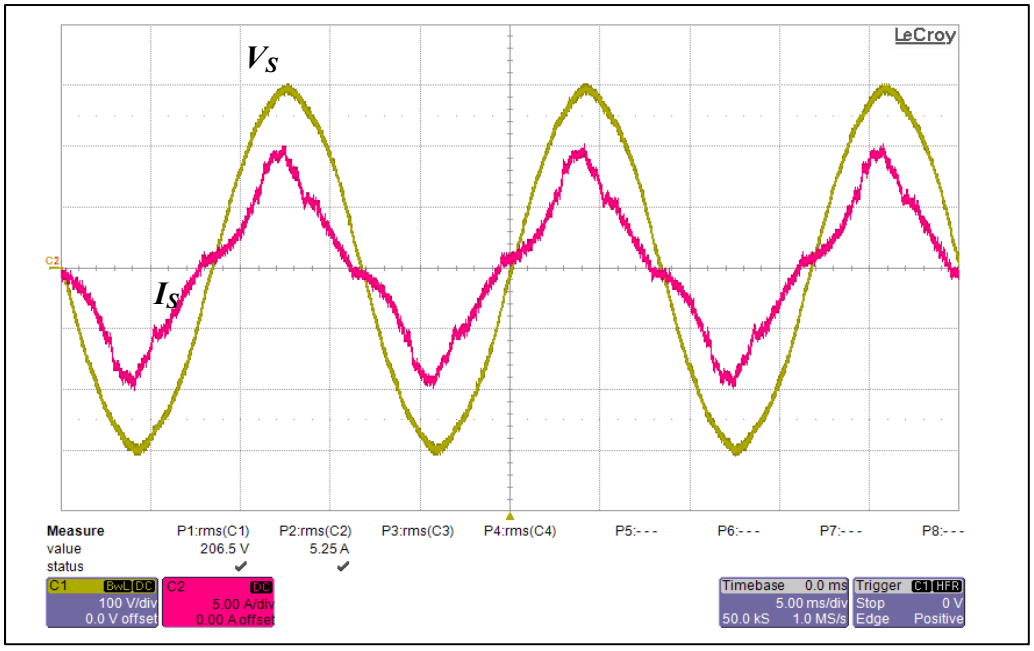

Figure 0.2 Nissan LEAF®, voltage and current waveforms during charging

Current Unbalance: The unbalance current in three-phase or multiphase systems is a condition in which the three phases do not have the same magnitude at fundamental frequency or they are not equally phase shifted in time. Severe current unbalance could cause multiple problems for the power systems, such as vibration in electrical generators. The primary cause of current unbalance is the non-equally distributed single-phase loads on a three-phase system.

Reactive Power: In AC system, the voltage and current have sinusoidal waveforms. The power calculation becomes complicated when these two waveforms do not line up perfectly. The resultant apparent power (S) which is the cross operation of the two waves has two components; one flowing from source to the load, performing work at the load, and the other portion, due to the delay between voltage and current (phase angle), cannot do useful work at the load. This portion is known as the reactive power. The reactive power reduces power flow efficiency in terms of the power consumed versus the installed capacity.

Voltage Distortion: Similar to current harmonics, voltage distortion or voltage harmonics are undesired components at a different frequency other than the fundamental one. The voltage harmonics can cause failures in the electrical equipment, loss of synchronization in sensitive devices and faults in zero crossing detectors, are some problems that such distortions may create (Roncero-Sanchez et al., 2009; Rudnick, Dixon et Moran, 2003).

Voltage Unbalance: If the three phases of a 3P3W or 3P4W system have not exactly the same voltage magnitude and phase shift, they contain an unbalance component. The voltage unbalance can cause harmful effects in devices such as motors and transformers why the IEEE std 1159 (IEEE Recommended Practice for Monitoring Electric Power Quality, 1995) imposes restrictions to power operators. In single-phase system, this variation causes worsen damages in electrical device.

Voltage Sags: According to established standard (IEEE Recommended Practice for Monitoring Electric Power Quality, 1995), it is a short duration voltage decrease and more precisely a decrease between 0.1 and 0.9 p.u. in rms voltage for a duration of 0.5 cycle to 1 min. This short-duration variation is almost always caused by fault conditions, the starting of large loads requiring high starting currents, or intermittent loose connections in power wiring. Voltage sags can also be caused by large load changes or motor starting where, an induction motor consume six to ten times its nominal rated current during startup.

Voltage Swells: A swell is a short duration rise in rms voltage from 0.5 cycles to 1 min. The typical magnitude varies between 1.1 and 1.8 p.u. As with sags, but much less common, swells could also be associated with system fault conditions. Swells can occur by switching off a large load or switching on a large capacitor bank.

With regards to the mentioned issues, the research guidelines and objectives are deuced. In this section the importance of compensating these pollutions phenomenon which affect directly the power quality are discussed. A brief introduction of necessary power quality key devices will be presented. Following the described objectives in this work, the methodologies to achieve them are depicted in detail. To conclude this chapter, the contribution of this project on the improvement of power quality enhancement is highlighted.

Importance of Power quality enhancement

Power system generators produce a clean sinusoidal voltage waveform at their terminals. This sinusoidal waveform is regarded as the pure form of the AC voltage and any deviation from it, is described as distortion. Power quality is related to the amplitude, frequency and distortion of the supply system. While the amplitude and frequency of the supply are largely controlled by the utility at high and middle level of transmission, the distortion of the wave (voltage or current) is attributed to the consumer loads at distribution levels. Linear loads like an induction motor, an incandescent bulb, resistive heating or a capacitor bank draw a sinusoidal current which follows the wave shape of the supplied voltage and require only reactive compensation. On the other hand, most of the common loads nowadays are non-linear, like VSDs (Variable Speed Drives), rectifiers, UPS-systems, computers, TV sets, energy efficient (fluorescent) lamps, photocopiers. These loads draw a current from the source which does not follow the voltage wave shape and hence introduce current distortion. The distorted current drawn by these nonlinear loads distorts the supply voltage which may then give rise to harmonic currents at distribution networks, even when at these locations no harmonic generating equipment is present. Moreover, the resonance phenomenon issue should be taken into account, e.g. the interaction between the (inductive) supply system and

capacitor banks, amplify the harmonic distortion when they occur around harmonic frequencies.

Furthermore, circuit breakers may go wrong and trip due to higher thermal or a false instantaneous value, fuses may blow, capacitors may be damaged and power meters may give faulty readings. Other harmful effects are: excessive increase in winding and iron losses of motors, perturbing torques on the shaft, as well as sensitive electronic equipment may be damaged. Equipment which uses the supply voltage as a reference may not be able to synchronize properly and either apply wrong firing pulses to switching elements or switch off. Interference with electronic communications equipment may also occur.

Ideally, voltages and currents should have a sinusoidal waveform with predetermined frequency and magnitude. However, the increase of modern nonlinear loads has increased current harmonic distortion levels. Additionally, harmonic pollution has become more apparent with the proliferation of power electronic converters and electronic devices. Consequently, reactive power compensation under non-sinusoidal conditions has become one of crucial complications that power systems are facing. The importance of current harmonic pollution causing number of problems is not hidden and thus, should be taken into account for compensation. While, current issues should be compensated, consumer requiring a sustainable energy, free of distortions, unbalances, sags, and swells forces the authorities to take actions to overcome voltage related issues. Altogether, the necessity to implicate renewable energies creates a much more prerequisite to think about more advance and sophisticated compensation techniques and devices.

Solutions to power quality issues

To overcome aforementioned issues, the use of filters seems unavoidable in present circumstances. There exist two major categories of filters for power quality enhancement.

Passive Filter: The first and traditionally installed over the power systems are the conventional passive filters. These filters are built up from passive components; resistors (R), Capacitors (C), and inductors (L). They are designed to form a tuned circuit. The tuning frequency is matched to the harmonics in question. Conventionally, to overcome current issues and correct the power factor, passive filters were the primary solution. These large preset filters are able to improve the power factor and reduce current harmonics. After installation, they are not able to behave as a dynamic compensator during a change in conditions of the system. If not properly designed, they could give rise to resonance phenomena in the system. As well, the distorted current drawn by nonlinear loads could distort the PCC voltage which may then give rise to harmonic currents, even if at these locations, no harmonic generating equipment are present. Furthermore, voltage unbalances, sags, and swells are other power quality issues related to the supply voltage required to be considered for compensations that passive filters are unable to solve.

Active Filter: The second category is active filters (AF); which offers an unprecedented ability to actively clean the network from harmonics, to perform smooth reactive power compensation and to do load balancing. Furthermore, AFs are able to overcome voltage related issues. The effectiveness and efficiency of active compensators compared to large passive components promote their industrial application for smart grids. They could also help higher penetration of renewable fluctuating power into the network. The development of low-cost power electronics made active filters able to compete with traditional passive filters. Active filters are classified, based on their electrical connection to the system. The following table gives a preview of various active filters and their ability over power quality problems.

Nowadays, passive filters are less intriguing due to the development of active filters based on controlled power electronics converters able to behave as dynamic device, follow changes and react spontaneously to control references. Shunt active filters have been proposed to be one of the best among possible equipment capable of eliminating electric harmonics, regulating power quality indices related to current and reactive power. Current distortions generally are injected from the no-linear loads to the grids. Although, the shunt active filter is

able to correct current related issues (Hamadi, Rahmani et Al-Haddad, 2010; Rahmani, Hamadi et Al-Haddad, 2012), it has not the ability to resolve voltage issues initiated by the power system implementation and thus protecting the consumers.

Table 0.1 Comparison of Power quality improving compensators

		Passive Filters	Active Filters				
	Power quality Parameters	Operation	Shunt AF	Series AF	Series AF/ DVR operation	Hybrid Series AF	Transformerless Hybrid Series AF (THSeAF)
Load Initiated Problems	Current Harmonic	Yes	Yes	Yes	No	Yes	Yes
	Reactive Power Compensation	Yes	Yes	Yes	No	Yes	Yes
	Current Unbalance	No	Yes	Yes	No	No/ Yes *1	No/ Yes *1
Grid Initiated Problems	Voltage Distortion	Yes	No	No	Yes	Yes	Yes
	Voltage Unbalance	No	No	No	Yes	Yes/ No *2	Yes/ No *2
	Voltage Sags	No	No	No	Yes	Yes	Yes
	Voltage Swells	No	No	No	Yes	Yes	Yes
	Voltage Interruption	No	No	No	Yes	Yes	Yes
*1	"Yes" if the Voltage unbalance at the load is not selected for compensation						
*2	"No" if the Current unbalance is been compensated						

To solve mentioned voltage issues and other power supply related problems, series active filters have been developed. Although, the technology of Series active filters is in his early stages of development, hypothetically they are able to filter voltage distortions. The complexity of series compensators compared to shunt active filters already commercially available, make them to remain at a prototype level. Dynamic voltage restorers (DVR) with similar topology as of Series active power filters are been installed at critically point of the distribution system on weak Point of common coupling (PCC) to overcome voltage issues in the network (Babaei et Kangarlu, 2011; Jimichi, Fujita et Akagi, 2011) and guarantee a sinusoidal balanced voltage on the load terminals despite the presence of perturbations in the source voltage such as unbalance, harmonic distortion, sags and swells, and other disturbances. Combined with a passive component SeAFs could treat voltage and current related issues under the label of Hybrid Series Active Filters (HSeAF). The series compensators as powerful and flexible compensators are kept and exploited in this research work to overcome aforementioned power quality threats. A detailed comparison of active filters will be given in the first chapter.

Research Objectives

The general objectives of this work were defined under four goals; *I*) to carry out a study on series compensators and develop a smart power electronic compensator to enhance the static and dynamic behavior of electrical network carrying high percentage of fluctuating renewable energy sources. *II*) To study the real-time behavior of the proposed compensator under a realistic condition realized by an experimental prototype, and should result in a laboratory benchmark. *III*) To develop a control approach in which the system performance under critical scenarios is improved. *IV*) To adapt the compensator to operate in single-phase household systems along with the three-phase distribution system and thus contribute in the ongoing research works in the area of power quality enhancement of smart grids.

The Specific research objectives are summarized below:

- To perform an in-depth analytical study on power quality issues their influence on the system behavior. The purpose of this study is to understand and clarify how non-linear load are behaving and how is it possible to reduce their noxious effects on the grid. And thus, evaluation of different compensators via real-time simulations to overcome power quality issues. It was essential to analyze behavior of Series compensators under unbalanced heavy fluctuation of network power initiated by the distributed sources and other perturbation sources. The energy storage element contributing in the application of renewables was similarly considered in this work;

- To carry out development of an advanced detection and control algorithm to accomplish real-time compensation of addressed issues for the single and three-phase systems. The Controller should be implemented on a real-time simulator where the state variables of the system are visualized instantaneously. The control strategy should be sufficiently versatile in number of calculations and memory while being reliable for normal operation. It should also be quite powerful to consider all constraints for different applications;

- To realize a novel system topology to improve weakness of available HSeAFs. This was resulted in the realization of the Transformerless-HSeAF. A financial evaluation and comparison of the new configuration over conventional topologies should be conducted. Analysis on the effectiveness of the proposed actively variable compensator to insure instantaneous compensation in a real-time laboratory environment;

- Based on the theoretical investigation and performed simulations, the controller should be tested in an experimental implementation. The Rapid Control Prototyping (RCP) will allow improvement of the control strategy and resolution of possible bugs in an iterative process. The setup consisting of the novel configuration connected to radial system should be tested and evaluated in a laboratory environment aiming to improve power quality indices of a critical system;

- While the system becomes smart, loads are implicated into the energy markets increasing their responsibility and at the same time their expectation from suppliers. They will expect a reliable and permanent supply without any voltage distortions, sags and swells. Thus the study should characterize performance of the proposed THSeAF in satisfying mentioned requirements of such Smart consumers;

- To optimize the compensator configuration for various applications in single-phase and three-phase systems following experimental validation results.

Methodology

To realize and accomplish the objectives highlighted above the following steps are outlined as below:

- A Comprehensive review of the concepts of power quality should be performed. Followed by a complete and exhaustive literature review on series active compensators; topologies and control methods. This thesis made of comprehensive theoretical

development, presents approaches are put forward through rigorous mathematical formulation and verifications;

- Study of different control algorithms and topologies of series active filters used for instantaneous compensation under distorted and/or unbalanced supply. The developed control approach including the compensator and the electrical system are then modeled using the digital simulation tool of MATLAB/ Simulink in this work. The SimPowerSystems (SPS) block sets are predominantly used first in continuous and variable time steps simulations. Subsequently, the models are adapted for Discrete and Fixed-step-size development also used for real-time simulations and experimental implementation;

- In a parallel process the recently developed concepts on Smart grids are reviewed. Besides, the equipment and loads compromising the power quality of smart grids is investigated. The integration of a Smart active power filter is evaluated. The integration of renewable energies into the proposed novel compensator for smart grids is explored;

- Real-time laboratory implementation of the series active filter. Two experimental setups including the conventional HSeAF and the THSeAF are built. The setup interfaces the active compensator with a radial distribution system. The integration of the smart developed device into this system allows improvement of the configuration structure and parameters for a practical industrial application;

- Improving the control algorithm and topology for both single and three-phase system in an iterative workflow: Small details required lots of work to find workaround solutions to make a reliable operation of the setup. This RCP platform of dSPACE/ dsp1103 has allowed optimization of gains and other parameters of the controller. And the developed controller was tested under several critical operation conditions both in single and three-phase systems;

- Finally, the reported research work summarizing simulation and experimental validation should be analyzed and discussed for future developments.

Thesis Contributions

This work was initiated with the project of feasibility analysis of emerging series active compensators for possible industrial applications to enhance power quality of distribution power systems.

The foundation of this thesis relies on instantaneous powers and harmonic distortions. These quantities in both three-phase and single-phase systems contribute in calculation of several important power quality problems. The source has the responsibility to deliver a clean, balanced and sustainable supply to consumers. In contrast, consumers should draw a sinusoidal balanced (in case of 3-phase system) and harmonic-free current from the source. Ideally, it is preferred that, the source supplies only active power and non-active powers be compensated or kept away from propagating into the grid. This goal raised up the idea of a hybrid series compensator to isolate the load from the distribution grid in terms of power quality problems. In the course of action, several configurations concepts and controller approach are proposed in this work. Important topologies are highlighted such as: shunt active power filter, series APF, and Hybrid series APF. The choice of controllers varies depending on the single or three phase system.

The remarkable accomplishment of the proposed work is the development of both a novel configuration for the series compensator and the control philosophy for this later. This interesting topology called the Transformerless-HSeAF is proposed for three-phase systems (3P3W and 3P4W), single-phase, and bi-phase applications. The proposed topology created the independent single phase compensator which gives an easy expansion to bi-phase and three-phase systems. Since this active compensator is a series device, the neutral wire does not create interruption or nuisance to the operation process.

A key accomplishment of this work as previously mentioned is the development of instantaneous controllers for both single and three phase systems. A controller is composed of two sections; the issue detection block, producing the reference compensation signal and the regulator block which takes care of producing the reference voltage at the compensator's output. The fundamentals of power quality detection concepts for single and three phases systems are described by providing detailed theoretical developments serving as benchmarks for this thesis. On the other hand, similar regulators are applied for case studied systems in this work. Regulators such as PI, Sliding mode, and proportional plus resonant (P+R) controllers are proposed with in depth mathematical analysis for a better understanding. Proposed controller including the detection and regulation loops are supported through discrete simulations and were successfully validated experimentally.

Two experimental prototypes were fabricated as shown in Figure 0.3 in the *Groupe de recherche en électronique de puissance et commande industrielle* (GRÉPCI) laboratory at ÉTS to implement the proposed topology and control algorithms. One prototype was a conventional configuration for Hybrid series APF shown in the following figure, with a three-phase four-leg converter and three separate single-phase transformers. This setup has been used to implement control approaches and better understanding of practical challenges. The second prototype realizes the THSeAF topology as shown in the next picture demonstrating a securely built setup. This setup comprised of three separate H-bridge converters housing Semikron's IGBT with homemade drivers. The Opal-RT probes are adapted for the setup for a precise and noise-free measurement.

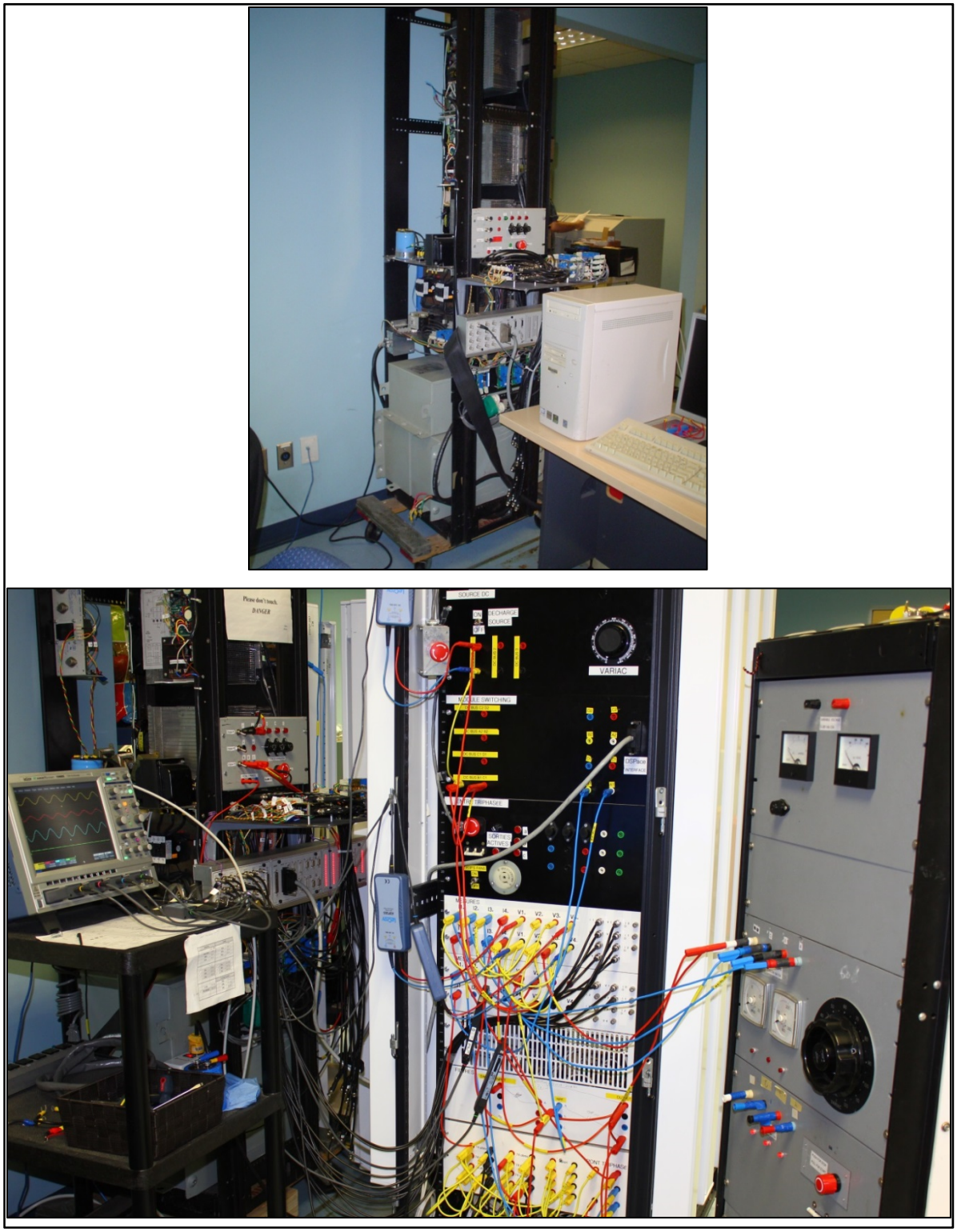

Figure 0.3 Laboratory setups. a) Three-phase conventional Hybrid APF, b) Transformerless-HSeAF experimental prototype

To realize the RCP application, the dsp1103 realize control algorithms in real-time. The dSPACE simulator is predominantly utilized to generate compensating voltage reference signals, which are sent to an FPGA based pulse-width modulator (PWM) board to perform switching gate pulses up to 5 MHz. The realization of this setup has required development of several boards for various tasks such as isolation, etc. The developed system performance is then verified under critical voltage and loading current conditions. The experimental results promises and supports the theoretical simulations reported in the proposed work.

Finally, this work contributes to the development of active power filters for power quality improvement and assists enhancement of smart technologies along with scientific and technical progress.

Thesis Outline

This thesis consists of five chapters. It starts with an introduction, followed by chapter one on literature review, three other chapters on various research tasks, and a chapter on substantial summary of the work presented, which links the outcomes of each chapter to proposed research objectives. Finally some conclusions, recommendations and future plans will be presented. The experimental conditions and parameters used in this research work are presented at the beginning of each chapter.

This work is organized as follows:

CHAPTER 1 presents a thorough review of the past and the most recent research work being done in the development of Smart Grids and the area of power quality compensation using Series active filter. Reported literatures on these topics are briefly discussed. The concept of smart girds and the application of Active power filtering in the power quality improvement of such system are also introduced. In this chapter various type of nonlinear loads are described along with their theoretical modeling. A study on conventional harmonic compensation techniques such as passive compensators is conducted in deep. After which a brief review of

active filtering and the state of the art in active compensation is presented. The basics of power quality, including key concepts and theoretical backgrounds, are explained which serve as a foundation to ease the understanding of this thesis work (Javadi et Al-Haddad, 2011; Javadi et al., 2012; Javadi, 2009).

CHAPTER 2 is fully dedicated to an extend review and the feasibility of a series active power compensator to improve power quality of a weak system. The chapter presents a comprehensive state of the art on Series compensator history, configurations, control strategies, and related involvements in this field. It provides a perspective of Series active compensator's technology to researchers dealing with power quality issues. A short-term study providing simulation results is carried out on the choice of components to realize the controlled voltage source of the SeAF by means of passive components and semiconductor converters. Furthermore, in this chapter a new control approach is proposed and analyzed to improve series harmonic compensation. To conclude some complementary studies on the stability of the system are presented along with experimental results. This chapter is partially based on two published papers (Javadi, Hamadi et Al-Haddad, 2014; Javadi et al., 2015).

CHAPTER 3 presents a single-phase Transformerless Hybrid Series Active Filter (THSeAF) to enhance power quality of an electrified transportation system consisted of single-phase current fed type of non-linear load. The proposed control strategy is designed to prevent current harmonic distortions of a CSC type of non-linear loads to flow into the utility and corrects its power factor. It will be demonstrated how the proposed configuration protects sensitive loads from voltage disturbances, sags, and swells initiated by the power system, ride of the series transformer. The rating and design of this new configuration for a practical implementation are presented. The validation of the proposed concept is done through simulation and experimental studies. Finally results presented in this work were carried out on a laboratory prototype demonstrating the effectiveness of the proposed topology where the compensator is subjected to several critical scenarios. This chapter is partially based on the published paper entitled "A Single-Phase Active Device for Power Quality Improvement of Electrified Transportation", (Javadi et Al-Haddad, 2015).

CHAPTER 4 thoroughly presents a Transformerless active power compensator using a sliding mode control algorithm and a Notch harmonic detection technique to improve power quality of a single-phase distribution feeder. It provides compensation for current harmonics coming from a voltage fed type of nonlinear load simulating an electric vehicle charging station. It will be demonstrated that the proposed configuration and based on the developed controller, the active power compensator is able to enhance the power quality while cleaning the point of common coupling (PCC) from possible voltage distortions and corrects the reactive power of a residential consumer. To overcome problems faced in a real-time control, accurate compensation methods are proposed. The validation is based on offline simulations and experimental results. Furthermore, an advance promoting Multilevel THSeAF with a PR controller onboard is presented in this chapter. Over again, this configuration improves power quality by means of an NPC multilevel converter and the Proportional plus Resonant (PR) controller. This chapter investigates aspects of harmonic compensation and asses the influence of the controller's choice and the delay time during a real-time implementation. The work presented in this chapter is based on three papers (Javadi, Hamadi et Al-Haddad, 2015), (Javadi et Al-Haddad, 2014), and (Javadi, Hamadi et Al-Hadda, 2015).

CHAPTER 5 is dedicated to a thorough study of three-phase system with poor power quality. In this chapter the power quality issues of three-phase system is treated where a three-phase series compensator is proposed to overcome power quality at low level distribution systems. Similar to single-phase SeAF, the proposed series active power filter adapted for the three-phase system with four-wire system is able to clean the grid's current from harmonics, unbalance and correct the power factor. Moreover, it would have the capability of cleaning the load side voltage problems and ensuring a stable and without supply perturbation. The chapter includes an advanced comprehensive control approach for three-phase Hybrid series active power filters with high efficiency response. Further in the chapter a novel transformerless configuration based on auxiliary current sources is presented. The proposed topology ride of the bulky transformer is capable of compensating current harmonics at the source and voltage distortion at the load terminals. Using the developed controller the three-phase THSeAF could perform superior to a conventional HSeAF and operate similar to a

Unified power quality conditioner (UPQC). Thereafter, a novel three-phase Transformerless Hybrid Series Active Filter (THSeAF) based on voltage fed converters to address major power quality issues related to residential and commercial buildings is presented. The developed inner-loop of the controller is a combination of Synchronous Reference Frame (SRF) and *p-q* theory extracting voltage and current harmonics and unbalances to be compensated. The controller's outer-loop producing gate switching signals for the three-phase THSeAF uses a proportional-integral controller. Simulation results illustrate the efficiency of the proposed techniques. Experimental results are demonstrated to validate and show the fidelity of the practical implementation towards real-time and offline simulations (Javadi, Fortin Blanchette et Al-Haddad, 2012a; 2012b).

The key conclusions of this thesis work and concluding remarks and recommendations for future work are also reported. Finally, at the end of the thesis, the list of key references and appendices are provided.

CHAPTER 1

SMART GRID'S CONCEPT AND ACTIVE FILTERING BASICS

1.1 Introduction

This chapter is aimed to give a global overview of Smart grids and develop necessary background knowledge of Series active filters. It will briefly discuss the latest development in the field of power quality enhancer's device. The chapter begins with a literature review on smart girds and the application of Active power filtering in their power quality improvement. It describes interests and benefits of an intelligently controlled power system while taking benefits of renewable energies. Later in this chapter various type of nonlinear loads are modeled and analyzed for harmonic compensation purpose. The traditional series passive compensation is deeply evaluated. After which a brief review of active filtering and the state of the art in active compensation is presented. To analytically study the power quality indices a mathematical notice on Fourier decomposition is presented. The chapter is followed by an extended study on power definitions found in the literature for time-domain and frequency domain applications. Regarding the fact that this thesis work is established on power semiconductors, a practical clarification on switching techniques and various type of pulse width modulation is presented for an experimental real-time implementation. Altogether this chapter should contribute to facilitate the understanding of this thesis dissertation along with some useful hint on real-time laboratory implementations.

1.2 Smart Grid Overview and Application

This section is dedicated to a brief review of Smart Grid concepts and the necessity of using advanced active compensators to improve its power quality. An overview of the recently established *Smart Grid* concept, elucidate the idea of updating the current power system with current informatics and telecommunication tools. An inclusive perceive on the state of the art led to the following description:

The Smart Grid contains several layers of decision centers, dispatched from main generation power plants to low level consumers. Each of these layers communicating over available internet infrastructure or a more sophisticated communication system. With regards to the increase of the renewable power sources and distributed generations, the current dispatching system will no more be able to carry on an efficient control over the network. Moreover, with implementation of smart consumer (electronic devices able to communicate and coordinate their behavior over an external control signal) able to change their loading behavior to optimize the global efficiency, it became a colossal dilemma to manage such huge flow of data. Meanwhile, if these setups are installed and the smart grid became operational, the future modern power system will be more reliable and much more efficient than the current conventional power systems.

1.2.1 Literature Review

A try to study the existing communication structure for the power grids is presented in (Iyer et Agrawal, 2010; Keyhani et Chatterjee, 2012). The paper discusses the emerging smart grid initiatives and analyzes the cyber security threats to such smart grid systems. This author and others researchers in this field believe that the communication technologies in a traditional power system is vulnerable and the dependency of load to the power system will increase manifold in the near future with more systems being computerized and a plethora of new electronic devices emerging for household, commercial and industrial applications. In such a scenario, the availability of secure, reliable and efficient power is crucial to sustaining current development and economic growth trends. With existing systems, power grids are not stable enough and can result in cascading failures.

In (Zhenhua, Fangxing et Pei, 2009), Jiang et al. present their vision of smart transmission grids in which they believe future modern power grids are required to become smarter in order to provide an affordable, reliable, and sustainable supply of electricity. As the backbone to deliver electricity from points of generation to consumers, the need of transmission grid development has been highly recognized to deal with more diversified

challenges, environmental challenges, market/customer needs, infrastructure challenges, and innovative technologies. Smart transmission grid regarded as an integrated system that functionally consists of different interactive, smart components; smart control centers, smart transmission networks, and smart substations. In (Rahimi et Ipakchi, 2010) the authors present the demand response as a market resource under the smart grid paradigm and mentioned that basic concepts on smart grid are related to advance metering infrastructure to improve demand-side management, energy efficiency, and a self-healing electrical grid to improve supply reliability.

Three main axes differentiate the smart grid over traditional systems as shown in Figure 1.1, where several developments have led to the expansion of the initially perceived scopes. The emphasis on environmental protection, including renewable energies and demand response (DR) are one. The drive for better asset utilization, including operating closer to the "knee of the curve" while maintaining reliable system operation and the need for enhanced customer choice are the two other backbone of smart grids.

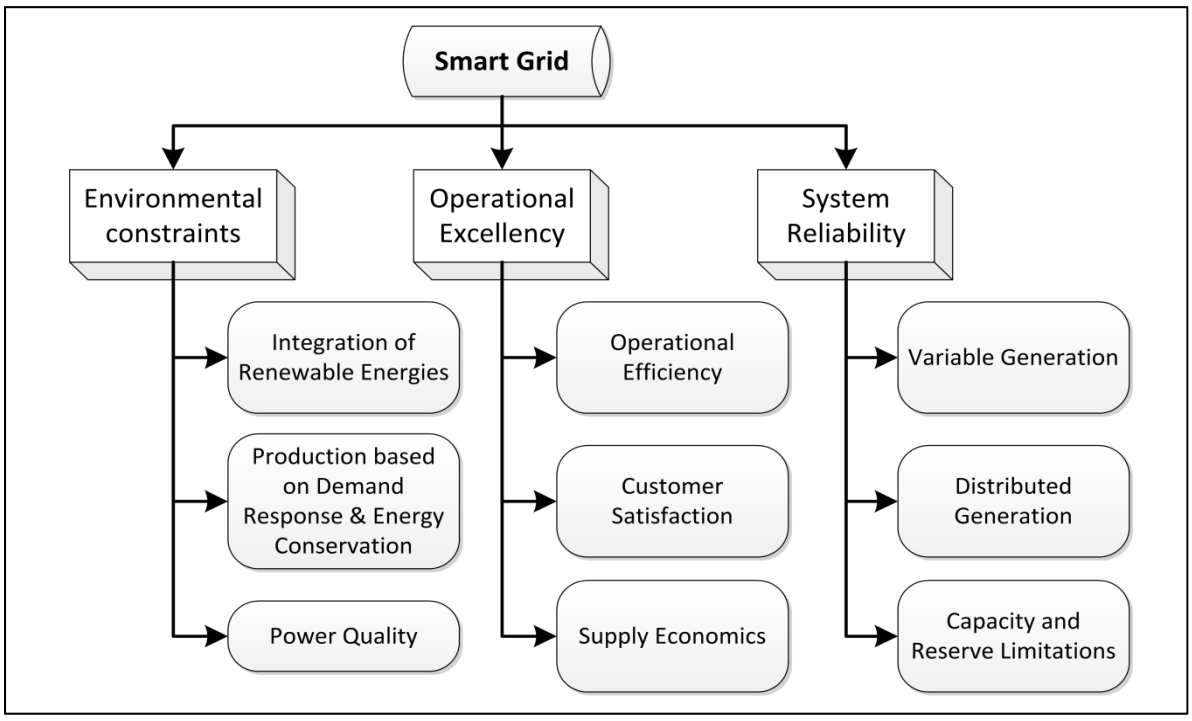

Figure 1.1 Overview of a smart grid operational flowchart

Under the pressure of climate challenges, in (Monti et Ponci, 2010) authors presents an analysis of the possible evolution of the power grids in the near future. While the platform for the smart grid is still under development, it is hard to predict the complexity that this system could contain. Many experts wish to see the power systems being operated like the communication networks, by a group of providers within the same infrastructure. Accordingly, it is safe to say that the power system will represent an interesting union of technologies from classical Power Systems to Power Electronics, Digital Control and Communications. Furthermore, researchers have investigated the catastrophe predictors from an ensemble decision-tree learning of wide-area severity indices (Kamwa, Samantaray et Joos, 2010). Much more works are still required to evaluate the reliability and viability of smart grids in all aspects of development. With regards to such developments in (Kurohane et Funabashi, 2010) authors introduce power electronics into Smart grids and give a vision of a hybrid smart ac/dc power system, where a smart grid based on a dc power grid is studied.

There exist some intuitive attempts to create new class of power electronics applications able to create small but discernible signals instantaneously, utilized for monitoring, power line communication and other information-oriented purposes. The signaling oriented power electronic techniques will have many potential applications in power systems and can be a major source of innovation for the smart grid development. While the importance of real-time simulations are pointed in (Podmore et Robinson, 2010), the implementation of highly realistic real-time and multi–time frame simulations are significant means to build a common vision of smart grid functions among politicians, regulators, managers, operators, engineers, and technicians.

To help a better understanding of the utility of smart grids in concern of efficiency, Figure 1.2 demonstrates a typical load curve during a day and the whole year in the USA (U.S. Energy Information Administration and Federal Energy Regulatory Commission, 2011). The difference between the deep point and the peak is between 0.7 and 1.3 (p.u.). The surface between the 1.3 and the red curve corresponds to the not used energy. While to have a higher efficiency the system should consume this power which the system is designed to have the

capacity to generate. If no outage and shedding on some part of the power system are considered, the installed generation capacity should be at least equal to the peak load. In this case, a huge amount of the installed capacity is not used. This portion can represent thousands of MW in reality. In addition a great amount of financial investment is needed to satisfy only the peak load.

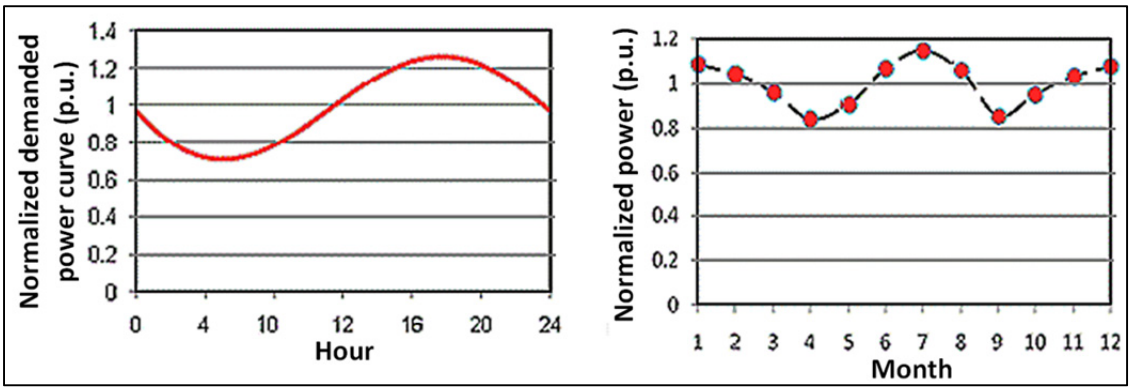

Figure 1.2 A typical daily and annually load curve in the United States
Taken from U.S. Energy Information Administration and
Federal Energy Regulatory Commission (2011)

To increase the system usage efficiency, many researchers, scientists and companies suggested different approaches. Some suggest to perform load shedding during the peak times, and the central controls should handle the anticipated load peaks and unanticipated generator outages (International Energy Agency (IEA), 2010). Some other approaches are based on the energy storage. A method to do so is the Hydrogen process. It has been developed as electric power medium energy storage. Hydrogen is not a primary energy source, but a portable energy storage method, because it must first be manufactured by other energy sources in order to be used. However, as a medium storage, it may be a significant factor in using renewable energies with fluctuating generated power. The widely used method is to store the energy by pumping the water to a higher elevation natural tank or artificial one during the low load, then regenerating power during peak loads. Other methods consist of using pumped storage methods, in compressed air, or in spinning flywheels. Compressed air energy storage technology stores low cost off-peak energy, in the form of

compressed air in an underground reservoir. The air is then released during peak load hours and heated with the exhaust heat of a standard combustion turbine. This heated air is converted to energy through expansion turbines to produce electricity.

However, these methods are costly and demand installation's sites and have environmental impacts, resulting in a significant reason to encourage the power grids to become smarter. By creating a smart marketing and a smart pricing it will be possible to encourage the consumers to contribute to reduce the peak of the load by consuming during off-peak periods. The smart electrical energy pricing make a better control on the power system and the power flow feasible. The drastic reduction of carbon emission cannot be realized without a significant involvement of electricity sectors as described in (Varaiya, Wu et Bialek, 2011). More power should be produced from renewable energy resources and an effective consumer's demand response must be implemented along with high-capacity energy storage systems. This highlights the necessity of a smart grid to manage and control the complex future grids.

Generation of power plants in traditional power systems depends on the load demand. In these systems, the information of the load is sent to the grid and central control to schedule the electric generation dispatch. By the increase of renewable plants and distributed generators (DG), the power system is required to adjust its production and management with this new constraint. By realizing electrical power systems more smart at all levels, it became possible to overcome these new challenges and it will be possible to increase efficiency and reducing the environmental impact of power systems. In an innovative vision of smart grids, loads and renewable plants along with available power plants are connected and the information flow between them. This implicates the consumers to be more responsible and more engaged toward their surroundings and been able to satisfy their own consumptions by installing renewable sources.

1.3 Power Quality Enhancement in Smart Grid

Multiple methods to overcome power quality issues exist, especially those related to harmonic pollutions. Load conditioning which is well documented in the literature consisted of changing the load's configuration in order to improve its behavior by reducing harmonic content of its consumed current. External solutions consisted of adding a compensator to address such issues. In this category two principal configuration are available; Passive Filters and Active Filters.

1.3.1 Passive Filter

Traditional filters made of passive components widely contributed to improve current and voltage harmonics of power systems. These filters have the advantage to be created of relatively simple electrical components like capacitors, inductors, and resistors. From the point of view of industries these combinations are quiet clear to understand. Meanwhile, they have significant weakness; they require a precise overview of the load and system parameters such as the impedances to be tuned properly. When installed, they behave operational during a specific state of the system and are not adapted to load variation and changes to the system specifications. Consequently, in particular conditions, not they cannot only help improving power quality but may also worsen this later by creating resonance or simply not operating as expected. Thus, they require re-tuning periodically to be effective as no control exist on their operation state. To better understand harmonic compensation process using passive filter on two types of non-linear loads, a passive filter made of a shunt and series branch is studied briefly. The issued IEEE standard 1531 cover application of such filters for harmonic compensation (IEEE Guide for Application and Specification of Harmonic Filters, 2003).

1.3.1.1 Current fed type of nonlinear load

In the first case the passive filter is applied to a current source converter (CSC) commonly known as current fed type of loads. These nonlinear loads are modeled using the Norton

equivalent model, a harmonic current source in parallel with an impedance. This impedance represents the active power consumed by the load. A single-phase representation of a current fed type of nonlinear load and a series bank of passive filter along with a shunt connected passive filter bank are depicted in Figure 1.3. It should be noted that a considerable efforts have been made in this thesis dissertation to follow electrical representation of the international standards for graphical representation of electrical diagrams (IEEE Standard American National Standard Canadian Standard Graphic Symbols for Electrical and Electronics Diagrams (Including Reference Designation Letters), 1993). For the aim of simple representation, a tuned combination of a fifth, seventh and a low-pass filter is used for the series branch, while any other combination could be applied. Likewise is for the shunt branch, where a fifth, seventh and a high-pass tuned filter are implemented to absorb current harmonics of the load. This combination of filter is practical for a robust compensation of current harmonics.

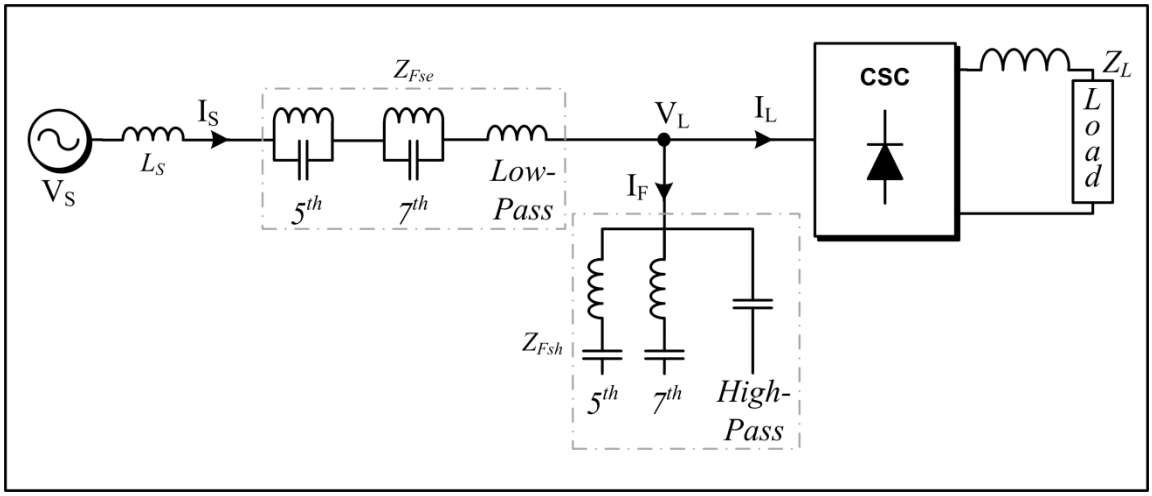

Figure 1.3 Single-phase representation of passive filter used to compensate a current fed type of non-linear load

The equivalent circuit is represented in Figure 1.4 where the non-linear load is modeled using its Norton equivalent model. A modest combination of passive filter is used and represented in the Figure 1.4. The I_L represents the loads current, I_F the current of the shunt passive filter, I_S the current fed through the grid, and Z_L is the equivalent impedance of the non-linear load.

The independent current source (I_h) represents current harmonics of the non-linear load. The grid is modeled by a voltage source in series with the equivalent inductance (L_S) of the power system.

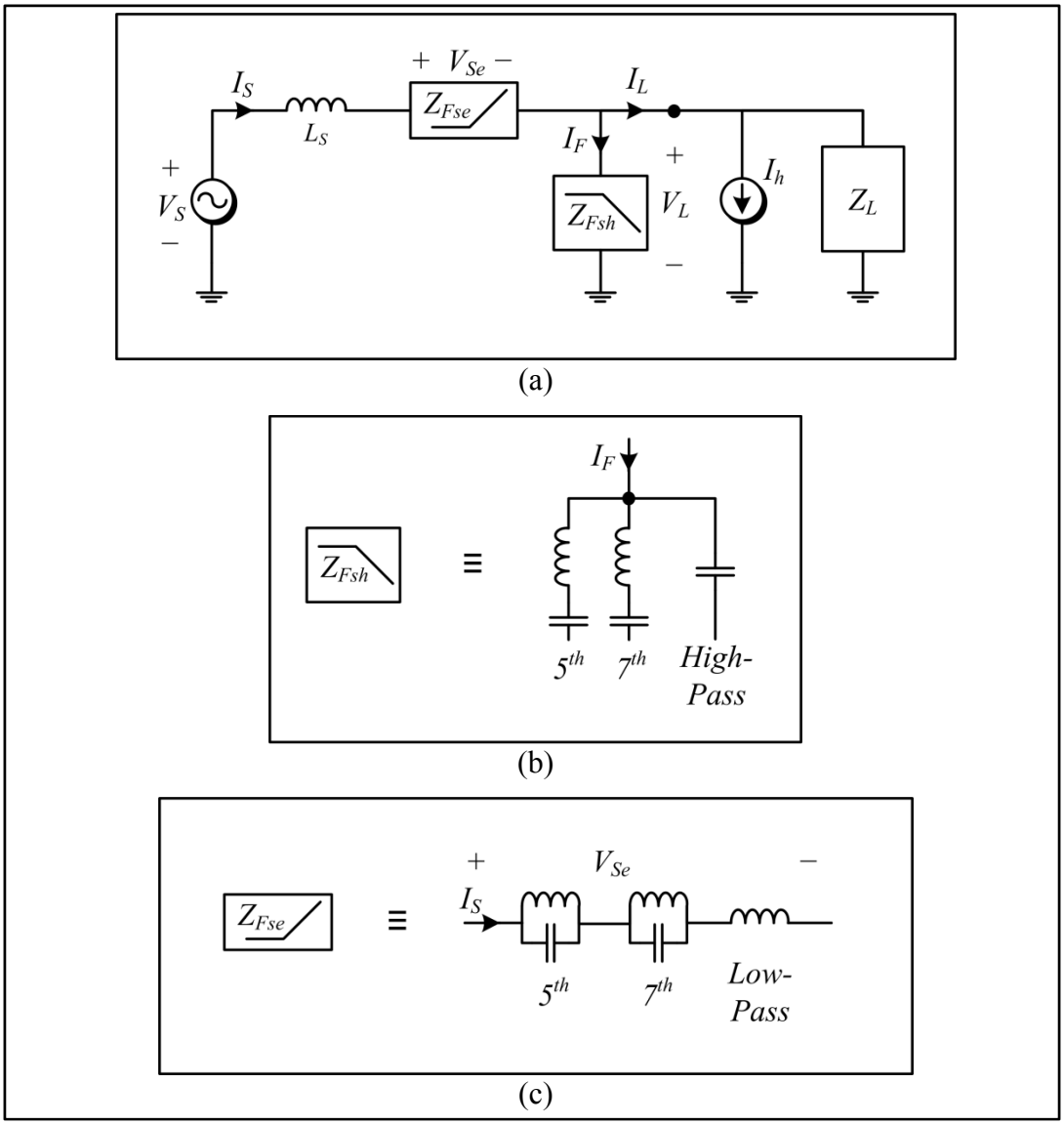

Figure 1.4 Equivalent circuit of the system using the Norton equivalent of the CSC

The circuit could be analyzed through linear circuit analysis. The source current is deduced using the Kirchhoff's voltage law.

$$I_S = \frac{(V_S - V_L)}{(X_{Ls} + Z_{Fse})} \tag{1.1}$$

For harmonic components the relationship (1.2) is obtained considering no voltage distortion at the source:

$$I_{Sh} = \frac{-V_{Lh}}{(X_{Ls} + Z_{Fse})} \tag{1.2}$$

Using the Kirchhoff's current law (KCL) at the connection point of the load, Eqn. (1.3) is obtained.

$$I_{Sh} = I_F + I_h + \frac{V_{Lh}}{Z_L} \tag{1.3}$$

Where the current of the shunt passive filter is

$$I_F = \frac{V_{Lh}}{Z_{Fsh}} \tag{1.4}$$

Substituting (1.2) and (1.4) in (1.3), the voltage distortion at the load's terminal is derived.

$$V_{Lh} = -\left(\frac{(X_{Ls} + Z_{Fse}) \cdot Z_{Fsh} \cdot Z_L}{Z_{Fsh} \cdot Z_L + (X_{Ls} + Z_{Fse}) \cdot Z_L + (X_{Ls} + Z_{Fse}) \cdot Z_{Fsh}}\right) \cdot I_h \tag{1.5}$$

Assuming that the series passive filter impedance is much greater than the source equivalent impedance for high frequency harmonics ($|X_{Ls}| << |Z_{Fse}|$) and supposing that Z_{Fsh} has a very low impedance toward same high frequency harmonics ($|Z_{Fsh}| << |Z_L|$), the following simplified relation is achieved.

$$V_{Lh} = -Z_{Fsh} \cdot I_h \tag{1.6}$$

Introducing (1.6) into (1.2), the source harmonic current over the loads produced harmonics is reached.

$$I_{Sh} = \frac{Z_{Fsh}}{(X_{Ls} + Z_{Fse})} \cdot I_h \tag{1.7}$$

With regards to the facts that the series passive filter represents high impedance for harmonics and the shunt passive filter has relatively low impedance for current harmonics, the source current is going towards a null value ($I_{Sh} \rightarrow 0$).

Table 1.1 Passive filter parameters

Definition	**Value**
Shunt passive filter, Z_{Fsh}	5^{th}: 20 mH, 14.1 µF 7^{th}: 10 mH, 14.4 µF C_{HP}: 2 µF
Series passive filter, Z_{Fse}	5^{th}: 5 mH, 57 µF 7^{th}: 10 mH, 14.4 µF L_{LP}: 0.5 mH
Supply equivalent inductance, L_S	250 µH
Load equivalent impedance	12.5 Ω, 20 mH
DC auxiliary power supply voltage	130 V

Thus with a precise tuning of passive filters it is possible to clean the source current from harmonic components of a CSC non-linear load. The typical ratio of attenuation of current harmonics in dB over the harmonic frequency is plotted in the Bode diagram of Figure 1.5.

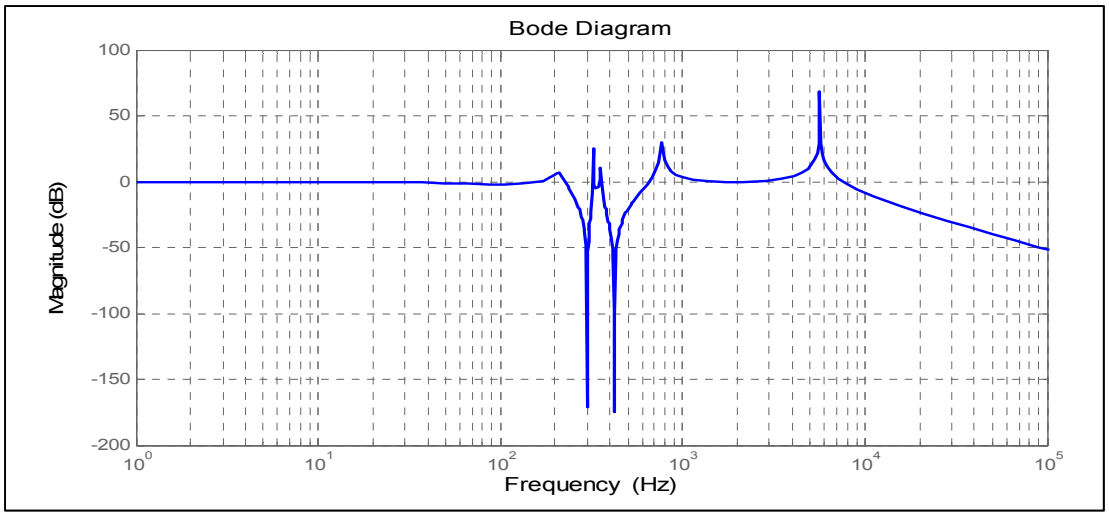

Figure 1.5 Typical compensation characteristic for the CSC type of loads, I_s/I_h

1.3.1.2 Voltage fed type of nonlinear load

The proliferation of VSC loads, having a semiconductor bridge at the entrance stage and a capacitor at the DC side, require harmonic compensation as well. This second case study is dedicated to voltage fed type of nonlinear loads. The single phase representation of a typical VSC load is illustrated in Figure 1.6, where the same passive filters as previously described are used to compensate current harmonics flowing into the grid.

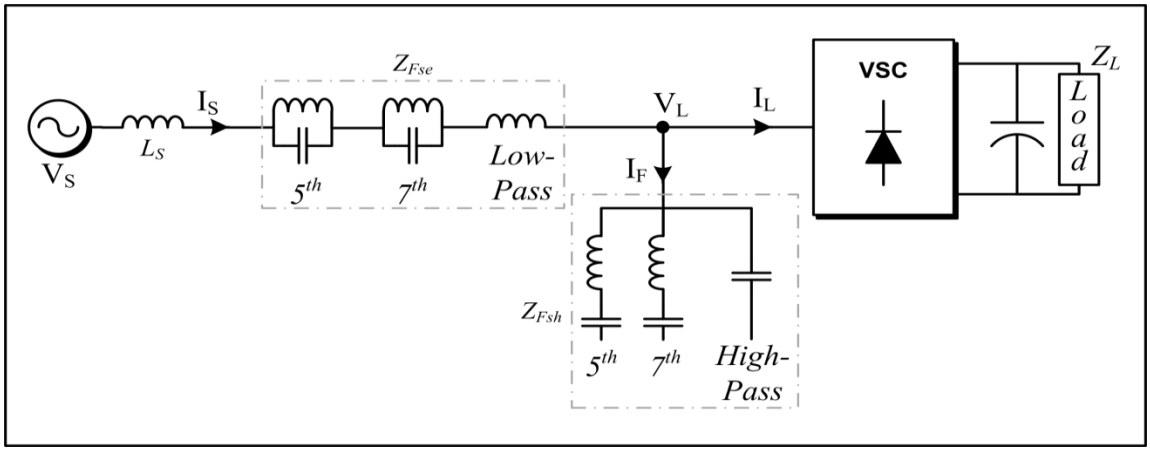

Figure 1.6 Single-phase representation of the system comprising a voltage fed type of non-linear load

The equivalent circuit is represented in Figure 1.7, where the non-linear load is modeled using its common Thévenin equivalent model for voltage fed type of loads. In this schematic I_L represents the loads fed current, I_F is the current of the shunt passive filter, and I_S is the source current. The source V_h represents voltage harmonics of the non-linear load. The grid is modeled by a voltage source in series with the grid's characteristic impedance (X_{Ls}) of the power system.

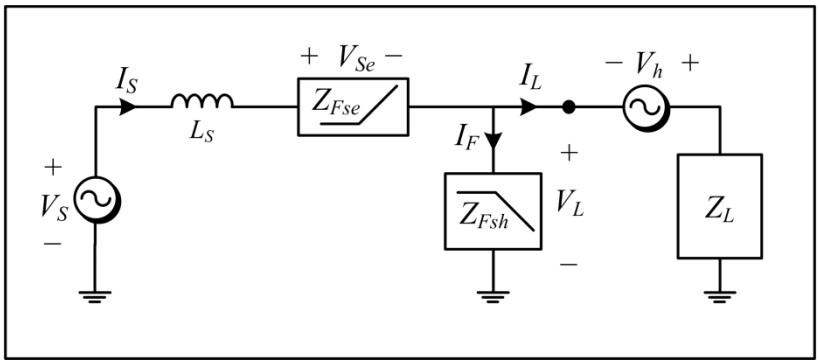

Figure 1.7 Equivalent circuit of the system using the Thévenin equivalent of the VSC load

Appling the ohm's law, it is possible to compute for the current source harmonics. The source current for harmonics is achieved using the KVL law of circuits, while source voltage harmonics V_{Sh} is absent.

$$I_{Sh} = \frac{-V_{Lh}}{(X_{Ls} + Z_{Fse})} \tag{1.8}$$

For the right hand loop, the load current at harmonic frequency is

$$I_{Lh} = \frac{V_{Lh} + V_h}{Z_L} \tag{1.9}$$

The voltage across the shunt passive filter or the load terminal is also reached from the following equation assuming I_F contain no fundamental component.

$$V_{Lh} = Z_{Fsh} I_F = Z_{Fsh} \cdot (I_{Sh} - I_{Lh}) \tag{1.10}$$

Substituting (1.9) into (1.10) the load harmonic voltage is derived.

$$V_{Lh} = A \cdot (Z_L I_{Sh} - V_h) \qquad , \qquad \left(A = \frac{Z_{Fsh}}{Z_{Fsh} + Z_L}\right) \tag{1.11}$$

Substituting (1.11) in (1.8), the relation for the compensation of source current harmonics over the voltage producing harmonics is reached.

$$I_{Sh} = \left(\frac{A}{X_{Ls} + Z_{Fse} + AZ_L}\right) \cdot V_h \tag{1.12}$$

Assuming that $|Z_{Fsh}|$ has an enough low value, the parameter A will have a quite small value. Consequently, the relation (1.12) illustrates that if the passive filters are adequately tuned, the Z_{Fsh} to have a small value and Z_{Fse} high impedance value for harmonic components, the current harmonics flowing through the source will be eliminated ($I_{Sh} \approx 0$).

The typical ratio of attenuation (I_S/V_h) of source current harmonics in dB over the harmonic frequency is depicted in the Bode diagram of Figure 1.8. This figure illustrated that using the tuned passive filter it is possible to clean the source current from harmonics produced by a voltage type of non-linear load.

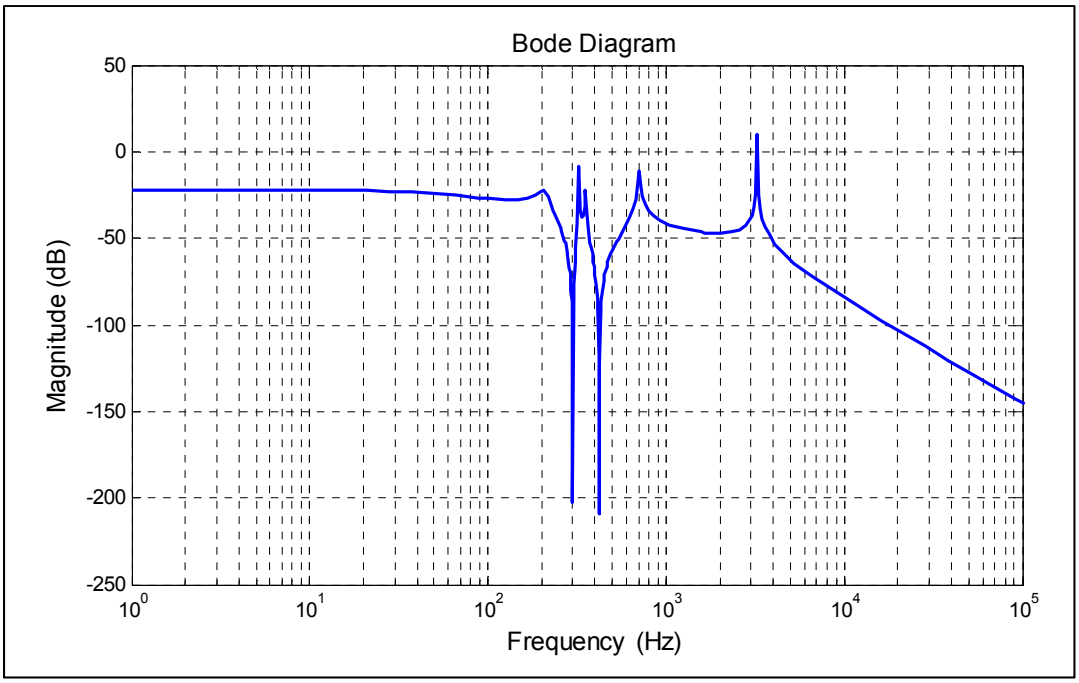

Figure 1.8 Typical compensation characteristic for the VSC type of loads, I_s/V_h

1.3.2 Active Filtering Techniques

With the advances in power electronics, the active filtering is gaining in popularity in recent decades. The shunt active filters are among the first AFs been commercially available for small and medium voltage applications. They have numerous advantages over conventional passive filters. They do not require tuning and are independent of the state of the systems parameters. They respond instantaneously to load variations without any difficulties. And their compensation efficiency is much less susceptible to external parameters. The operator has instantaneous control over the device and could perform all kind of desired modification without the necessity of modifying the hardware. In this way, there exists numerous types of active filters; Shunt AFs, Series AFs, Hybrid AFs, and Unified power quality conditioner (UPQC) are among popular active compensators. The Table 0.1gives a general overview of aforementioned active devices. The IEEE-1409 standard describes applications of power electronics for power quality improvement on distribution systems rated from 1-kV through

38-kV (IEEE Guide for Application of Power Electronics for Power Quality Improvement on Distribution Systems Rated 1 kV Through 38 kV, 2012).

With the technological advances in manufacturing and the decrease in production cost of power electronic converters the application of Active compensators seems inevitable. The introduction of Smart grids has promoted application of these alternative compensators to enhance power quality over traditional passive filters. Having similar topology to FACTS devices, the industry is convinced on their reliability during critical operating states. Thus, in this section a brief overview of these various categories of active compensators are presented.

1.3.2.1 Shunt Active Filter

The harmonic mitigation using shunt active filtering was initially introduced by Gyugyi in 1979 (Gyugyi, 1979). Nowadays, Shunt filtering is well developed and numerous industrial applications are available and the traditional approach of using passive filters to address current issues and power factor correction is modernized by the application of power electronic devices (Javadi, Olivier et Sirois, 2010; Rahmani, Mendalek et Al-Haddad, 2010; Yi et al., 2012). Accordingly, the shunt active filter has been replacing passive filters in industrial applications, while their robust and reliable operation has convinced industry to make them commercially available. They have a remarkable performance in compensating current harmonics and correcting power factors simultaneously (Chudamani, Vasudevan et Ramalingam, 2009; Zhikang et al., 2009). Their real-time controller determines the compensating current reference and forces the electronic converter to synthesize it precisely. They give the ability to operators to perform a selective and adaptive compensation as well as the degree of power factor correction. The SAF can compensate only for a specific harmonic order of a non-linear load, and can continuously track changes in its harmonic content (Javadi, 2009). There exist several configurations for 3P3W or 3P4W systems respectively. The principle of shunt current compensation is depicted in the following figure.

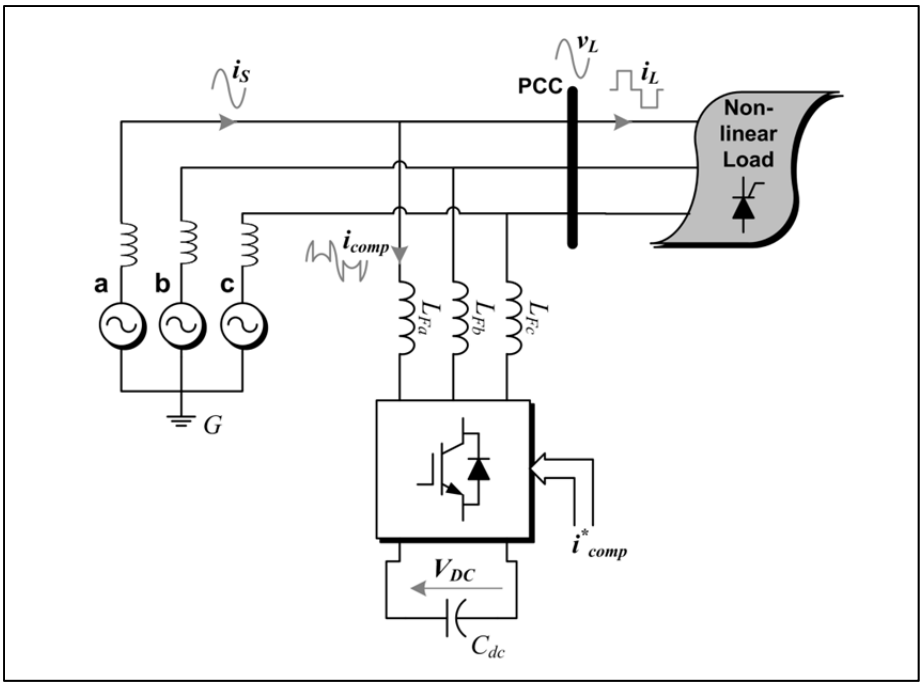

Figure 1.9 Three-phase shunt-AF for current harmonics of a nonlinear load
Taken from Javadi et al. (2012)

Similarly Shunt-AFs have the distinct advantage that they do not resonate with the power system and they work independently with respect to the system impedance characteristics. They are used in difficult circumstances where passive filters don't operate successfully because of resonance problems and they don't have any interference with other elements installed anywhere in the power system. They can also address more than one harmonic at the same time and solve other power quality problems like flicker, etc. Shunt active filter has the ability to be adjusted instantly with the load changes without any energy storage components, so it can compensate harmonics completely without consuming any active power. In addition, they can provide compensating current from zero to their maximum capacity according to the load currents; so if the load does not need any compensating current, the compensators will not inject any current and even if the frequency of harmonics of the load changes, the filters can easily adapt to compensate the new harmonics without any need for tuning in the hardware. Active filters inject a current to the connection point in a way that the sum of the compensating and the load current become a sinusoidal waveform seen from the source as illustrated in Figure 1.9.

1.3.2.2 Series Active Filter

Problems with passive filters include the fact that they are extremely expensive and represent a fairly inaccurate solution push the experts to look for alternative solutions. Passive filters are typically hard to install because a precise evaluation of system parameters is required before installation, and such an evaluation can be long and arduous. Moreover, as the power grid evolves, its parameters change, and the passive filters must be adjusted to account for these changes. This reduces the efficiency of the passive filter as a solution, and increases the related maintenance expenses. Shunt active filters, which have been used to replace passive filters, are limited to compensating current harmonic pollution produced by nonlinear loads and correcting the power factor. To mitigate power quality related problems, line conditioning systems are used that suppress or counteract the power system disturbances. “Series Active Filters (SeAF)” and “Dynamic Voltage Restorers (DVR)” are among the compensation devices used to reduce voltage distortions and to compensate for current issues. However, due to the complexity of series active compensators, as compared with more conventional shunt active filters, the use of such devices is still limited to specific application where PQ requirement is very stringent.

In addition to compensate current issues, it is essential to protect the PCC and sensitive loads from voltage distortions, sags, and swells, a dynamic voltage restorer is required. The DVR and the SeAF share similar topologies which is relatively complex in part due to the isolation transformer for coupling to the grid. This provides good isolation of the compensating system, but the transformer, in addition to being quite expensive, introduces a number of detrimental performance issues, such as electrical losses, hysteresis phenomena, and the need to be short-circuited during a fault condition on the secondary.

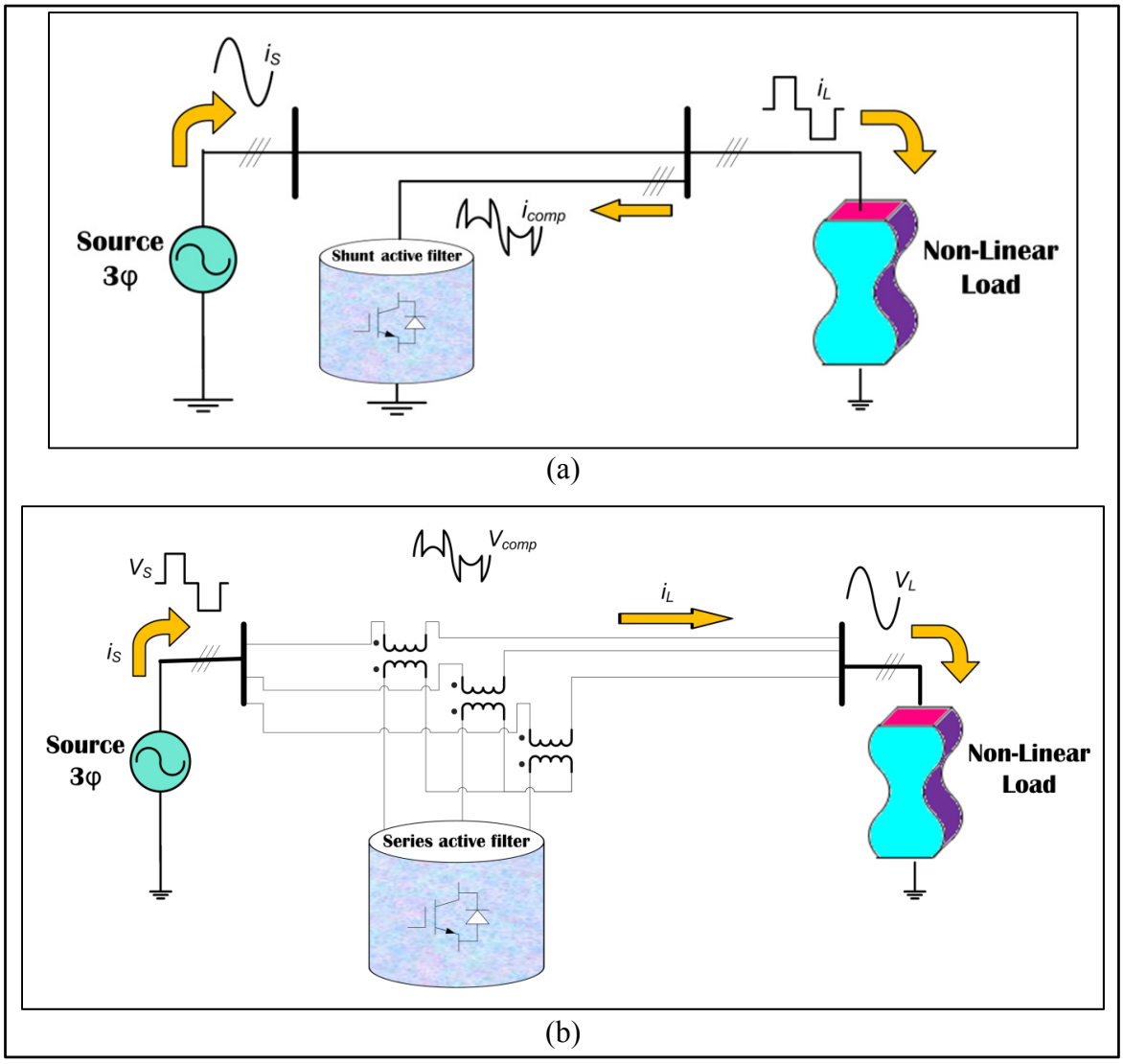

Figure 1.10 Operation schematics of Shunt versus Series compensation
(a) Shunt compensation, (b) Series compensation
Taken from Javadi et Al-Haddad (2011)

The operation principle of Series compensation is illustrated in Figure 1.10. In comparison to the shunt compensator, the Series compensator injects a voltage to the line to resolve voltage or current issues. The DVR and SeAF share a common configuration which is depicted in Figure 1.11.

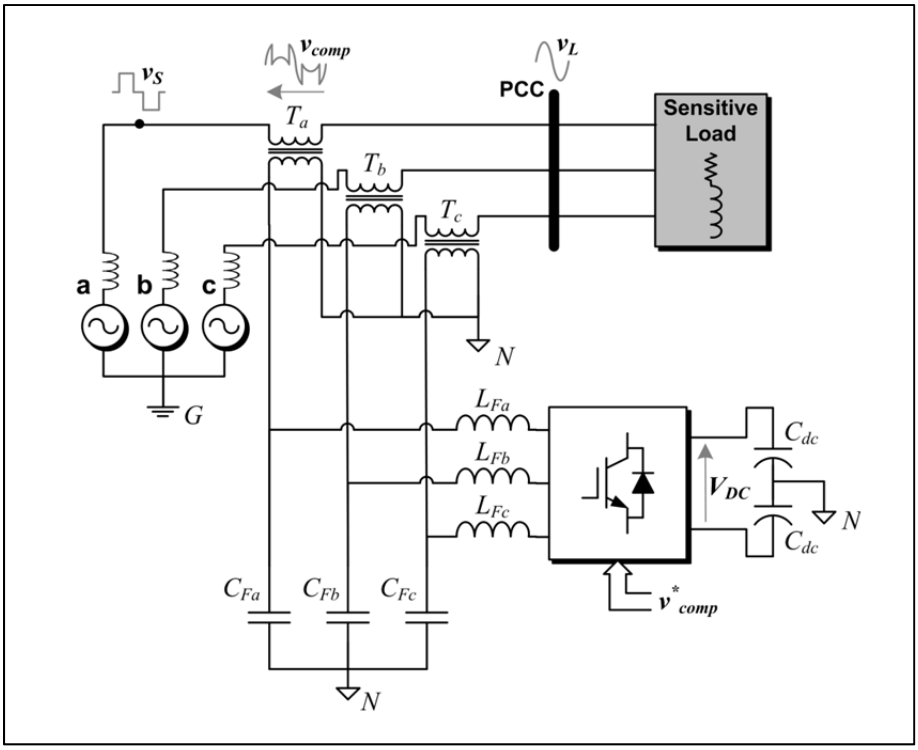

Figure 1.11 Three-phase Series compensator connected to the grid
Taken from Javadi et al. (2012)

The series compensation been the subject of this research work, will be described in detail in this thesis dissertation.

1.3.2.3 Hybrid Active Filter

Nowadays, modern electrical equipment requests stringent demands on supply voltage quality and stability. On the other hand, power networks have to be free from harmonics and other electrical disturbances. Compensating these issues has several benefits such as; a higher power factor, improved voltage stability and decrease in network losses. Elimination of undesired harmonics in the system, avoidance of resonance problems, and amplification of electrical disturbances are among multiple benefits of enhancing the power quality. Cleaning the network from perturbations has the advantage of imposing less strain on equipment and lengthens its life span; this means a lower cost of replacing worn-out equipment and

consequently a lower maintenance cost. Altogether, this makes operators seeking to improve power quality aspects of the network. To take advantages of both passive and active filters, Hybrid filters were created. There exist various types of hybrid filters which are out of context for this study. The Hybrid Filter shown in Figure 1.12 consists of a Series active filter in parallel to a passive filter bank. This configuration will be studied in detail in following chapter. This configuration is able to address current related issues while, taking into account the restoration of a reliable and sustainable supply for the loads.

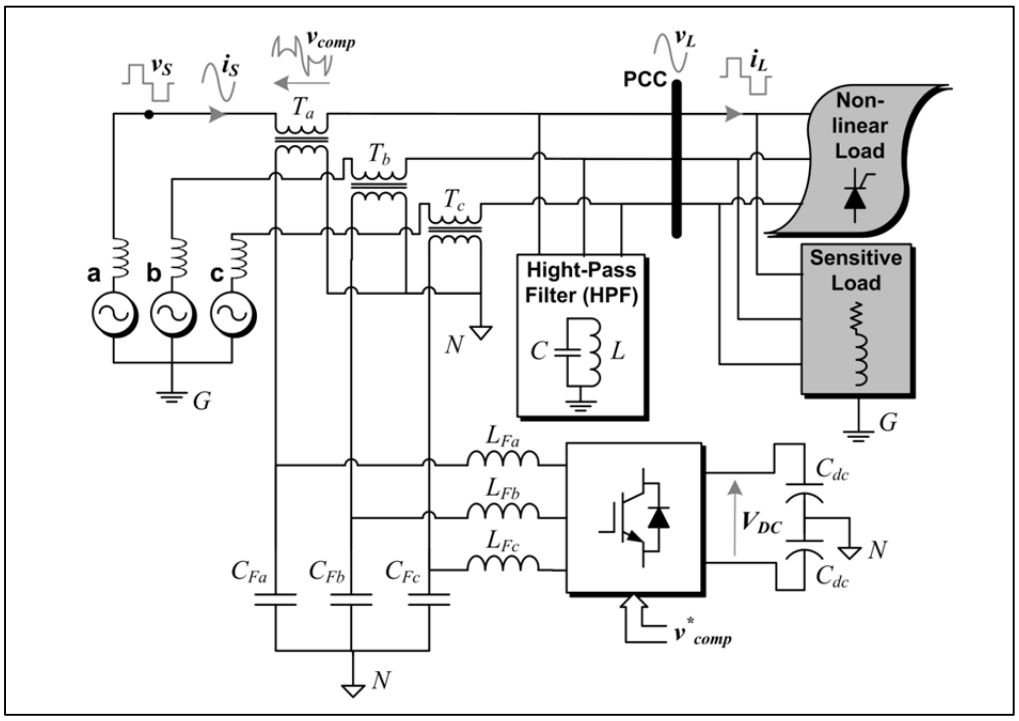

Figure 1.12 Hybrid Series Active filter compensating voltage and current issues

These filters, take advantages of the high dynamic provided by the active part and the simplicity of the passive section. This combination gives more interesting structure which ensures high VAR compensation as well than Active or Passive filters alone.

1.3.2.4 Unified Power Quality Conditioner

An ultimate solution is the Unified power quality conditioner (UPQC), a combination of a shunt and a series active filters (Khadkikar, 2012). The series connected active filter compensates for voltage harmonics and related issues, while the shunt part connected across the load eliminates current distortions (Ganguly, 2014). The extremely expensive UPQC could be an effective response to power quality issues, but due to its complexity is less commercially available and has therefore seen only scattered application. The following diagram illustrates a typical configuration for a UPQC to be linked to the power system.

The UPQC come from the same family as of Active filters where shunt and series AFs functionalities are unified together to reach superior control over several power quality problems instantaneously (Quoc-Nam et Hong-Hee, 2014). The back-to-back converter configuration came into attention when Fujita and Akagi (Fujita et Akagi, 1998) proved the practical application of this topology with 20 kVA experimental results and they named this device a “unified power quality conditioner”.

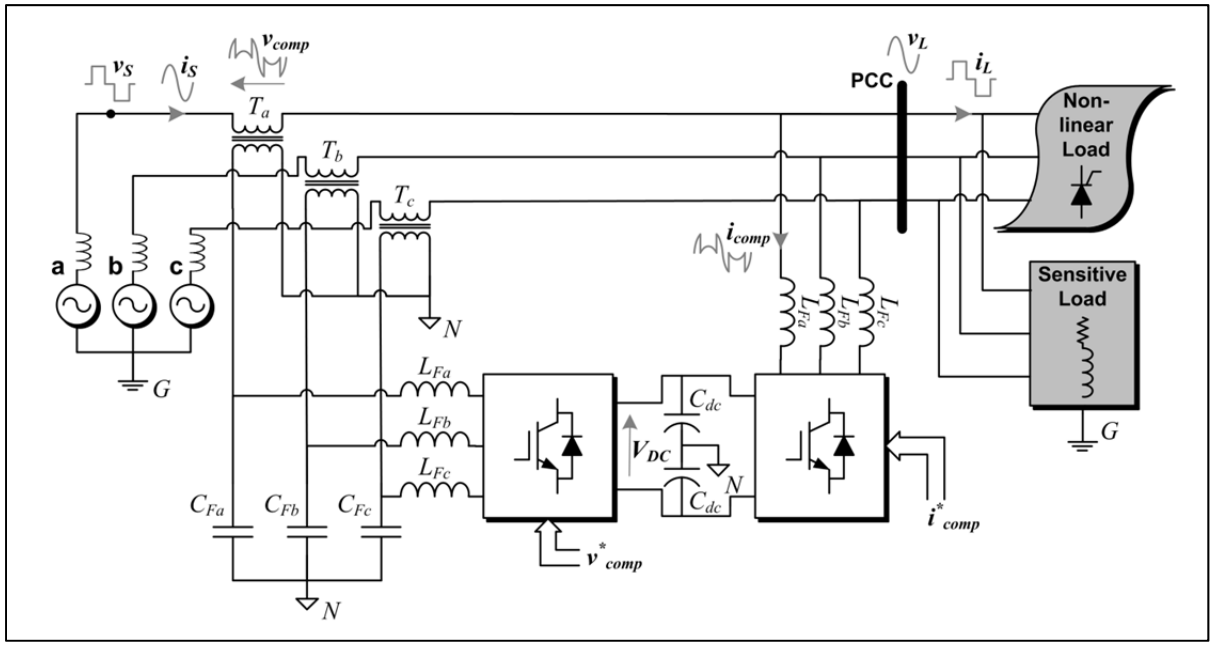

Figure 1.13 Unified Power Quality Conditioner addressing power quality problems

1.4 Fourier Series Decomposition

The decomposition of a signal into multiple frequency oscillating signals is the basis of power quality analysis. This way of representation a periodical function as the sum of simple sine or cosine waves allow definition of harmonics. A periodical waveform could be represented by the following Fourier equation.

$$f(t) = A_0 + \sum_{h=1,2,3,\cdots,N}^{\infty} (A_h \cos(h\omega_o t) + B_h \sin(h\omega_o t)) \tag{1.13}$$

Where

$$A_0 = \frac{1}{T}\int_0^T f(t).dt \tag{1.14}$$

and

$$A_h = \frac{2}{T}\int_0^T f(t)\cos(h\omega_o t)\,dt \quad , \quad B_h = \frac{2}{T}\int_0^T f(t)\sin(h\omega_o t)\,dt \tag{1.15}$$

To make simpler the decomposition, the notion of Even and Odd waves are introduced.

$$\begin{cases} Even\ if & g_{(-x)} = g_{(x)} \\ Odd\ if & g_{(-x)} = -g_{(x)} \end{cases} \tag{1.16}$$

The following relations are always true when crossing two signals.

$$\begin{cases} even \times even = even \\ even \times odd = odd \\ odd \times odd = even \end{cases}$$

Based on the established definitions it became possible to generalize some simplified rules when decomposing a periodic signal:

1. For Even signals, the terms B_h are not present (B_h=0, h=1,2,3, …,n).

2. For Odd signals, the terms A_h are not present (A_h=0, h=1,2,3, …, n).

3. If a waveform has a "Half-wave" behavior, the even orders of harmonics are not present.

$$if \quad f(t) = -f\left(t + \frac{T}{2}\right) \;\Rightarrow\; A_h \; and \; B_h = 0 \quad for \quad even \; h = 2,4,6, \ldots 2n \tag{1.17}$$

And

$$\begin{cases} A_h = \dfrac{4}{T}\displaystyle\int_0^{T/2} f(t)\cos(h\omega_o t)\,dt \\ B_h = \dfrac{4}{T}\displaystyle\int_0^{T/2} f(t)\sin(h\omega_o t)\,dt \end{cases} \qquad h = 1,3,5,\cdots,2n-1 \tag{1.18}$$

4. If a waveform is a "Quarter-wave" signal then following relations are derived:

   a. For Even signals:

$$\begin{cases} f(t) = f(-t) \\ f(t) = -f\left(t + \dfrac{T}{2}\right) \end{cases} \Rightarrow \quad f(t) = -f\left(\frac{T}{2} - t\right) \quad (Odd \; quarter - wave) \tag{1.19}$$

The terms A_0 and B_h are not present as well as A_h for components with even orders (h=2, 4, 6,…2n). Thus, we have

$$A_h = \frac{8}{T}\int_0^{T/4} f(t)\cos(h\omega_o t)\,d_t \qquad h = 1,3,5,\cdots,2n-1 \tag{1.20}$$

   b. For Odd signals:

$$\begin{cases} f(t) = -f(-t) \\ f(t) = -f\left(t + \dfrac{T}{2}\right) \end{cases} \Rightarrow \quad f(t) = f\left(\frac{T}{2} - t\right) \quad (Even \; quarter - wave) \tag{1.21}$$

The terms A_0 and A_h are not present as well as B_h for components with even orders (h=2, 4, 6,…2n). Thus, we have

$$B_h = \frac{8}{T}\int_0^{T/4} f(t)\sin(h\omega_o t)\,dt \qquad h = 1,3,5,\cdots,2n-1 \tag{1.22}$$

As reminder, following definitions are helpful regarding the DC component and the mean value of a periodic signal.

$$V_{dc} = V_{mean} = A_0 = \frac{1}{T}\int_0^T v(t).dt \tag{1.23}$$

The rms or the effective value became as follow.

$$V_{rms} = V_{eff} = \sqrt{\frac{1}{T}\int_0^T v(t)^2.dt} \tag{1.24}$$

The relation between the oscillating and the DC component as well as some definitions is as follow.

$$\begin{cases} \left|{V_{rms}}^2\right| = \left|{V_{ac}}^2\right| + \left|{V_{dc}}^2\right| & \\ FF = \dfrac{V_{rms}}{V_{dc}} & Form\ Factor \\ RF = \dfrac{V_{ac}}{V_{dc}} = \sqrt{FF^2 - 1} & Ripple\ Factor \\ TVF = \dfrac{P_{dc}}{V_{Seff}\cdot I_{Seff}} & Transformer\ Factor \end{cases} \tag{1.25}$$

1.4.1 Power Quality Indices

According to the IEEE-519 standard, the following definitions on the harmonic related issues are briefly enumerated in this section.

1.4.1.1 Total harmonic distortion, THD

The total harmonic distortion (THD) is a measurement of the harmonic distortion present in a waveform and is the ratio of the sum of the powers of all harmonics to the power of the fundamental frequency (IEEE Recommended Practices and Requirements for Harmonic Control in Electrical Power Systems, 1993). It is practically used to characterize the power quality of electrical systems. It reflects the effect of harmonics on the power system voltage or current respectively. It is almost always expressed as a percent of the fundamental rms value.

$$THD_{\%} = \frac{\sqrt{\sum_{h=2}^{\infty} {V_h}^2}}{V_1} \cdot 100\% \qquad h = 1\ (fundamental), 2,3, \cdots, n \tag{1.26}$$

The effective (rms) value of a waveform containing harmonics could be depicted as follow:

$$V_{eff} = V_1\sqrt{1 + THD^2} \tag{1.27}$$

1.4.1.2 Distortion index, DIN

The DIN is the ratio of the root-mean-square of the all harmonic content to the root-mean-square value of all components including the fundamental quantity. The relation between the distortion index and the THD could be expressed as follow.

$$DIN = \sqrt{\frac{\sum_{h=2}^{\infty} {V_h}^2}{\sum_{h=1}^{\infty} {V_h}^2}} = \sqrt{\frac{THD^2}{1 + THD^2}} \qquad (0 < DIN < 1) \tag{1.28}$$

1.4.1.3 Total demand distortion, TDD

The total demand distortion, harmonic current distortion in % of maximum demand load current (fundamental frequency component) at PCC for a measurement period of 15 to 30 minutes. The TDD is practically equal to the THD value in percentage.

$$TDD_{\%} = \frac{\sqrt{\sum_{h=2}^{\infty} {I_h}^2}}{I_{L1}} \cdot 100\% \tag{1.29}$$

1.4.1.4 Telephone interference, TIF

The presence of harmonics in both voltage and current in circuitry associated with power conversion apparatus can produce electro-magnetic fields that will affect and disturb the performance of communication systems by virtue of their proximity and susceptibility. For a given physical arrangement, the disturbance is a function of both the amplitude and the frequency of the perturbation in the communication device. An easy calculation of TIF is presented in Eqn (1.30).

$$TIF = \frac{\sqrt{\sum_{h=2}^{\infty} (V_h W_h)^2}}{V_{eff}} \cdot 100\% \tag{1.30}$$

where W_h is the single frequency TIF weighting at frequency h.

1.5 Power Definitions

The electrical power definitions have longtime been subject of discussions. Regarding the fact that classical definitions; active, reactive and apparent power, are emphasized mainly under normal conditions. During the presence of harmonics and unbalance conditions these definitions in their initial form have some ambiguities. Consequently, various power definitions and calculation methods have been proposed in both the frequency domain and the time domain to cover as much as possible all aspect that power could represent. The main definitions in frequency domain and time domain are summarized in this section.

1.5.1 Budeanu's General Power Definitions

The commonly used definition of power established by Budeanu for a frequency domain analysis can be applied for a steady state analysis (Javadi, 2009). That means for a steady state study voltages and currents could be decomposed in Fourier series to calculate harmonics and each parameter of the system like powers and power factors. It should be noticed that since the method use frequency domain it cannot be instantaneous in the time domain. Budeanu globally defines four types of power for the single-phase system as follows (Emanuel, 2004).

Apparent power S:

$$S = V \cdot I = \sqrt{\sum_{h=1}^{\infty} V_h^2} \times \sqrt{\sum_{h=1}^{\infty} I_h^2} \qquad h = 1\ (fundametal), 2,3, \cdots, n \tag{1.31}$$

where phasors V and I are the voltage and current rms value respectively. The Active power P, which contribute to the work or heating supplied by the electrical source:

$$P = \frac{1}{T}\int_0^T v_{(t)}.\, i_{(t)}.\, d_t = \sum_{h=1}^{\infty} P_h = \sum_{h=1}^{\infty} V_h I_h \cos\varphi_h \tag{1.32}$$

Reactive power Q:

$$Q = \sum_{h=1}^{\infty} Q_h = \sum_{h=1}^{\infty} V_h I_h \sin\varphi_h \tag{1.33}$$

Distortion power D:

$$D = \sqrt{S^2 - P^2 - Q^2} \tag{1.34}$$

For the three-phase (3P4W) unbalanced system, the definitions are derived as follows in the frequency domain, using the Fourier series and the Sequence Transformation, voltages and currents are decomposed in their rms values. Thus, the active power (W) became:

$$\begin{aligned} P_{3\varphi} = \sum V_h I_h \cos(\theta_h) &= P_d + P_i + P_0 \\ &= V_{1d} I_{1d} \cos(\theta_{1d}) + V_{2d} I_{2d} \cos(\theta_{2d}) + \cdots \\ &+ V_{1i} I_{1i} \cos(\theta_{1i}) + V_{2i} I_{2i} \cos(\theta_{2i}) + \cdots \\ &+ V_{10} I_{10} \cos(\theta_{10}) + V_{20} I_{20} \cos(\theta_{20}) + \cdots \end{aligned} \tag{1.35}$$

where *d,i,0* are suffix for the direct, inverse, and the zero-sequence components. The reactive power is respectively defined as follow.

$$\begin{aligned} Q_{3\varphi} = \sum V_h I_h \sin(\theta_h) &= Q_d + Q_i + Q_0 \\ &= V_{1d} I_{1d} \sin(\theta_{1d}) + V_{2d} I_{2d} \sin(\theta_{2d}) + \cdots \\ &+ V_{1i} I_{1i} \sin(\theta_{1i}) + V_{2i} I_{2i} \sin(\theta_{2i}) + \cdots \\ &+ V_{10} I_{10} \sin(\theta_{10}) + V_{20} I_{20} \sin(\theta_{20}) + \cdots \end{aligned} \tag{1.36}$$

It is possible to define two different apparent powers; the arithmetic and the vectors one. The Arithmetic apparent power $S_{3\varphi}$, the sum of magnitude of apparent power of each separate phase, is an extension of the Budeanu's apparent power for single-phase systems is almost implemented in all commercial Power Analyzers.

$$S_a = \sqrt{P_a^2 + Q_a^2 + D_a^2}\ ,\quad S_b = \sqrt{P_b^2 + Q_b^2 + D_b^2}\ ,\quad S_c = \sqrt{P_c^2 + Q_c^2 + D_c^2} \tag{1.37}$$

The following arithmetic apparent power is obtained:

$$S_{3\varphi} = S_a + S_b + S_c \tag{1.38}$$

The power factor is then defined as follow.

$$PF = \frac{P}{S_{3\varphi}} \tag{1.39}$$

Consequently the Distortion power (var), is calculated.

$$D_{3\varphi} = \sqrt{{S_{3\varphi}}^2 - {P_{3\varphi}}^2 - {Q_{3\varphi}}^2} \tag{1.40}$$

1.5.2 Instantaneous Powers

The previous definitions in the frequency domain using phasors are useful for off-line studies and statistical investigations. Meanwhile for a practical and real-time application, time-domain definitions are required. The instantaneous power is defined in the time-domain to emphasis the necessity of power calculation based on direct measurements. This power differs from the general active power in frequency domain which is an average of the instantaneous power in a cycle of fundamental period.

This time domain approach was proposed by Akagi (Akagi, Tsukamoto et Nabae, 1990) under the name “p-q theory” or “instantaneous power theory”. This widely spread theory for three-phase shunt active filters is among attractive approaches for an instantaneous variable compensator. Akagi proposes a different approach based on the instantaneous calculations for the shunt active filter in three-phase systems (Akagi et Isozaki, 2012a). The *p-q theory* is well adapted for shunt active filters and performs an instantaneous compensation with a better transient response compared to other control algorithms. This control approach uses the Clarke’s transformation to link voltages and currents from the three-phase ‘*abc*’ to a two-phase orthogonal system ‘*αβ0*’. Many definitions of active and reactive power in distorted and even unbalanced systems have been proposed, a summary of which can be found in (Akagi, Watanabe et Aredes, 2007).

The instantaneous power in three-phase system, with 3 or 4 wires the instantaneous voltages and currents are shown as an instantaneous space vector $\boldsymbol{v}$ and $\boldsymbol{i}$.

$$v = \begin{bmatrix} v_{an} \\ v_{bn} \\ v_{cn} \end{bmatrix} \quad , \quad i = \begin{bmatrix} i_a \\ i_b \\ i_c \end{bmatrix} \tag{1.41}$$

Where v_{kn} is the phase to ground voltage and i_k is the phase current. The instantaneous active power is obtained by the dote product of voltage and current.

$$p = \vec{v} \cdot \vec{i} = v_{an} i_a + v_{bn} i_b + v_{cn} i_c \tag{1.42}$$

For a balanced three wire system where $i_a + i_b + i_c = 0$, it is possible to take one of the voltages as reference, and obtain the following relations in which v_{ab}, v_{bc}, and v_{ca} are the instantaneous line-to-line voltages.

$$p = v_{ab} i_a + v_{cb} i_c = v_{ac} i_a + v_{bc} i_b = v_{ba} i_b + v_{ca} i_c \tag{1.43}$$

It should be noted that the total Active power is the mean of the instantaneous power in one cycle. This active power is equal to the general power from the Budeanu's approach.

$$P = \frac{1}{kT}\int_{\tau}^{\tau+kT} v_i i_i dt \qquad i = a, b, c \tag{1.44}$$

The *p-q theory* uses the Clark transformation to transform voltages and currents from three phases '*abc*' to related vectors in *αβ0* coordinates, where instantaneous active and reactive powers are derived.

$$i_{\alpha\beta 0} = \begin{bmatrix} i_\alpha \\ i_\beta \\ i_0 \end{bmatrix} = \underbrace{\sqrt{\frac{2}{3}} \begin{bmatrix} 1 & -1/2 & -1/2 \\ 0 & \sqrt{3}/2 & -\sqrt{3}/2 \\ 1/\sqrt{2} & 1/\sqrt{2} & 1/\sqrt{2} \end{bmatrix}}_{C} \times \begin{bmatrix} i_a \\ i_b \\ i_c \end{bmatrix} \tag{1.45}$$

And

$$v_{\alpha\beta 0} = \begin{bmatrix} v_\alpha \\ v_\beta \\ v_0 \end{bmatrix} = C \times \begin{bmatrix} v_{an} \\ v_{bn} \\ v_{cn} \end{bmatrix} \tag{1.46}$$

where *C* is the Clark's matrix. Instantaneous powers are then defined as in Eqn (1.47).

$$\begin{bmatrix} p \\ q \\ p_0 \end{bmatrix} = \underbrace{\begin{bmatrix} i_\alpha & i_\beta & 0 \\ -i_\beta & i_\alpha & 0 \\ 0 & 0 & i_0 \end{bmatrix}}_{B} \begin{bmatrix} v_\alpha \\ v_\beta \\ v_0 \end{bmatrix} \tag{1.47}$$

The total instantaneous active power supplied by the source can be redrafted in the *αβ0* coordinates by means of the Eqn. 1.47 as follow.

$$p_{3\varphi} = \vec{v} \cdot \vec{i} = v_{an} i_a + v_{bn} i_b + v_{cn} i_c = v_\alpha i_\alpha + v_\beta i_\beta + v_0 i_0 = p + p_0 \tag{1.48}$$

Instantaneous three-phase power is in fact the sum of real power p and the zero-sequence power p_0. In the case of a three-phase three-wire (3P3W) system, p_0 does not exist and $p_{3\varphi}$ became equal to p. The power $p_{3\varphi}$ is a function of voltage and current in an interval of time $p_{3\varphi}(v,i)$. With reference to the $\alpha\beta 0$-coordinates, currents can be obtained from the power expressions (p, q). Then, these currents can be decomposed into active and reactive components. And then used for compensations in the shunt active filter. Instead, for the series active filter similar to the shunt-AF, it is possible by duality to apply the same principle to calculate the compensating voltage references of the Series-AF.

$$v_{Comp} = \begin{bmatrix} v_{Comp\_a} \\ v_{Comp\_b} \\ v_{Comp\_c} \end{bmatrix} = \begin{bmatrix} v_{Sa} \\ v_{Sb} \\ v_{Sc} \end{bmatrix} - \begin{bmatrix} v_{La} \\ v_{Lb} \\ v_{Lc} \end{bmatrix} \tag{1.49}$$

The suffix S and L refer to the source and load side, and the suffix $Comp$ refer to the compensation voltage.

$$\begin{bmatrix} v_\alpha \\ v_\beta \end{bmatrix} = \frac{1}{{i_\alpha}^2 + {i_\beta}^2} \begin{bmatrix} i_\alpha & -i_\beta \\ i_\beta & i_\alpha \end{bmatrix} \begin{bmatrix} p \\ q \end{bmatrix} \tag{1.50}$$

These orthogonal voltages (v_α and v_β) can be split into their active (v_p) and reactive (v_q) parts.

$$\begin{bmatrix} v_\alpha \\ v_\beta \end{bmatrix} \triangleq \overbrace{\begin{bmatrix} v_{\alpha p} \\ v_{\beta p} \end{bmatrix}}^{v_p} + \overbrace{\begin{bmatrix} v_{\alpha q} \\ v_{\beta q} \end{bmatrix}}^{v_q} = \tag{1.51}$$

$$= \frac{1}{{i_\alpha}^2 + {i_\beta}^2} \begin{bmatrix} i_\alpha & -i_\beta \\ i_\beta & i_\alpha \end{bmatrix} \begin{bmatrix} p \\ 0 \end{bmatrix} + \frac{1}{{i_\alpha}^2 + {i_\beta}^2} \begin{bmatrix} i_\alpha & -i_\beta \\ i_\beta & i_\alpha \end{bmatrix} \begin{bmatrix} 0 \\ q \end{bmatrix}$$

The previous equation lead to the instantaneous active voltages ($v_{\alpha p}$, $v_{\beta p}$) and instantaneous reactive voltages ($v_{\alpha q}$,$v_{\beta q}$). Due to the presence of both zero-sequence currents and voltages for the case of a three-phase four wires system, p_0 must also be considered (Javadi et Al-Haddad, 2011). In some cases, it is proposed not to compensate the zero-sequence power, based on the need for a storage element for compensating p_0.

$$B^{-1} = \begin{bmatrix} \frac{i_\alpha}{{i_\alpha}^2 + {i_\beta}^2} & \frac{-i_\beta}{{i_\alpha}^2 + {i_\beta}^2} & 0 \\ \frac{i_\beta}{{i_\alpha}^2 + {i_\beta}^2} & \frac{i_\alpha}{{i_\alpha}^2 + {i_\beta}^2} & 0 \\ 0 & 0 & \frac{1}{i_0} \end{bmatrix} \tag{1.52}$$

$$= \frac{1}{{i_0}^2({i_\alpha}^2 + {i_\beta}^2)} \begin{bmatrix} {i_0}^2 i_\alpha & -{i_0}^2 i_\beta & 0 \\ {i_0}^2 i_\beta & {i_0}^2 i_\alpha & 0 \\ 0 & 0 & i_0({i_\alpha}^2 + {i_\beta}^2) \end{bmatrix}$$

The instantaneous active component of the voltage in quadrature space is obtained.

$$v_p(\alpha\beta 0) = B^{-1} \times \begin{bmatrix} p \\ 0 \\ p_0 \end{bmatrix} \rightarrow \ v_p = C^{-1} \times v_p(\alpha\beta 0) \tag{1.53}$$

The reactive portion of the voltage is obtained using the instantaneous reactive power q.

$$v_q(\alpha\beta 0) = B^{-1} \times \begin{bmatrix} 0 \\ q \\ 0 \end{bmatrix} \rightarrow v_q \ = C^{-1} \times v_q(\alpha\beta 0) \tag{1.54}$$

Both active and reactive powers can be divided into a constant amplitude component and an oscillating component: $p = \bar{p} + \tilde{p}$ and $q = \bar{q} + \tilde{q}$. It is then possible to split voltages into ac and dc values. By compensating the reactive portion of the voltage, the load's voltage and current will became in phase and a unity power factor ($\cos\theta \cong 1$) will be achieved, there would not be any phase shifting between the voltage and current.

$$if \ \ v_q = 0 \ \ \xrightarrow{yields} \ \ v = v_p \ \ \rightarrow \ \ S = P \ \ \rightarrow \ \ \lambda \ or \ PF = 1 \tag{1.55}$$

To have a physical representation of instantaneous powers the illustrates the total instantaneous energy flow per time unit (p) from the source to the load, and the energy

exchanged between the phases without transferring energy to the load (q) are presented. The unit value of the instantaneous reactive q is "vai" or volt-ampere imaginary. Thus it is proposed to use this time-domain approach for calculation of powers in a real-time application, where the average of instantaneous p and q represent the conventional powers.

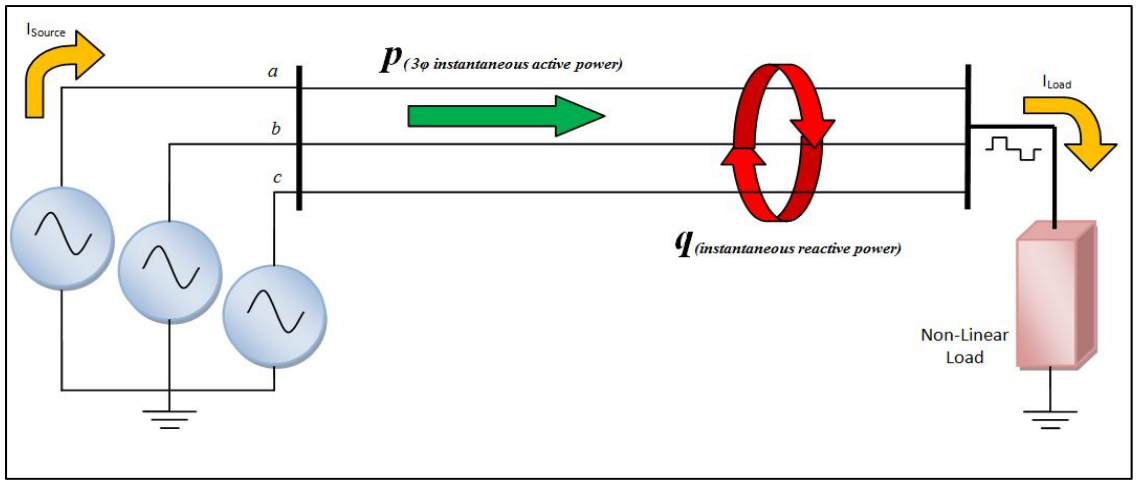

Figure 1.14 Schematic representation of instantaneous power flow in a three-phase system.

1.6 Modulation Techniques

Modulation in electronics and telecommunications is the process of varying properties of a periodic signal with a modulating signal. In telecommunication, the aim of pulse modulation methods is to transfer a narrowband analog signal over a wideband channel or as a bit stream over another digital transmission line. For digital systems, the analog signal is modulated by a discrete signal. In power electronics, the analog signal is modulated in order to produce a digital signal which is then applied to semiconductors switches. There exist multiple modulation techniques to achieve desired objectives depending on the configuration constraints. Hereafter, three main techniques are discussed and reviewed for a real-time practical implementation.

1.6.1 Pulse Width Modulation (PWM)

The pulse width modulation technique is used to encode a continuous waveform into a pulsing signal. Even if, this type of modulation seems attractive for encoding telecommunication information for transmission, its main use is in power electronic drives. In this technique the average value of the output signal is controlled by switching converters semiconductors On and Off. In the PWM modulation a reference signal is compared to a fixed frequency carrier waveform as shown in Figure 1.15. The fixed PWM switching frequency has to be higher (at least 10 times higher) than the dynamics of the output voltage or current reference. To make the resultant waveform to be as smooth as possible the switching has to be done several times a second up to tens of kilohertz (kHz) and well into the hundreds of kHz in audio amplifiers and power supplies.

The duty cycle describes the proportion of the time the switch is ON, over the period interval of time. A key advantage of the PWM is a low power loss in the switching devices. The reference signal or the "Duty Cycle" (dark red in Figure 1.15) is compared with a triangle waveform (black). When the latter is less than the former, the PWM signal (magenta) is in Low (0) state where S_1 is "Off" and S_2 is "On". Otherwise it is in the high state (1) where S_1 is "On" and S_2 is "Off". This sequence could be any other combination of switches depending on the desired PWM state.

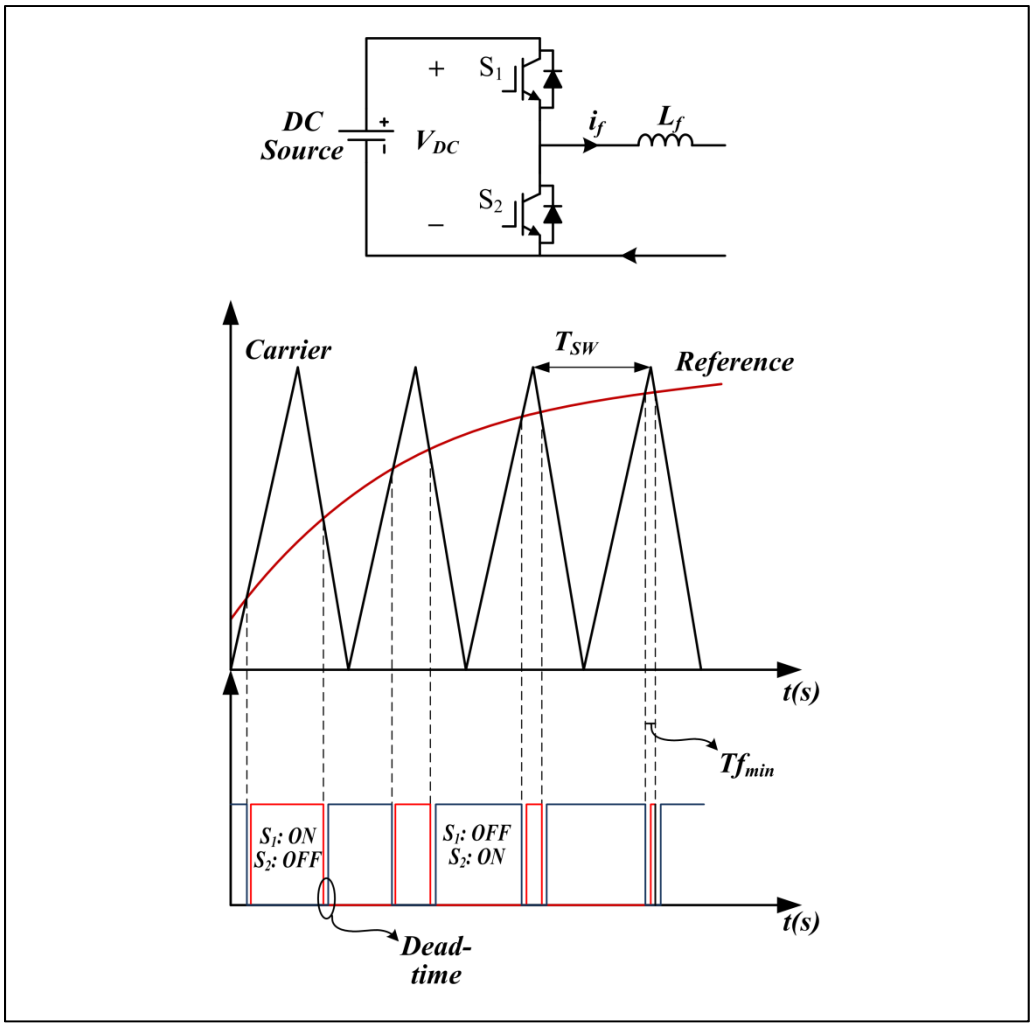

Figure 1.15 A simple Pulse-width modulation method to generate the Gate signals

It should be noted that, there exists some key constraint to respect for a reliable experimental implementation. Based on the pre-defined sampling-time step for the Controller (T_S), it is possible to tune the switching frequency (F_{SW}) and the dead-time (ds) of the PWM according to the following constraints.

1. At first the lowest value that could be chosen for delay between the changing states of the PWM commonly known as “dead-time”, is equal to the discrete Time-step “Ts”.

$$\textit{Dead-time}\ (\text{ds}) \geq T_S$$

2. To have a marginally low accuracy for the PWM, the triangle waveform should have at least more than four sampling points. Consequently, the highest switching frequency for the PWM became, supposing no constraint from the semiconductor hardware, as follow:

$$F_{SW}(Hz) = \frac{1}{T_{SW}\ (s)} \qquad \leq \qquad \frac{1}{4T_S} \tag{1.56}$$

3. Consequently, the minimum time in which a state could be kept unchanged (Tf_{min}) will be greater than T_S. This is called the Precision of the PWM generator.

4. The last limitation that should be kept in mind is the fact that the frequency of the reference signal or the Duty-cycle signal should be less than four times the carrier frequency.

$$F_{ref}(Hz) = \frac{1}{T_{modulation}\ (s)} \qquad \leq \qquad F_{SW}(Hz) = \frac{1}{4T_{SW}} \tag{1.57}$$

If a DSP or a digital controller with a sampling time of T_S=40µs is used to implement the PWM generator, the highest switching frequency that could be reached will be 6.250 kHz as shown in Figure 1.16. Therefore, it can be deduced that the frequency of the reference modulated signal (duty-cycle) as the input of the PWM should be less than 1.56 kHz equal to the 26th harmonic order. Even though, this will result in a marginal stable operation point in which the experimental results will not have enough precision for an accurate study. When such low resolution frequencies are chosen, the Aliasing phenomenon has a colossal influence on the obtained results.

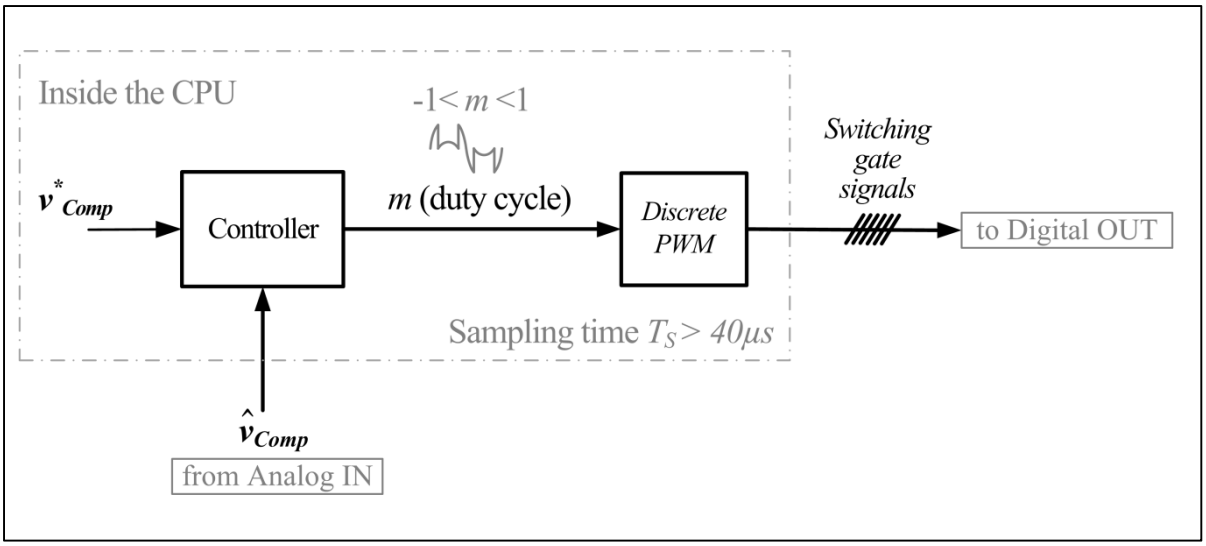

Figure 1.16 Real-time implementation block diagram of a PWM generated in the CPU

In a common laboratory implementation, if the dSPACE controller or the Opal-RT real-time simulators are used for the Rapid control prototyping (RCP) application, it has been tested that in the best case the sampling period could not go beyond 30 to 40 micro-seconds for a simple closed loop HIL application. Consequently If the PWM is generated inside the main CPU unit, it results in a low profile performance for active filtering or any other application requiring fast switching ability. An alternative solution adopted is to implement the PWM generator outside the main CPU unit on an FPGA as represented in Figure 1.17. This technique already available on dSPACE and Opal-RT module allow reaching switching frequency up to 5 MHz, thanks to the FPGA fast sampling time of Nano-seconds. In an RCP application this external PWM will operate independent of the CPU time-steps.

As a useful hint, under tested laboratory experiments, the lowest step size (sampling time) that the dSPACE module dsp1103 could reach in a closed loop with Analog inputs and digital outputs, is 40-µs. The less powerful module, the dsp1104, could reach 50-µs with reduced number of Analog inputs. Finally, the Opal-RT WANDA modules could reach 30-µs in a closed loop implicating their Analog-In and Digital-OUT mezzanines.

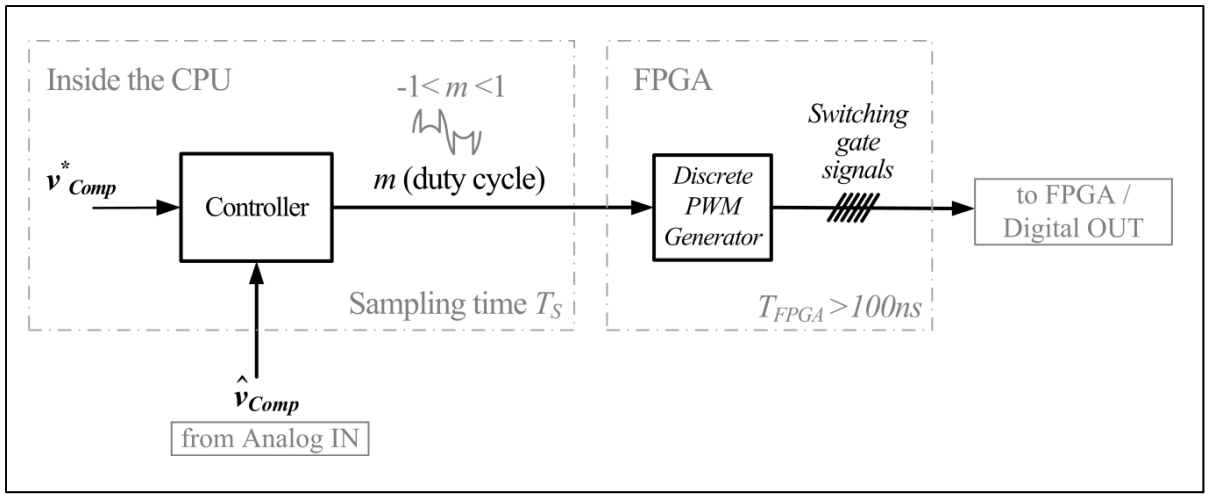

Figure 1.17 Real-time implementation schematic of the PWM generated by the FPGA

1.6.2 Space Vector Modulation (SVM)

In the field of power electronics, space vector modulation is of paramount importance for a detailed understanding of three-phase modulation techniques. This modulation technique apply the PWM control algorithm for multi-phase systems, in which after each sampled reference signal, the non-zero active switching vectors adjacent to the reference vector and one of zero switching sectors are selected for the appropriate fraction of the time period in order to synthesize the reference signal as the average of a combination of vectors.

The harmonics pollution drawn by converters in the system has always been a concern for pulse-width modulation techniques. The space vector modulation (SVM) tries to reduce feasibly the distortions in the output waveforms of an inverter while maintaining the performance of the PWM. The optimization of modulation's behavior has made this technique to be among the most popular techniques in minimizing the commutations and consecutively losses in the inverter. The SVM over comes the drawbacks of other modulation algorithms and increase the overall system efficiency. It gives the ability to have a higher modulation index (m) and an optimized commutation, as a result a reduction in the switching frequency, compared to conventional modulators is observed. Some authors proposed the vector modulation for inverters based on IGBTs (Rodriguez et al., 1994). They present a

design of a three-phase inverter using the space vector modulation to generate the switch control signals. Vander Broeck and K. Zhou analyze greatly contributed in the development of the SVM technique and compared it with carrier-based PWMs (Keliang et Danwei, 2002; Van der Broeck, Skudelny et Stanke, 1988). A digital implementation was presented in (Mehrizi-Sani et Filizadeh, 2009), while the transient behavior of a practical application of the SVM is analyzed. A survey on the Pulse width modulation written by Joachim Holtz (Holtz, 1992), review the SVM and other feed-forward schemes compared with feedback PWM controllers. Chen has simplified the space vector modulated scheme for a three-phase switch mode rectifier in (Chern-Lin et al., 1999). Some intuitive were made to simplify the comprehension of space vector modulation. The control in power electronics (Kazmierkowski, Krishnan et Blaabjerg, 2002) gives some advanced approaches of the space vector modulation and the behavior of SVM during over-modulation.

In this technique the objective is to produce a three-phase sinusoidal waveform from a reference voltage (*Vs*) without using a fixed frequency carrier waveform inside the model. While other pulse-width modulations require a carrier time basis, the space vector modulation is free of any time basis. Thus, the reference signal could be the positive sequence of a three-phase system or the resultant vector in the d-q orthogonal system. Essential information deduced from this vector is the magnitude of the vector and the phase rotational angle of the vector instantaneously in the time domain as shown in Figure 1.18, by which the SVM will produce the pulse control signals. Any three-phase system's instantaneous values (e.g. [112, -20, -92]) can be represented uniquely by a rotating vector V_S (e.g. V_S= 112-j41= 119∟-20°).

$$\vec{V}_S = \frac{2}{3}\left(v_a + \delta v_b + \delta^2 v_c\right) = 2V_{Positive\ Seq.} \qquad \left(\delta = e^{j\left(\frac{2\pi}{3}\right)}\right) \tag{1.58}$$

Using the transform "$\alpha\beta\gamma$" described in Eqn 1.60, for a balanced system, the vector V_S can be defined in the complex plane by the following quadrature components.

$$\vec{V}_S = \vec{v}_\alpha + j\vec{v}_\beta = \hat{V}\angle\varphi = \hat{V}\angle(\omega t + \theta) \tag{1.59}$$

Where

$$\begin{bmatrix} v_\alpha \\ v_\beta \end{bmatrix} = \frac{2}{3}\begin{bmatrix} 1 & -1/2 & -1/2 \\ 0 & \sqrt{3}/2 & -\sqrt{3}/2 \end{bmatrix} \times \begin{bmatrix} v_a \\ v_b \\ v_c \end{bmatrix} \tag{1.60}$$

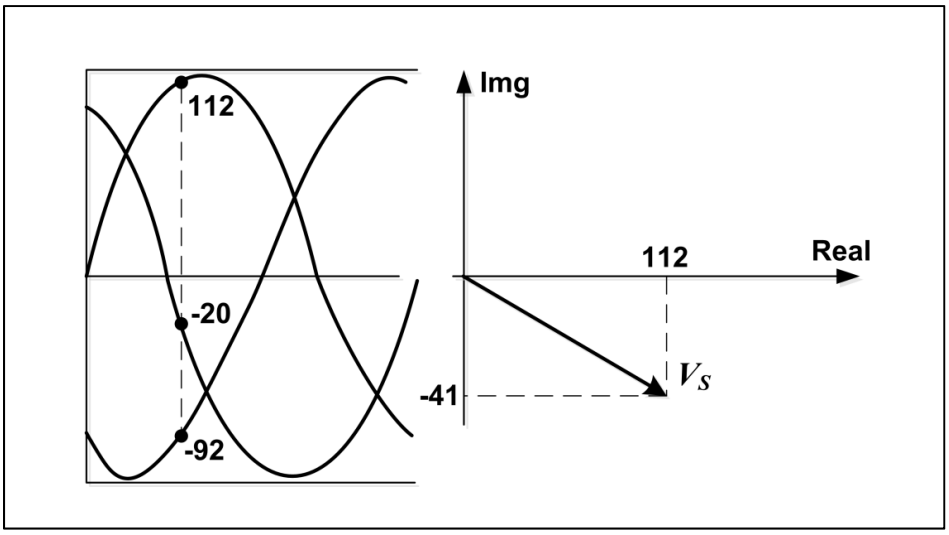

Figure 1.18 Voltage vector representation of a set of three instantaneous phase voltages in the complex plane

As a case study for a two level converter, the output voltage has six state leads to six switching vector in the complex plane $V_1, V_2, ..., V_6$ as shown in Figure 1.20. The magnitude of these six vectors in this case is equal to $2V_{dc}/3$.

$$\overrightarrow{V_1} = \frac{2}{3}\left(\frac{2Vdc}{3} + \frac{-Vdc}{3}e^{+120} + \frac{-Vdc}{3}e^{-120}\right) = \frac{2}{3}Vdc\ \angle 0° \tag{1.61}$$

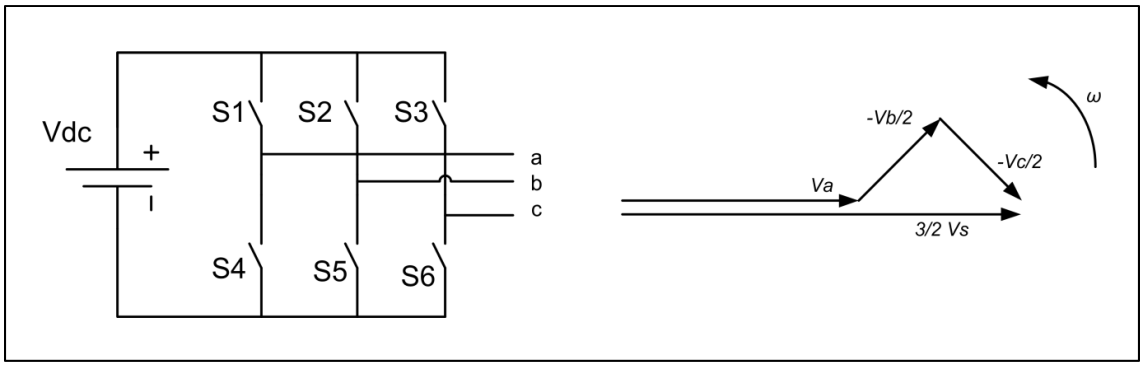

Figure 1.19 Three-phase inverter topology and
the resultant space vectors representation

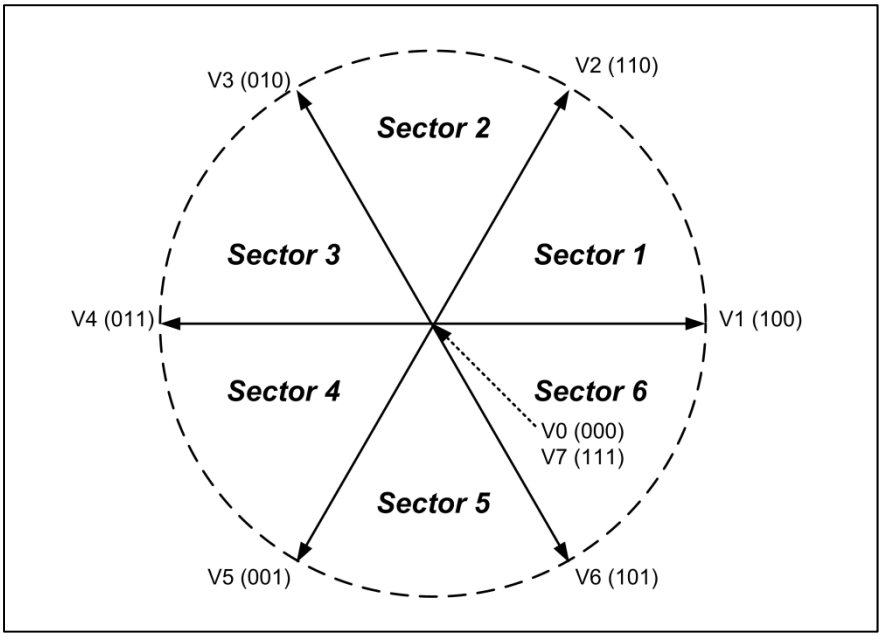

Figure 1.20 Space vectors for a three-phase two level inverter
involving eight switching states

The vector V_S could be decomposed in infinite ways into these eight vectors. But typically it is decomposed with a zero vector and two nonzero vectors framing the output voltage vector. Here, the vector V_S is decomposed in two adjacent vectors as shown in Figure 1.21.

$$V_y = \frac{2}{\sqrt{3}}\hat{V}\sin(\varphi) \tag{1.62}$$

The area between the inscribed circle and the hexagon defines the over-modulation in the SVM technique. The definition of the modulation index for carrier based PWM is defined as follow.

$$M = \frac{A_r}{A_C} \tag{1.63}$$

Where A_r is the magnitude of reference signal and A_C is the magnitude of the carrier. Consequently for the configuration described earlier, the modulation index became:

$$m = \frac{\hat{V}_S}{V_{dc}} \tag{1.64}$$

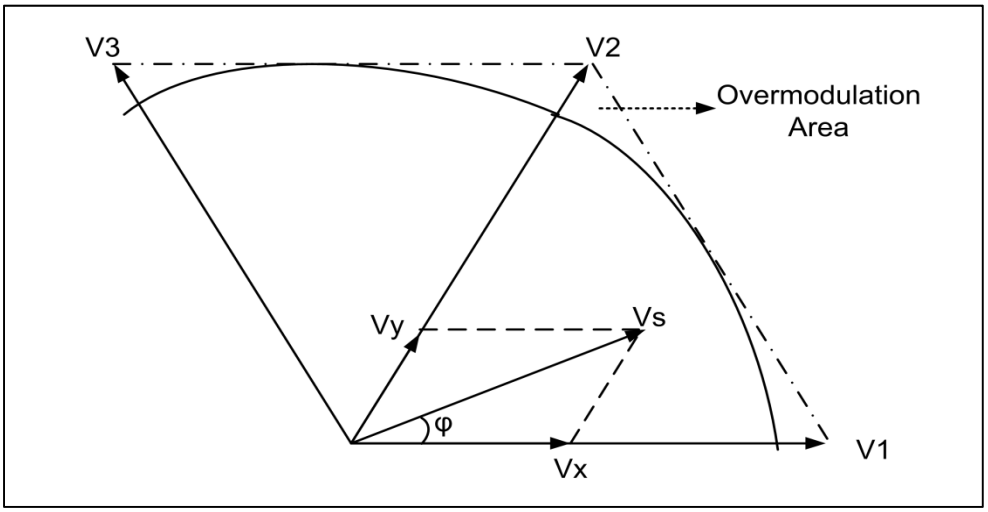

Figure 1.21 Voltage space vector decomposition, space vector hexagon with modulation areas

By means of the modulation index, the limitations for linear and the over modulation area could be depicted. During the linear operation, the modulation is calculated as follow.

$$\hat{V}_{max} = \frac{V_{dc}}{\sqrt{3}} \quad \Longrightarrow \quad m = \frac{1}{\sqrt{3}} = 0.577 \quad or \quad M = \frac{\pi}{2\sqrt{3}} = 0.907 \tag{1.65}$$

where V_{max} is the radius of the inscribed circle in the hexagon. The over modulation is defined regarding following equations.

$$\hat{V}_{max} < \hat{V}_s < V_1 \tag{1.66}$$

If the vector V_S is equal to one of the reference vectors like V_1, the modulation index became:

$$m = \frac{{}^{2}/_{3}\, V_{dc}}{V_{dc}} = \frac{2}{3} = 0.66 \qquad or \qquad M = {}^{\pi}/_{3} = 1.04 \approx 1 \tag{1.67}$$

The vector V_S in a time interval T is constituted by a set of three vectors; V_x, V_y, and (V_0 or V_7). The time interval associated to each of these vectors could be defined regarding the modulation index and the total interval time T.

$$\vec{V}_S = \frac{t_{0,7}}{T}\vec{V}_{0,7} + \frac{t_1}{T}\vec{V}_1 + \frac{t_2}{T}\vec{V}_2 + \frac{t_3}{T}\vec{V}_3 + \frac{t_4}{T}\vec{V}_4 + \frac{t_5}{T}\vec{V}_5 + \frac{t_6}{T}\vec{V}_6 \tag{1.68}$$
$$T = t_{0,7} + t_1 + t_2 + t_3 + t_4 + t_5 + t_6$$

In Eqn. 1.68, only the two nearest vectors to the reference voltage V_S, are kept as defined previously. Consequently, the time allocated to vectors V_x and V_y in each sector could be calculated by means of following trigonometric relations.

$$\begin{cases} t_x = \sqrt{3}.m.T.\sin\left(\frac{\pi}{3} - \varphi\right) \\ t_y = \sqrt{3}.m.T.\sin(\varphi) \\ t_0 = T - \left(t_x + t_y\right) \end{cases} \tag{1.69}$$

With regards to the time periods calculated, the total interval T could be distributed using the pattern illustrated in Figure 1.22. Noted that V_x and V_y depend on the sector in which V_S is placed.

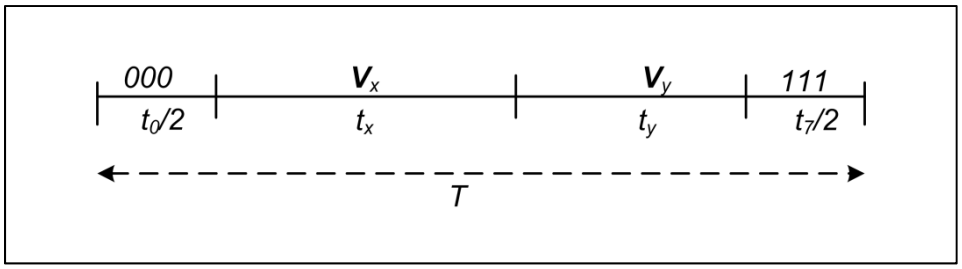

Figure 1.22 Typical Space vector modulation sequence

1.6.3 Hysteresis PWM

A widely inspired PWM technique is the hysteresis band (HB) control used mostly in offline simulations. Shown in the following figure, this method is basically an instantaneous feedback control method in which the actual measured signal, continuously tracks the command reference signal within a pre assigned hysteresis band. There exist advanced Hysteresis technique for specific applications (Malesani et Tenti, 1990).

Meanwhile, this technique has some ambiguity for industrial applications. In this technique the operator could control the hysteresis band-width which will results in the variation of the switching frequency. But, there is no direct control on the switching frequency itself. As a result, for digital and discrete applications it became less attractive as no control on the switching frequency is available.

The Hysteresis PWM produces the impulsions for a converter using the hysteresis band width as input for modulation. In a hysteresis current control method, the current is compared with the reference with a bandwidth tolerance and each time it reach this limit a control pulse signal is generated. As shown in Figure 1.23, half of the tolerance band is the distance that the backup current could diverge from the reference current waveform. The step size and the maximum frequency supported by the inverter are the factors that limit the tolerance band width. Some factors limit the decrease of the margin value in the hysteresis PWM; the maximum switching frequency of the hardware (power converter), the minimum step size supported by the real-time simulator, and the dynamics of the system output including

passive components. These three factors are such that they should be adjusted accordingly to each set of conditions creating a complex calculation for a practical implementation.

The decrease of the dynamic response of the physical system has the same impact as increasing the dc-side voltage. Decreasing the stiffness of the passive component response, within the suitable margins, improves the dynamic response of the active filter. At all-time the following condition should be satisfied.

The minimum time for the measured signal, related to the dynamism of the system, to increase within the hysteresis dead band should not be smaller than the time step value. Thus, to prevent the system to go out of control, the dynamic behavior of the measured signal should be a couple time greater than the discrete step size ($T_S \leq t_{min}$).

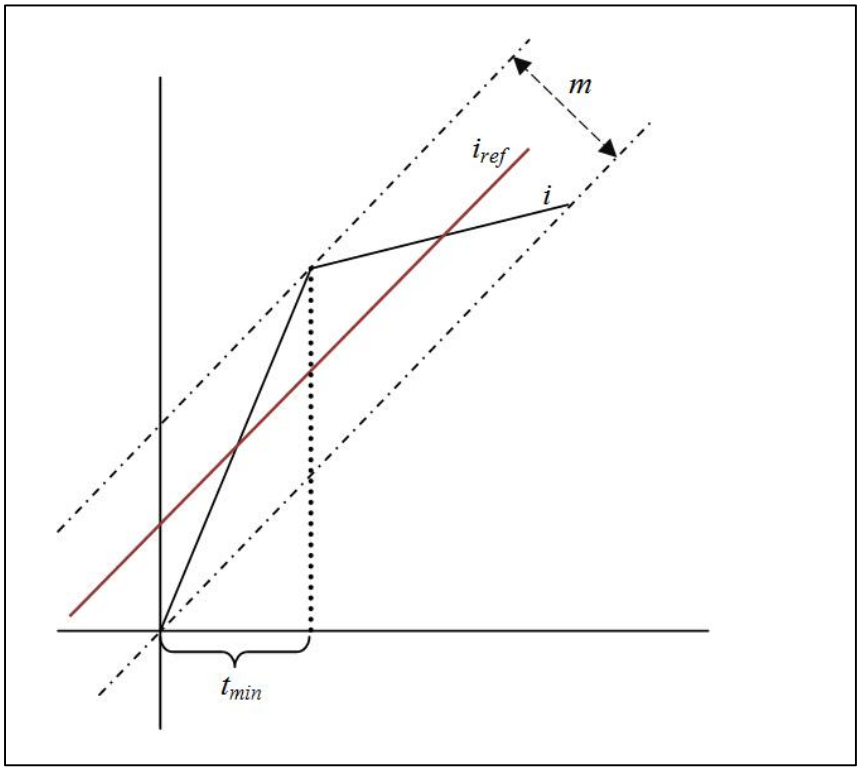

Figure 1.23 Hysteresis pulse-width modulation for a current controller

1.7 Conclusion

In this chapter, the essential basics to understand the Smart grids concepts, power quality related issues, and background of harmonic compensation have been highlighted. A state of the art on development of Smart Grids and application of Active power filtering to improve their overall power quality was presented. Later in this chapter various type of nonlinear loads leading to drop the power quality were analyzed and the effect of applying traditional passive components on the harmonic compensation had been presented. To overcome passive filtering deficiencies active filtering seems the preeminent solution. Consequently this research work is apprehending this path to improve power quality by means of active power filters. A brief review of active filtering and the state of the art in active compensation was presented followed by prompting mathematical development of power quality indices and harmonic component decomposition method. The chapter presented an extend study on power definitions for multiple types of applications. Finally, due to the importance of semiconductor's switching phenomenon, some practical pulse modulation were stated and evaluated for practical implementations. In conclusion this chapter aimed to give required background to the reader to facilitate the read and comprehension of this thesis work.

CHAPTER 2

SERIES ACTIVE COMPENSATION FUNDAMENTALS

2.1 Introduction

This chapter is dedicated to the feasibility of a series active compensator in a realistic distribution network. Nowadays, the harmonic pollution not only affects equipment in the polluting plant but may also disturb equipment in other plants, a reason for operators to impose limits for disturbances by setting standards for maximum allowable distortions. Two approaches are available to the mitigation of power quality problems. The load conditioning, this method ensures that the equipment is less sensitive to power disturbances and allow the operation under significant voltage distortion. The other solution is to install line conditioning systems that suppress or counteract the power system disturbances (Rudnick, Dixon et Moran, 2003).

The development of active power compensators and power conditioners lead to eminent solutions to improve power quality. Among these emerging solutions, the Series Active Filter, which is relatively less comprehended and developed compared with the shunt configuration. This chapter presents a comprehensive review of the Series compensator; configurations, control strategies, and related involvements in this field. It provides a perspective of Series active hybrid compensator's technology to researchers dealing with power quality issues. The study is completed with simulation results where effects of passive components employed in the series compensator capability to compensate for harmonics are evaluated. Furthermore, in this chapter a new control approach is proposed and analyzed to improve series harmonic compensation accurately. To conclude, complementary study on the stability of the system is presented along with experimental results.

2.2 Series Compensation Concepts

The concept of a series active compensation was introduced by the end of the 1980s to operate as a voltage regulator for sensitive loads (Gyugyi, 1979). The series-connected filter protects the consumer from an inadequate supply-voltage quality. They are supposed to guarantee a sinusoidal balanced voltage on the load's side despite the presence of perturbations in the source voltage such as unbalance, harmonic distortion, sags and swells, as well as disturbances in the current load such as step changes, unbalance and distortion by harmonics. Later, it was found that it has the capability of isolating current harmonics of a voltage fed type of nonlinear load (VSC) from the power system. In most cases, the series active power filters as a controllable voltage source, must operate in conjunction with the shunt passive filters in order to compensate load current harmonics. If passive LC filters are connected in parallel, the series active power filter operates as a harmonic isolator, forcing the load current harmonics to circulate mainly through the passive filter rather than the power system.

As previously explained this approach is recommended for compensation of voltage unbalances and voltage sags and swells from the ac supply and for low-power applications and represents an economically attractive alternative to UPS, since no energy storage on the DC bus is required the overall rating of the components became fairly smaller. Since, the high efficiency of active compensators promotes their industrial application for Smart grids, they could contribute to simplify facilitate higher penetration of renewable fluctuating power into the grid (Singh, Al-Haddad et Chandra, 1999). The development of low-cost power electronics made active filters more attractive than before. Active filters as affordable solution will be indispensable to improve the power quality of future grids with as smart and adaptive devices. Shunt active filters (SAF) are currently applied at a distribution level in conditions where passive filters failed to operate safely and accurately.

To overcome both current and voltage issues an overall expensive solution is the Unified Power Quality Conditioner (UPQC) (Brenna, Faranda et Tironi, 2009; Han et al., 2006;

Khadkikar et Chandra, 2008). To enhance the power quality, it combines a shunt and a series active filter to regulate current and voltage issues simultaneously. The shunt active part compensates current harmonics and corrects the power factor of a non-linear load, while the series active part eliminates voltage distortions and regulates the three-phase voltage at the PCC (Khadkikar et Chandra, 2009; 2011). This is a tremendous and reliable solution to improve power quality (Basu, Das et Dubey, 2008). There exist different topologies for the UPQC; i.e. the shunt active filter connected in the left or right side of the series active part (Kesler et Ozdemir, 2011). However, regarding the complexity of components it became an unaffordable solution (Mohammadi, Varjani et Mokhtari, 2009). The main disadvantage of this configuration is the non-isolation of the DC bus bar and the three-phase power system. Thus, hereafter the series-AF with/without passive filter is emphasized and different configuration and topologies are discussed.

2.3 System Configurations and State of The Art

Even if series active compensators are not industrially incorporated in power systems, they remain among potential active compensators able to enhance the electric power quality of Smart grids. The complexity of series compensators make engineers hesitating on their application. So far, it is considered as the last alternative to power quality issues. However, Series compensators could be the preeminent choice if well matured. Depending on their application, Series compensators are classified into two categories; Series active filter (SeAF) and Dynamic voltage restorer (DVR). The dynamic voltage restorer and the series active filter are both complex, and are coupled to the grid using an isolation transformer. This provides good isolation of the compensating system, but the transformer, in addition to being quite expensive, introduces a number of detrimental performance issues, such as electrical losses, hysteresis phenomena, and the need to be short-circuited if there is a fault in secondary. Transformerless DVR technology has been proposed, but these devices are still in a development stage, and are currently only able to compensate for voltage issues at the PCC, and are not capable of addressing current perturbations in the power grid.

2.3.1 Dynamic Voltage Restorer (DVR) Operation

To mitigate voltage related issues initiated by the utility, the load conditioning which ensures that the equipment is less sensitive to power disturbances and allow the operation under significant voltage distortion, is one solution. The other solution is to install a line conditioning system known as DVR or dynamic voltage restorer, to suppress or counteract the power system disturbances actively (Choi, Li et Vilathgamuwa, 2000; Nielsen et Blaabjerg, 2005; Yun Wei et al., 2007a; Yun Wei et al., 2007c). This application of a series compensator is a key solution for a reliable PCC where sensitive loads are installed (Abdel-Rahman et al., 2008; Bingsen et Venkataramanan, 2009; Vilathgamuwa, Wijekoon et Choi, 2006). A common configuration for a DVR installed on a single-phase distribution system is illustrated in Figure 2.1. It is obvious that the topology is similar to a Series-AF excepting the passive filter and that the control strategy employed to drive the converter relies on a voltage detection algorithm (Chi-Seng, Man-Chung et Ying-Duo, 2008; Jing et al., 2010). There exists improvement done on DVR using multilevel or cascaded techniques (Al-Hadidi, Gole et Jacobson, 2008; Babaei, Kangarlu et Sabahi, 2010; Massoud et al., 2010; Roncero-Sanchez et Acha, 2009; Shangyang et al., 2009).

2.3.1.1 Simulation Results

The installed DVR is to compensate for voltage issues such as distortions, sags, and swells. In the following Simulation, A single-phase DVR is applied for load with a weak utility supply. The utility is subjected to various critical power quality issues while the DVR compensating them, delivers a clean and stable supply to the load’s feeder.

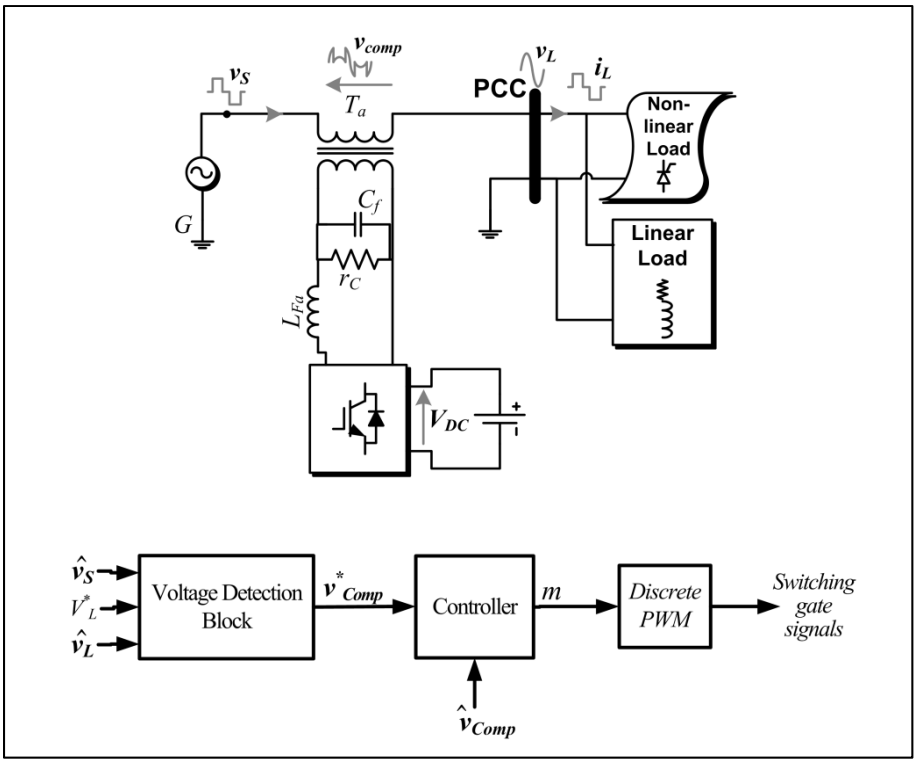

Figure 2.1 A Single-phase Dynamic voltage restorer (DVR) in series with combination of loads, the DVR control structure

The system simulated consisted of a linear and a nonlinear load is subjected to utility voltage distortions, sag and swell. The control algorithm illustrated that by detecting load voltage and extracting compensating components, the DVR is able to protect loads from perturbation initiated by the grid.

The Table 2.1 describe system's parameters. The source voltage is subjected to a deep sag where it magnitude decrease to 60V and a swell where the magnitude of the grid's voltage reach 156 V. Active and reactive powers are depicted during normal operation. During sags and swells, the deference of powers as shown in Figure 2.2 is supplied by the auxiliary dc source. During normal operation the DVR consumes 20W which is less than 1.4% of the load rated power while it compensate efficiently grid's voltage harmonics. It is noteworthy to mention that the DVR has no influence on the current pattern. Thus, the source current I_S is

equal to the load current I_L. During sags and swells the DVR restore the voltage at the PCC to its nominal value.

Table 2.1 Voltage compensation using a single-phase DVR

	Load PCC		**Grid (Source)**	
Measures	V_L (V rms)	I_L (A rms)	V_S (V rms)	I_S (A rms)
THD (%)	2.9	13.5	25	13.5
Fund. (rms)	120	14	120, 60, 156	14
Active power, P (W)	1340		1360	
Reactive power, Q (var)	1100		1060	
Power, S (VA)	1733		1724	
Compensator	S_{Comp} = + 20W – j 40var = 45VA			

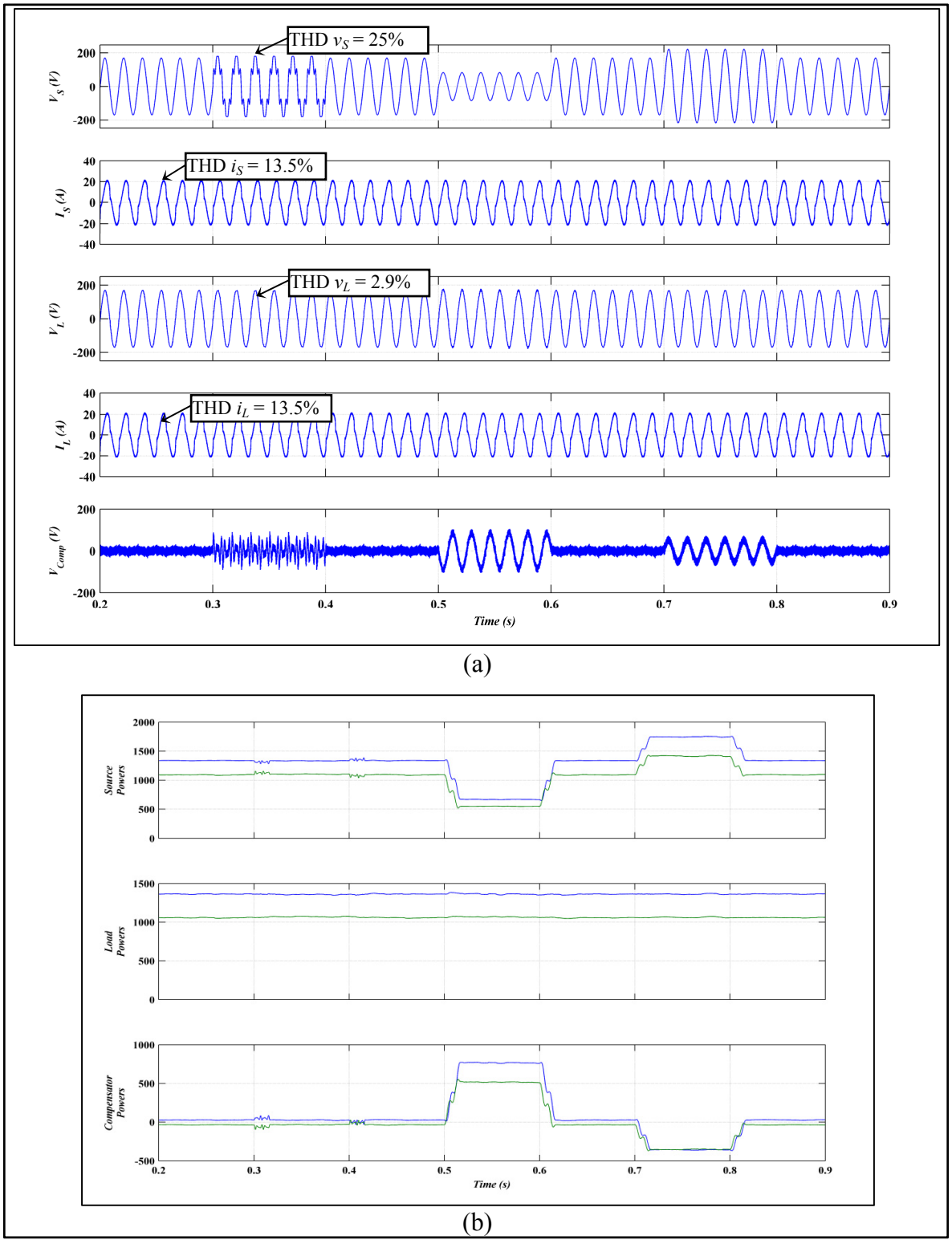

Figure 2.2 DVR to clean voltage at the PCC. (a) Voltage and current waveforms, (b) Active and reactive powers in blue and green respectively

2.3.2 Series Active Filter (SeAF) Function

Series active filters are intended to behave as current harmonic isolators. In most cases, the SeAF, as a controllable voltage source, must operate in conjunction with a shunt passive filter in order to compensate load current harmonics (Dixon, Venegas et Moran, 1997; Gupta, Ghosh et Joshi, 2011; Peng, Akagi et Nabae, 1993). This configuration is commonly known as hybrid series topology or HSeAF (Akagi et Kondo, 2010; Huayun et Shiyan, 2008; le Roux, Mouton et Akagi, 2009). In the hybrid approach shown in Figure 1.12, the combination operates as a harmonic isolator, forcing the load current harmonics to circulate mainly through the passive filter rather than the power system. This approach is an attractive alternative to shunt active filters, since no energy storage is required and the overall rating is reduced (Barbosa, Santisteban et Watanabe, 1998; Salmero et Litra, 2010). An advantage of this topology is the isolation of the DC side from the power system (Lee, Dong-Choon et Jul-Ki, 2004; Senturk et Hava, 2009; Shigenori, Toshihisa et Keiji, 2007). Note that if the active part is used alone without the passive component and the control approach is to compensate current distortions, The SeAF will distort the load side voltage at the PCC in order to force the load to draw a sinusoidal waveform current. In the literature, there exist couples of papers implementing such approach (Fujita et Akagi, 1991c; Peng, Akagi et Nabae, 1990). However, the load side terminal voltages are not presented. The series-AF without the shunt passive component has a configuration similar to a DVR.

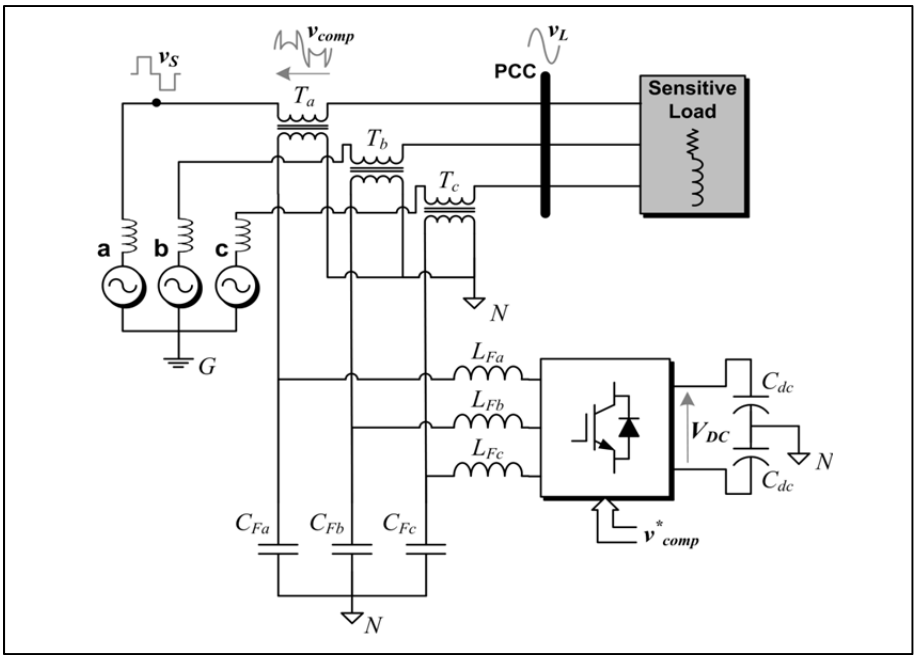

Figure 2.3 Three-phase Series active power filter connected to the grid

Nowadays, it is imperative to compensate current harmonic pollution generated by nonlinear loads. As illustrated for a current fed type of nonlinear load in Figure 2.4, composed of a diode bridge with resistive and inductive components in the dc side, the distorted current produces undesired voltage distortion at the loads feeder, one more reason along with the efficiency, and losses to address current related power quality issues. In this case the current contains 25.1% of THD with a power factor of 97% and the supply voltage has 4% of THD. The compensation of these current related issues will be studied in the next chapters along with experimental results.

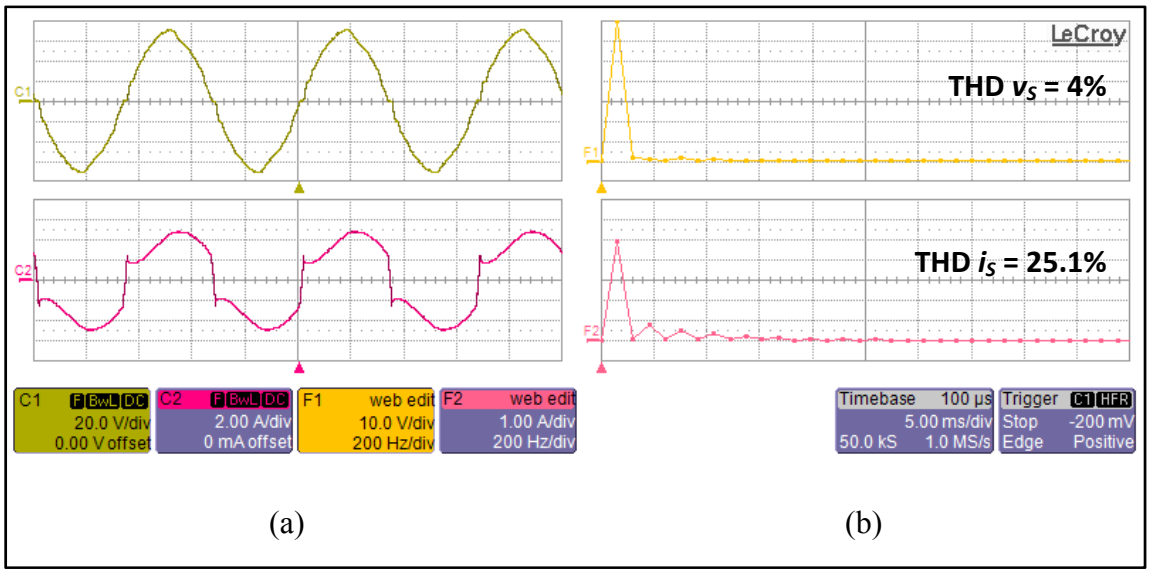

Figure 2.4 Current fed type of nonlinear load (CSV). (a) Voltage and current measured waveforms, (b) Respective harmonic FFT in % of fundamental value

In the Figure 2.5 a voltage fed type of nonlinear load is illustrated as well as its impact on deteriorating the supply voltage. The load consumes a current with a THD of 82% with a power factor of 72%and the voltage has 8.2% of pollution.

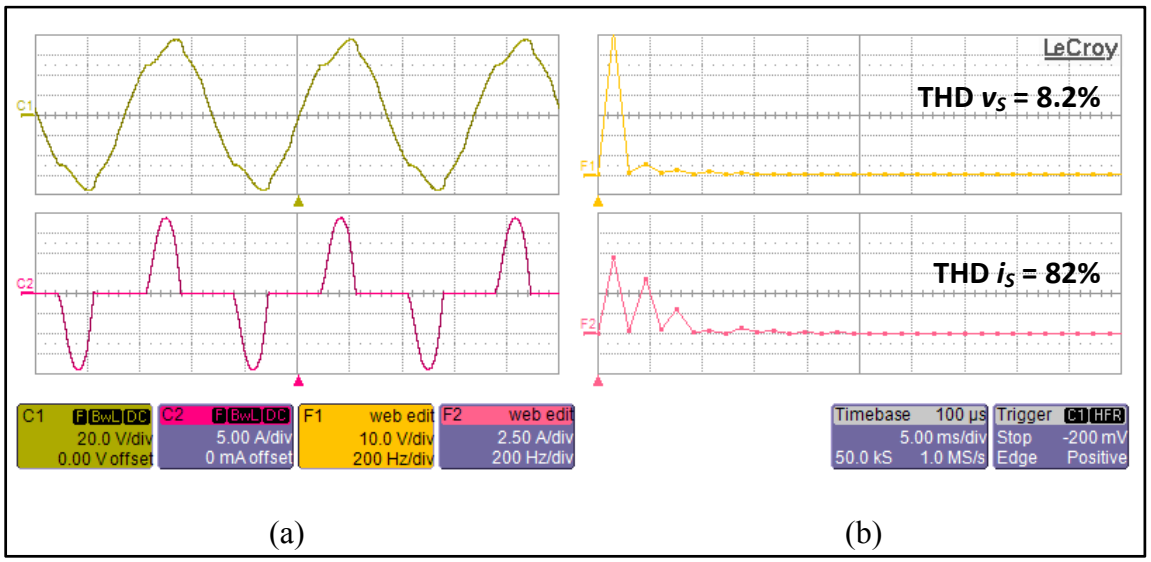

Figure 2.5 Voltage fed type of non-linear load (VSC). (a) Voltage and current measured waveforms, (b) Respective harmonic components

2.3.3 Transformerless-DVR

To isolate the DC bus from the power systems, the series active filter is connected to the grid across three single-phase transformers. This structure complicates the series compensator in both practical realization and modeling aspects. Different approaches are available to eradicate this pricey component off the DVR (Li, Choi et Vilathgamuwa, 2002; Sng, Choi et Vilathgamuwa, 2004). The promoting transformerless configuration could be an affordable solution to substitute shunt AF and UPQCs in future Smart grids (Ghosh, Jindal et Joshi, 2004; Pinto et al., 2011). Figure 2.6 shows a novel configuration for the DVR application (Goharrizi et al., 2012). The elimination of transformers reduces obviously the production cost and the installation complexity for a practical application. The behavior of such configuration is being analyzed in the following sections.

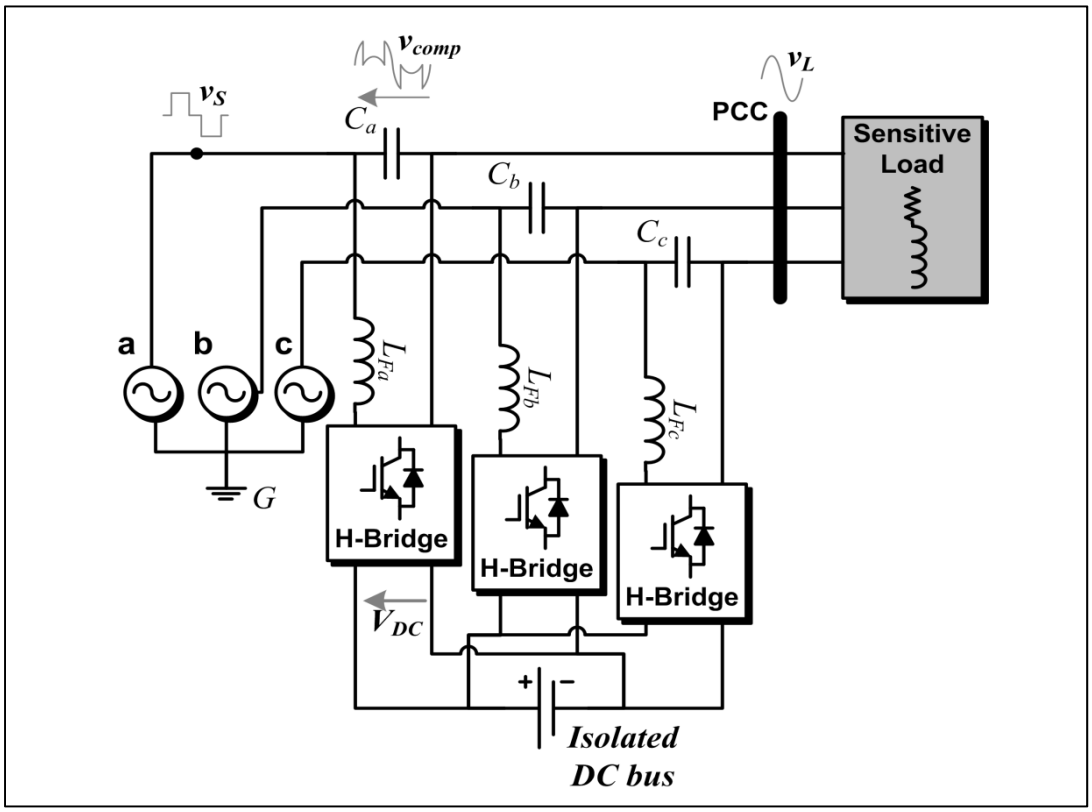

Figure 2.6 A three-phase transformerless dynamic voltage restorer schematic (T-DVR)

2.4 Choice of Inverter to Operates as Voltage Source

The series compensator should behave as a controllable voltage source. Two options are available to realize such device using power electronics; the voltage source converter (VSC) and the current source converter (CSC). Each converter having different designs could be operated as controlled voltage or current sources. Figure 2.7 and Figure 2.8 show the circuit schematic for each configuration. It is possible in application not requiring power supply to replace the DC source by only energy storage elements, capacitor for the VSC and inductor for the CSI. In addition, the converter should be designed to keep the average dc voltage constant for the VSC, and the average dc current for the CSC. A critical comparison of these two configurations is beyond scope of this thesis work. One can prefer the CSC due to its robustness (Fukuda et Endoh, 1995) or the VSC for its efficiency and small physical size while having a lower production cost (Akagi, 2005).

2.4.1 Voltage Source Converter (VSC) Configuration

In the VSC configuration (sometimes refereed as voltage source inverter, VSI), semiconductor switches in any of the legs of the inverter cannot be switched off simultaneously due to this resulting in the voltages being dependent on the respective line current's polarity, resulting in the line currents freewheeling through either the upper or the lower diodes. Moreover, popular IGBTs available in the market nowadays have integrated free-wheeling diode connected in antiparallel with each IGBT, making them more suitable for a VSC configuration. The voltage source converter is illustrated in Figure 2.7 with arbitrary passive components tuned at the switching frequency.

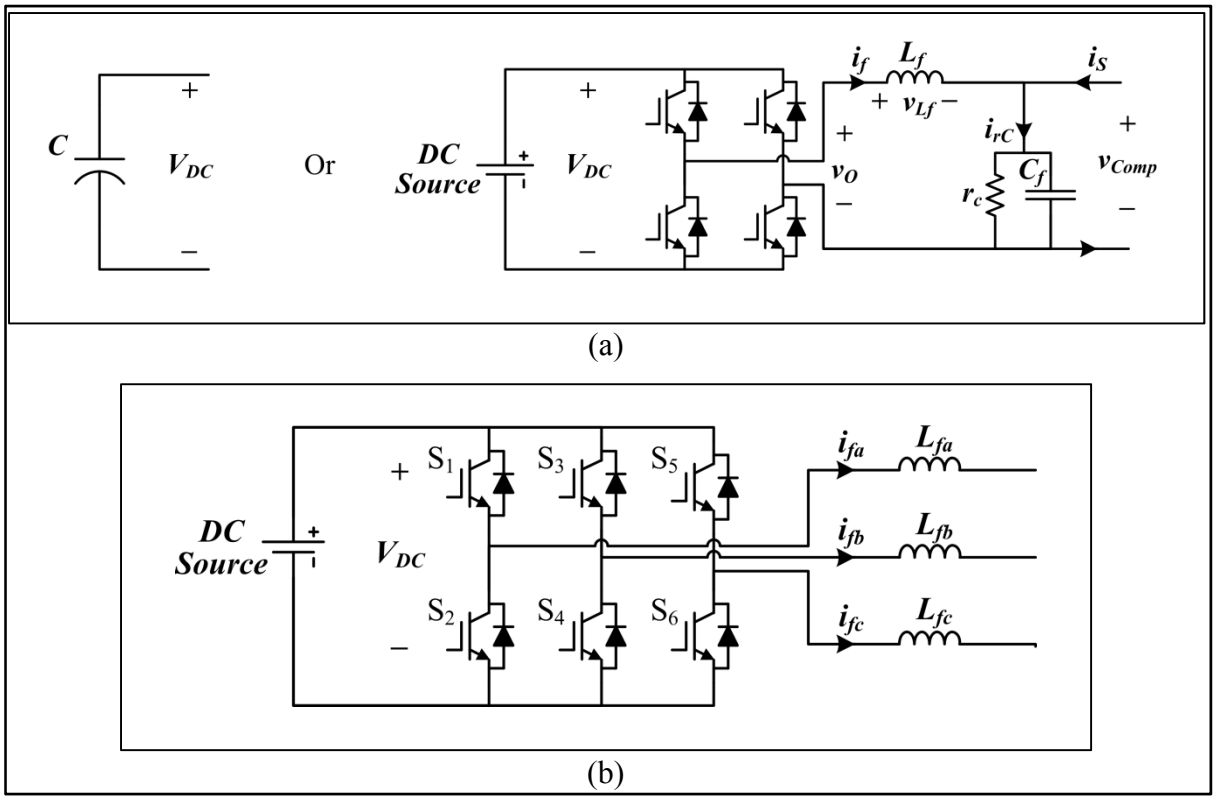

Figure 2.7 Voltage source converter schematic
(a) Single-phase H-Bridge configuration, (b) three-phase configuration

2.4.2 Current Source Converter (CSC)

On the other hand, CSC (in some case refereed as current source inverter, CSI) transforms a DC current into an AC current waveform for applications requiring sinusoidal waveforms. As previously mentioned, due to the absence of antiparallel diodes, the electrical circuit is reduced in size and weight, and tends to be more reliable than VSCs. In general form, a three-phase CSC employs the similar conduction sequence as of a VSC, while instead of a dead-time between switches conducting in the same leg, there should be a superposition to allow current to create a short circuit path for the inductive current to flow through. The current source converter is illustrated in Figure 2.8 with passive components tuned at the switching frequency.

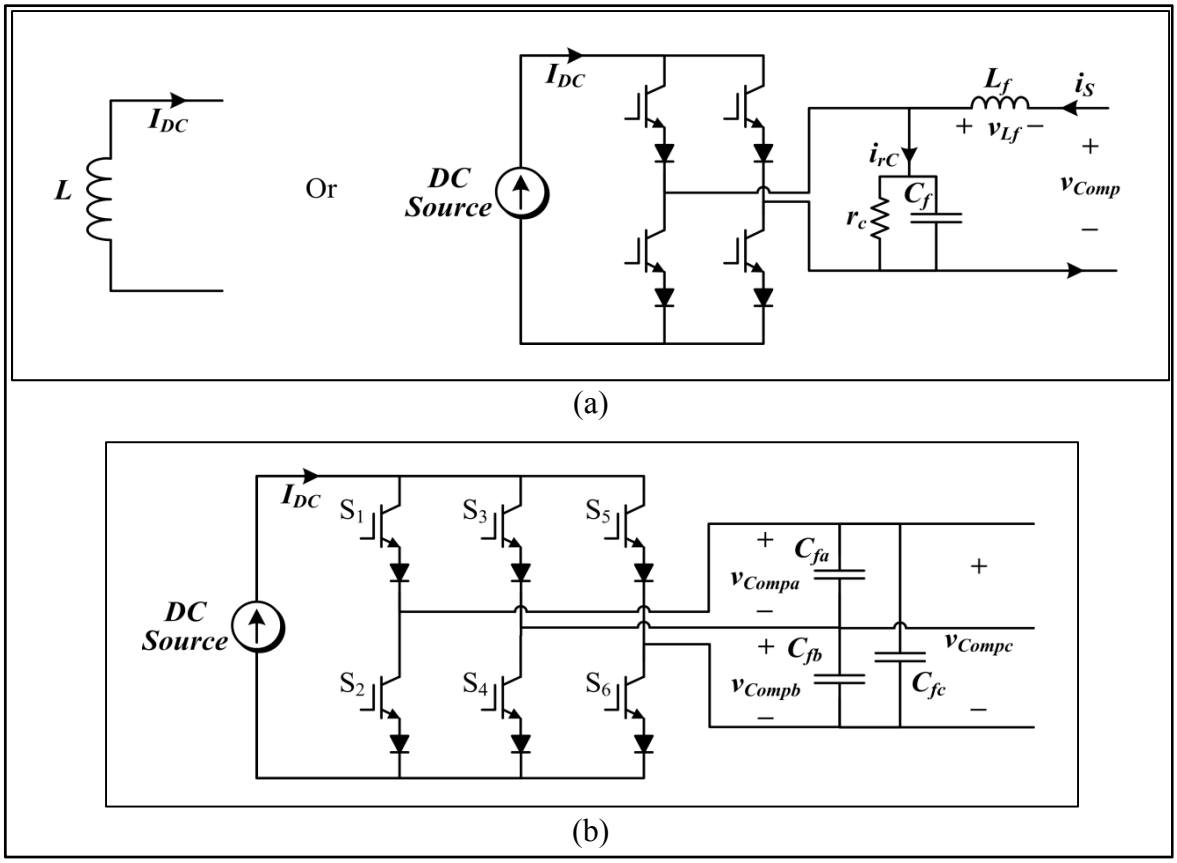

Figure 2.8 Current source converter schematic
(a) Single-phase H-Bridge configuration, (b) three-phase configuration

Most pulse width modulation and carrier-based techniques used for VSCs can also be implemented for their counterparts CSCs with few modifications. Consequently the CSC's line currents will behave in the same way as VSC's line voltages. Meanwhile, the development of higher rated insulated-gate bipolar transistors (IGBTs) and gate turn-off thyristors (GTOs) has made VSC's configurations more economical than ever.

2.4.3 Switching Passive Filter Components

To produce the desired voltage waveform with the given shape, a passive filter is required to filter switching frequency components and give the output waveform, in our case the voltage, is a clean noise-free wave shape. In fact the filter should behave as a short circuit at switching frequency and should have an adequate damping to prevent production of spikes

on the output voltage. Although, series compensators including dynamic voltage restorer and series active filters in general are considered reliable, a stability analysis of their configuration is mandatory before their large propagation in the power system. Therefore, this section focuses on the stability of passive filters implemented in series compensators to eliminate high frequency harmonics off the power converter output. Then, the effect of passive dampers is evaluated. Moreover, simulation and experimental results are presented to validate the theoretical approach. Tuning the LC, second order filter is practically difficult. In application where a transformer is employed in series with the grid, the impedance of the later creates an LCL filter even more complex to tune (Arcuri et al., 2011). However, as the leakage impedance of transformer is negligible compared to its magnetizing impedance (L_{eq}), a solution to damp the resonance is the application of resistive dampers (Dannehl, Liserre et Fuchs, 2011; Ricchiuto et al., 2011). To evaluate the behavior of the passive filter, it could be useful to consider the configuration in Figure 2.7 connected to the LC filter in Figure 2.9.

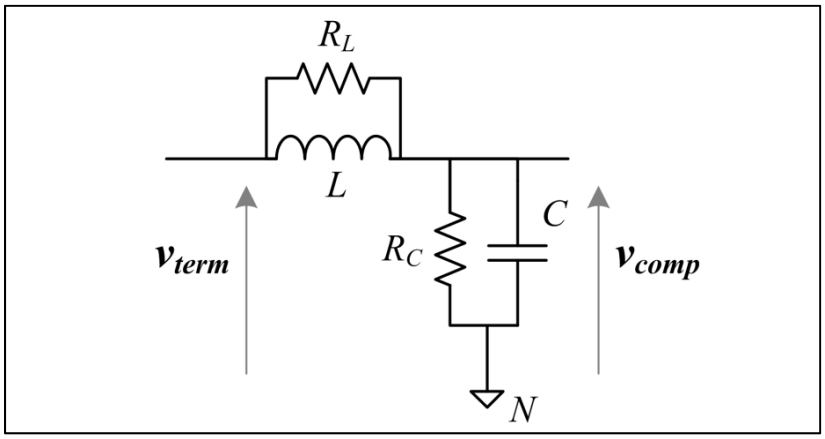

Figure 2.9 The single-phase LC filter with passive damping method

The transfer function of the passive filter without the damping resistances could be described in the Laplace domain.

$$H_1(s) = \frac{V_{comp}}{V_{term}} = \frac{1}{1 + LCs^2} \tag{2.1}$$

Where V_{comp} is the output voltage and V_{term} is the voltage generated at the inverter's terminal before the passive filter. Note, that the *H(s)* should not be confused with the equivalent impedance *Z(s)* of the passive filter. The poles of such a filter are situated on the imaginary axes with positive values creating a marginally stable (oscillating) system where oscillations will not attenuate rapidly and for practical application could be considered unstable.

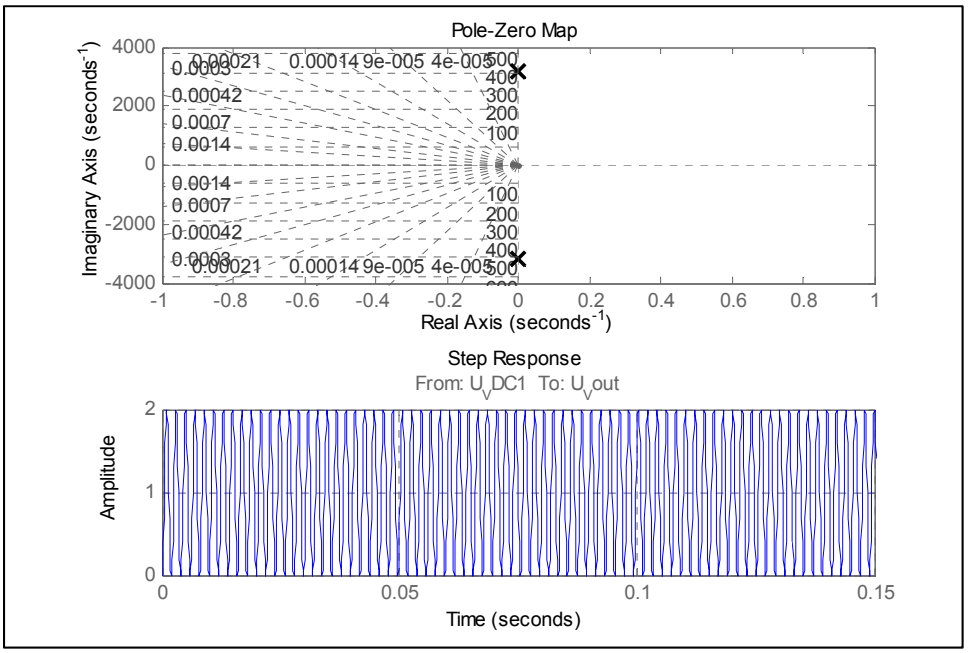

Figure 2.10 Poles and zeros of the LC filter and response to a Heaviside function

With regards to the position of poles of the system without damping, this configuration represents an uncontrollable oscillation. The behavior of the system by simulation is shown in the Figure 2.11.

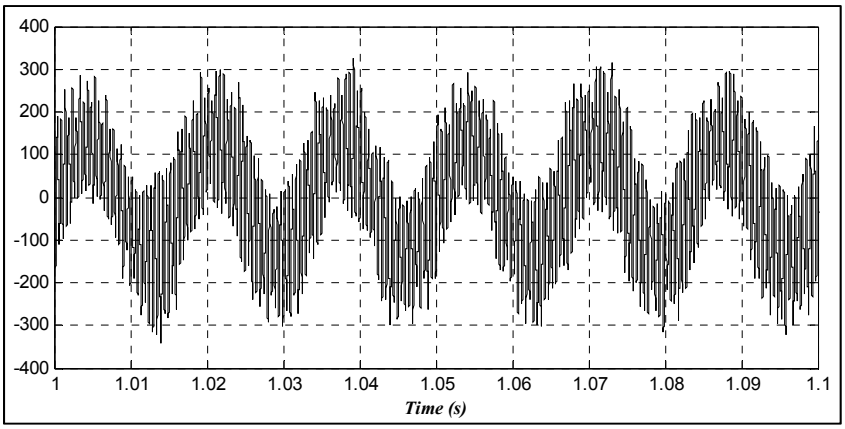

Figure 2.11 Oscillation of the load voltage (V_{La}) of a system without damping, L_F=1mH and C_F=10uF

The following experimental result shows the same configuration connected to a non-linear load. As predicted by simulations, Figure 2.12 shows an inappropriate oscillating voltage across the load terminals resulting in a load voltage THD of 49.8%.

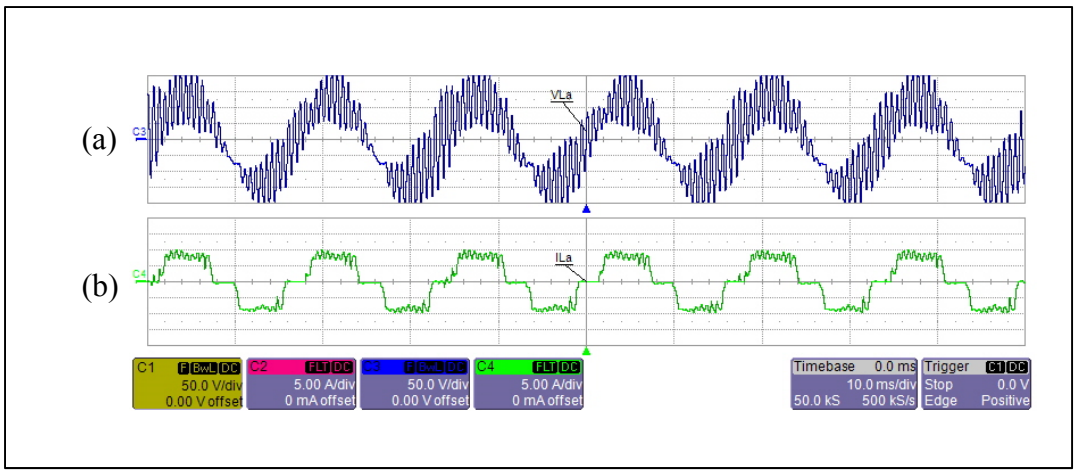

Figure 2.12 Experimental results without damping
(a) Load terminal voltage v_L, (b) load current i_L

To attenuate such oscillations as discussed previously an efficient technique is the application of passive damping method. Now the damping resistors in parallel with the *LC* components of Figure 2.9 are installed and their effect is analyzed. It is noted that, the use of series resistors is prohibited by the facts that they annoy the generated output voltage and produces

higher losses. The impact of both resistors is analyzed regarding the transfer function for each configuration. The overall transfer function including the two damping resistors is described as follow.

$$H_2(s) = \frac{V_{comp}}{V_{term}} = \frac{R_C L s + R_L R_C}{R_C L C s^2 + R_C L s + R_L R_C} \tag{2.2}$$

The effect of each resistance is well analyzed in (Javadi, Hamadi et Al-Haddad, 2014). Hereafter, the response of the system without the resistor in parallel to the inductance is analyzed. The transfer function is then simplified as given by (2.3).

$$H_3(s) = \frac{V_{comp}}{V_{term}} = \frac{R_C}{R_C L C s^2 + L s + R_C} \tag{2.3}$$

The Table 2.2 describes response for various values of inductor, capacitor, and damping resistor of Eqn (2.3). Table 2.2 shows each case component's value. It should be noted that the switching frequency will vary from 6 kHz up to 10 kHz. Consequently as explained in the previous chapter, the attenuation ratio of the filter should be high enough in order that no spikes at switching frequency appear in the generated compensating voltage. Moreover, it is preferred to have a system with the lowest oscillation amplitude as possible.

Table 2.2 Components value for the LCR filter of H_3

Case study	**Capacitance, C (µF)**	**Inductance, L (mH)**	**Damping Resistance, R_C (Ω)**
Case 1	2	5	50
Case 2	2	5	100
Case 3	20	5	50
Case 4	2	1	50
Case 5	2	10	50
Case 6	1	2.5	50

Figure 2.13.a shows the response of each case to a step input. The Bode diagram as well as the Nyquist and the placement of poles and zeros of transfer functions are demonstrated. The chosen values for the practical application coincide with values of the case number one.

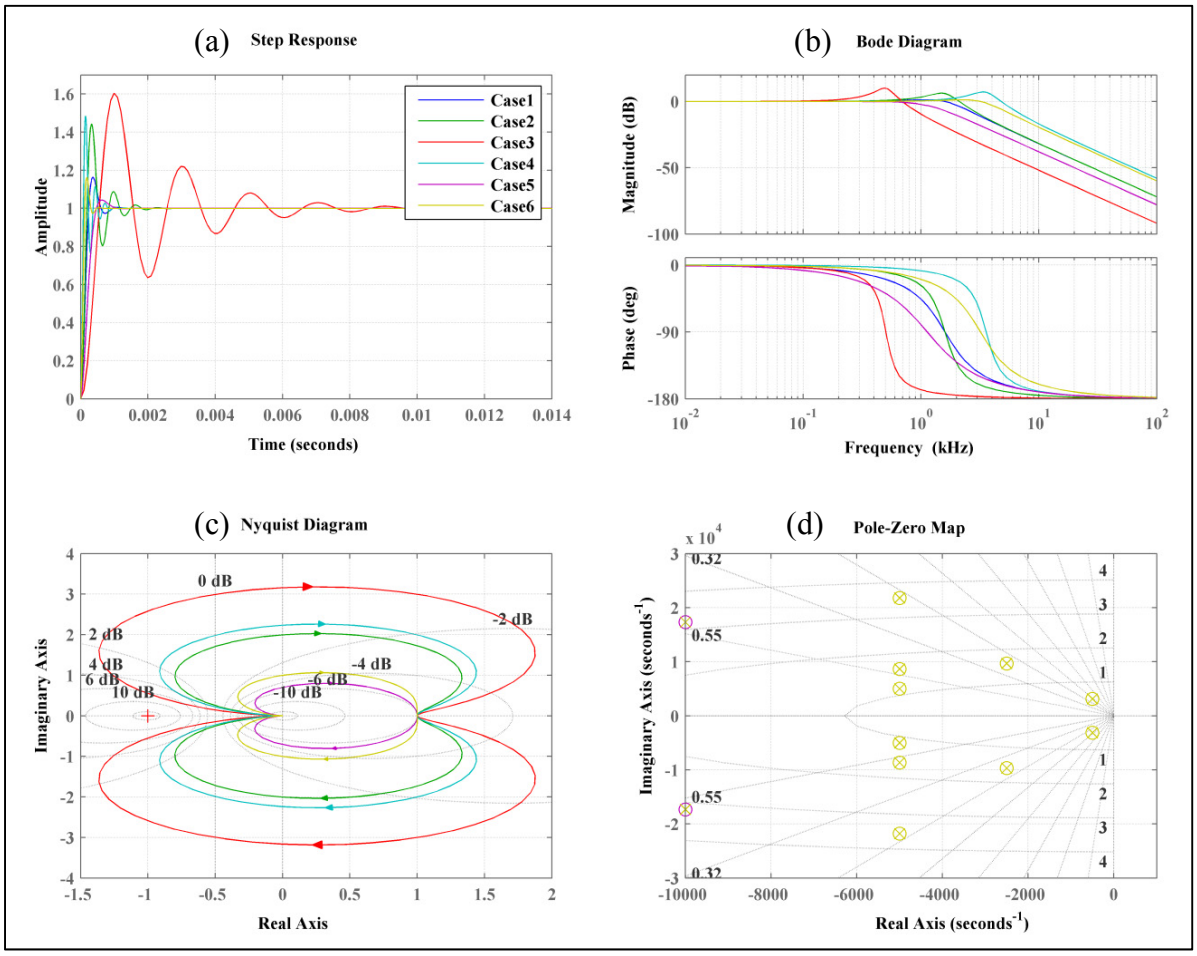

Figure 2.13 Response of the passive filter for different cases

The system with values of Case#1 has an infinite Gain margin (GM) and a 90 degrees phase margin (PM) at 3.2 kHz according to the Bode diagram. This frequency is high enough for compensation purpose of the SeAF and at least two times less than the switching frequency. Consequently, for a practical Rapid Control Prototyping (RCP) application this passive filter combination at the output of the converter will have a satisfactory performance to generate appropriately the compensating voltage.

2.5 Steady State Power Flow of Active Series Compensation

As apprehended earlier, the series compensator behaves as a controllable voltage source generating waveforms having harmonic components up to the tuned allowable limits imposed by the designer based on parameters of the compensator, in this work 3 kHz is chosen to remain in the stable operating point. In this section the equivalent circuit of the standalone Active compensator without the shunt passive filter as shown in the diagram of Figure 2.14 is taken into account. The load flow performed for steady state condition assumes a lagging load. In the case if V_{Comp} is absent, the load and source voltage will be equal ($V_S = V_L$).

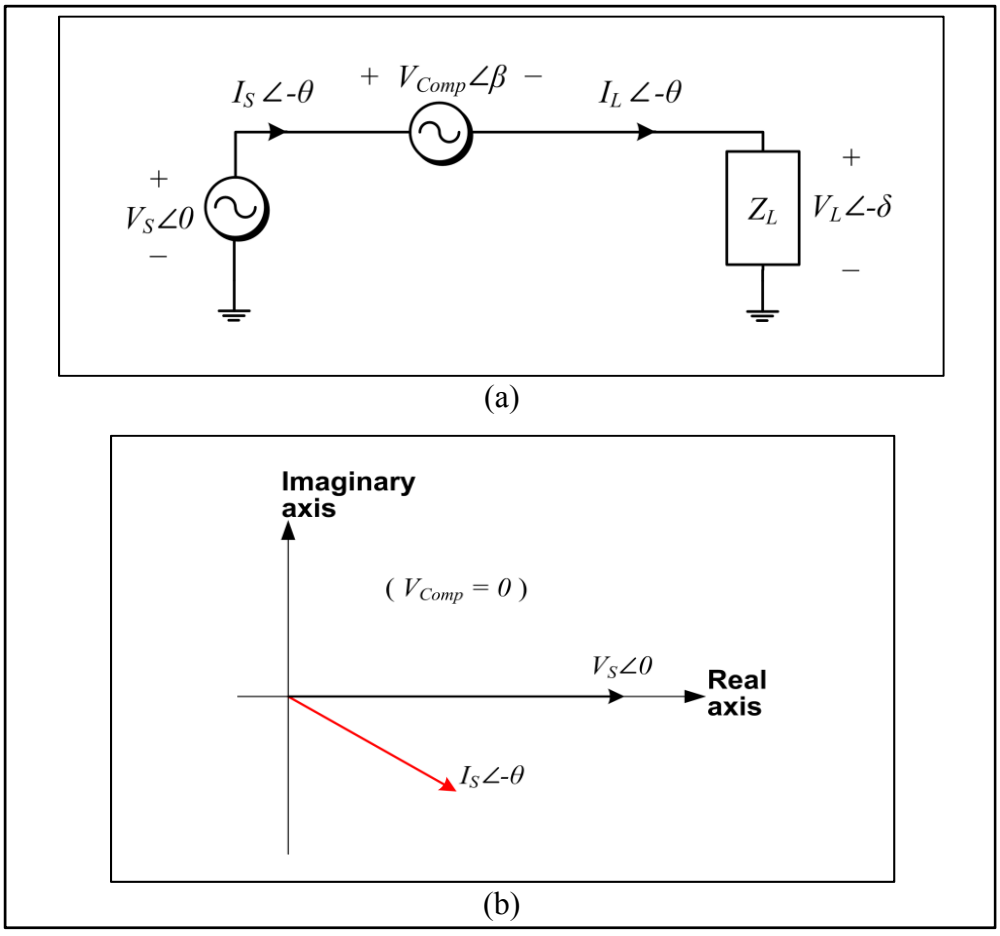

Figure 2.14 (a) Circuit diagram of a radial system with the series active compensator, (b) Phasor diagram of the radial system before compensation with VS as reference

It is noteworthy to mention the three following principles to remember for the series compensation:

1. The series source does not inject or absorb current. This lead to the fact that the load current and source current are identical. As the duality of a shunt active filter, here the line current passes directly through the series compensator ($I_S = I_L$);

2. The load flow is performed at the fundamental frequency, and thus the harmonics are not considered in this study ($I_h = 0$);

3. In a general form, it is impossible to control the DC bus voltage of the compensator and correcting the power factor simultaneously by acting on the phase shift of the compensating voltage.

To give a clear explanation on the third notice, two circumstances are considered; the first is the compensation of the power factor, and the other is the regulation of the DC bus. For sake of simplicity, the load voltage amplitude is considered equal to the source voltage rms value.

2.5.1 Power Factor Compensation

The polar representation of the system become as of Figure 2.15, while the line current and the source voltage are in phase. The power flow for each component of the radial circuit for the inductive load could be found. By shifting the load voltage, the compensator forces the load to drift a current which will be in-phase with the source voltage respectfully.

In a general form, the auxiliary dc supply should be designed according to the maximum compensating voltage that the compensator is tasked to provide at the fundamental frequency. Consequently, the DC bus voltage could not be less than the maximum peak value of the compensation voltage at fundamental frequency that the SeAF will provide.

$$V_{DC} \geq V_{Comp\_max} \quad \Rightarrow \quad 0 \leq |V_{Comp}| \leq V_{DC} \tag{2.4}$$

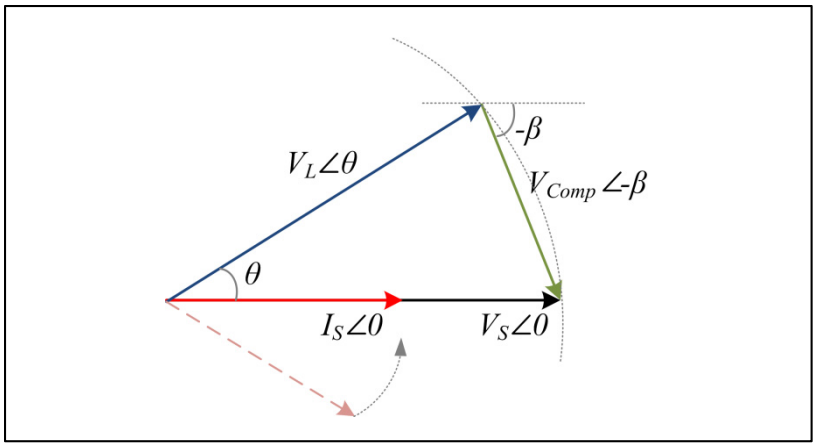

Figure 2.15 Phasor diagram while correcting the power factor

The compensator rating will be equal to the percentage of the produced compensation voltage. Thus, the rating of the SeAF could vary from around 30% of the load power up to the full load. The rated power to design the compensator could be calculated as follows.

$$S_{SeAF} = V_{Comp} I_L^{*} \qquad (I_{Comp} = I_S = I_L) \tag{2.5}$$

Back to the previous vector representation the angle of the produced compensating voltage could be calculated as follow:

$$\beta = \frac{180 - \theta}{2} \tag{2.6}$$

By assuming that $|V_L|$ is equal to $|V_S|$, the complex apparent power which is the product of the voltage and the conjugate of the current could be calculated as follow. The power supplied by the grid is:

$$S_S = (V_S\angle 0)(I_S\angle 0)^{*} = |V_S||I_S|\angle 0 = P_S \tag{2.7}$$

The amount of power consumed by the load is:

$$S_L = (V_L \angle \theta)(I_L \angle 0)^* = |V_S||I_S| \angle \theta = P_L + jQ_L \tag{2.8}$$

The amount of power supplied by the compensator is:

$$S_{Comp} = \left(V_{Comp} \angle -\beta\right)(I_S \angle 0)^* = \left|V_{Comp}\right||I_S| \angle -\beta = P_{Comp} - jQ_{Comp} \tag{2.9}$$

With regards to calculated powers, it is obvious that the source supply only active power, while the load continue to consume and exchange the same active and reactive power respectively as before compensation. The compensator is absorbing the arithmetical difference of active powers between the source and load and supply the difference of reactive power again between the source and the load.

$$\begin{cases} P_{Comp} = P_S - P_L \\ Q_{Comp} = -Q_L \end{cases} \tag{2.10}$$

The direction of the power flow for the compensator has arbitrary been chosen as follow: if the compensator absorbs the power it has a positive value and if it inject or supply power, the power will have a negative value.

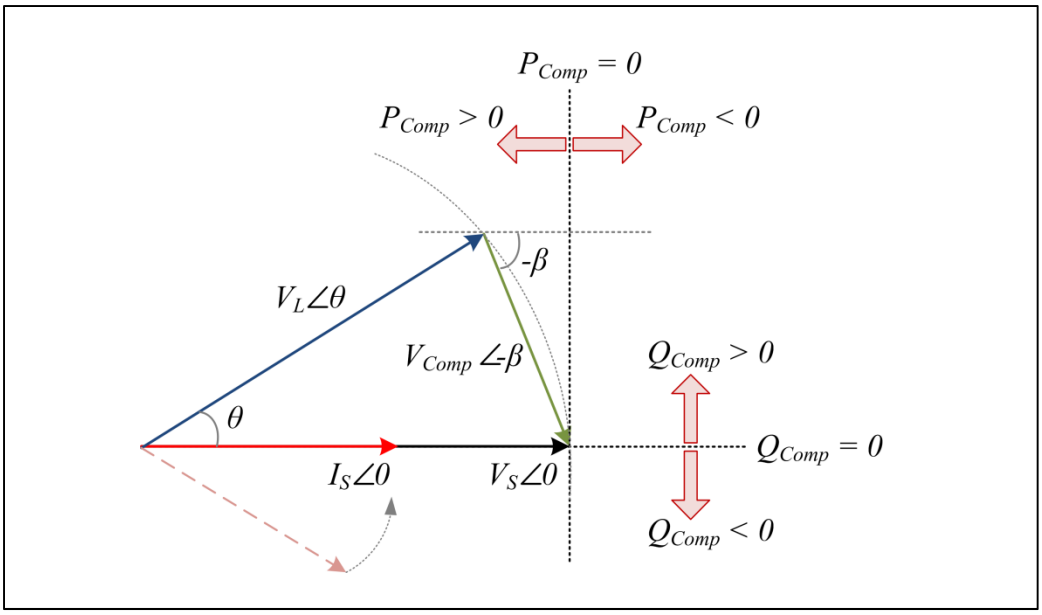

Figure 2.16 Phasor diagram and compensator's power representation

It is noteworthy to mention that, if the source voltage amplitude is equal to the load's voltage, the compensator will absorb power, while if the load voltage is much greater than the source one, then the compensator will start to supply active power as illustrated in Figure 2.16. Likewise for the reactive power; if the load has a lagging power factor (inductive load) the compensator will supply reactive power and if the load has a leading power factor (capacitive load) the compensator will absorb the desired amount of reactive power to finally achieve a unity PF.

Figure 2.17 shows simulation results of a series compensator (a DVR) correcting the power factor. A unity power factor is reached even during a dynamic change in the load power. The DVR has shifted the load voltage by applying a compensating voltage at fundamental frequency where as illustrated in Figure 2.16, the V_{Comp} is the difference of V_S and V_L.

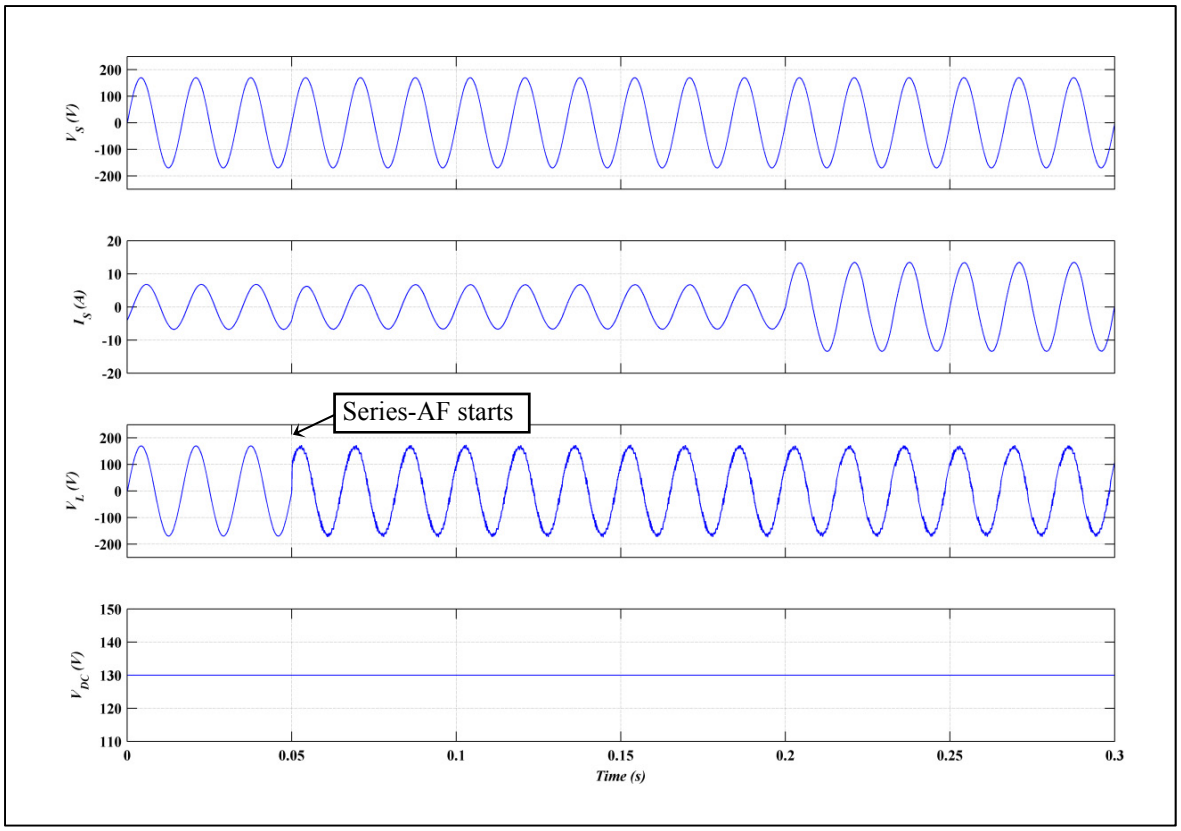

Figure 2.17 Series compensator with DC source to correct the power factor
(a) Grid voltage v_S, (b) source current i_S, (c) load voltage v_L, (d) DC bus voltage V_{DC}

By sweeping the load voltage, the load current will follow in the same direction. As a consequence the line current become in phase with the grid voltage resulting in a unity PF. The compensator will keep the PF at unity value even when the load has increased at 0.2s by supplying more reactive power. The calculated powers in Figure 2.18 illustrate the amount of active and reactive powers flow in each section and show the exceeding amount of power absorbed or injected by the auxiliary DC source. As soon as the Series compensator starts operating (at 0.05s), by performing a PF correction, the reactive power exchanged with the grid drop down, while the load power flow is not affected. The amount of powers that each source will provide could be calculated by Eqn 2.7 to Eqn 2.9. This auxiliary source ensures a constant voltage in the DC side of the converter and the compensator's controller does not require having an integrated DC bus regulator.

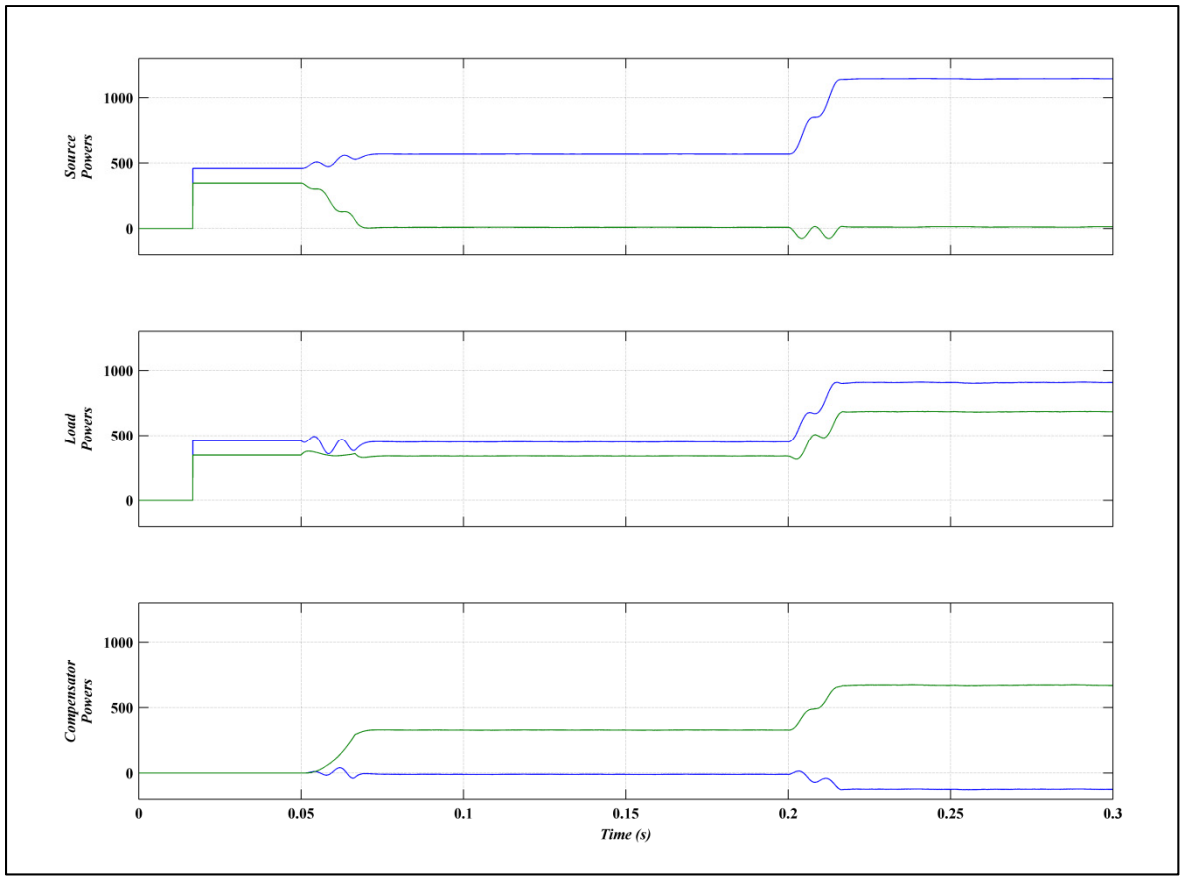

Figure 2.18 Series compensator with DC source correcting the power factor, calculated powers; Active power (blue), and Reactive power (green)

2.5.2 DC voltage regulation

The second case concerns the DC voltage regulation of the compensator. In the previous case study, it was assumed that the series compensator has an auxiliary DC supply to make the compensator operate as desired in all four quadrant. It was also observed that if the load has a resistive behavior with a unity power factor, the DVR would have not produced any compensating voltage at fundamental frequency ($V_{Comp} = 0$). It is not possible to achieve such an outcome without a dc supply according to the upcoming clarifications. If no auxiliary supply is available and the converter has a DC capacitor connected to its DC bus, then the control algorithm should be adapted to take into account the dc regulation. Consequently, to perform a dc regulation the converter should operate similar to a rectifier by absorbing active

power. Regarding the fact that the source current (I_S) is flowing through the series compensator, and that the harmonics have been eliminated, the converter has no choice other than absorbing power at fundamental frequency. To do this, the DVR in this case is forced to produce a V_{Comp} at fundamental in order the product with its respective current results in the absorption of active power to charge the energy storage component C_{dc}. Regarding the derived rules for a rectifier, to maintain the DC bus regulated the input voltage in this case V_{Comp} could not be equal to zero and should absolutely have a no-zero value. Consequently, the lower limit of Eqn. 2.4 should be greater than zero. Thus a unity power factor could never be achieved.

As the series compensator should also maintain a constant voltage at the load's terminal, thus the amplitude of the later is also fixed. Consequently the two possible options are illustrated in the Figure 2.19 with following suppositions.

$$\left|V_{Comp}\right| = Constant \quad , \quad |V_L| = |V_S| = Constant \tag{2.11}$$

According to the vector diagrams of Figure 2.19.a, the leading compensating voltage has shifted the inductive load's voltage phase angle and the power factor is improved. While, in the diagram of Figure 2.19.b a lagging compensation voltage is applied. In this case the load's voltage is still kept constant, but the power factor has been deteriorated as a consequence. For a capacitive load the opposite result are found. As mentioned previously, one can observe that it is impossible to regulate the DC voltage and correcting the PF simultaneously. Both control strategies operate by shifting the V_{Comp}.

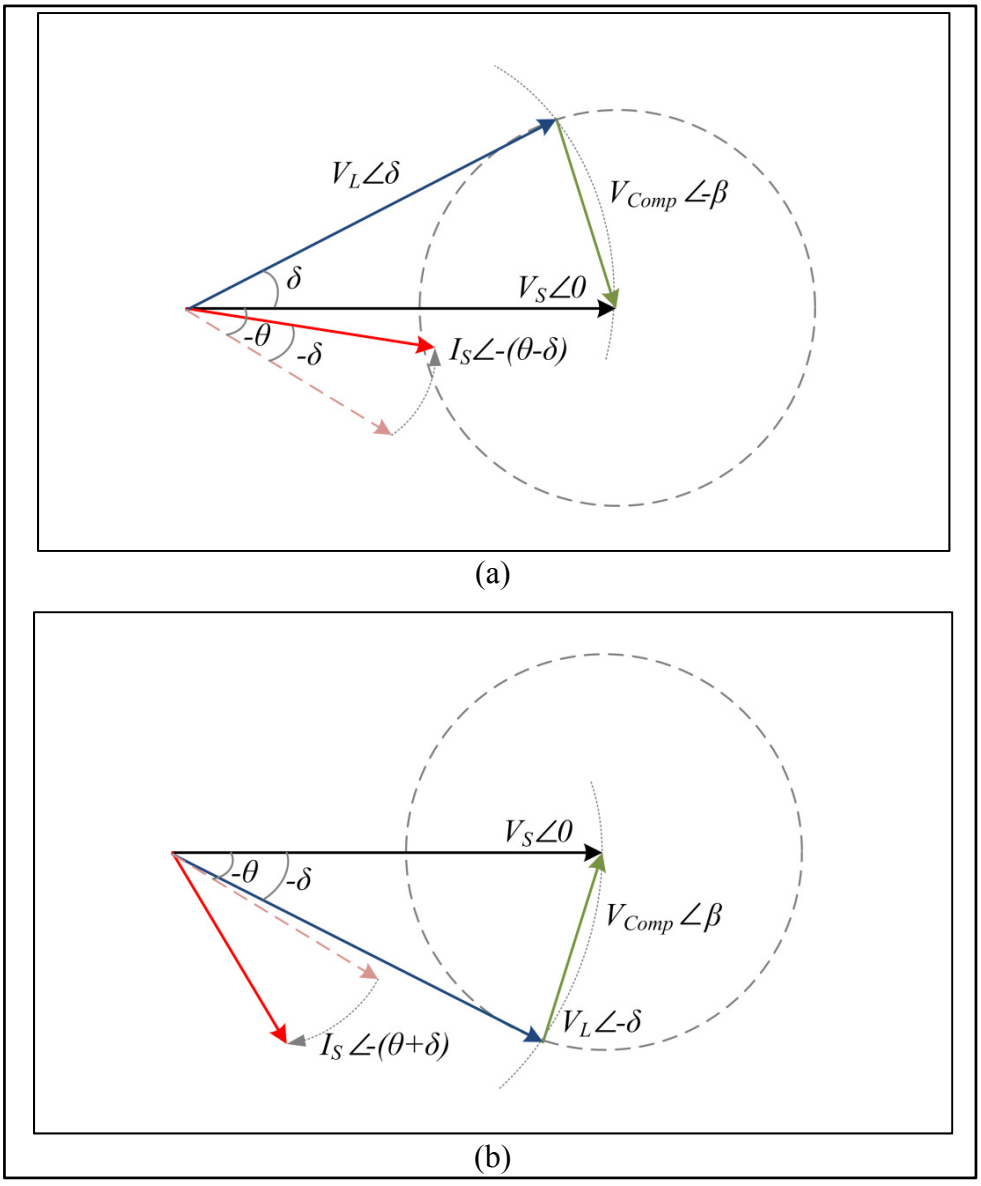

Figure 2.19 Vector representation with constant load voltage and constant compensation voltage, (a) Leading V_{Comp}, (b) Lagging V_{Comp}

This phenomenon makes the operator to take the decision of either using a DC capacitor as an energy storage component and regulate its voltage or using an auxiliary regulated bidirectional DC supply which takes care of keeping the DC voltage constant and allow the DVR or SeAF to correct the power factor. The phase angle is then equal to Eqn. 2.12, where δ is the phase angle that the compensator has shifted the load voltage.

$$\beta = \frac{180 - \delta}{2} \tag{2.12}$$

In this work a DC auxiliary source is used to maintain an adequate supply on the load terminals during sags or swells. It absorbs or injects power to keep the voltage magnitude at the load terminals within the specified margin. However, as desired in this section a dc capacitor is used instead of the auxiliary source. To maintain a constant regulated DC bus voltage across the capacitor, a PI controller is therefore used. Regarding the enlightened background, the amount of active power transferred from AC to the DC side is achieved by generating a sinusoidal voltage signal in phase with the source current i_s. The output signal v_{O_DC} is added to the fundamental active component of the global controller. Figure 2.20 shows the block diagram of the DC-link control regulation which should be added to controllers requiring a DC voltage regulation.

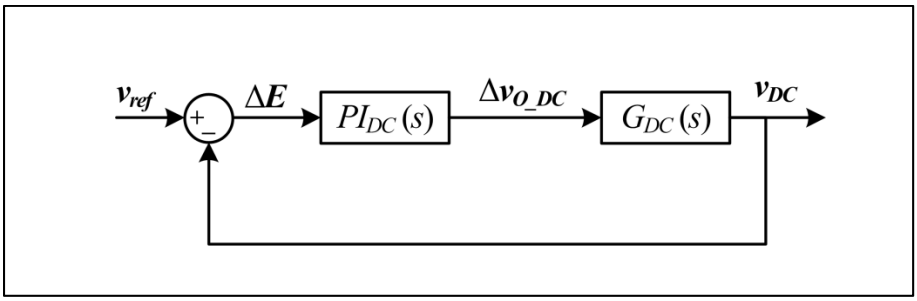

Figure 2.20 Capacitor's DC voltage regulation block diagram

The $PI_{DC}(s)$ is the PI control transfer function and $G(s)$ is the transfer function between the capacitor voltage v_{DC} and the compensation output voltage generated by the PI regulator v_{O_DC}. The energy stored in the capacitor is evaluated by the following equation.

$$E_{DC} = \frac{1}{2} C_{DC} \cdot v_{DC}^2(t) \tag{2.13}$$

The power flow into the capacitor in steady state is then derived. This provides a power balance between the dc and ac side of the converter. The transfer function G_{DC}(s) is obtained

by small-signal perturbation and considering the V_{DC} as the steady state reference voltage for the capacitor.

$$\Delta p_{DC} = C_{DC} \cdot V_{DC} \cdot \frac{d}{dt} v_{DC}(t) = v_{O_{DC}}(t) \cdot I_S \cos\varphi \tag{2.14}$$

where I_S is the effective value of line current. Taking the Laplace transformation of Eqn 2.14, *G(s)* can be obtained as follow.

$$G_{DC}(s) = \frac{\Delta v_{DC}}{\Delta v_{O_{DC}}} = \frac{I_S \cdot \cos\varphi}{s \cdot C_{DC} \cdot V_{DC}} \tag{2.15}$$

The PI transfer function is

$$PI_{DC}(s) = K_{pDC} + \frac{K_{iDC}}{s} \tag{2.16}$$

Where, *Kp* is the proportional gain and *Ki* the integration gain of the controller. Thus, the closed-loop transfer function of the DC control system is achieved.

$$T_{DC} = \frac{\Delta v_{DC}}{\Delta v_{ref}} = \frac{G_{DC} \cdot PI_{DC}}{1 + G_{DC} \cdot PI_{DC}} \tag{2.17}$$

$$= \frac{\frac{K_{pDC} \cdot I_S \cdot \cos\varphi}{C_{DC} \cdot V_{DC}} \cdot s + \frac{K_{iDC} \cdot I_S \cdot \cos\varphi}{C_{DC} \cdot V_{DC}}}{s^2 + \frac{K_{pDC} \cdot I_S \cdot \cos\varphi}{C_{DC} \cdot V_{DC}} \cdot s + \frac{K_{iDC} \cdot I_S \cdot \cos\varphi}{C_{DC} \cdot V_{DC}}}$$

According to this equation the damping factor ζ and the natural angular velocity ω_n can be calculated. In order to have a damped response within few cycles, ζ=0.8 and ω_n = 50 rad/s were chosen. Afterward, the PI gains are calculated. Consequently, this controller will remain stable as the poles of the system are situated to the left side of the s-plane.

$$\zeta_T = \frac{K_{pDC}}{2}\sqrt{\frac{I_S \cdot \cos\varphi}{K_{iDC} \cdot C_{DC} \cdot V_{DC}}} \tag{2.18}$$

and

$$\omega_n = \sqrt{\frac{K_{iDC} \cdot I_S \cdot \cos\varphi}{C_{DC} \cdot V_{DC}}} \tag{2.19}$$

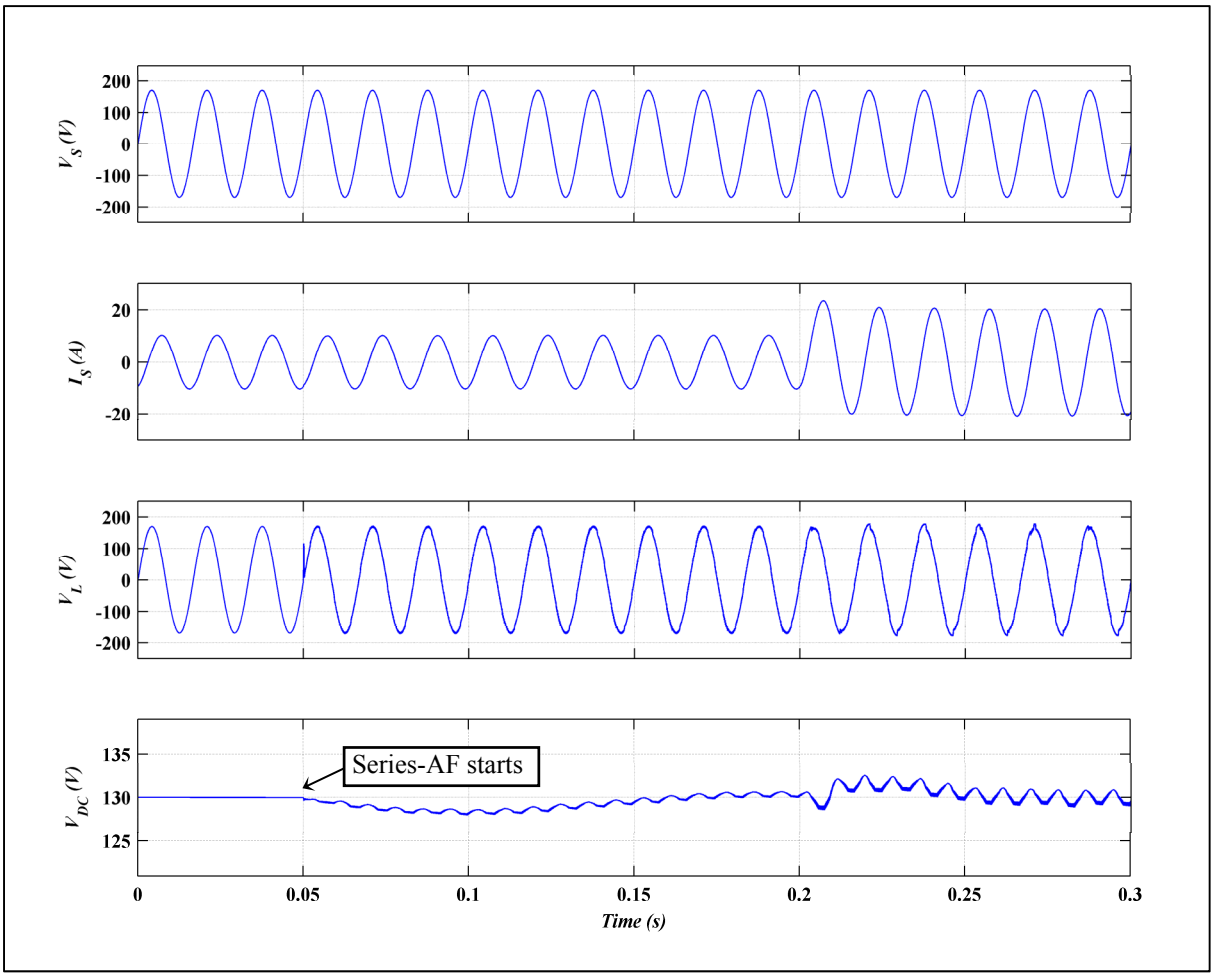

Figure 2.21 Series compensator with Capacitor and DC regulation
(a) Grid voltage v_S, (b) source current i_S, (c) load voltage v_L, (d) DC bus voltage V_{DC}

The simulation results of Figure 2.21 show a series compensator (a DVR) performing its compensation task, while taking into consideration the DC voltage regulation. It shows that

the DC voltage is regulated by only shifting the loads voltage in order for the compensator to absorb the required amount of active power to maintain its DC voltage regulated at 130Vdc. The load flow is demonstrated in the Figure 2.22, in which the powers are not noticeably modified, and only few amount of active power is absorbed to regulate the DC bus voltage.

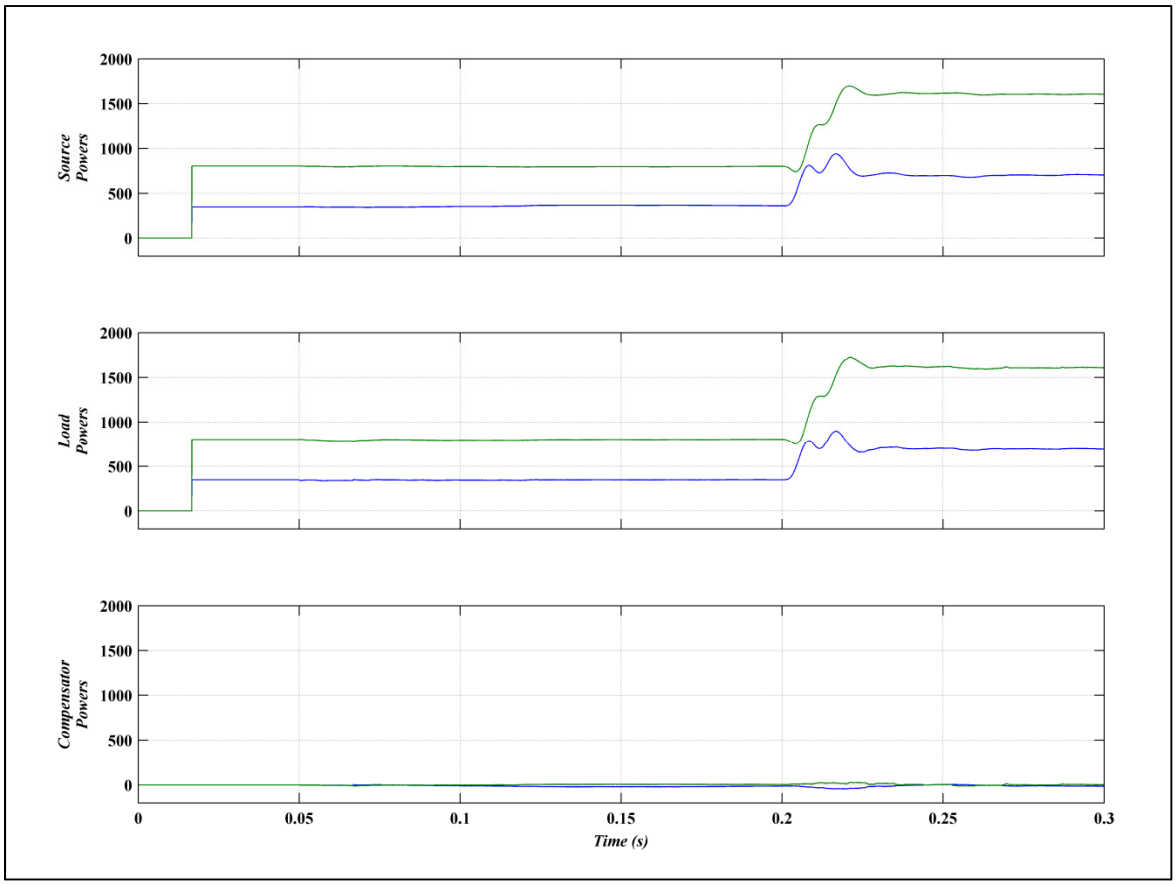

Figure 2.22 Series compensator with Capacitor and DC regulation, calculated powers; Active power (blue), and Reactive power (green)

2.6 Current Harmonic Compensation, a Novel Hybrid Detection Approach under Grid Perturbation

In this section a novel hybrid harmonic compensation approach for non-linear loads is developed and analyzed (Javadi et al., 2015). This technique provides compensation for current harmonics coming from a nonlinear load and reactive power regulation even during grid's voltage disturbances. The method could be implemented on any Series Active Filter. A single-phase Transformerless configuration (TSeAF) is selected to address power quality issues of a non-linear load. In the first step the source current distortions are extracted from the sensed nonlinear load currents. Then, to improve the compensation's behavior this new strategy uses voltage harmonic distortions to make the grid current remain as clean as possible with a small gain *G* proportional to current harmonic components. At first the strategy is evaluated on an Ideal polluted CSC load with non-linear behavior, and then a single-phase bridge rectifier with R–L load is taken as nonlinear load to implement the controller. This strategy operates in regular conditions, while it keeps a high quality sinusoidal current waveform during disturbances initiated by the grid.

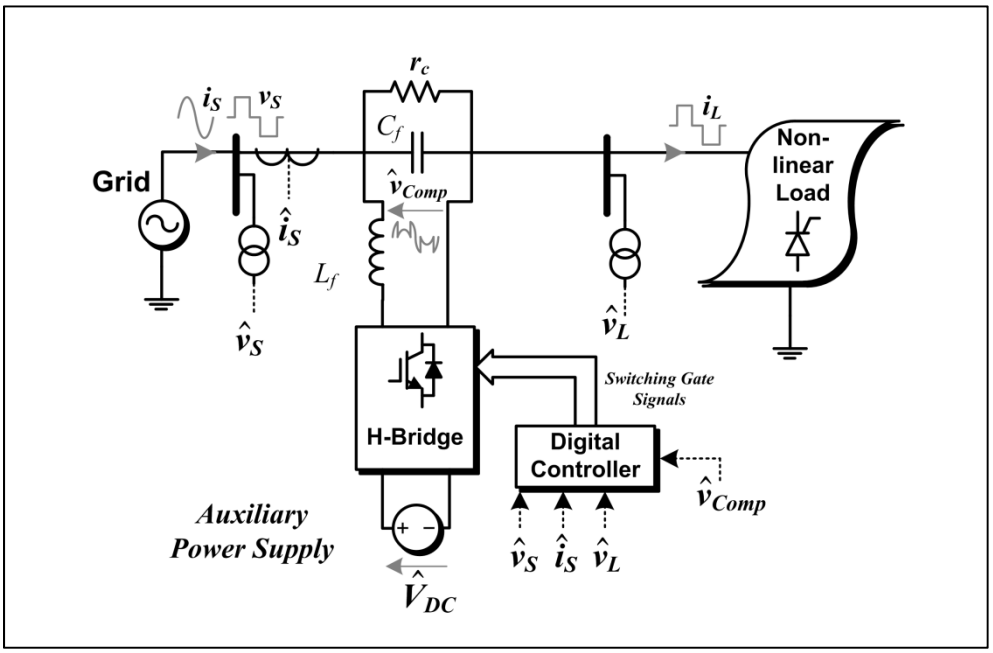

Figure 2.23 The TSeAF connected to a single-phase radial system

The transformerless hybrid series active filter shown in Figure 2.23 is used to implement the proposed control strategy. It is created of an H-bridge converter connected in series between the grid and the load. To stay in the scope of this section a bidirectional source is applied in the DC side. This will prevent DC regulation and let focusing on the main control approach. However, one can place a DC storage capacitor and regulate it as required as described in (Sng, Choi et Vilathgamuwa, 2004). The namely rating of the implemented system is adjusted to 1.2 kVA. The source is set at residential voltage of 120Vrms and is connected to a current fed non-linear load.

The TSeAF connected in series will inject the compensating voltage as produced by the developed control technique. Parameters of the system are meticulously explained in Table 2.3. Meanwhile, the controller will be first applied to an ideal current polluting source. As the load current will stay intact and independent from its voltage distortion, this will allow an explicit demonstration of proposed controller's behavior.

Table 2.3 System Parameters for current harmonics compensation

Symbol	**Definition**	**Value**
v_s	Line phase-to-neutral voltage	120 Vrms
f_g	Grid frequency	60 Hz
S_L	nonlinear load rating	1.2 kVA
Lf	Switching ripple filter inductance	5 mH
Cf	Switching ripple filter capacitance	2 µF
T_S	Simulations discrete sampling time	10 µs
f_{PWM}	PWM frequency	10 kHz
V_{DC}	DC bus voltage of the TSeAF	120 V

Active filters compensate generally distortions of current type of non-linear loads. Thus, the distorted current waveform of the 1.2 kW non-linear load is depicted in Figure 2.24. In this simulation the compensator is out of service and current harmonics flow directly into the grid. In this section the proposed active filter is connected to the grid without the series injection transformer. The active compensator is then able of compensating current

harmonics from polluting the grid side. Same controller could be applied to a configuration with isolating transformer. As the objective of this subsection is to put forward the control principle and not the configuration itself, such comparison is out of the aims of the current work. Assuming up to the nineteen's harmonic order, the non-linear load current could be reconstructed from its components as shown in the following figure.

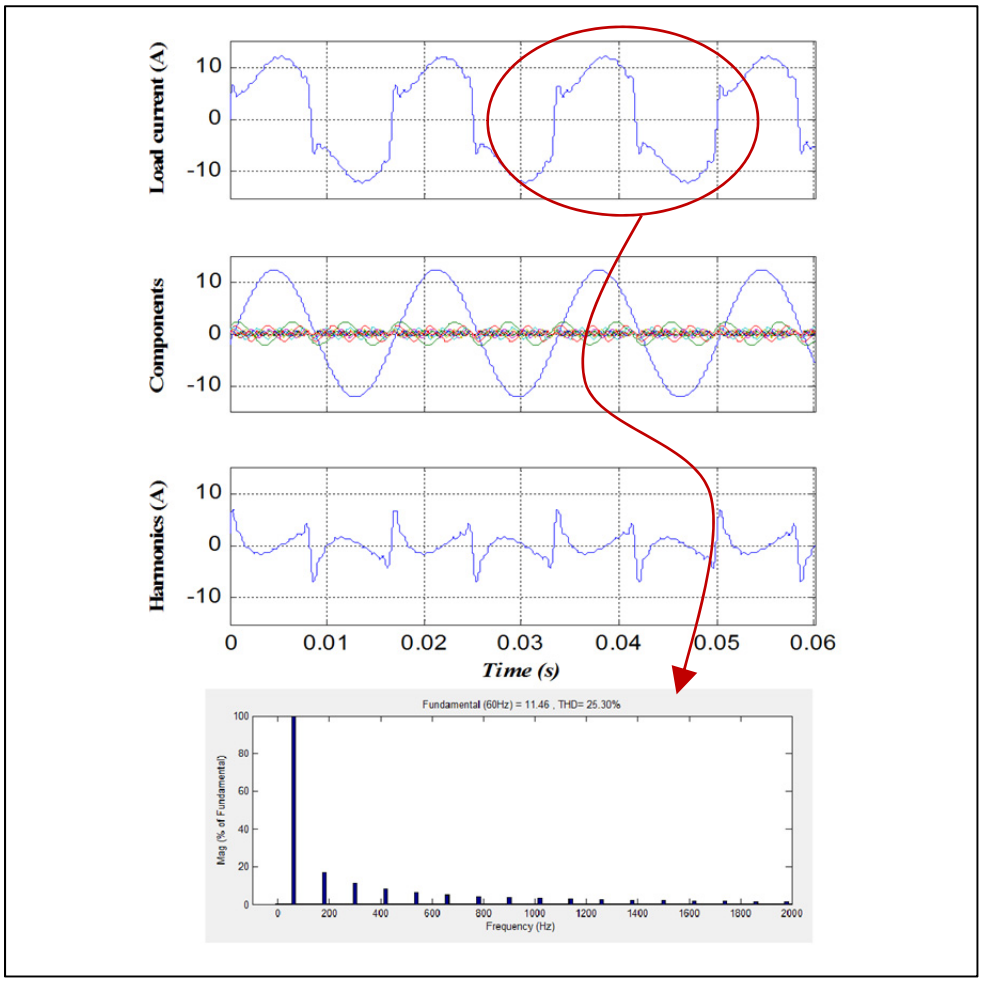

Figure 2.24 Current harmonic components of a typical CSC non-linear load up to 19th harmonic

The closed-loop control compensation introduced in early 21th century by Wang (Wang et al., 2001) had great contribution in series compensation. In order to prevent current harmonics I_h to flow into the grid side, Series active filter considered as controlled voltage

sources (VSI) was proposed to present low impedance for the fundamental component and high impedance for those harmonics. The equivalent circuit is presented in Figure 2.25. This principle of compensation is been implemented in most series AFs (Fujita et Akagi, 1996). Meanwhile, this work proposes a new hybrid approach to improve behavior and performances of compensation even during grid voltage perturbations. The behavior of the series compensator for a harmonic current control could be studied from the equivalent circuit demonstrated in Figure 2.25. As commonly used, the non-linear load is modeled by a resistance and a current harmonic source. The impedance Z_L represents the load and its active power consumption. In this section, the fundamental and harmonic components are not separated to keep a wide overview of the electrical circuit.

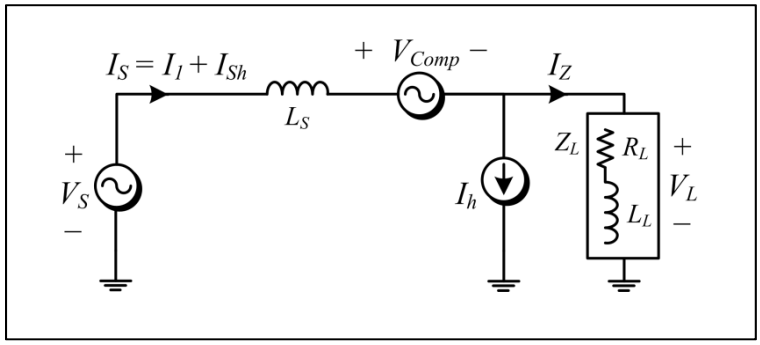

Figure 2.25 Single-phase phasor circuit representation

The output voltage V_{Comp} is produced by the Active compensator. There exist three approaches to achieve a closed-loop control compensation of current harmonics.

2.6.1 Detection of Source Current Harmonics

The first is to assuming the compensating voltage is only equal to the current harmonics with a gain (***G***) high enough to prevent them to flow into the grid.

$$V_{Comp} = +G.I_{sh} \tag{2.20}$$

The grid's equivalent circuit for the fundamental and harmonics components could be depicted as follow:

$$V_S = V_{s1} + V_{sh} \tag{2.21}$$

$$V_L = V_{L1} + V_{Lh} = Z_L I_Z = Z_L(I_S - I_h) \tag{2.22}$$

$$I_S = I_{S1} + I_{Sh} = I_Z + I_h \tag{2.23}$$

Applying electrical circuit's law, following equation is obtained.

$$V_S = Z_S I_S + V_{Comp} + Z_L I_Z = Z_S I_S + G I_{Sh} + Z_L(I_S - I_h) \tag{2.24}$$

The source current could be separated into a fundamental and harmonic component.

$$\begin{cases} I_{S1} = {V_{S1}}/{(Z_S + Z_L)} \\ I_{Sh} = {(Z_L I_h + V_{Sh})}/{(Z_S + Z_L + G)} \end{cases} \tag{2.25}$$

When the compensator generates a V_{Comp}, the load voltage is consequently equal to Eqn 2.26. The harmonics distortion of the load voltage could be then separated and calculated.

$$V_L = V_S - V_{Comp} - Z_S I_S \tag{2.26}$$

$$V_{Lh} = \left(\frac{Z_L}{Z_S + Z_L + G}\right) \cdot (V_{Sh} - Z_S I_h - G I_h) \tag{2.27}$$

One can clearly observe that by increasing the gain ***G*** high enough, the source current harmonics will be equal to an infinitely small value. And it is possible to consider the load voltage harmonics are equal to Eqn. 2.29. In a comprehensive explanation, one can deduce somehow that, in this approach the whole current harmonics of the load are turned back into the load impedance and thus Eqn 2.28 holds assuming I_{Sh} is eliminated.

$$V_{Comp} = \left(\frac{G \cdot Z_L}{Z_L + G}\right) \cdot I_h \tag{2.28}$$

And

$$G \gg Z_L \quad \rightarrow \quad \begin{cases} I_{Sh} \approx 0 \\ V_{Lh} = -V_{comp} \approx -Z_L I_h \end{cases} \tag{2.29}$$

It should be mentioned that the harmonic gain in this approach require to have an extremely high value. Even more with such a high compensating gain the source current harmonics are not totally compensated. And if the grid's voltage became distorted, they are reflected on its related current. For this first case, Figure 2.26 shows simulation results with an ideal system. The Active filter starts to operate at 0.05s while the gain ***G*** continuously has been increased to show its influence on the source current.

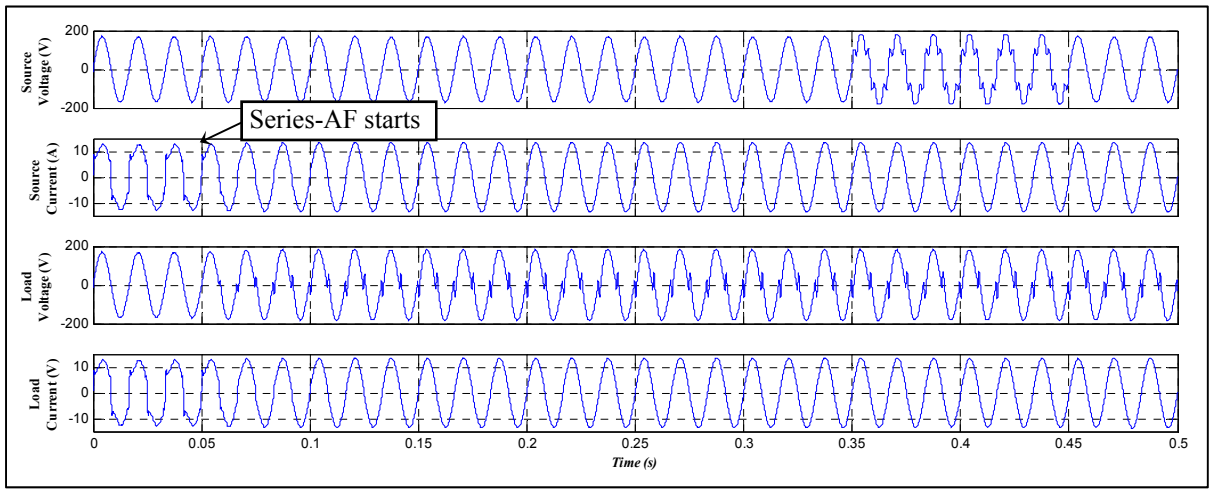

Figure 2.26 Simulation of the ideal system with $V_{Comp} = +G.I_{Sh}$

The Figure 2.26 demonstrates that by increasing the gain ***G*** up to 250, the source current harmonics will be eliminated. However, there will be a residual amount of distortions in the waveform. This coincides with the control approach explained previously that requires a huge gain value and confirms the theoretical developments. Thus, two weaknesses of this

approach are the steady state error on the harmonic distortions and the facts that during source voltage perturbation, this perturbation is affecting the compensation performances. The grid voltage became highly polluted between 0.35s and 0.45s with fifth and seventh order harmonics as shown in Figure 2.26.

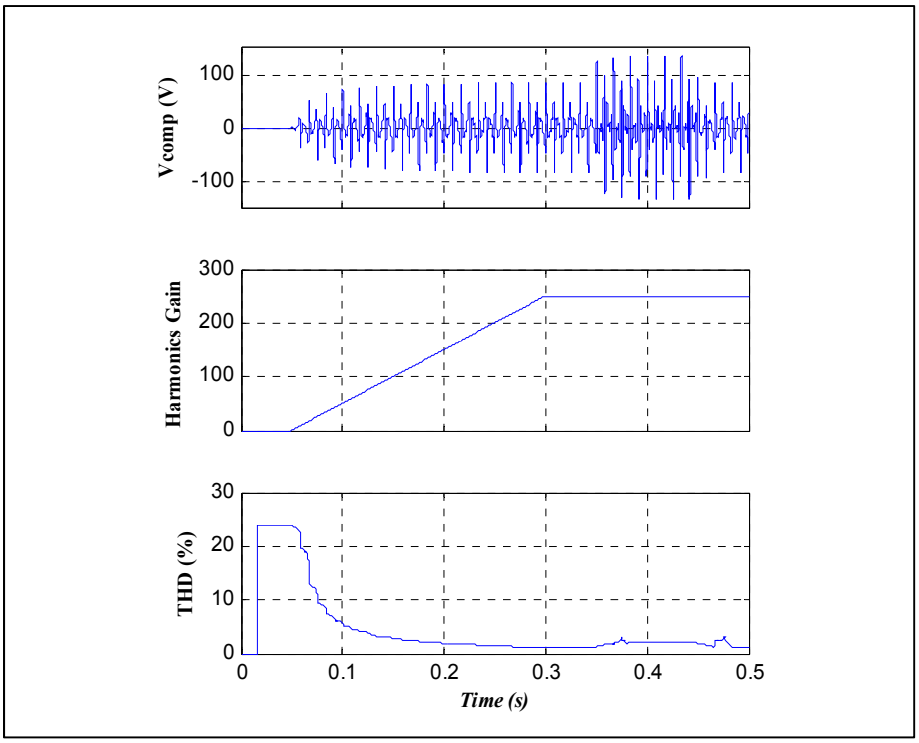

Figure 2.27 Compensating voltage V_{Comp}, the gain G, and the current's Total Harmonic Distortion (THD)

2.6.2 Detections of Load Voltage and Source Current Harmonics

To improve the compensation performances, as detailed in (Peng, Akagi et Nabae, 1990), the load voltage harmonics are added to the controller. As seen in the previous subsection, by injecting a compensating voltage related to the current harmonics, the load voltage terminals became distorted with the same harmonics order as of its current generated harmonics. To counterpart this distortion the use of a shunt passive filter became mandatory to absorb these voltage distortions by creating a low impedance path for current harmonics initiated by the non-linear load. Regarding the fact that in this section the aim is to focus on the current

control approach the load terminal voltage distortions are not required to be compensated. Contrary, one can deduce that in case of a perfect current compensation as developed in the succeeding section the load distortion should be exactly equal to the product of current harmonics and the load impedance. In the second approach the load voltage harmonics are also detected and added to the closed-loop controller. Thus the compensating voltage is as follow.

$$V_{Comp} = +G.I_{sh} - V_{Lh} \tag{2.30}$$

The source current could be derived by same mathematical principles as of the earlier section. The Eqn. 2.31 demonstrates the harmonic component of the source current. The fundamental active component remains unaffected.

$$I_{Sh} = \left(Z_L I_h + V_{Sh} + V_{Lh}\right) \Big/ \left(G + Z_S + Z_L\right) \tag{2.31}$$

By introducing Eqn. 2.31 into the generic equation Eqn. 2.22, the load distortion is derived.

$$V_{Lh} = \left(\frac{Z_L}{Z_S + G}\right) \cdot \left(V_{Sh} - Z_L I_h\right) \tag{2.32}$$

Substituting Eqn 2.24 in 2.25, the source current harmonic component is reached.

$$I_{Sh} = \left(\frac{1}{Z_S + G}\right) \cdot V_{Sh} \tag{2.33}$$

Hence as it is possible to observe in Figure 2.28, if the source voltage harmonic V_{Sh} is neglected the current harmonic distortion will be equal to an imperative zero value.

$$G > 0 \quad (V_{Sh} = 0) \rightarrow \quad \begin{cases} I_{Sh} = 0 \\ V_{Lh} = -Z_L I_h \end{cases} \tag{2.34}$$

However, during grid's voltage perturbation, the gain should be high enough to prevent it to influence the current waveform.

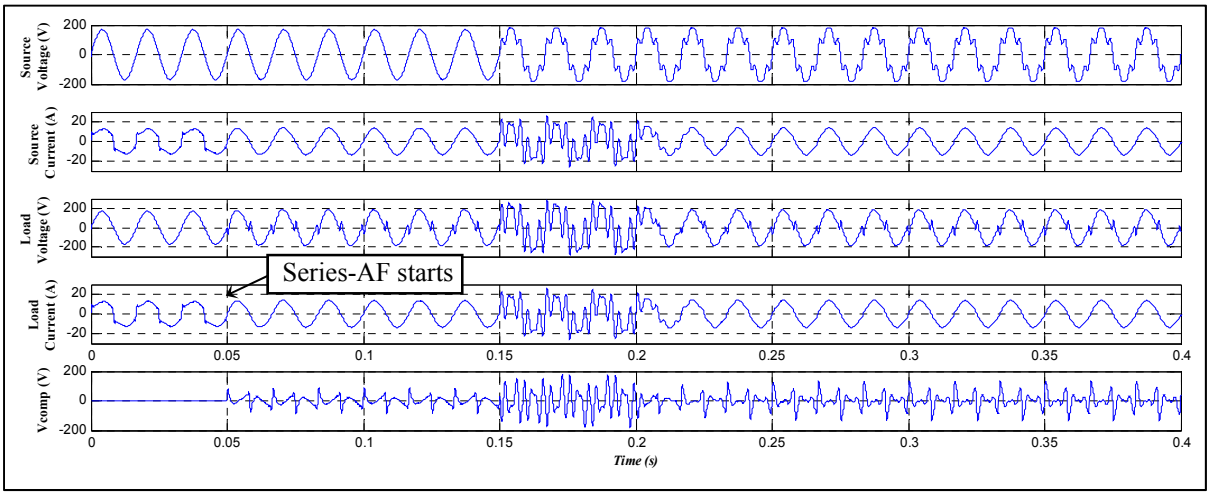

Figure 2.28 Simulation of the ideal system with $V_{Comp}= +G.I_{Sh}-V_{Lh}$

$$G \gg 0 \quad (V_{Sh} \neq 0) \rightarrow \quad \begin{cases} I_{Sh} \approx 0 \\ V_{Lh} \approx -Z_L I_h \end{cases} \tag{2.35}$$

In fact in this approach, the added voltage distortion component is considered as the residual error of the closed loop control of the later section. Thus, it allows achieving a zero steady-state error even with low gain ***G*** values. Figure 2.28 illustrates the simulation for this second approach. The AF starts at 0.05s and even with a low gain ***G*** equal to 3, it compensates bulk of harmonic components and reduces the source current THD before 0.15s.

However, this gain is not sufficient to compensate current harmonics while the source voltage became distorted as shown in Figure 2.28 from 0.15s to 0.4s. Thus, this gain should be increased to prevent voltage harmonics to disturb the current harmonic compensation performance as illustrated in Figure 2.29 between 0.15s and 0.4s.

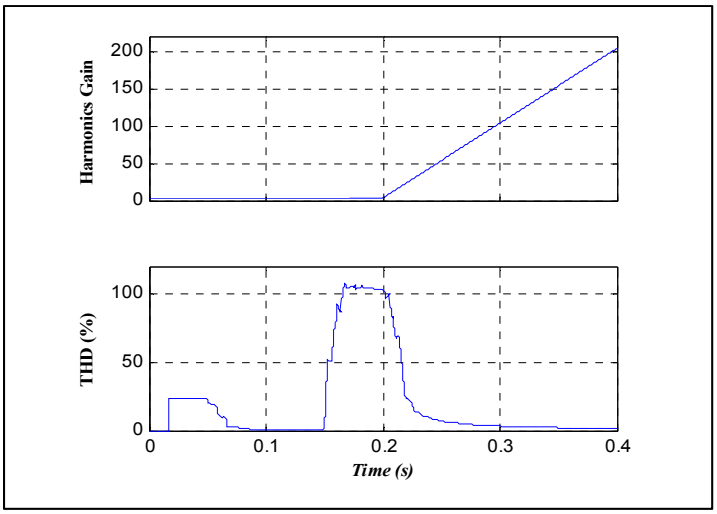

Figure 2.29 Compensating voltage V_{Comp}, the gain G, and the current's THD

2.6.3 Proposed Hybrid Control Approach

As comprehended from previous section, the hybrid compensation is interesting when the grid voltage is clean of any perturbations. However, in this proposed approach the previous hybrid compensation approach will be improved as demonstrated hereafter. With regards to mathematical developments, if the compensating voltage takes into account the source voltage harmonics a novel approach is achieved with improved performances during all kind of perturbations no matter of their origins. This established Hybrid approach gives an unprecedented performance and is less sensitive to the gain value of the current harmonics ***G***.

$$V_{Comp} = +GI_{Sh} - V_{Lh} + V_{Sh} \tag{2.36}$$

By introducing Eqn 2.36 in generic equations; Eqn 2.21 to Eqn 2.23, the source current harmonics as well as load voltage harmonics are obtained.

$$I_{Sh} = \frac{(Z_L I_h + V_{Lh})}{(Z_S + Z_L + G)} \tag{2.37}$$

$$V_{Lh} = Z_L(I_{Sh} - I_h) \tag{2.38}$$

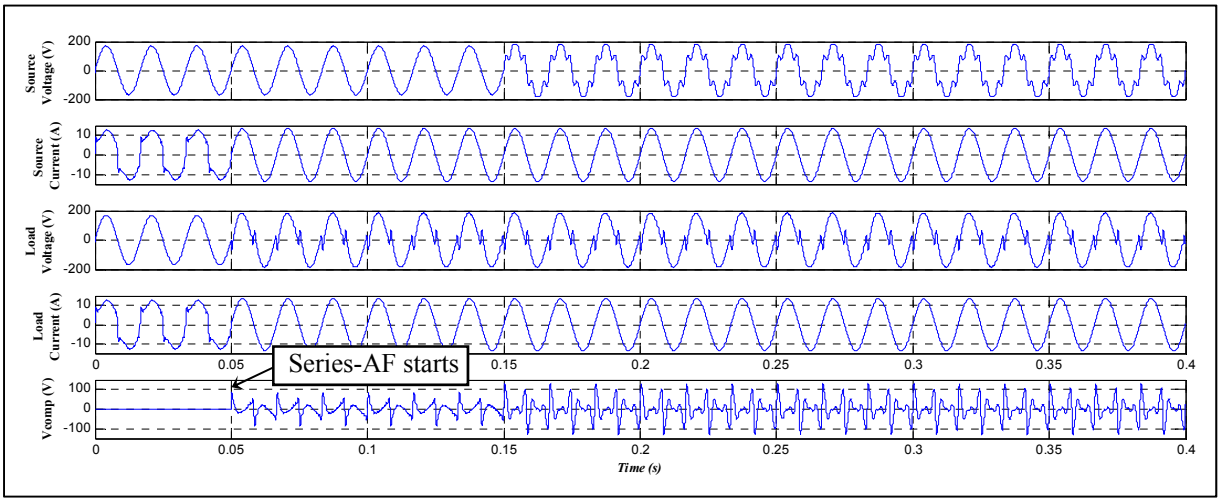

Figure 2.30 Simulation of the system with V_{Comp}= +$G.I_{Sh}$ - V_{Lh}+ V_{Sh}

By solving the previous relations it is clear that the source current harmonic became equal to an absolute zero value and these harmonics are definitely compensated independent of the gain *G*. However, in a practical application with all delays and noises, a minimum and positive value should be set for *G* to ensure the proper operation of the controller. In fact, the gain *G* should be set equal or over the equivalent impedance of the shunt passive filters at harmonic frequencies.

$$I_{Sh} = \frac{+Z_L I_h - Z_L I_h}{Z_S + Z_L + G} = 0 \tag{2.39}$$

The load terminal voltage harmonics are obtained by substituting equation 2.39 in 2.38.

$$V_{Lh} = -Z_L I_h \tag{2.40}$$

As one can recognize the value of load harmonics corresponds to the case where absolutely no current harmonics are flowing into the grid. Furthermore, in this approach even in presence of voltage harmonics the source current remain clean of harmonic component. As

shown in the Figure 2.31, independent of the gain *G*, as far as it has a positive value the controller operates smoothly. And during source voltage distortions it compensates current harmonics and achieves a near zero THD.

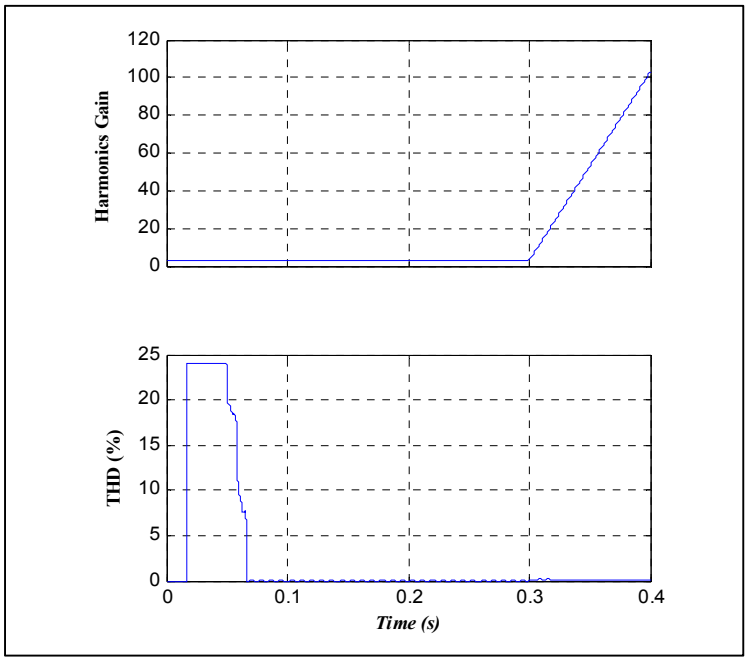

Figure 2.31 Compensation voltage V_{Comp}, the gain *G*, and the source current's THD

The analysis on the developed control principle shows the effectiveness of the control principle in an ideal environment. To properly evaluate the real implementation of this approach the controller is applied to the configuration of Figure 2.23. The Transformerless-SeAF configuration was simulated in MATLAB/Simulink using a discrete time steps of (T_S = 10µs) and mentioned circuit parameters.

The complete results are depicted in Figure 2.32. The compensating voltage reference produced by the proposed hybrid control technique forces the nonlinear loads to draw a sinusoidal current reducing therefore from 26% Total Harmonic Distortion (THD) to less than 2% and keeps this exceptional performance during high source voltage perturbations initiated in the grid supply from 0.15s.

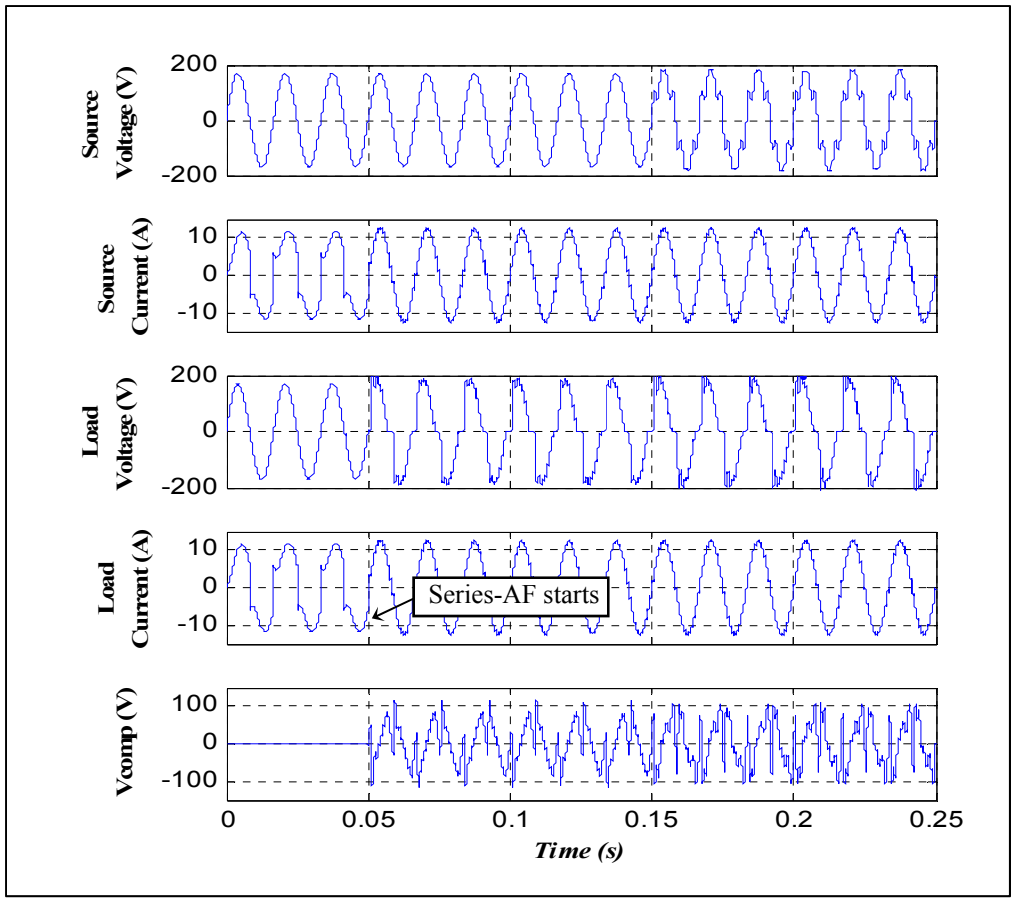

Figure 2.32 SPS response for compensation of a current-fed non-linear load with TSeAF and the proposed Hybrid approach

2.6.4 Laboratory Experimental Results

The performance of the proposed harmonic compensation is also validated through laboratory experimental study. The experimental prototype consists of a Transformerless-SeAF with an H-Bridge converter connected to an auxiliary source in the dc bus. The rapid prototyping board, ds1103 from dSPACE is used to implement and control the converter. The electrical pictogram illustrated in Figure 2.23 is implemented for two types of loads; a current fed type of non-linear load (a diode bridge rectifier followed by a series R-L on the DC side) as well as a voltage fed type of non-linear load (a diode bridge followed by a shunt R-C on the DC side). A PI controller is used to regulate the compensating voltage output by producing the required duty cycle for the PWM modulator.

2.6.4.1 Single-phase Transformerless-SeAF with CSC load

The performance of the proposed hybrid compensation strategy for a CSC type of load is illustrated in the Figure 2.33 captured using an oscilloscope LeCroy 104MXi. This current fed type of nonlinear load was realized using a diode bridge rectifier followed by a RL load (R=12.5 Ω, L=20 *mH*). The load current profile shown in Figure 2.33 has a THD of 25.1%.

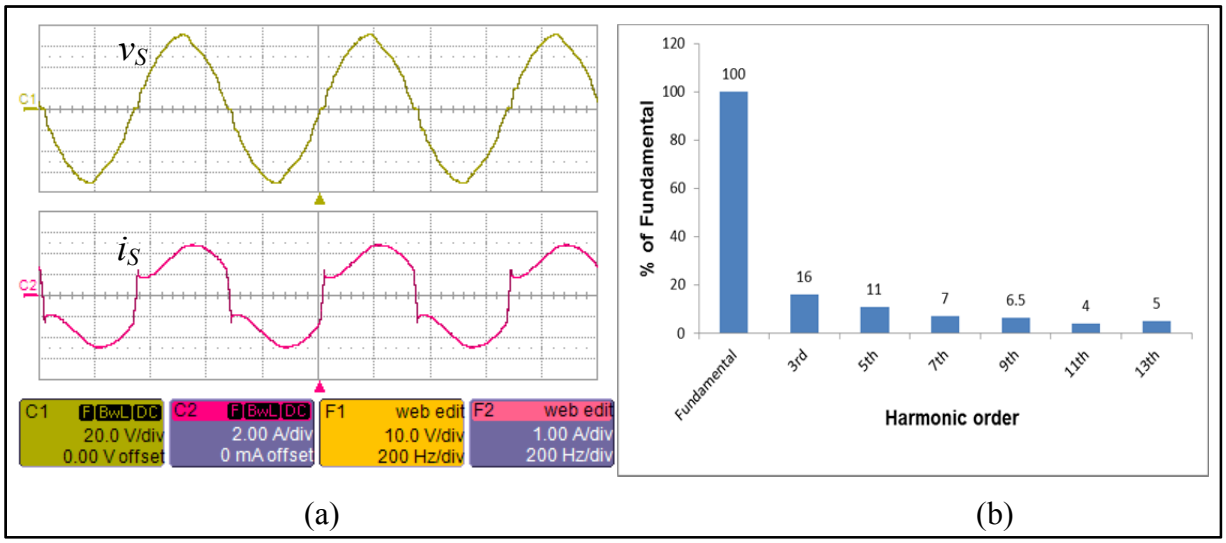

Figure 2.33 The CSC non-linear load profile. (a) Voltage and current waveforms, (b) current harmonic spectrum and individual harmonic values as % of fundamental

While performing the experimental investigation on the TSeAF with Hybrid control approach, an interesting fact on PI controller based series converter is observed. The Figure 2.34 illustrates the results after compensation of the TSeAF. The Series compensator distorts the load's terminal voltage in order to force the nonlinear load to draw a sinusoidal waveform current.

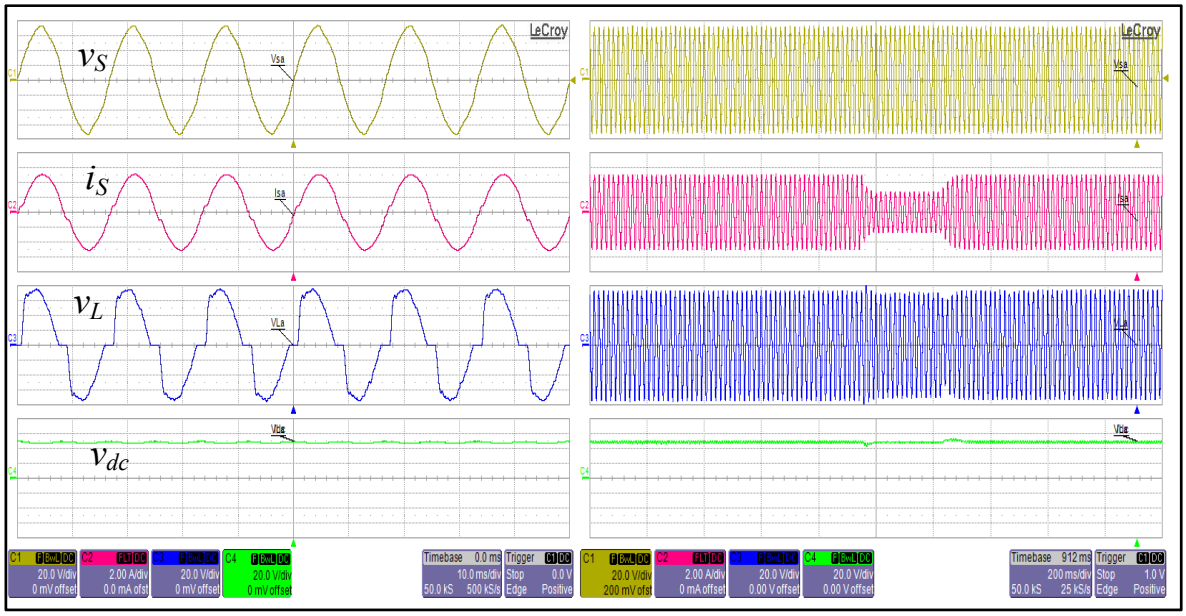

Figure 2.34 Experimental results: Current harmonics compensation of a Hybrid approach for CSC load

The performance of this practical implementation are summarized in the Table 2.4, in which the source current THD decreased to less than 5%.

Table 2.4 Current harmonic compensation using TSeAF for Single-phase CSC load

	Load PCC		**Source**	
Measures	Voltage, V_L (V)	Current, I_L (A)	Voltage, V_S (V)	Current, I_S (A)
THD (%)	21.3	3.8	3.2	3.8
Fund. (rms)	50.3	3.5	50.6	3.5
Active power, P (W)	160		173.7	
Reactive power, Q (var)	70		21	
Power, S (VA)	175		175	
Power Factor, PF (%)	90		99	

2.6.4.2 Single-phase Transformerless-SeAF with VSC load

The behavior of the proposed hybrid compensation strategy for a VSC type of load is illustrated in the following figures. This voltage fed type of nonlinear load was realized using

a diode bridge rectifier followed by a RC load (R=12.5 Ω, L=1000 μF).To limit the current of such loads a small inductance of 0.3mH is used before the rectifier and the essay was performed at reduced voltage. The load current profile shown in Figure 2.35 has a THD of 82.4% with a fundamental magnitude of 8.7 A. This highly polluted current distorts the source voltage by flowing through the grids impedance resulting in a supply voltage distortion of 8.2%.

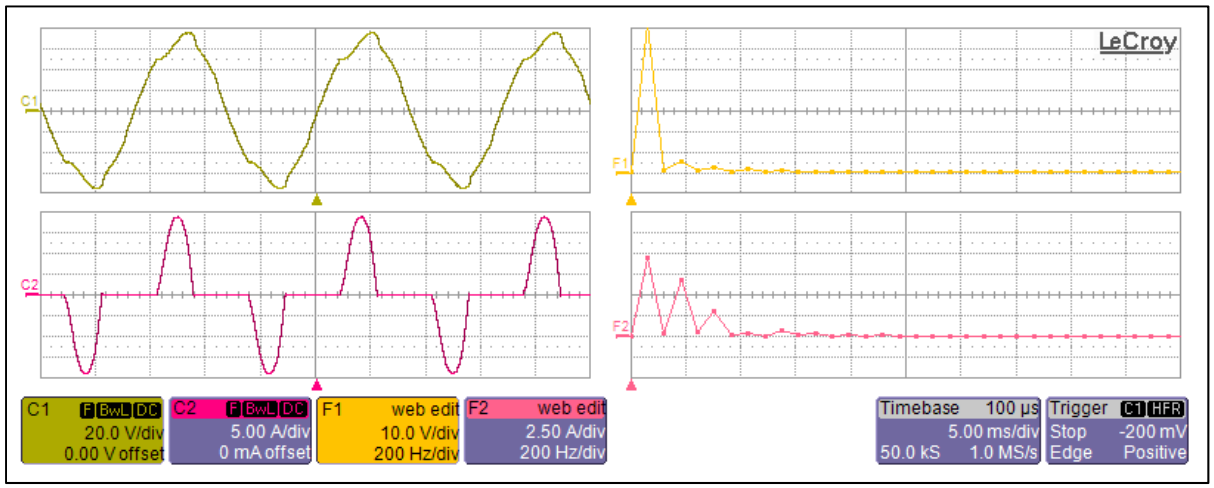

Figure 2.35 The VSC non-linear load profile. (a) Voltage and current waveforms, (b) Respective harmonic spectrum and individual harmonic values

Such highly distorted current have negative influence on voltage quality and thus on other load installed on the same PCC. Cooncequently, the series compensator should produce a compensating voltage in order to force the non-linear load to draw a sinusoidal waveform. Likewise its dual configuration, a diode rectifier connected to a dc capacitor requires a square voltage waveform in order to draw a sinusoidal current. As observed in Figure 2.36, it is practically impossible to produce such a stiff square waveform due to transient response of the converter's LC output filter. Thus, after compensation a discontinuity is observed in the source compensated current. It is important to note that somehow it is practically impossible to eliminate this phenomenon due to a stiff voltage variation required across the load to eliminate this discontinuity. Meanwhile, it is possible to increase the transient behavior of the LC filter which will cost the production of undesirable high frequency harmonics. The

performance of this implementation is tabulated as follow in which the source current THD decreased to less than 8% from 82% before compensation. As a consequence, the source voltage distortion has drastically improved to 3%.

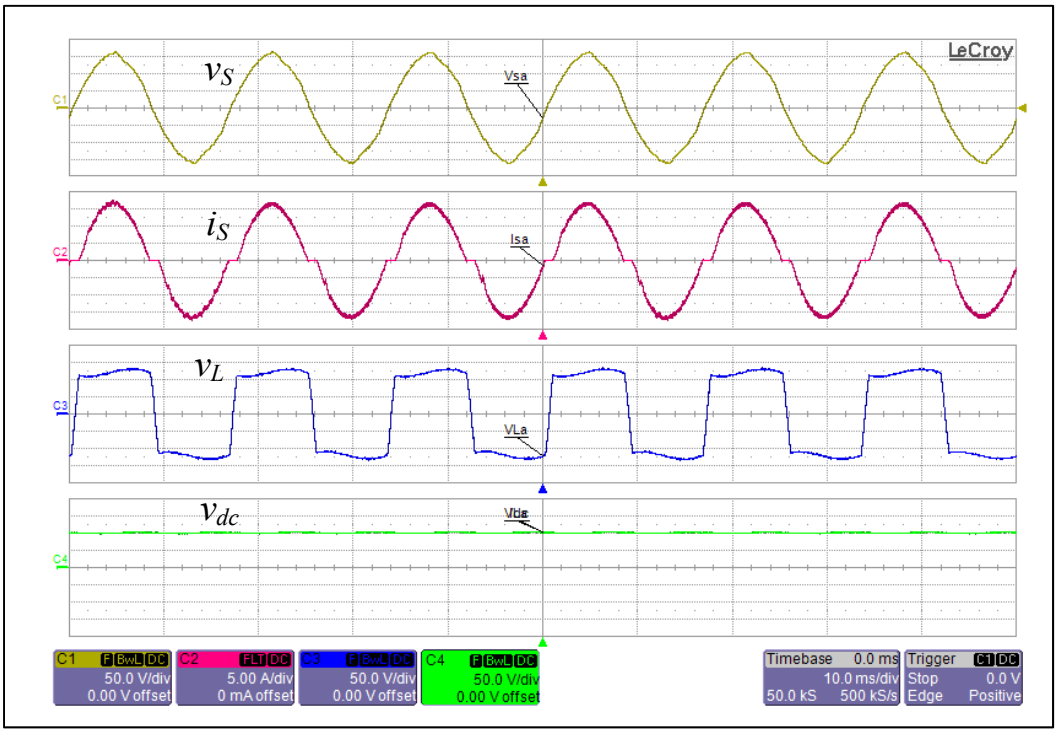

Figure 2.36 Experimental results: Current harmonics compensation of a Hybrid approach for VSC load

Table 2.5 Current harmonic compensation using TSeAF for Single-phase VSC load

	Load PCC		**Source**	
Measures	Voltage, V_L (V)	Current, I_L (A)	Voltage, V_S (V)	Current, I_S (A)
THD (%)	38	7.8	3	7.8
Fund. (rms)	102	12	110	12
Active power, P (W)	1210		1312	
Reactive power, Q (var)	-190		144	
Power, S (VA)	1225		1319	
Power Factor, PF (%)	98 (leading)		99 (lagging)	

2.6.4.3 Three-phase Series active filter with transformer

The performance of the approach for a three-phase application is tested over a conventional three-phase SeAF using isolation transformer shown in Figure 2.37. The SeAF with isolation transformer is used to compensate harmonics of current fed type non-linear load.

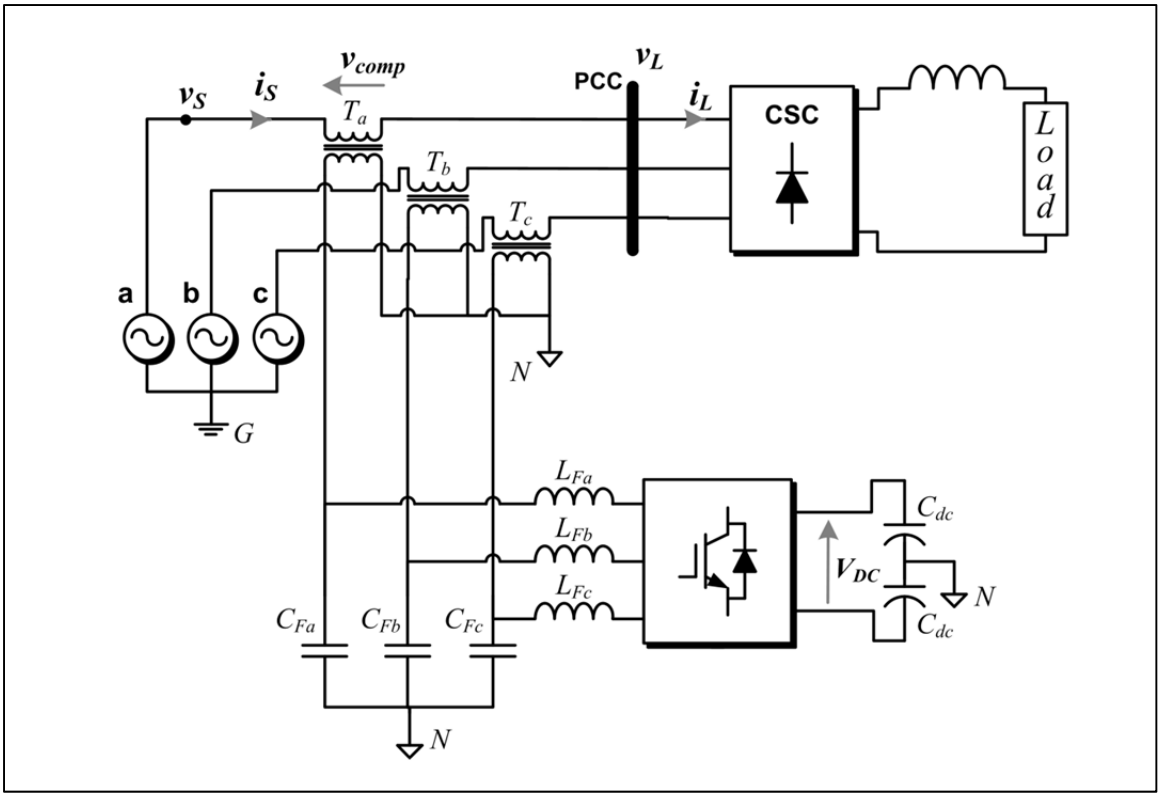

Figure 2.37 Electrical circuit schematic of the Three-phase SeAF compensating current harmonics

The experimental results after compensation of the setup shown in Figure 2.38 are illustrated in Figure 2.39 in which the first pictogram is the oscilloscope recorded waveform for one phase before compensation at nominal voltage and the second is the results after compensation on the same phase. The electrical design of this setup is illustrated in the Appendix II, while the shunt passive filter was disconnected in this application.

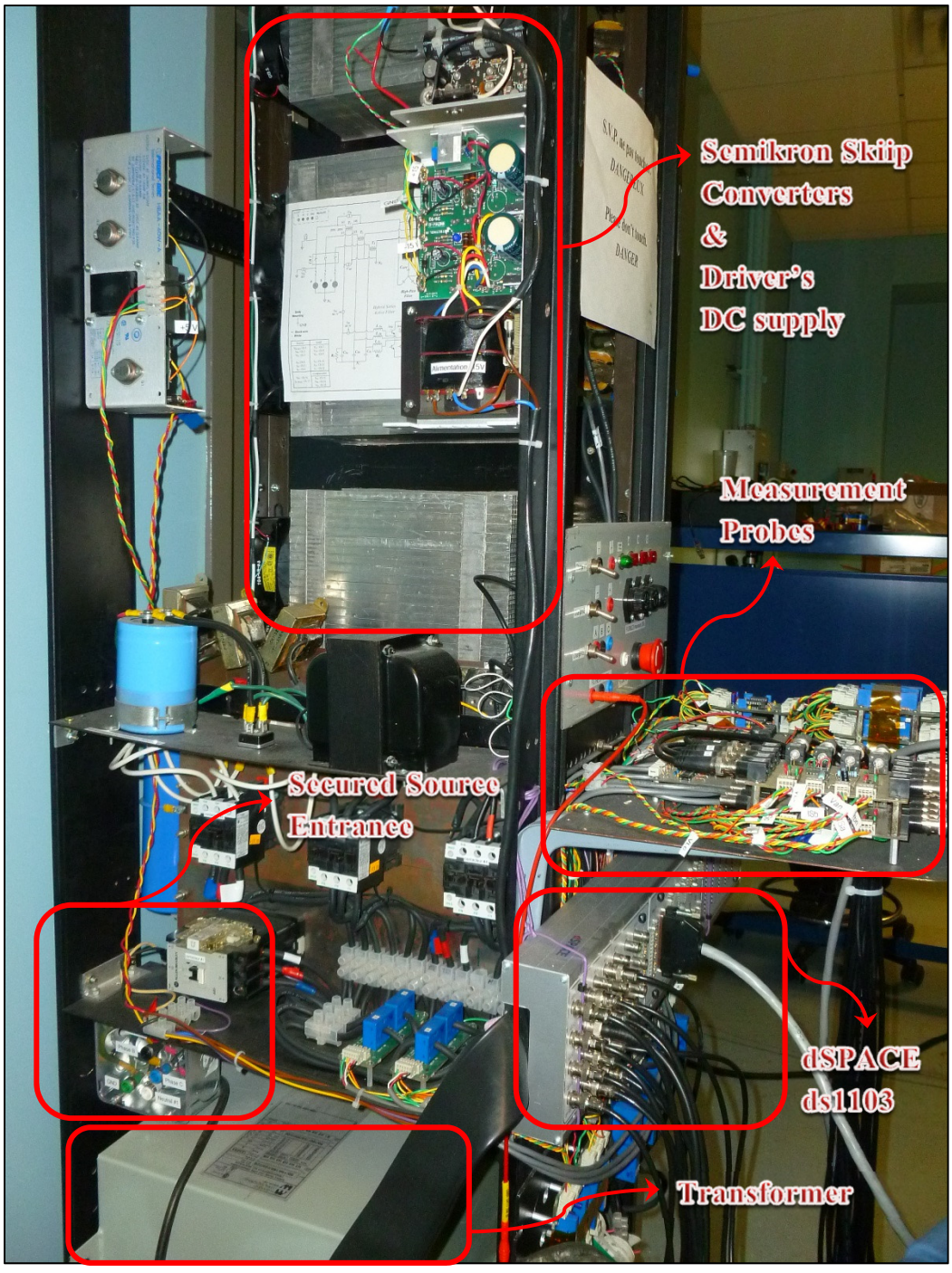

Figure 2.38 Experimental setup of 3P4W SeAF with isolating transformer

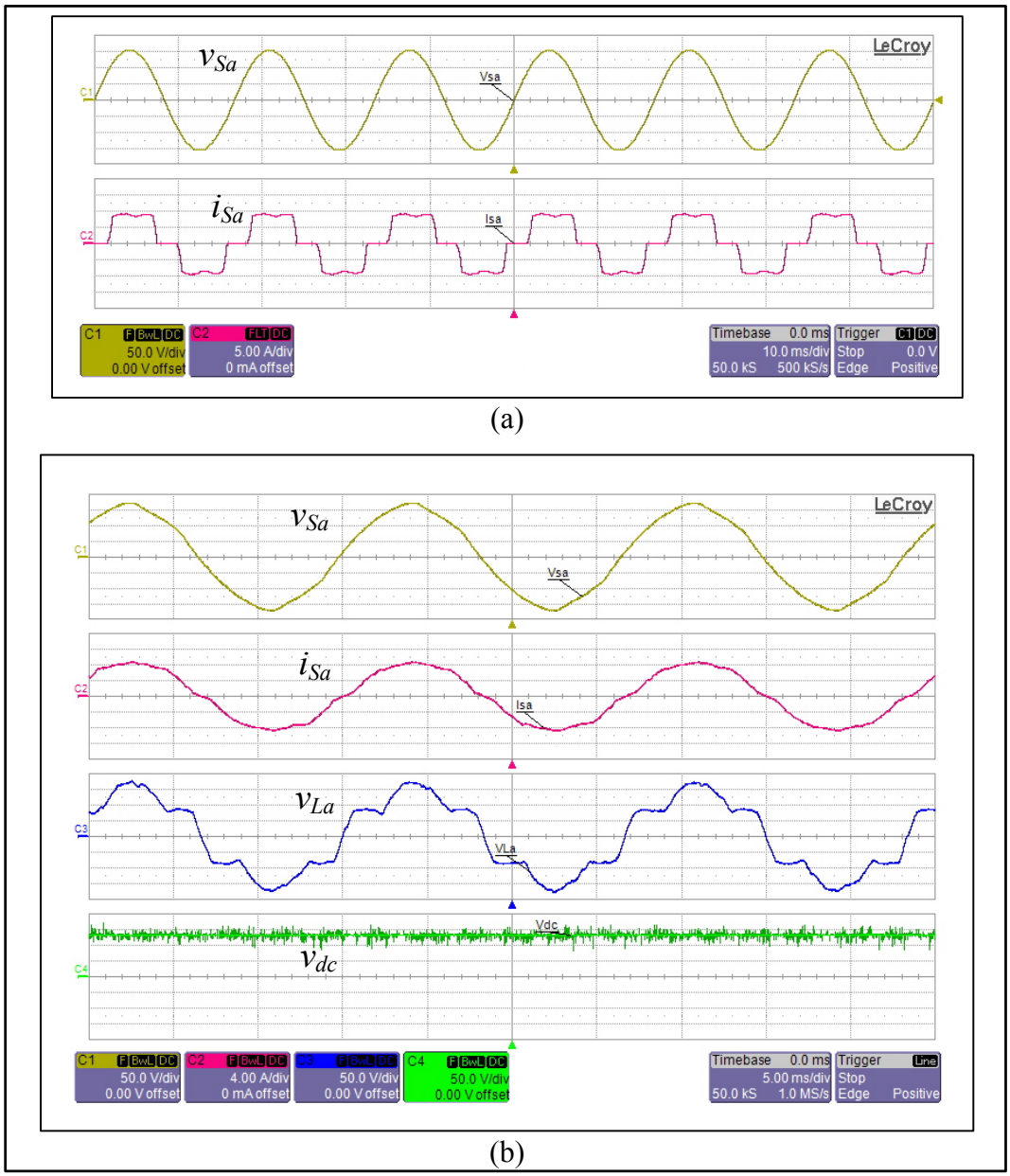

Figure 2.39 Experimental results: voltage (ph-N) and current profile, (a) before compensation, (b) with hybrid compensation

The experimental results of the three phases are depicted in Figure 2.40, illustrating a real-time snapshot of the twelve measured inputs visualized in ControlDesk powered by dSPACE. Moreover, the instantaneous powers are sketched simultaneously on the screen.

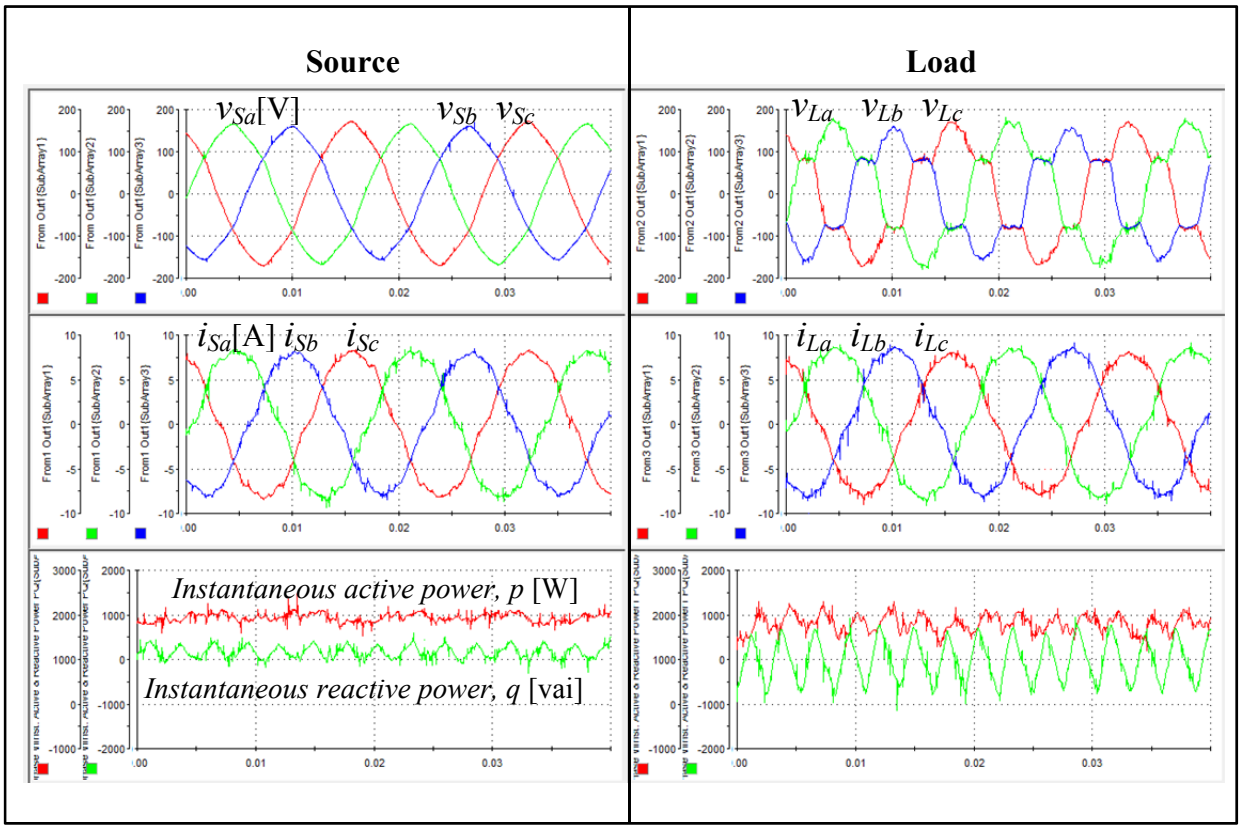

Figure 2.40 Three-phase real-time measurements of the Hybrid compensation performed by DS1103 with sampling time of 40µs

2.7 Control Strategies and Algorithm for the SeAF

The control part shown in Figure 2.41 consists of two distinct main blocks; the signal processing section which is the Active controller or reference detection part (Inner-Loop) and the power processing section or the Controller and Modulator (Outer-Loop). As shown in the Controller schematic, various strategies could be used for the harmonic detection section depending on the objectives and hardware configuration. Finally, the output (reference signals) could be adapted for a three-phase system (three separate signals) or for a single phase system (one dimensional reference). This reference (v_{ref_abc}) is the desired compensating voltage. This signal and the corresponding measurement ($v^{\wedge}_{Comp}$) are both sent to the regulator section, which consists of a Regulator and a Pulse width modulator. This section of the controller is taking care of producing a compensating voltage which follows

with high accuracy the reference input signal. To give an example of stability evaluation in the frequency domain, the controller of a DVR shown in Figure 2.41 is selected as example for this practice. This simple controller is based on a Synchronous Reference Frame (SRF) algorithm to detect anomalies in the grid's voltage.

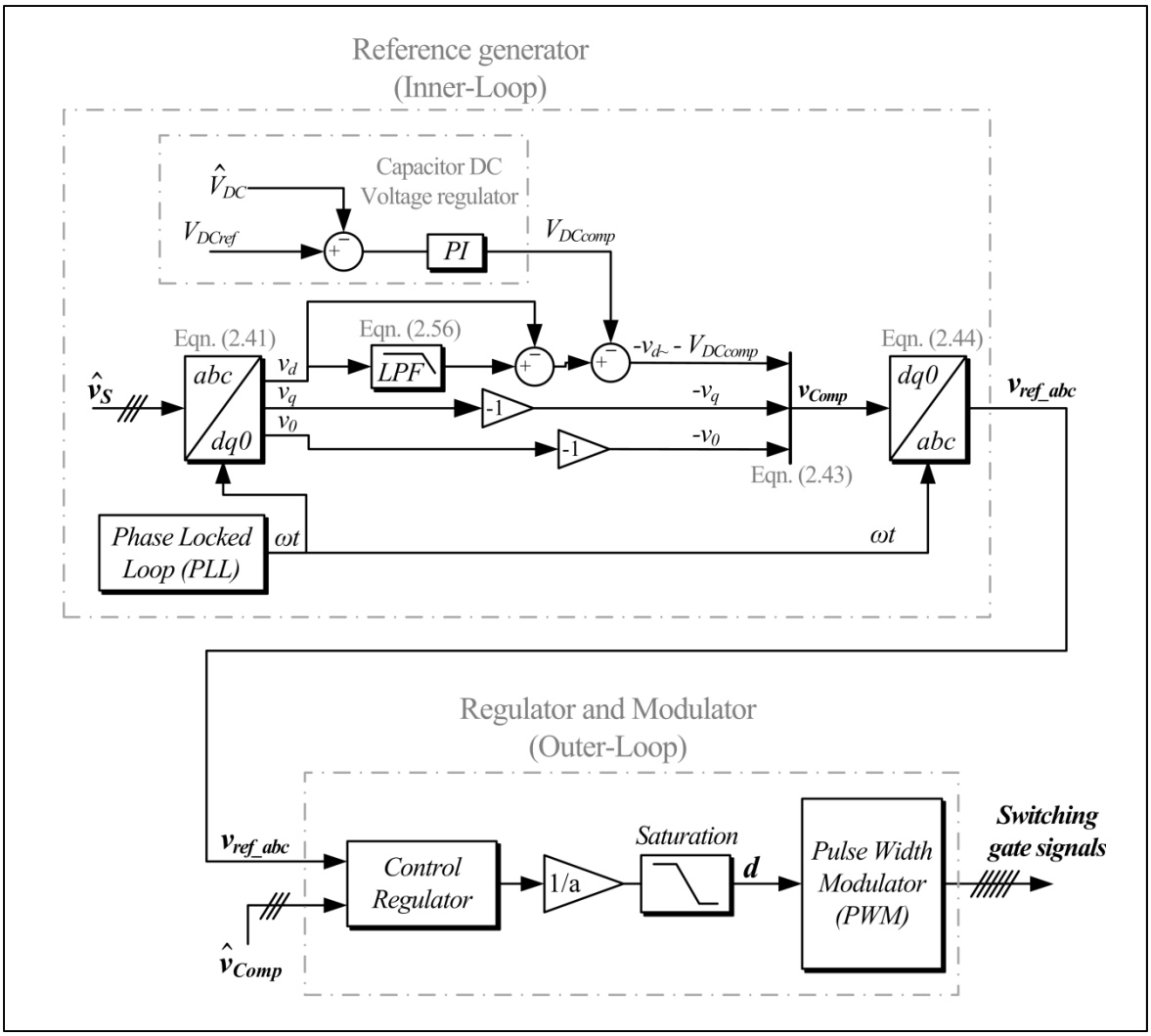

Figure 2.41 Functional block diagram for a three-phase load voltage controller

Many theories have been developed to control active filters and then performing compensation of load voltage; voltage harmonic distortions, unbalances, sag, and swells (Ajaei et al., 2011; Jurado, 2004; Nielsen et al., 2004; Yun Wei et al., 2007b). In this application the Dynamic voltage restorer (DVR) operation ensures a sinusoidal and balanced

voltage for sensitive loads in presence of any perturbation in the distribution system (Nguyen Xuan, Fujita et Horikoshi, 2010). A comprehensive approach which is only used for stability purpose is the Synchronous reference frame (SRF) shown in Figure 2.41. The *dq0* transformation converts the three-phase stationary frame to a synchronous reference frame. Where, the oscillating portions are extracted then compensated. This allows the voltage distortions, sag, swells, and unbalances to be attenuated from the load terminals.

This approach extracts the fundamental, and compensates the remaining unwanted harmonic voltages. By compensating the oscillating portion of the direct voltage and the whole quadrature component, the compensation voltage in *dq* frame is obtained (Eqn 2.43). An inverse Park's transformation (Eqn. 2.44) is required to obtain the three-phase compensation voltage references. Then, the $\boldsymbol{v}_{ref\_abc}$ is given to a PWM or a Hysteresis modulator to generate the gate signals for the converter. The stationary frame quantities are transformed to the synchronous *d-q* frame variables in time domain before the filtering is applied given by

$$\left[v_s^{dq0}(t)\right] = [T][v_s^{abc}(t)] \tag{2.41}$$

where,

$$T(\omega t) = \sqrt{\frac{2}{3}}\begin{bmatrix} \cos(\omega t) & \cos\left(\omega t - \frac{2\pi}{3}\right) & \cos\left(\omega t + \frac{2\pi}{3}\right) \\ \sin(\omega t) & \sin\left(\omega t - \frac{2\pi}{3}\right) & \sin\left(\omega t + \frac{2\pi}{3}\right) \\ 1/\sqrt{2} & 1/\sqrt{2} & 1/\sqrt{2} \end{bmatrix} \tag{2.42}$$

and ω is the angular frequency extracted using a phased locked loop detector. A low-pass filter (LPF) tuned at 30Hz is then used to extract the oscillating portion of the direct components and obtain the compensating voltage in *dq0* coordinates.

$$\left[v_{comp}(t)\right] = \begin{bmatrix} -\tilde{v}_d(t) - V_{DCreg}(t) \\ -v_q(t) \\ -v_0(t) \end{bmatrix} \tag{2.43}$$

And

$$\left[v_{ref}(t)\right] = [T]^{-1} \times \begin{bmatrix} -\tilde{v}_d - V_{DCreg} \\ -v_q \\ -v_0 \end{bmatrix} = [T]^{-1} \times \left[v_{comp}(t)\right] \tag{2.44}$$

This strategy compensates the zero sequence voltage as well as unbalances, leaving only the direct fundamental component (v_{d1}) of the load voltage. To maintain a constant regulated DC bus voltage across the capacitors, a PI controller is therefore used. The required voltage (V_{DCreg}) is then added to the oscillating direct voltage quantity to account for the power losses in the converter.

$$v_L(t) = v_S(t) - v_{comp}(t) = v_{d1}(t) \tag{2.45}$$

In this section the frequency domain of an SRF controller is developed. The developed model could be used for further stability analysis. The transfer function of the Inner –loop excluding the dc regulation is presented in Eqn 2.47. It includes the transform function from *abc* frame time varying quantities to stationary *d-q* frame time varying quantities. In *d-q* frame a low pass filter *LPF* (Eqn. 2.56), is implemented to extract the dc component of v_d given to a reverse *d-q* to *abc* transform. The time-domain synchronous *d-q* frame transformation of a three-phase stationary voltage controller is derived as follow.

$$\begin{bmatrix} -\tilde{v}_d(t) \\ -v_q(t) \\ -v_0(t) \end{bmatrix} = \begin{bmatrix} LPF(t) - 1 & 0 & 0 \\ 0 & -1 & 0 \\ 0 & 0 & -1 \end{bmatrix} \begin{bmatrix} v_d(t) \\ v_q(t) \\ v_0(t) \end{bmatrix} \tag{2.46}$$

There is no assumption in where the same treatment is applied to each component in the stationary frame space resulting in a cross coupling and unequal direct path coefficients.

$$\left[v_{ref}^{abc}(t)\right] = \underbrace{[T]^{-1}\begin{bmatrix} LPF(t)-1 & 0 & 0 \\ 0 & -1 & 0 \\ 0 & 0 & -1 \end{bmatrix}[T]}_{M} \times [v_s^{abc}(t)] \tag{2.47}$$

And

$$\begin{bmatrix} v_{ref}^{a}(t) \\ v_{ref}^{b}(t) \\ v_{ref}^{c}(t) \end{bmatrix} = [M]\begin{bmatrix} v_s^{a}(t) \\ v_s^{b}(t) \\ v_s^{c}(t) \end{bmatrix} \tag{2.48}$$

The full derivation of this transformation is:

$$\boldsymbol{M}(\omega t) = \begin{bmatrix} A & B & C \\ B & D & E \\ C & E & F \end{bmatrix} \tag{2.49}$$

$$A = \frac{2}{3}LPF(t)\cdot\cos^2(\omega t) - 1$$

$$B = \frac{\sqrt{3}}{6}LPF(t)\cdot\sin(2\omega t) - \frac{1}{3}LPF(t)\cdot\cos^2(\omega t)$$

$$C = -\frac{\sqrt{3}}{6}LPF(t)\cdot\sin(2\omega t) - \frac{1}{3}LPF(t)\cdot\cos^2(\omega t)$$

$$D = \frac{2}{3}LPF(t)\cdot cos^2\left(\omega t - \frac{2\pi}{3}\right) - 1$$

$$E = \frac{1}{6}LPF(t)\cdot(2\cos(2\omega t) - 1)$$

$$F = \frac{2}{3}LPF(t)\cdot\cos^2\left(\omega t + \frac{2\pi}{3}\right) - 1$$

To develop the frequency-domain *abc*-Stationary to *dq0* Transformation for the voltage controller described earlier the following theoretical background is adopted. The formal theoretical development of the Laplace domain is as follow regarding that multiplication in the frequency domain is equivalent to a convolution in the time-domain which means:

$$f(t) \otimes g(t) = \int_0^t f(\tau) \cdot g(t-\tau) \cdot d_\tau \tag{2.50}$$

Similarly the following convolution is used in the frequency *s*-domain to obtain following results. Thus, the convolution in s-domain is:

$$L\{f(t) \cdot g(t)\} = \frac{-j}{2\pi} \lim_{T\to\infty} \int_{c-jT}^{c+jT} F(\sigma)G(s-\sigma)d\sigma \qquad (\Re(\sigma) = c) \tag{2.51}$$

Thus the following relation will be employed to find Laplace transform of ***M***.

$$L\{f(t) \cdot \cos(\omega t)\} = L\{f(t)\} \otimes \frac{s}{s^2+\omega^2} = \frac{1}{2}\{F(s+j\omega) + F(s-j\omega)\} \tag{2.52}$$

And

$$L\{f(t) \cdot \sin(\omega t)\} = L\{f(t)\} \otimes \frac{\omega}{s^2+\omega^2} = \frac{j}{2}\{F(s+j\omega) - F(s-j\omega)\} \tag{2.53}$$

In order to simplify the components of the transformation matrix ***M***, the cosine terms could be replaced using algebraic calculations of

$$\cos\left(\omega t \pm \frac{2\pi}{3}\right) = -\frac{1}{2}\cos(\omega t) \mp \frac{\sqrt{3}}{2}\sin(\omega t) \tag{2.54}$$

In Eqn 2.47 the phase separation of one-third cycle (2π/3) between phase voltages should be considered for further calculations. However, for stability analysis these lags do not play a significant role. Assuming G_1 and G_2 being stable functions in Laplace environment having negative real roots, the function *G* would also be stable with negative real parts respectively.

$$G_1(s) = \frac{A}{B} \quad , G_2(s) = \frac{C}{D} \qquad \Rightarrow \qquad G(s) = G_1(s) \cdot G_2(s) = \frac{AB}{CD} \tag{2.55}$$

The second order low pass filter used in great number of controller, the *s*-plane Laplace function is described as follow.

$$L\{LPF(t)\} = K_p + \frac{K_i \omega_c}{s + \omega_c} \tag{2.56}$$

In a specified application such as the one mentioned earlier, the cutoff frequency is tuned at 30Hz and the gains K_p, K_i, and ω_c are set to 25, 0.1, and 5.12 respectively. Substituting Eqn2.54 into Eqn2.47 and apply methods described in Eqn 2.52-3 and 2.56, the Laplace transform of the matrix ***M(s)*** in *s*-plane is achieved. In control system terms, the Inner-loop transfer function described in Figure 2.41 could be illustrated as a Multiple-Input and Multiple-Output (MIMO) system in this case three-input variable control system with the Laplace domain transfer function as follow.

$$\begin{bmatrix} V_{ref}^a(s) \\ V_{ref}^b(s) \\ V_{ref}^c(s) \end{bmatrix} = \begin{bmatrix} M_{11}(s) & M_{12}(s) & M_{13}(s) \\ M_{21}(s) & M_{22}(s) & M_{23}(s) \\ M_{31}(s) & M_{32}(s) & M_{33}(s) \end{bmatrix} \begin{bmatrix} V_s^a(s) \\ V_s^b(s) \\ V_s^c(s) \end{bmatrix} \tag{2.57}$$

The matrix Laplace transfer function ***M(s)*** is the general form of the widespread three-phase SRF control algorithm. A similar manipulations and development could be used for further stability analysis of three-phase control strategies. Note that Eqn. 2.57 shows the general form of the controller allowing cross coupling between control variables through off-diagonal terms. The transfer function constituted of the direct and inverse Park's transformations allows study of its impact on the stability of controllers in the synchronous reference frame systems. A full derivation of the transfer function ***M(s)*** in the *s*-plane is provided in the Appendix-I.

As a further development, the stability of this SRF voltage regulator could be analyzed as follow. A basic criterion of a stable linear system (BIBO) is that the output should stay bounded for any bounded input. Mathematically, this means that to remain stable, all of the poles (roots of the characteristic equation Δ) of the transfer function must have a negative real value. However, a multivariable system (MIMO) is stable if and only if all poles of the transfer function of each terms of the matrix has a negative real part. Thus according the developed terms in the appendix, the reference for each phase is a combination of self and mutual function as follow:

$$V_{ref}^{a}(s) = M_{11}(s)V_{ref}^{a}(s) + M_{12}(s)V_{ref}^{b}(s) + M_{13}(s)V_{ref}^{c}(s) \tag{2.58}$$

It is essential to note that the sum of multiple stable functions will be also a stable function. Accordingly, the stability study must be performed once for each individual transfer function of the transfer function matrix. Following plot shows the zeros and poles of each element of the matrix ***M(s)*** whose entries are given in the Appendix-I. By taking values defined in the previous exercise and according to the position of poles, the roots of all characteristic equations have a negative real part, leading to a stable output.

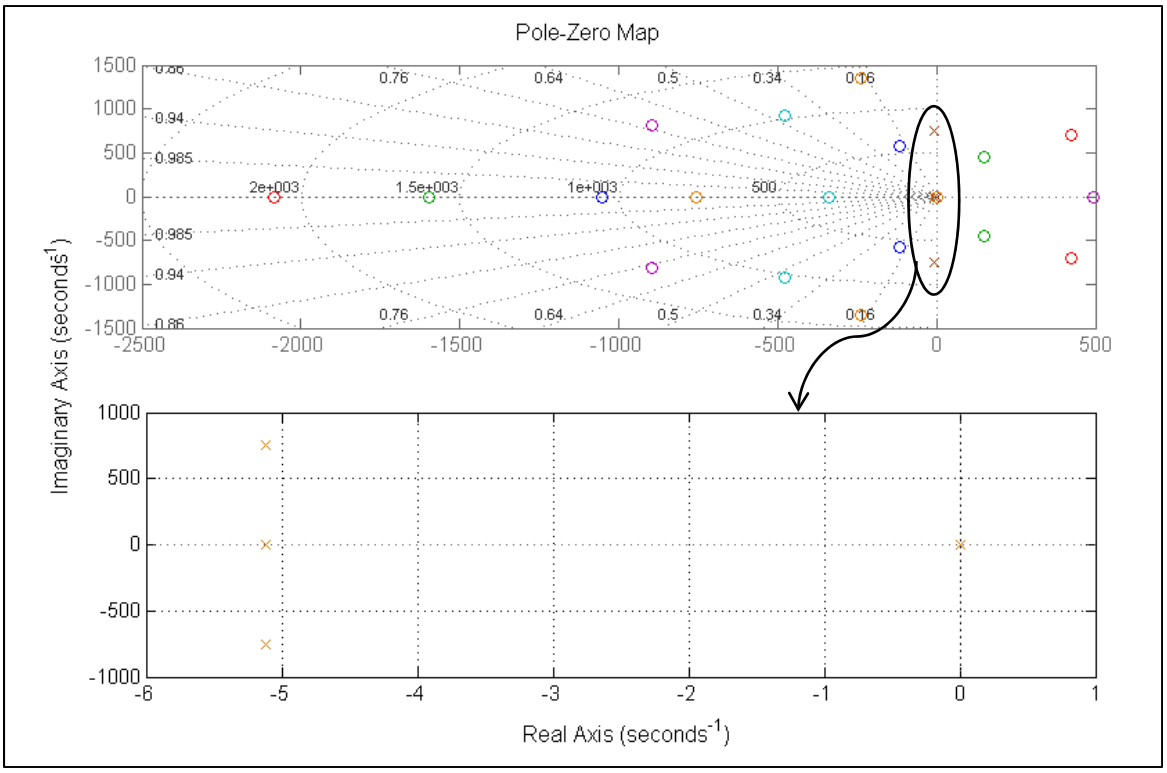

Figure 2.42 Poles and zeros of the transfer function matrix with $K_p = 25$, $K_i = 0.1$, and $\omega_c = 5.12$. (a) Zeros of matrix entries, (b) Poles of matrix terms entries

2.8 Conclusion

In this chapter a comprehensive review of the Series compensator history, key components, various configurations, control strategies, and related involvements in this field have been highlighted. An in-depth and up-to-date literature review on Series active compensation dealing with power quality issues along with related articles was provided. For easy understanding, the operation principle of series compensation has been explained theoretically and results of simulation in Matlab/SPS were also provided. Moreover, the study is pointing out the importance of tuning the converter's output passive filter for an optimal operation. Simulation results were also presented to validate the effects of passive components employed in the series active power filter.

Besides building the first milestone of the basic understanding of a series active power filter (SeAF), a new control approach is proposed and analyzed to improve series harmonic compensation. This novel hybrid harmonic compensation approach developed for non-linear loads reduces the dependency of the compensation to the harmonics current gain. The strategy used to improve the power quality was tested on a single-phase system. Furthermore, it was demonstrated that the presented technique compensates current harmonics coming from a nonlinear load and also regulates the reactive power. To conclude some complementary studies on the stability of the system are carried out along with experimental results. Eventually, the study results in hand tool to select the SeAF components values and ratings into consideration.

CHAPTER 3

A SINGLE-PHASE ACTIVE DEVICE FOR POWER QUALITY IMPROVEMENT OF ELECTRIFIED TRANSPORTATION

3.1 Introduction

In this chapter the application of a Transformerless Hybrid Series Active Filter (THSeAF) is proposed to enhance the power quality in single-phase systems with a current fed type of non-linear load. This chapter assists the energy management and power quality issues related to electric transportation, and focuses on improving electric vehicles loads connection to the grid (Javadi et Al-Haddad, 2015). The control strategy is designed to prevent current harmonic distortions of CSC type of non-linear loads to flow into the utility and corrects the power factor of this later. While, protecting sensitive loads from voltage disturbances, sags, and swells initiated by the power system, ridded of the series transformer, the configuration is advantageous for an industrial implementation. This polyvalent hybrid topology allowing harmonic isolation and compensation of voltage distortions could absorb or inject the auxiliary power to the grid. Beside practical analysis this work also investigates on the influence of gains and delays in the real time controller stability. The simulation and experimental results presented in this chapter were carried out on a 2.2 kVA rated laboratory prototype demonstrating the effectiveness of the proposed topology.

This chapter is organized as follows: The system architecture is introduced in following section. Then the operation principle of the proposed configuration is explained. The third section is dedicated to the modeling and analysis of the control algorithm implemented in this work. The dc voltage regulation and its considerations are briefly explained and the voltage and current harmonic detection method is explicitly described. To evaluate the configuration and the control approach, some scenarios are simulated. Experimental results performed in laboratory are demonstrated to validate simulations. And finally the chapter is summarized with a conclusion.

3.2 Electric Transportation Backbones

The forecast of future Smart Grids associated with electric vehicle charging stations has created a serious concern on all aspects of power quality of the power system, while widespread electric vehicles battery charging units (Jun-Young et Hyung-Jun, 2014; Seung-Hee et al., 2014) have detrimental effects on power distribution system harmonic voltage levels (Staats et al., 1998). On the other hand, the growth of harmonics fed from nonlinear loads like electric vehicle propulsion battery chargers shown in Figure 3.1 (Amjadi et Williamson, 2011; Kuperman et al., 2013), which indeed have detrimental impacts on the power system and affect plant equipment, should be considered in the development of modern grids. Likewise, the increased rms and peak-value of the distorted current waveforms increase heating and losses and cause failure of the electrical equipment. Such phenomenon reduces effectively the system efficiency and should be addressed properly (Akagi et Isozaki, 2012a; Zobaa, 2014).

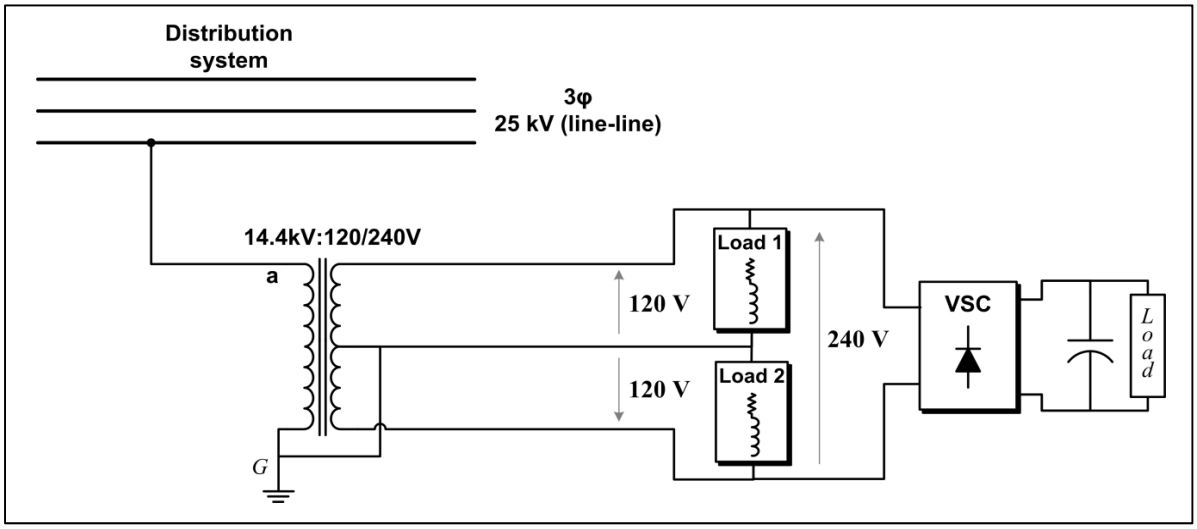

Figure 3.1 Electric diagram of typical North-American distribution system for residential consumers

Moreover, to protect the point of common coupling (PCC) from voltage distortions, using dynamic voltage restorer function is advised. A solution is to reduce the pollution of power electronics based loads directly at their source. Although several attempts are made for

explicit case study, a generic solution is to be explored. Between the two existing types of active power devices to overcome power quality issues, the series type are less scattered than shunt type of active filters (Hamad, Masoud et Williams, 2014; Sixing, Jinjun et Jiliang, 2013). One important advantage of series active filter compared to shunt type is the inferior rating of the compensator versus load nominal rating (Liu et al., 2013). However, the complexity of the configuration and necessity of an isolation series transformer had decelerated their industrial application in distribution system.

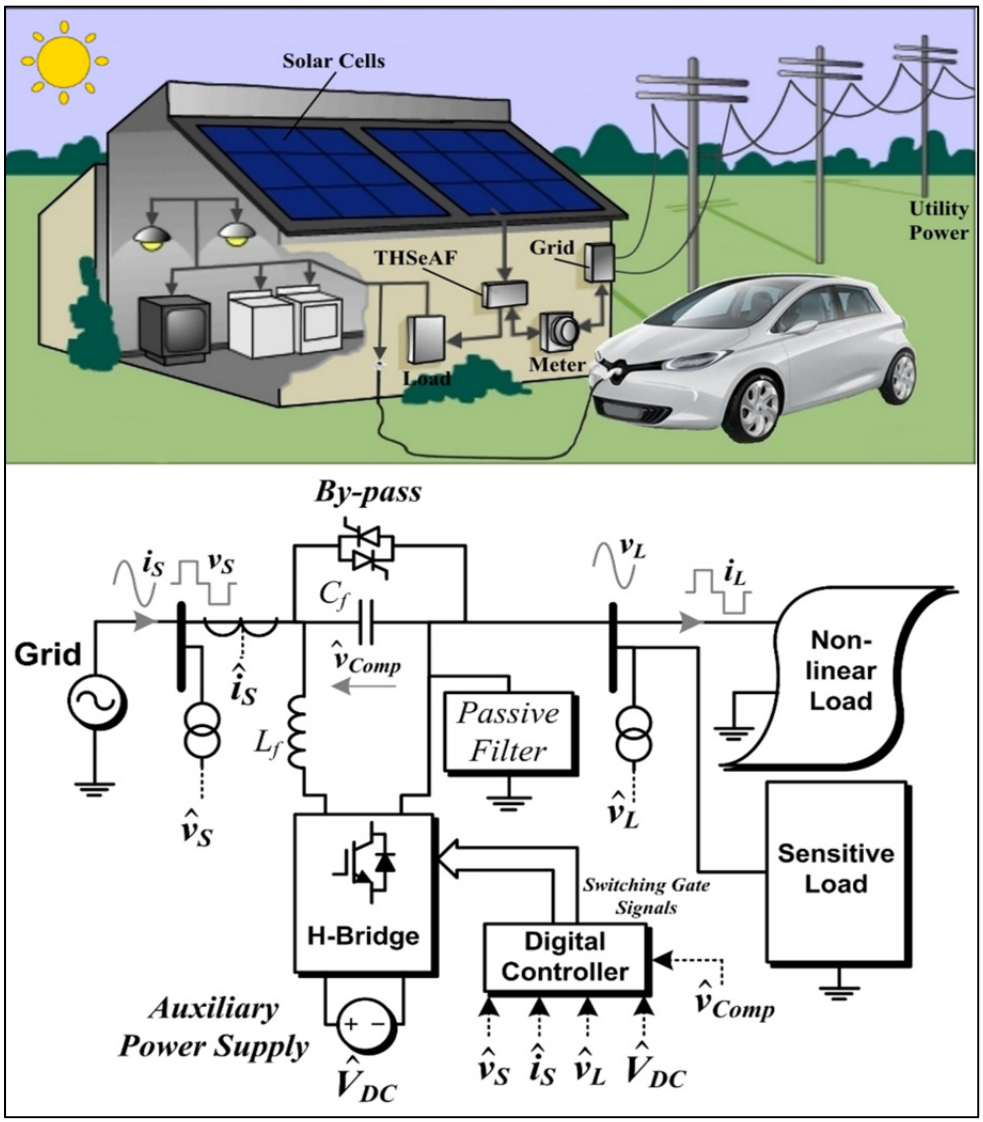

Figure 3.2 a) Schematic of a single-phase smart load with the compensator installation, b) Electrical diagram of the THSeAF in a single-phase utility

Hybrid series active filter (HSeAF) was proposed to address above aforementioned issues with only one combination. Hypothetically, they are capable to compensate current harmonics, ensuring a power factor correction, and eliminating voltage distortions at the PCC (Javadi, Fortin Blanchette et Al-Haddad, 2012a; Senturk et Hava, 2011). These properties make it an appropriate candidate for power quality investments. The three-phase series active filters are well documented (Abu-Rub, Malinowski et Al-Haddad, 2014; Goharrizi et al., 2012), whereas limited research works reported the single-phase applications of series active filters in the literature. The proposed single-phase transformerless-HSeAF is capable of cleaning the grid side connection bus bar from current harmonics generated by a non-linear load (Rahmani, Al-Haddad et Kanaan, 2006). With a smaller rating up to 10%, it could easily replace the shunt active filter (Nogueira Santos et al., 2014). Furthermore, it could restore a sinusoidal voltage at the load point of common coupling. Advantage of the proposed configuration is that non-linear harmonic voltage and current producing loads could be effectively compensated. The THSeAF is an alternative option to conventional power transferring converters in distributed generation systems with high penetration of renewable energy sources, where each phase can be controlled separately and could be operated independently of other phases (Javadi, Fortin Blanchette et Al-Haddad, 2012b). The proposed configuration shows that the separation of a three-phase converter into single-phase H-bridge converters has allowed the elimination of the costly isolation transformer and promotes industrial application for filtering purposes. The setup has shown great ability to perform requested compensating tasks for correction of current and voltage distortions, power factor correction, as well as voltage restoration on the load terminal (Liqun et al., 2014).

3.3 System Architecture

3.3.1 Proposed System Configuration

The transformerless hybrid series active filter shown in Figure 3.2 is consisted of an H-bridge converter connected in series between the source and the load. A shunt passive capacitor

ensures a low impedance path for current harmonics. A DC auxiliary source could be connected to inject power during voltage sags. The DC link energy storage system is described in (Sng, Choi et Vilathgamuwa, 2004). The system is implemented for a rated power of 2200 VA. To ensure a fast transient response with sufficient stability margins over a wide range of operation, the controller is implemented on a dSPACE/dsp1103. The system parameters are identified in Table 3.1. A variable source of 120 Vrms is connected to a 1.1 kVA non-linear load and a 998 VA linear load with a 0.46 power factor. The THSeAF is connected in series in order to inject the compensating voltage. On the DC side of the compensator, an auxiliary dc-link energy storage system is installed. Similar parameters are also applied for practical implementation.

Table 3.1 Configuration parameters

Symbol	**Definition**	**Value**
v_s	Line phase-to-neutral voltage	120 Vrms
f	System frequency	60 Hz
$R_{non\text{-}linear\ load}$	Load resistance	11.5 Ω
$L_{non\text{-}linear\ load}$	Load inductance	20 mH
P_L	Linear load power	1 kVA
PF	Linear load power factor	46 %
L_f	Switching ripple filter inductance	5 mH
C_f	Switching ripple filter capacitance	2 μF
T_S	dSPACE Synchronous sampling time	40 μs
f_{PWM}	PWM frequency	5 kHz
G	Control gain for current harmonics	8 Ω
V_{DCref}*	VSI DC bus voltage of the THSeAF	70 V
PI_G	Proportional gain (K_p), Integral gain (K_i)	0.025(4*), 10 (10*)

* Adopted value for the experimental setup

The HSeAFs are often compensating distortions of current type of non-linear loads. For instance, the distorted current and voltage waveforms of the non-linear system during normal operation and when the source voltage became distorted are depicted in Figure 3.3. The THSeAF is bypassed ($v_L = v_S$) and current harmonics flew directly into the grid. As one can perceive, even during normal operation the current harmonics (with a THD of 12%) distort the PCC, resulting in voltage THD of 3.2%. The behavior of the system when the grid is highly polluted with 19.2% of THD is also illustrated. The proposed configuration could be solely connected to the grid with no need of a bulky and costly series injection transformer, making this topology capable of compensating source current harmonics and voltage distortion at the point of common coupling. Even if the number of switches has increased, the transformerless configuration is more cost-effective than any other series compensators, which generally uses a transformer to inject the compensation voltage to the power grid. The passive filter is composed of a 5th, 7th, and a High-pass filter.

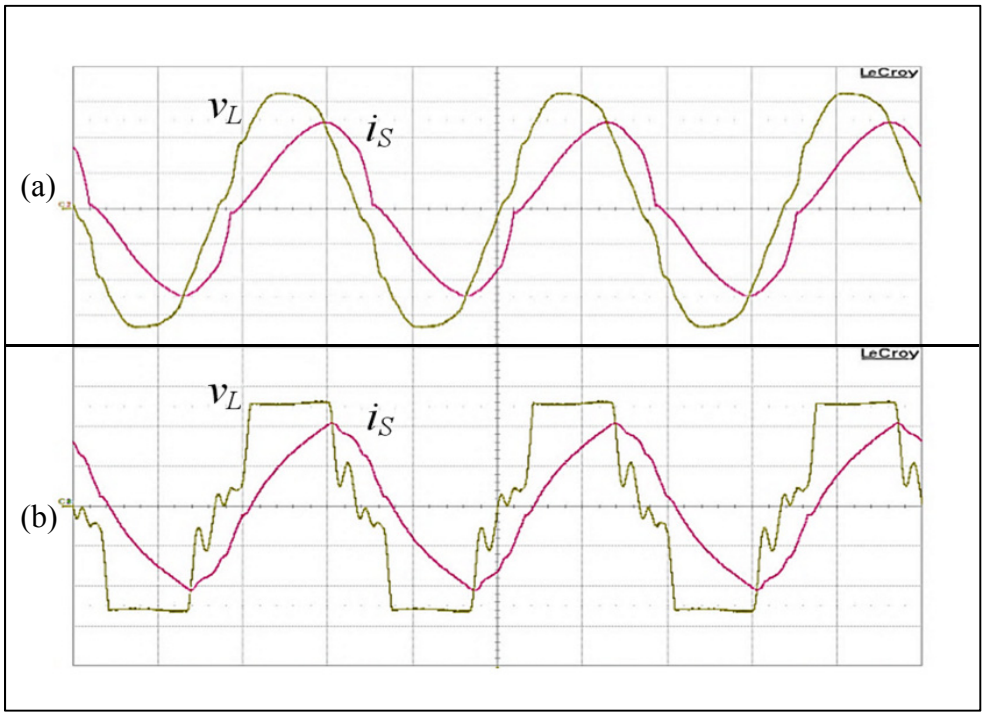

Figure 3.3 Terminal voltage and current waveforms of the 2kVA single-phase system without compensator. a) Regular operation, b) Grid's voltage distortion (scales: 50 V/div for channel 1 and 10 A/div for channel 2)

A comparison between different existing configurations is given in Table 3.2. It is aimed to point out the advantages and disadvantages of the proposed configuration over the conventional topologies. To emphasize the comparison Table fairly, equivalent single-phase of each configuration is considered in the evaluation. Financial production evaluation demonstrated a 45% reduction in components costs and considerable reduction in assembly terms as well.

3.3.2 Operation Principle

The series active filter represents a controlled voltage source (VSI). In order to prevent current harmonics i_{Lh} to drift into the source, this series source should present low impedance for the fundamental component and high impedance for all harmonics as shown in Figure 3.4. The principle of such modeling is well documented in (Fujita et Akagi, 1991c). The use of a well-tuned passive filter is then, mandatory to perform compensation of current issues and maintaining a constant voltage free of distortions at the load terminals. The behavior of the series active filter (SeAF) for a current control approach is evaluated from the equivalent circuit shown below. The non-linear load could be modeled by a resistance representing the active power consumed and a current source generating current harmonics. Accordingly, the impedance Z_L represents the non-linear load and the inductive load.

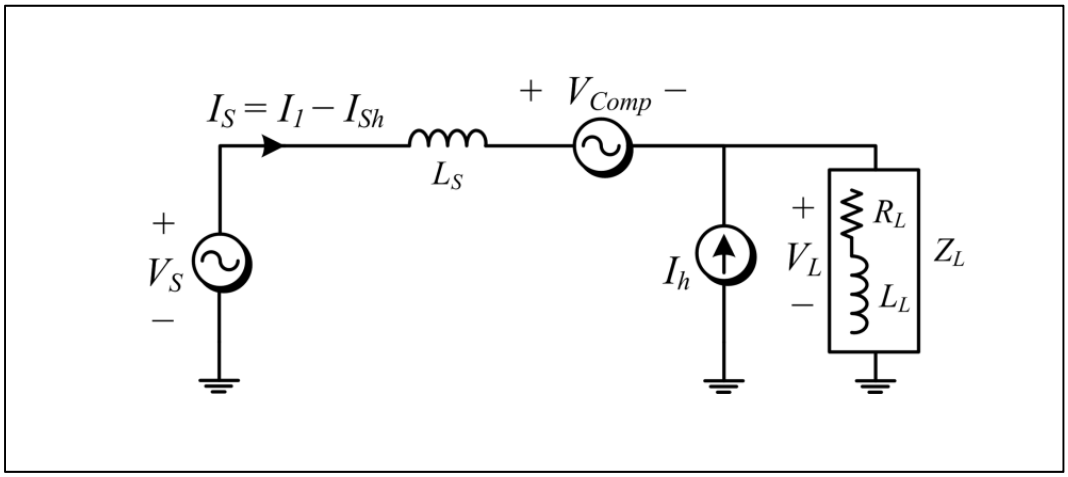

Figure 3.4 THSeAF equivalent circuit for current harmonics

Table 3.2 Comparison of single-phase THSeAF to prior HSeAFs

Definition	**Proposed THSeAF**	**(Varschavsky, Dixon et Rotella, 2010)**	**(Salmero et Litra, 2010)**	**(Senturk et Hava, 2011)**
Injection Transformer	Non	2 per phase	1 per phase	1 per phase
# of semiconductor devices	4	8	4	4
# of DC link storage elements	1+Aux. Pow.	1	2	1+Aux. Pow.
AF rating to the load power	10-30%	10-30%	10-30%	10-30%
Size and weight, regarding the transformer, power switches, drive circuit, heat sinks, etc.	The Lowest	High	Good	Good
Industrial production costs	The Lowest	High	Low	Low
Power losses, including switching, conducting, and fixed losses	Low	Better	Low	Low
Reliability regarding independent operation capability	Good	Low	Good	Good
Harmonic correction of Current source load	Good	Good	Good	Low
Voltage Harmonic correction at load terminals	Good	Better	Good	Good
Power factor correction	Yes	Yes	Yes	No
Power injection to the grid	Yes	No	No	Yes

The series active filter operates as an ideal controlled voltage source (V_{comp}) having a gain (G) proportional to the current harmonics (I_{sh}) flowing through the grid (V_s).

$$V_{comp} = G.I_{sh} - V_{Lh} \tag{3.1}$$

This allows having individual equivalent circuit for the fundamental and harmonics:

$$V_{source} = V_{s1} + V_{sh} \quad , \quad V_L = V_{L1} + V_{Lh} \tag{3.2}$$

The source harmonic current could be evaluated.

$$V_{sh} = -Z_s.I_{sh} + V_{comp} + V_{Lh} \tag{3.3}$$

$$V_{Lh} = Z_L(I_h - I_{sh}) \tag{3.4}$$

Combining Eqn3.3 and 3.4 leads to the following result:

$$I_{sh} = \frac{V_{sh}}{(G - Z_s)} \tag{3.5}$$

If gain G is sufficiently large ($G \rightarrow \infty$), the source current will became clean of any harmonics ($I_{sh} \rightarrow 0$). This will help improving the voltage distortion at the grid side. In this approach the THSeAF behave as high impedance open circuit for current harmonics, while the shunt high pass filter tuned at the system frequency, creates a low-impedance path for all harmonics and open circuit for the fundamental; it also help for power factor correction.

3.4 Modeling and Control of the Single-Phase THSeAF

3.4.1 Small-signal Modeling

Based on the average equivalent circuit of an inverter (Singh, Chandra et Al-Haddad, 2015), the small-signal model of the proposed configuration can be obtained as of Figure 3.5. Hereafter, d is the duty cycle of the upper switch during a switching period, whereas $\bar{v}$ and $\bar{\imath}$

denotes the average values in a switching period of the voltage and current of the same leg. The mean converter output voltage and current are expressed by Eqn. 3.6 and 3.7 as follow.

$$\bar{v}_O = \underbrace{(2d-1)}_{m} \cdot V_{DC} \tag{3.6}$$

And

$$\bar{\imath}_{DC} = m\bar{\imath}_f \tag{3.7}$$

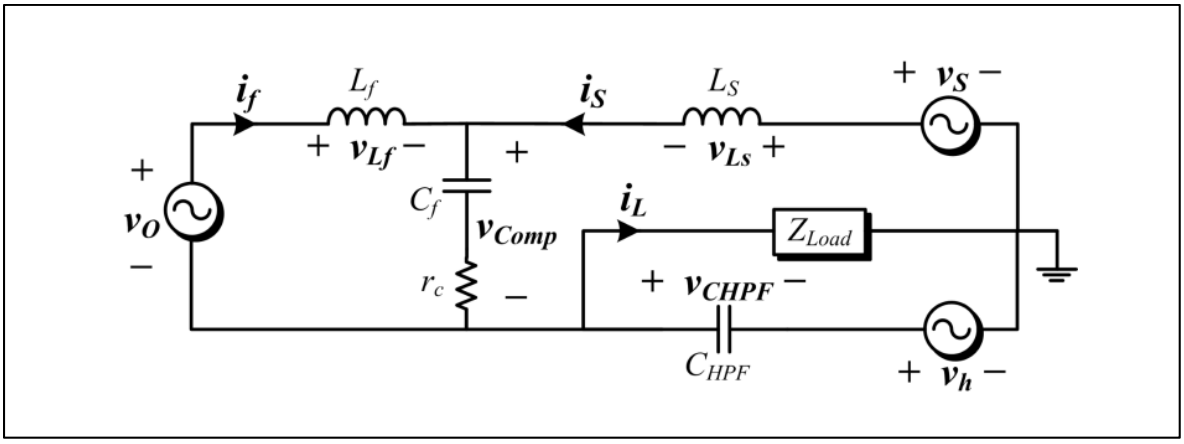

Figure 3.5 Small-signal model of transformerless HSeAF in series between the Grid and the load

Calculating the Thévenin equivalent circuit of the harmonic current source leads to the following assumption.

$$\bar{v}_h(j\omega) = \frac{-j\bar{\imath}_h}{C_{HPF} \cdot \omega_h} \tag{3.8}$$

If the harmonic frequency is high enough, it is possible to assume that there will be no voltage harmonics across the load. The state-space small-signal ac model could be derived by a linearized perturbation of averaged model as follow:

$$\dot{x} = Ax + Bu \tag{3.9}$$

Hence we obtain:

$$\frac{d}{dt}\begin{bmatrix} \bar{v}_{Cf} \\ \bar{v}_{CHPF} \\ \bar{\imath}_S \\ \bar{\imath}_f \\ \bar{\imath}_L \end{bmatrix} = \begin{bmatrix} 0 & 0 & {}^{1}/_{C_f} & {}^{1}/_{C_f} & 0 \\ 0 & 0 & {}^{1}/_{C_{HPF}} & 0 & {}^{-1}/_{C_{HPF}} \\ {}^{-1}/_{L_S} & {}^{-1}/_{L_S} & {}^{-r_c}/_{L_S} & {}^{-r_c}/_{L_S} & 0 \\ {}^{-1}/_{L_f} & 0 & {}^{-r_c}/_{L_f} & {}^{-r_c}/_{L_f} & 0 \\ 0 & {}^{1}/_{L_L} & 0 & 0 & {}^{-R_L}/_{L_L} \end{bmatrix} \times \begin{bmatrix} \bar{v}_{Cf} \\ \bar{v}_{CHPF} \\ \bar{\imath}_S \\ \bar{\imath}_f \\ \bar{\imath}_L \end{bmatrix} + \begin{bmatrix} 0 & 0 & 0 \\ 0 & 0 & 0 \\ {}^{1}/_{L_S} & 0 & {}^{1}/_{L_S} \\ 0 & {}^{m}/_{L_f} & 0 \\ 0 & 0 & {}^{-1}/_{L_L} \end{bmatrix} \times \begin{bmatrix} \bar{v}_S \\ V_{DC} \\ \bar{v}_h \end{bmatrix} \tag{3.10}$$

And the output vector is:

$$y = Cx + Du \tag{3.11}$$

Or

$$\begin{bmatrix} \bar{v}_{comp} \\ \bar{v}_L \end{bmatrix} = \begin{bmatrix} 1 & 0 & r_c & r_c & 0 \\ 0 & 1 & 0 & 0 & 0 \end{bmatrix} \times \begin{bmatrix} \bar{v}_{Cf} \\ \bar{v}_{CHPF} \\ \bar{\imath}_S \\ \bar{\imath}_f \\ \bar{\imath}_L \end{bmatrix} + \begin{bmatrix} 0 & 0 & 0 \\ 0 & 0 & -1 \end{bmatrix} \times \begin{bmatrix} \bar{v}_S \\ V_{DC} \\ \bar{v}_h \end{bmatrix} \tag{3.12}$$

By means of Eqn. 3.10 and Eqn 3.12, the state-space representation of the model in Figure 3.5 is obtained. The transfer function of the compensating voltage versus the load voltage, $T_{V\_CL}(s)$, and the source current, $T_{CI}(s)$, could as well be derived as follow. For the sake of simplicity the resistance r_c of the switching capacitor filter C_f is neglected and the L_f is a linear inductance. The relation of load voltage (V_L) and grid voltage (V_S) are obtained.

$$T_{V_{LS}}(s) = \frac{V_L(s)}{V_S(s)} = \frac{Z_{Load}}{L_S + Z_{out} + Z_{Load}} = \tag{3.13}$$
$$= \frac{L_f L_L C_f s^3 + L_f R_L C_f s^2 + L_L s + R_L}{A + B + C + D + E + F}$$

$$A = L_f L_L L_S C_f C_{HPF} s^5 \quad , \quad B = L_f L_S R_L C_f C_{HPF} s^4$$
$$C = \left(L_f L_L C_f + L_f L_L C_{HPF} + L_f L_S C_f + L_L L_S C_{HPF}\right) s^3$$
$$D = \left(L_f R_L C_f + L_f R_L C_{HPF} + L_S R_L C_{HPF}\right) s^2$$
$$E = \left(L_f + L_L + L_S\right) s \quad , \quad F = R_L$$

The steady-state transfer function between the load voltage (V_L) and compensating voltage (V_{Comp}) is obtained.

$$T_{V_{CL}}(s) = \frac{V_{Comp}}{V_L} = \frac{Z_{out}}{Z_{Load}} = \frac{L_f L_L C_{HPF} s^3 + L_f R_L C_{HPF} s^2 + L_f s}{L_f L_L C_f s^3 + L_f R_L C_f s^2 + L_L s + R_L} \tag{3.14}$$

To control the active part independently the derived transfer function should be autonomous from the grid configuration. The transfer function T_{Vm} presents the relation between the output voltages of the converter versus the duty cycle of the first leg converter's upper switch.

$$T_V(s) = \frac{V_{Comp}}{V_O} = \frac{r_C C_f s + 1}{L_f C_f s^2 + r_C C_f s + 1} \tag{3.15}$$

Thus we have,

$$T_{Vm}(s) = \frac{V_{Comp}}{m} = V_{DC} \cdot T_V(s) \tag{3.16}$$

A DC auxiliary source should be employed to maintain an adequate supply on the load terminals. During the sag or swell conditions, it should absorb or inject power to keep the

voltage magnitude at the load terminals within a specified margin. However, if the compensation of sags and swells is less imperative, a capacitor could be deployed. Consequently, the DC-link voltage across the capacitor should be regulated as demonstrated in Figure 3.6.

3.4.2 Voltage and Current Harmonic Detection

The outer-loop controller is used where a capacitor replaces the DC auxiliary source. This control strategy is well explained in the previous section. The inner-loop control strategy is based on an indirect control principle. A Fast Fourier Transformation (FFT) was used to extract magnitude and phase of the fundamental component of the source current. The control gain *G* representing the impedance of the source for current harmonics, has a sufficiently level to clean the grid from current harmonics fed through the non-linear load.

The second PI controller used in the outer loop, was to enhance the effectiveness of the controller when regulating the DC bus. Thus a more accurate and faster transient response was achieved without compromising compensation behavior of the system. According to the theory, the gain G should be kept in a suitable level, preventing the harmonics flows into the grid (Salmero et Litra, 2010; Salmeron et Litran, 2010). As previously discussed, for a more precise compensation of current harmonics, the voltage harmonics should also be considered. The compensating voltage for current harmonic compensation is obtained from Eqn 3.17.

$$v_{comp_i}(t) = (-G\hat{\imath}_S + \hat{v}_L) - [|-Gi_{S1} + v_{L1}| \cdot \sin(\omega_S t - \theta)] \tag{3.17}$$

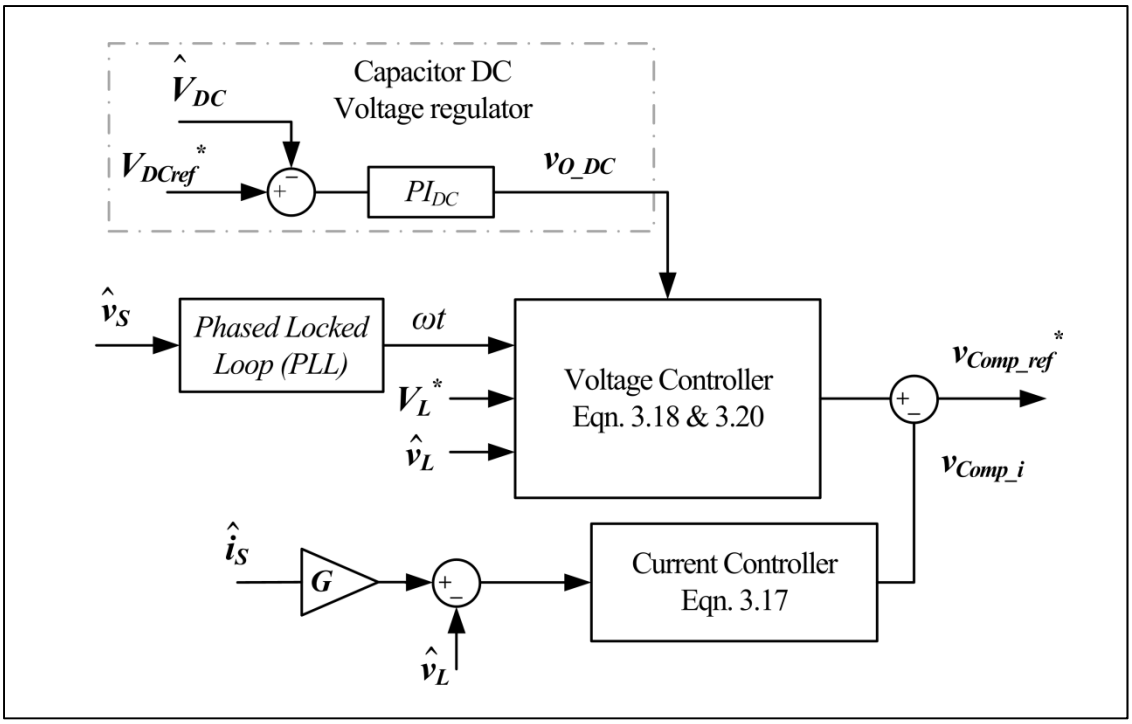

Figure 3.6 Control system scheme of the active part

Hereby, as voltage distortion at the load terminals is not desired, the voltage sag and swell should also be investigated in the inner-loop. The closed loop equation (3.18) allows to indirectly maintain the voltage magnitude at load side equal to V_L* as a predefined value, within acceptable margins.

$$v_{comp_v} = \hat{v}_L - V_L^* \sin(\omega_S t) \tag{3.18}$$

The control scheme for the THSeAF presented in Figure 3.6 was used and implemented in MATLAB/Simulink for real-time simulations and calculation of the compensating voltage. The real-time toolbox of dSPACE was used for compilation and execution on the dsp-1103 control board. The source and load voltages together with the source current are considered as system input signals. According to (Srianthumrong, Fujita et Akagi, 2002), an indirect control increases the stability of the system. The source current harmonics are obtained by extracting the fundamental component from the source current.

$$v^*_{comp_{ref}} = v_{comp_v} - v_{comp_i} + v_{DC_{ref}} \tag{3.19}$$

As explained previously, if the DC capacitor replaces the auxiliary source the DC regulation loop should be added. The v_{DC_ref} is the voltage required to maintain the DC bus voltage constant.

$$v_{DC_{ref}}(t) = V_{O_{DC}} \cdot \sin(\omega_S t) \tag{3.20}$$

A phase-locked loop (PLL) was used to obtain the reference angular frequency (ω_s). Accordingly, the extracted current harmonic $\hat{\imath}_{sh}$ contains a fundamental component synchronized with the source voltage in order to correct the power factor (PF). This current represents the reactive power of the load. The gain G representing the resistance for harmonics converts current into a relative voltage. The generated reference voltage v_{comp_i} required to clean source current from harmonics is described in Eqn 3.17. According to the presented detection algorithm, the compensated reference voltage $v^*_{Comp\_ref}$ is calculated. Thereafter, the reference signal is compared with the measured output voltage and applied to a PI controller to generate the corresponding gate signals as depicted in Figure 3.7.

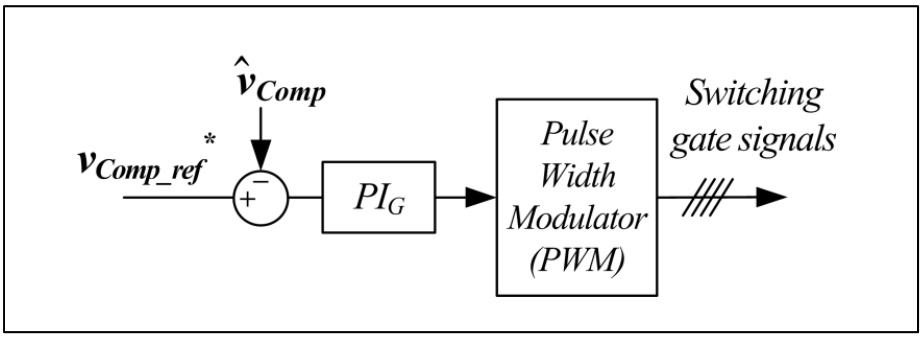

Figure 3.7 Block diagram of the v_{Comp} regulation showing the PI controller and the PWM circuit

3.4.3 Stability Analysis for Voltage and Current

The stability of the configuration is mainly affected by the introduced delay of a digital controller. This subsection studies the impact of the delay first on the inclusive compensated system according to works cited in the literature. Thereafter, its effects on the active compensator separated from the grid. Using purely inductive source impedance and the Kirchhoff's law for harmonic frequency components, Eqn. 3.21 is derived. The delay time of digital controller, large gain G and the high stiffness of the system seriously affect the stability of the closed-loop controlled system.

$$I_{sh}(s) = \frac{V_{sh} - V_{Comp} - V_{Lh}}{L_s s} \tag{3.21}$$

The compensating voltage including the delay time generated by the THSeAF in Laplace domain is

$$v_{Comp} = G \cdot I_{sh} \cdot e^{-\tau s} - V_{Lh} \tag{3.22}$$

Considering previous equations, the control diagram with delay is illustrated in Figure 3.8.

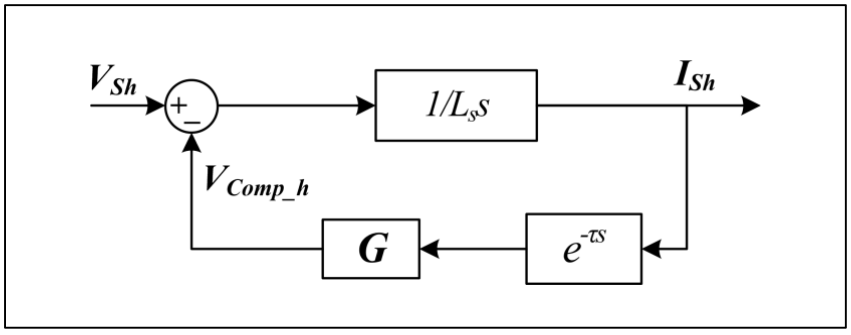

Figure 3.8 The control diagram of the system with delay

For the sake of simplicity, overall delay of the system is assumed to be a constant value τ. Therefore, the open-loop transfer function is obtained.

$$G(s) = \frac{G}{L_s s} e^{-\tau s} \tag{3.23}$$

From the Nyquist stability criterion, the stable operation of the system must satisfy the following condition:

$$G < \frac{\pi L_s}{2\tau} \tag{3.24}$$

A system with a typical source inductance L_S of 250 µH and a delay of 40 µs is considered stable according to Eqn 3.24, when the gain G is smaller than 10Ω. Experimental results confirm the stability of system presented in this work. Moreover, the influence of the delay on the control algorithm should also be investigated. According to the transfer functions Eqn 3.15 and 3.16, the control of the active part is affected by the delay introduce by the digital controller. Thus, assuming an ideal switching characteristic for the IGBTs, the closed-loop system for the active part controller is shown in the following diagram.

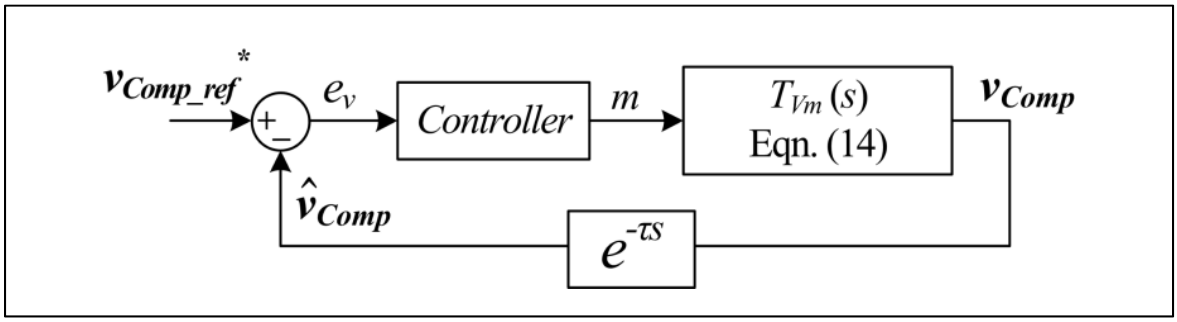

Figure 3.9 Closed-loop control diagram of the Active filter with a constant delay time τ

The open loop transfer function of Figure 3.9 turns to Eqn 3.26, where, the τ is the delay time initiated by the digital controller. The PI_G transfer function is as Eqn 3.25.

$$PI_G = K_p + \frac{K_i}{s} \tag{3.25}$$

$$F(s) = PI_G \cdot T_{Vm} \cdot e^{-\tau s} = \frac{\left(r_C C_f V_{DC} s \; + \; V_{DC}\right) \cdot \left(K_p s + K_i\right) e^{-\tau s}}{s \cdot \left(L_f C_f s^2 + \; r_C C_f s \; + \; 1\right)} \tag{3.26}$$

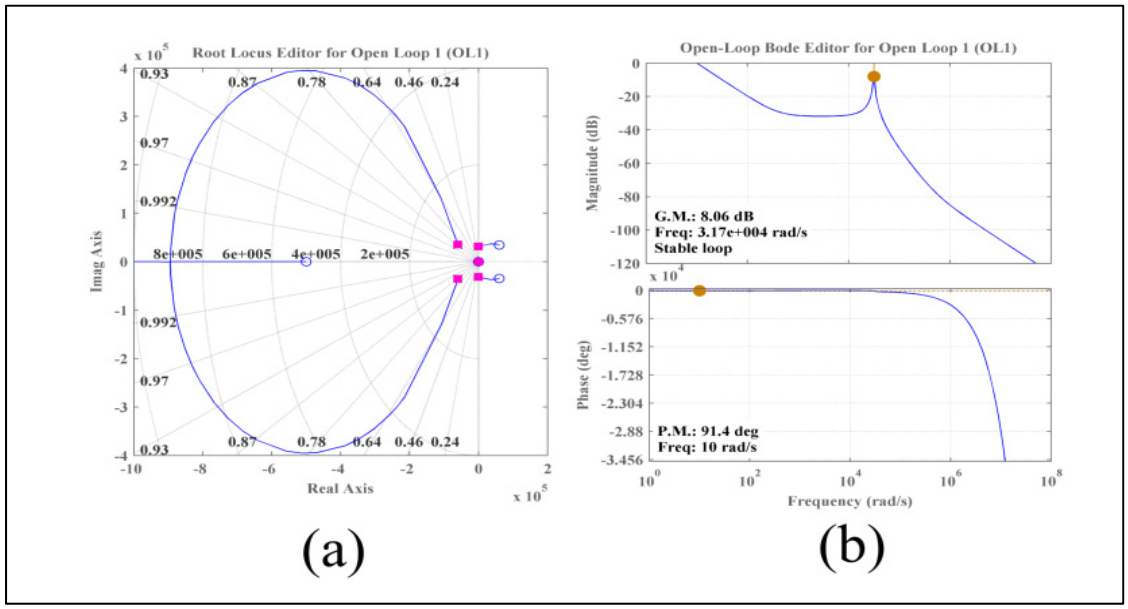

Figure 3.10 Compensated open-loop system with delay time of 40 µs, (a) Root Locus diagram. (b) Bode diagram

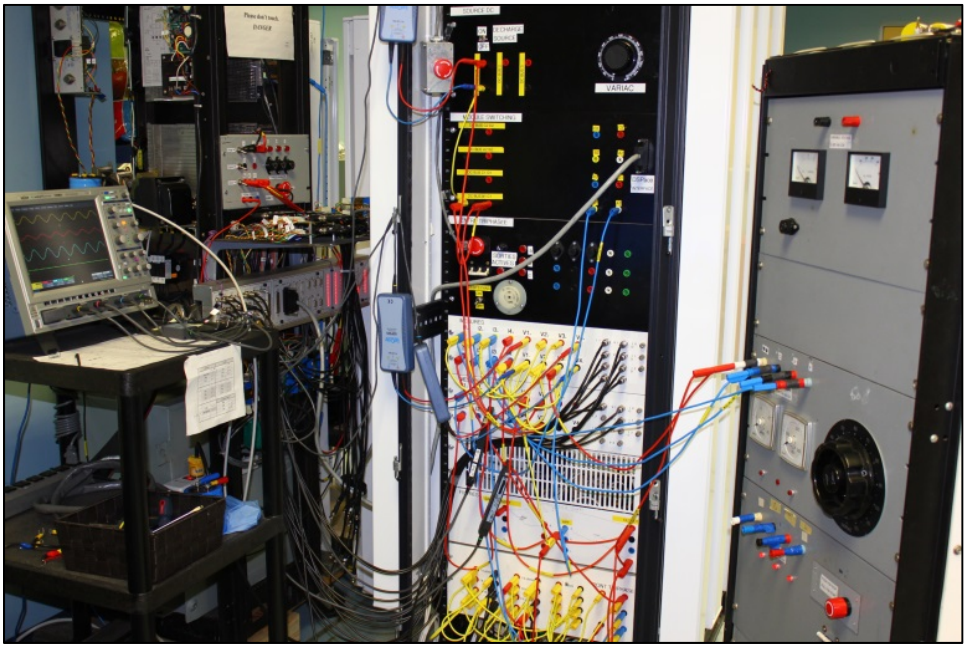

Figure 3.11 Transformerless-HSeAF prototype used for experiments

A PI controller with system parameters described in Table 3.1 demonstrates a smooth operation in the stable region. By means of MATLAB the behavior of the system's transfer function *F(s)* is traced in Figure 3.10. The Root Locus and the Bode diagram of the compensated open-loop system demonstrate a gain margin of 8.06 dB and a phase margin of 91 degree.

3.5 Simulations and Experimental Results

The proposed Transformerless-HSeAF configuration was simulated in MATLAB/Simulink using discrete time steps of T_S = 10µs. A dSPACE/dsp1103 was used for the fast control prototyping. To ensure an error free and fast implementation, the complete control loop was executed every 40µs. The parameters are identified in Table 3.1.

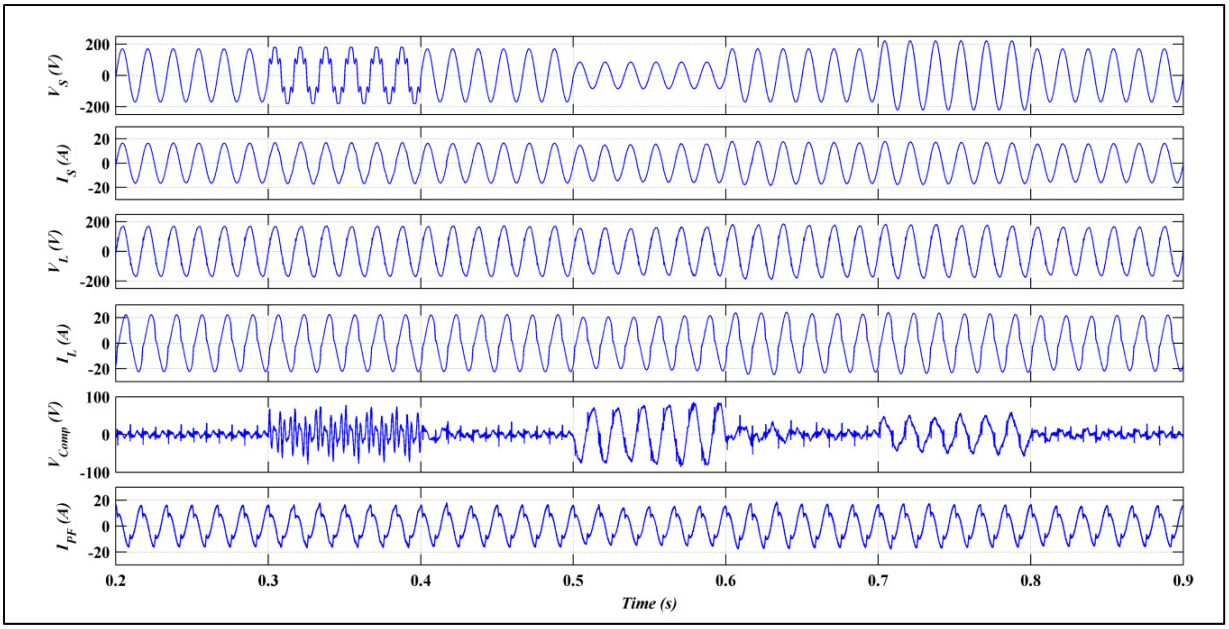

Figure 3.12 Simulation of the system with the THSeAF compensating current harmonics and load voltage regulation. (a) Source voltage v_S, (b) source current i_S, (c) Load voltage v_L, (d) load current i_L, (e) Active-filter voltage V_{Comp}, (f) Harmonics current of the passive filter i_{PF}

The combination of a single-phase non-linear load and a linear load with a total rated power of 2 kVA with a 0.74 lagging power factor is used for laboratory experiments and

simulations. For experiments and simulations a 2 kVA, 120 Vrms, and 60 Hz variable source is used. The THSeAF connected in series to the system compensates the current harmonics and voltage distortions. The complete experimental system is demonstrated in Figure 3.11. A gain G = 8 Ω equivalent to 1.9 p.u. was used to control current harmonics. As mentioned earlier, the capability of operation with low dc voltage is considered as one of the main advantages of the proposed configuration.

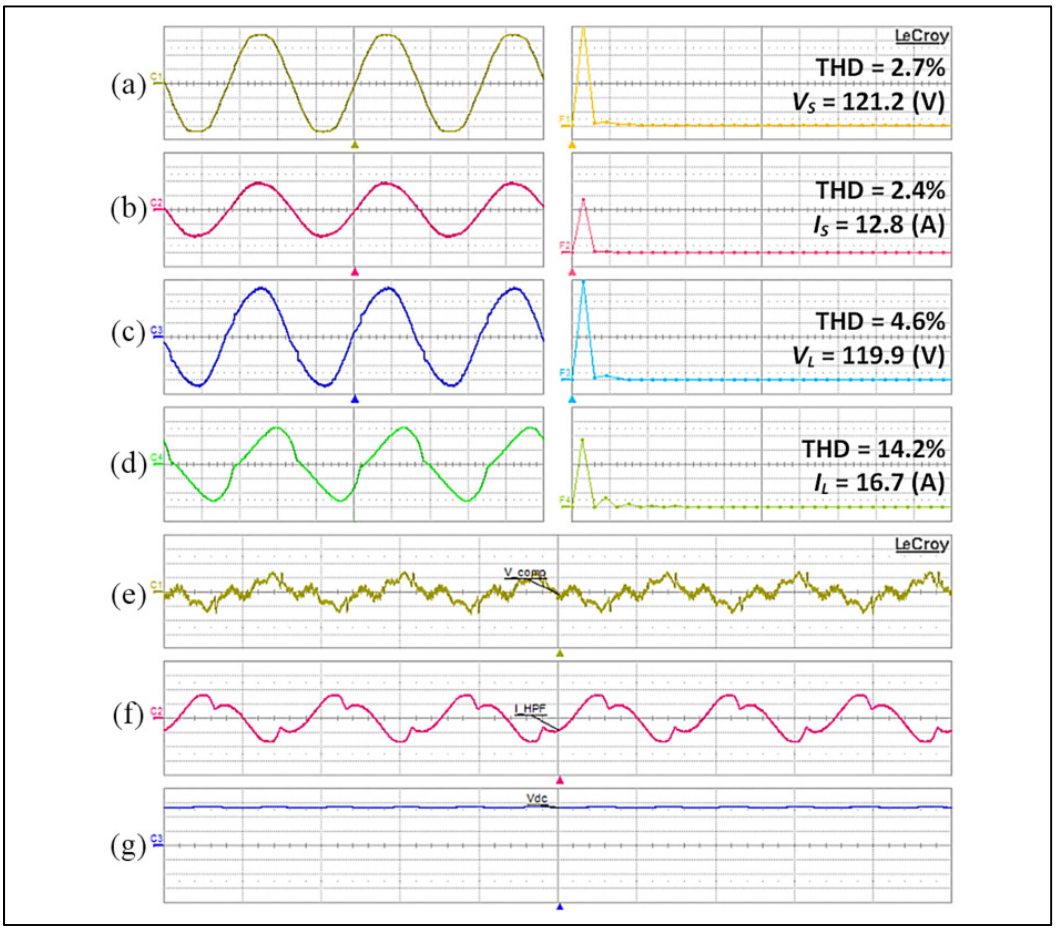

Figure 3.13 Experimental waveforms and harmonic spectrum under steady-state sinusoidal grid voltage. (a) Source voltage v_S [50V/div], (b) source current i_S [10A/div], (c) load terminal voltage v_L [50V/div], (d) load current i_L [10A/div], (e) THSeAF voltage v_{Comp} [20V/div], (f) passive filter current i_{PF} [10A/div], (g) DC voltage v_{DC} [50V/div]

For this experiment the DC voltage is maintained at 130 Vdc. During a grid's voltage distortion, the compensator regulates the load voltage magnitude, compensates current

harmonics and corrects the power factor. The simulated results of the THSeAF illustrated in Figure 3.12, demonstrates improvement in the source current THD. The load terminal voltage V_L THD i_S 4.3% while, source voltage is highly distorted (THD V_S= 25%). The grid is cleaned of current harmonics with a UPF operation and the THD is reduced to less than 1% in normal operation and less than 4% during grid perturbation. While the series controlled source clean the current of harmonic components, the source current is forced to be in phase with the source voltage. The series compensator has the ability to slide the load voltage in order for the power factor to reach unity. Furthermore, the series compensator could control the power flow between two PCCs.

Experimental results obtained in laboratory corroborate the successful operation of the THSeAF shown in simulations. Figure 3.13 shows the compensator during steady state operating with parameters described in Table I. The source current became sinusoidal and the load voltage regulated at rated 120 Vrms. The source current is in phase with the utility voltage achieving a unity power factor correction. The grid supplies 1.545 kW at a PF equal to 0.99, while the load consumes 2 kVA with a PF of 0.75. The compensator shows high efficiency in normal operation where the total compensator losses including switching, inductors resistances and damping resistances are equal to 44 W which is less than 2.5% of the system rated power. The power flow and THD of measured values are depicted in Table 3.3 for case demonstrated in Figure 3.13.

Table 3.3 Laboratory measured value and power flow analysis

	Load PCC		**Grid Utility (Source)**	
Measures	Voltage, V_L (V)	Current, I_L (A)	Voltage, V_S (V)	Current, $I_{S.}$ (A)
THD (%)	4.6	14.2	2.7	2.4
Fund. (rms)	119.9	16.7	121.2	12.8
Active power, P (W)	1499.7		1544.4	
Reactive power, Q (var)	1284.5		10.6	
Power, S (VA)	1998.6		1545.2	
Power Factor, PF (%)	75		99	
Compensator, THSeAF	S_{Comp}= + 44W - j1274var			

The experimental results illustrate a high fidelity with those observed in simulation. Therefore, the system is subjected to sag initiated from the utility source as shown in Figure 3.14. While cleaning the source current from harmonics and correcting the power factor the compensator regulates the load terminal voltage using the auxiliary source's power to maintain the supply at the load terminals despite grid's perturbations. The behavior of the proposed compensator during dynamic load variation could be depicted from Figure 3.15, where the load is suddenly varied. The THSeAF reacts instantly to this variation and do not interfere its operation functionality. Meanwhile, it is normal to observe a slight transient voltage variation depending on the momentum of the load disengagement or connection.

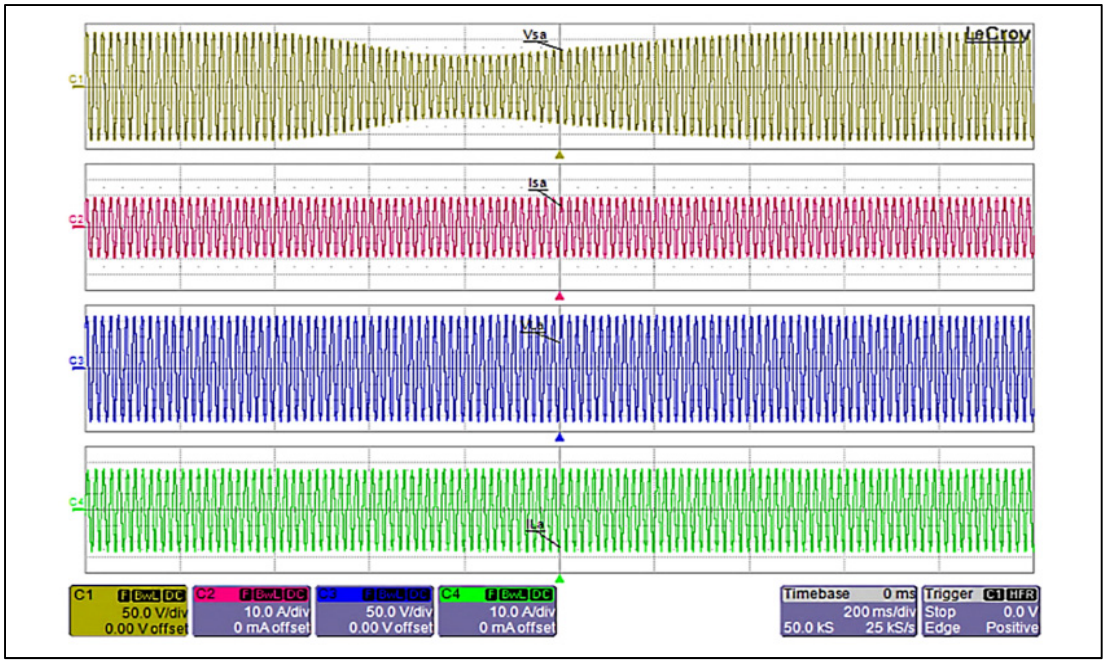

Figure 3.14 Waveforms during a variation of the source voltage
(a) Source voltage v_S [50V/div], (b) source current i_S [10A/div],
(c) load PCC voltage v_L [50V/div], (d) load current i_L [10A/div]

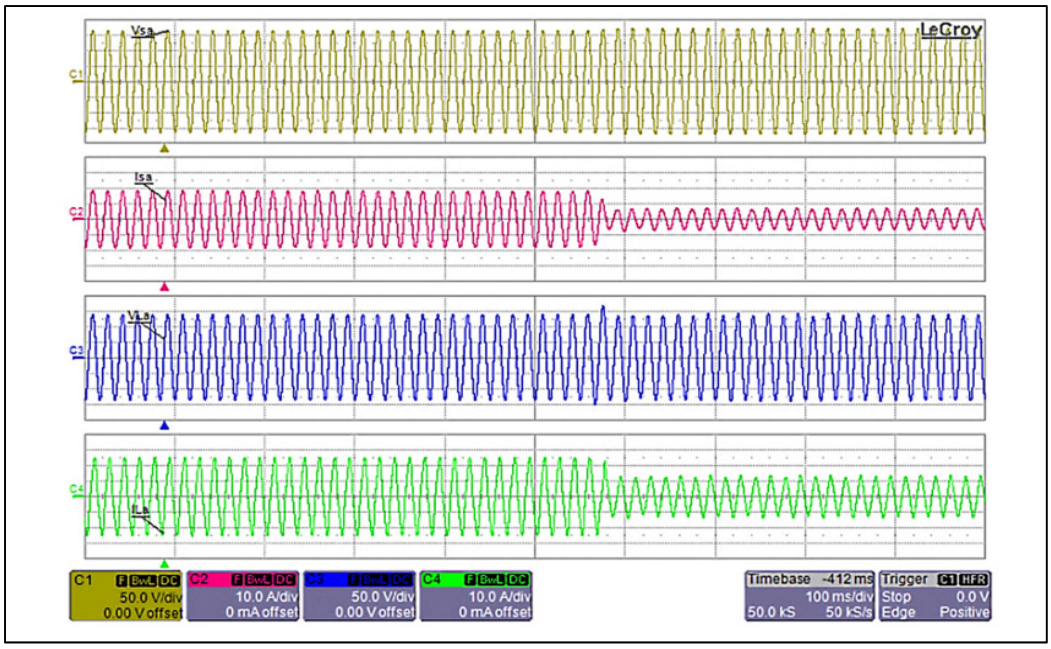

Figure 3.15 Waveforms during a dynamic load variation
(a) Source voltage v_S [50V/div], (b) source current i_S [10A/div],
(c) load PCC voltage v_L [50V/div], (d) load current i_L [10A/div]

To evaluate the compensator's response during utility's perturbation, the power source became distorted as depicted in Figure 3.16. The source current is cleaned of the majority of harmonics available in the load current and has a unity power factor. The THSeAF prevents existing perturbation on the grid's voltage to be propagated on the load's PCC. By doing this, it protects sensitive loads and maintains a sinusoidal and regulated voltage across the point of common coupling of loads with a 3.9% of distortion. Moreover, in a worst possible scenario, the already distorted utility's voltage is subjected to voltage magnitude variation. Thus, the compensator should also inject power to maintain the load PCC voltage regulated at desired level.

During voltage sags the auxiliary source should supply/absorb the difference of power to maintain the magnitude of the load side voltage regulated. The harmonic content and THD factor of the source utility and load PCC presented shows dramatic improvements in THD while the load draw polluted current waveforms. Furthermore, although the grid's voltage is

polluted the compensator in a hybrid approach regulates and maintains a harmonics-free load's voltage.

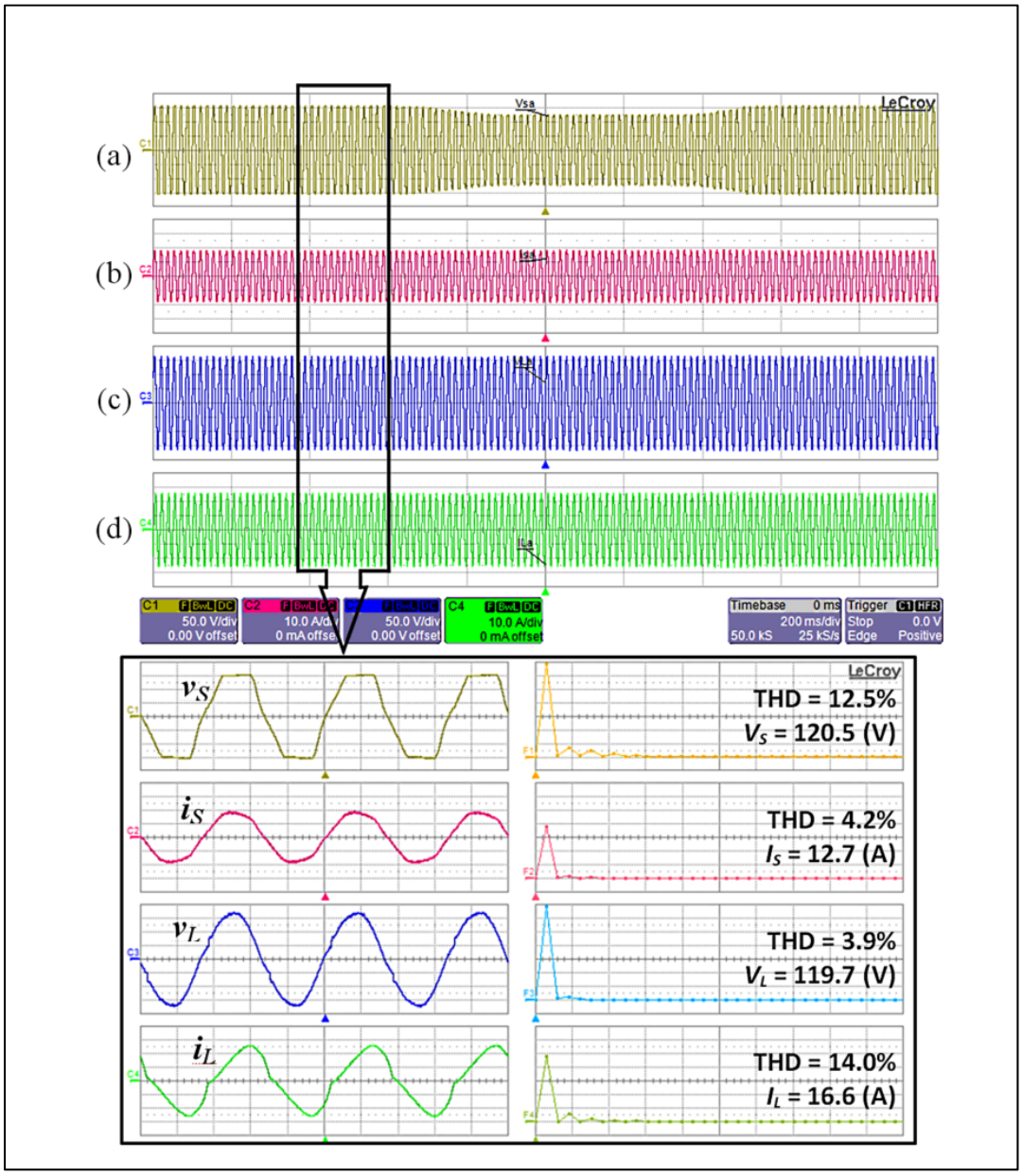

Figure 3.16 Experimental waveforms under utility voltage distortion and prolonged sags (a) Utility source voltage v_S [50V/div], (b) Utility current i_S [10A/div], (c) load PCC voltage v_L [50V/div], (d) load current i_L [10A/div]

3.6 Conclusion

In this chapter the application of a Transformerless-HSeAF for power quality improvement was developed and tested on a CSC type of non-linear load. The work highlighted the fact that with the ever increase of non-linear loads and higher exigency of consumer for a reliable supply, concrete actions should be taken into consideration for future Smart Grids in order to smoothly integrate electric cars battery chargers to the distribution network. The key novelty of the proposed solution is that the proposed configuration could improve power quality of the system in more general way by compensating a wide range of harmonics current. Even though, it can be seen the THSeAF regulates and improves the PCC voltage.

Connected to a renewable auxiliary source, the topology is able to counteract actively to the power flow in the system. This essential capability is required to ensure a consistent supply for critical loads. Behaving as high-harmonic impedance, it cleans the power system and ensures a unity power factor. The theoretical modeling of the proposed configuration was investigated. The proposed transformerless configuration was simulated and experimentally validated. It was demonstrated that this active compensator responds properly to source voltage variations by providing a constant and distortion-free supply at load terminals. Furthermore, it eliminates source harmonic currents and improves power quality of the grid without the usual bulky and costly series transformer.

CHAPTER 4

A THSEAF WITH SLIDING MODE AND RESONANT CONTROLLERS AND FIVE LEVEL TOPOLOGY FOR POWER QUALITY ENHANCEMENT OF A VSC TYPE OF NONLINEAR LOADS

4.1 Introduction

In this Chapter at first, a single-phase Transformerless Hybrid Series Active Filter (THSeAF) using a sliding mode control algorithm and a Notch harmonic detection technique is implemented on a single-phase distribution feeder. This method provides compensation for both current harmonics coming from a voltage fed nonlinear load (VSC), and provide reactive power compensation for a residential consumer. The realized compensator enhances the power quality while cleaning the point of common coupling (PCC) from possible voltage distortions, sags, and swells initiated through the grid. Furthermore, to overcome drawbacks of real-time control delay, a computational delay compensation method, which accurately generates reference voltages, is proposed. Based on an improved compensation strategy, while the grid current remains clean of harmonics even with a small compensation gain, voltage disturbances initiated by the power system are obstructed by the compensator, and the PCC became ridded of voltage harmonics and protected from sag and swell. Simulation and experimental results carried on a 1.6-kVA prototype are as well presented and discussed.

In the second step, a promoting solution to enhance the power quality of a typical household using a Multilevel THSeAF with a PR controller onboard is presented. The THSeAF is improved using an NPC multilevel converter and a Proportional plus Resonant (PR) controller. The Multilevel Transformerless Hybrid Series Active Filter (Multilevel-THSeAF) is proposed to enhance power quality of a single-phase residential non-linear load. The proposed topology reflects new trends of consumers towards electronic polluting loads and integration of renewable sources which in fact may lead to the scope of a reliable and sustainable supply. This section contributes to improvement of power quality for a modern single phase consumer, and focuses on integrating of a Photovoltaic (PV) modules with

energy storage capacity to ensure a continuous supply. A proportional plus resonant (PR) regulator is implemented in the controller to prevent current harmonic distortions of various non-linear loads to flow into the utility. The main significant features of the proposed topology include the great capability to instantly correct the power factor as well as cleaning the grid, while protecting consumers from voltage disturbances, sags, and swells during a grid perturbation. This chapter investigates aspects of harmonic compensation and assesses the influence of the controller's choice and the delay time during a real-time operation.

4.2 Voltage Fed Type of Non-Linear Load's Impacts on the Power Quality of the Grid

The predictions on a clean and hassle-free power system associated with the ever increase of switch-mode power converters, drives, as well as domestic and industrial nonlinear loads has created a serious concern on the power quality of the future smart grid distribution power systems as shown in Figure 4.1. In existing power systems current harmonic pollution fed from nonlinear loads have deteriorate the power quality (Liserre, Sauter et Hung, 2010; Singh, Chandra et Al-Haddad, 2015). This amplified distortion power increases heat dissipation losses and can cause serious failure of some sensitive electrical equipment, therefore reducing system efficiency (Jun-Young et Hyung-Jun, 2014; Zobaa, 2014). In a more inclusive vision, the points of common coupling (PCC) where sensitive loads are installed, will require additional protection to avoid voltage distortions, sags, swells (Munir et Yun Wei, 2013; Sixing, Jinjun et Jiliang, 2013) and therefore ensure complete decoupling from the other network branches.

As mentioned over this dissertation, to mitigate power quality issues, there exist three categories of compensators; the conventional and widespread used passive filters (Akagi et Isozaki, 2012b; Yi et al., 2012), the well-developed shunt active power filters (El Badsi, Bouzidi et Masmoudi, 2013; Nogueira Santos et al., 2014). As last resort comes the Series active filters (including Hybrid type ones) (Senturk et Hava, 2011; Tian, Chen et Xie, 2012; Varschavsky, Dixon et Rotella, 2010). These compensators have been developed to eliminate current harmonics produced by non-linear type of loads such as vehicle charging stations as

shows the waveform of grid current in Figure 4.1 with a THD of 28%. This current is drawn from the power system or from and established compensated PCC (Ajaei et al., 2011; Jimichi, Fujita et Akagi, 2011).

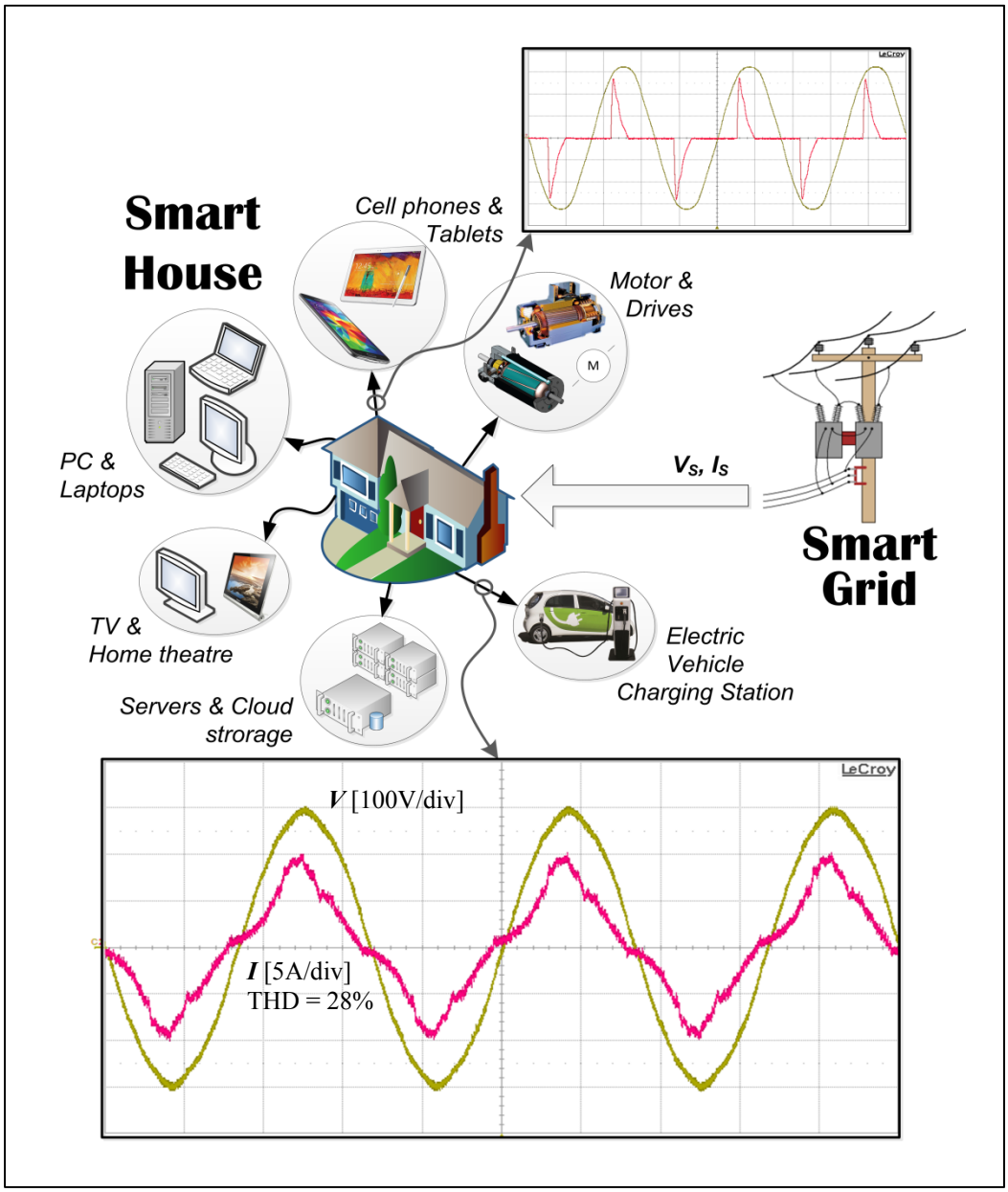

Figure 4.1 Typical residential consumer with electronic loads, and measured electric car (Nissan Leaf®) voltage and current patterns connected to a level-2 AC charging station

Series active filters (SeAF) less spread than shunt type, received fewer industrial investigations and little research is dedicated to such compensators due to their complex configuration and operation characteristics. Meanwhile, they are more advantageous compared to the shunt active filters, by having an inferior rating versus load nominal rating (Senturk et Hava, 2009). However, the complexity of the configuration and necessity of an isolation series transformer had decelerated their industrial widespread application in distribution system. There exists other application for SeAFs where they are employed to address voltage quality and regulation issues for sensitive loads. In this case they are commonly known as Dynamic Voltage Restorer (DVR) (Barros et Silva, 2010; Roncero-Sanchez et al., 2009). Thus, the SeAF and DVR are similar in topology but their control approach differentiates them from each other (Gupta, Ghosh et Joshi, 2011). This difference relies on the objective and their application. Found in the literature, the Hybrid series active filter (HSeAF) is proposed to address both aforementioned issues with only one combination. They are capable to compensate current harmonics, ensuring a power factor correction, and eliminating voltage distortions at the PCC (Salmeron et Litran, 2010). The major research works have contributed on three-phase HSeAFs, whereas limited researches were conducted in the state of the art on their single-phase application (Amjadi et Williamson, 2011; Rahmani, Al-Haddad et Kanaan, 2006).

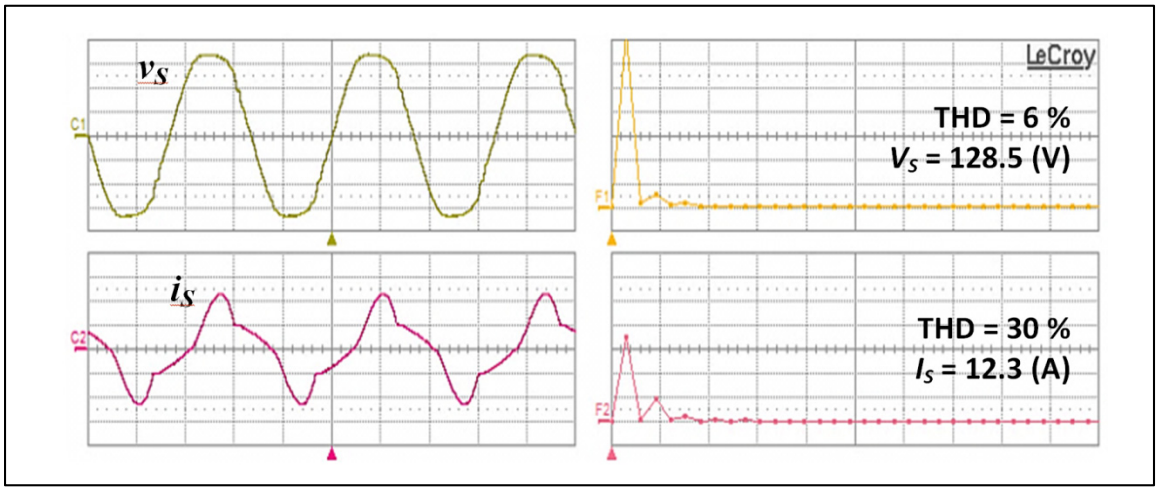

Figure 4.2 Steady state terminal voltage [50V/div] and current [10A/div] waveforms of a 1.6-kVA load without compensation (the THSeAF is by-passed)

The single-phase Transformerless-HSeAF is capable of cleaning the grid side bus from current harmonics generated by non-linear loads. Furthermore, it restores and provides a clean sinusoidal voltage for the load. Advantage of the proposed configuration relies on the fact that harmonic currents leading to voltage distortions could be efficiently compensated. In addition, this configuration could contribute to the integration of renewables in distributed generation systems with high penetration of renewable energy sources and more importantly it permit soft integration of charging stations in the residential and distribution network.

The use of a single-phase H-bride converter has allowed elimination of the costly isolation transformer and thus promotes its industrial application. For a three-phase application, it is suggested to use three independent compensators installed in series on each phase. Contrary to previously developed three-phase Series active power filters, which uses a three-phase converter, in the proposed topology the three-phase are operating independently and are electrically isolated from each other. The setup has shown a great capability to perform correction of current and voltage distortions produced by a VSC type of non-linear load, such as current harmonic elimination, power factor correction, as well as compensation of voltage distortions on the load terminal. The proposed compensator keen to compensate distortions of a voltage fed type of non-linear loads. For instance, the distorted current and voltage waveforms of the non-compensated 1.6 kVA non-linear load combined with a linear load are depicted in Figure 4.2. Note that a 12.3 Arms having a THD of 30% is causing 6% voltage distortion on a single feeder of 128Vrms. To ensure an acceptable quality of voltage at the feeder, this challenging task is addressed in this section.

4.3 System Architecture of the single-phase THSeAF

4.3.1 Configuration of the Setup

The THSeAF shown in Figure 4.3 is connected in series between the utility and the load. A bank of tuned shunt passive filters ensures a low impedance path for current harmonics and a dc source could be connected to inject power during voltage sags and absorbs it during

overvoltage. The dc source is consisted of a combination of PV and energy storage devices. The implemented system is rated at 1.6 kVA. To ensure a fast transient response with sufficient stability margins over a wide range of operation, the controller is implemented on a dSPACE/dsp1103. A variable source to simulate utility sag is connected to combination of a voltage fed non-linear load of 675 VA with a 0.8 lagging power factor and an 864 VA linear inductive load with a 0.7 power factor. Similar parameters are applied for simulation and practical implementation.

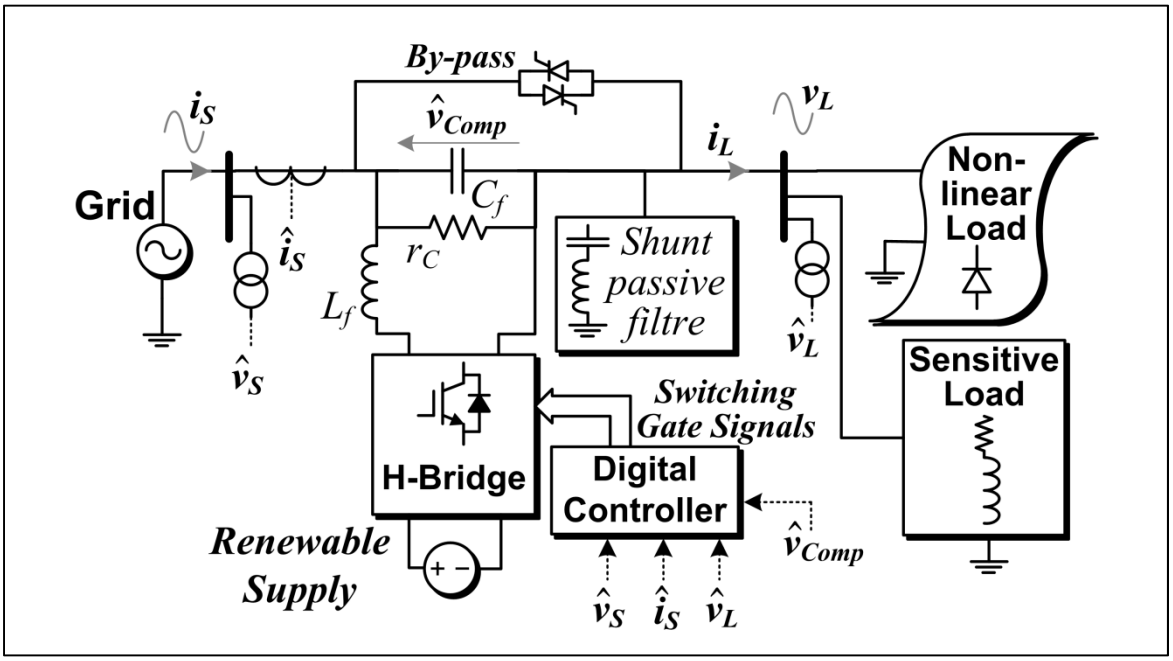

Figure 4.3 The THSeAF connected to the single-phase radial system with VSC load

The proposed topology could be solely connected to the grid without a bulky series injection transformer to compensate current harmonics at the source and voltage distortion at the PCC. Even if the number of switches has increased, the transformerless configuration is more cost-effective than any other series compensators, which generally uses a transformer to inject the compensating voltages to the grid.

4.3.2 Operation Principle of Proposed Current Compensation Approach

A voltage type of non-linear load could be modeled as a harmonic voltage source in series with an impedance $Z_{Non\text{-}Linear}$ or by its Norton equivalent modeled with a harmonic current source in parallel to the impedance. The Thévenin's model and the Norton equivalent circuit are depicted in Figure 4.4. In this section the common Norton equivalent is chosen to follow major related articles. The principle of such modeling is documented in (Javadi et al., 2015). In this research work the approach to achieve optimal behavior during perturbation is implemented on the controller. The use of a passive filter is mandatory to compensate current issues and maintaining a constant voltage free of distortions at the load terminals.

The non-linear load is modeled by a resistance representing the active power consumed and a current source generating harmonics current. Accordingly, the impedance Z_L is the equivalent of the nonlinear ($Z_{Non\text{-}linear}$) and the linear load (Z_{RL}). The Series active filter, whose output voltage V_{Comp} is considered as an ideal controlled voltage source is generating a voltage based on the detecting source current, load voltage, and also the source voltage to achieve optimal results as of Eqn. 4.4. This established hybrid approach gives good result and is quite less sensitive to the value of the gain G to achieve low level of current harmonics. The gain G is proportional to the current harmonics (I_{sh}) flowing to the grid. Assuming the grid contains voltage distortions, the equivalent circuit for the fundamental and harmonics are:

$$V_S = V_{S1} + V_{Sh} \tag{4.1}$$

$$V_L = V_{L1} + V_{Lh} = Z_L I_Z = Z_L(I_S - I_h) \tag{4.2}$$

$$I_S = I_{S1} + I_{Sh} = I_Z + I_h \tag{4.3}$$

$$V_{Comp} = +GI_{Sh} - V_{Lh} + V_{Sh} \tag{4.4}$$

where I_Z represents the load current in Z_L shown in the following pictograms. Using the Kirchhoff's law the following equation is depicted for both the fundamental and harmonics.

$$V_S = Z_S I_S + V_{Comp} + V_L \tag{4.5}$$

$$V_{L1} = Z_L I_{S1} \quad , \quad V_{Lh} = Z_L (I_{Sh} - I_h) \tag{4.6}$$

By substituting the fundamental of Eqn 4.6 in 4.5, the source current at fundamental frequency is obtained.

$$I_{S1} = \frac{V_{S1}}{Z_S + Z_L} \tag{4.7}$$

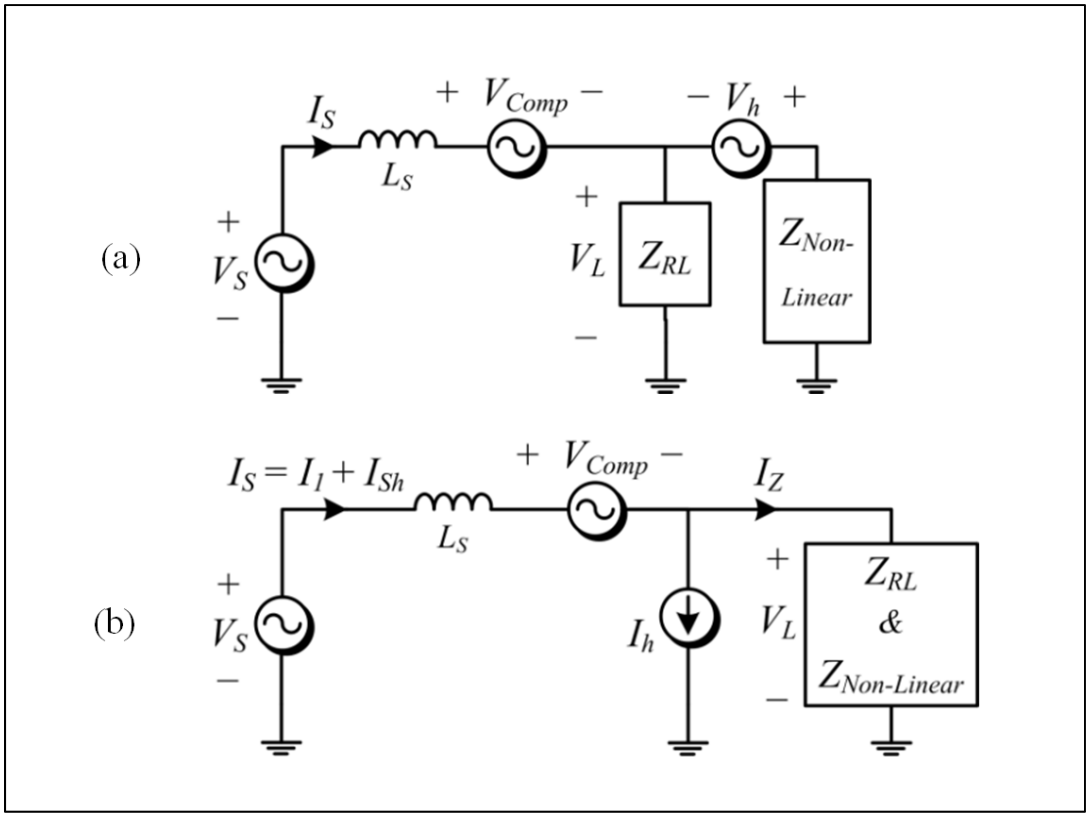

Figure 4.4 Single-phase equivalent phasor model for VSC type of loads, (a) Thévenin's model, (b) Norton equivalent

By substituting Eqn 4.4 in 4.5 for the harmonic components, the harmonic source current is reached as follow.

$$V_{Sh} = Z_S I_{Sh} + G I_{Sh} - V_{Lh} + V_{Sh} + V_{Lh} \quad \rightarrow \quad I_{Sh} = 0 \tag{4.8}$$

By introducing Eqn. 4.8 into the harmonic component of the load PCC voltage Eqn 4.6, following equation is achieved.

$$V_{Lh} = -Z_L I_h \tag{4.9}$$

Consequently under this approach even in presence of source voltage distortions the source current will remain clean of any harmonic components. To some extent in this approach the filter behaves as high impedance likewise an open circuit for current harmonics, while the shunt high pass filter tuned at the system frequency, could create a low-impedance path for all harmonics and open circuit for the fundamental component. This argument explains the need of a Hybrid configuration to create an alternative path for current harmonics fed from a current source type of nonlinear loads.

The rating of the compensator is designed based on the required power consumers desire to restore during sags in the grid supply. For the 1.6 kVA load, in order to restore a 40% voltage sag, and at the same time compensating source current harmonics and correcting the power factor following sizing is suggested.

The rating of the compensator depends on following constraints to consider during performing the design of the compensator. The auxiliary supply should be designed accordingly as: $S_{DCsource}$ = 1.6×40% = 650VA. The converter should transfer the load RMS current and have the following characteristics: $I_{Converter} = I_L$ = 1.6kVA/120Vrms = 13Arms. The nominal voltage of the converter is then $V_{Converter}$ = 650VA/13Arms = 50Vrms. The DC bus voltage is then required to be $V_{DCsource}$>70Vdc and the more DC voltage is, the compensation will have a better performances. The bank of series resonant tuned shunt

passive filters, assuming a 20% of 5th harmonic component, should have the following parameters: V_{SPF}=120Vrms with a rated current of I_{SPF} = 2.6A. To have an optimized design a primary study of the nonlinear load characteristic is required and then the same design process should be taken for the other tuned branches if required.

4.4 Modeling and Control of the THSeAF

A Transformerless Hybrid series Active filter configuration is considered in this section in order to avoid current harmonic pollution along the power line caused by a single-phase diode bridge rectifier load, followed by a capacitor C_{NL} in parallel with a resistor R_{NL}. The THSeAF which structure is illustrated in Figure 4.5 acts as a controlled voltage source connected in series with the loads between the grid and the PCC.

4.4.1 Modeling of Transformerless Series Active Filter

According to Figure 4.3, and the average equivalent circuit of an inverter developed in (Figueres et al., 2009), the small-signal model of the proposed configuration can be obtained as shown in the following electric scheme. Kirchhoff's rules for voltages and currents, as applied to this system, provide us with the differential equations including the *LC* filter. Thereafter, *d* is the duty cycle of the upper switch of the converter leg in a switching period, whereas $\bar{v}$ and $\bar{\imath}$ denotes the average values in a switching period of the voltage and current of the same leg. The mean converter output voltage and current are expressed by Eqn. 4.10 and 4.11 as follow.

$$\bar{v}_O = \underbrace{(2d-1)}_{m} V_{DC} \tag{4.10}$$

$$\bar{\imath}_{DC} = m\bar{\imath}_f \tag{4.11}$$

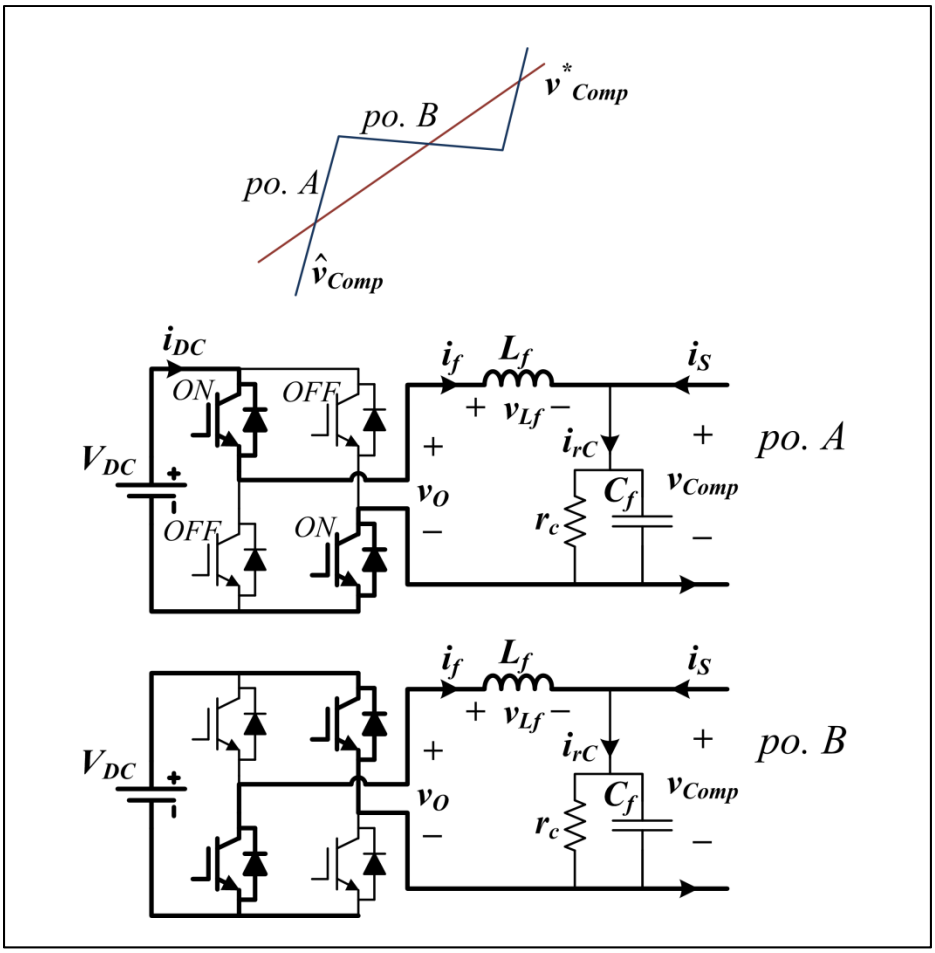

Figure 4.5 Sequence of operation of the transformerless-HSeAF

According to the previous scheme, the arbitrary direction of i_f is leaving the H-bridge converter. For dynamic studies the accurate model is considered.

$$mV_{DC} = L_f \frac{di_f}{dt} + v_{Comp} \tag{4.12}$$

$$r_C C_f \frac{dv_{Comp}}{dt} = -v_{Comp} + r_C(i_f + i_S) \tag{4.13}$$

The state-space model could be derived by a linearized perturbation of averaged model as follow:

$$\dot{x} = Ax + Bu \tag{4.14}$$

Hence we obtain:

$$\frac{d}{dt}\begin{bmatrix} \bar{\imath}_f \\ \bar{v}_{Comp} \end{bmatrix} = \begin{bmatrix} 0 & -\frac{1}{L_f} \\ \frac{1}{C_f} & -\frac{1}{r_C C_f} \end{bmatrix} \times \begin{bmatrix} \bar{\imath}_f \\ \bar{v}_{Comp} \end{bmatrix} + \begin{bmatrix} \frac{V_{DC}}{L_f} & 0 \\ 0 & \frac{1}{C_f} \end{bmatrix} \times \begin{bmatrix} m \\ i_S \end{bmatrix} \tag{4.15}$$

The output vector is then:

$$y = Cx + Du \tag{4.16}$$

or

$$y = [0 \quad 1] \times \begin{bmatrix} \bar{\imath}_f \\ \bar{v}_{Comp} \end{bmatrix} \tag{4.17}$$

By means of Eqn. 4.15 and 4.17, the state-space representation of the model could be obtained.

The second order relation between the compensating voltage and the duty cycle could be reached as follow.

$$C_f \frac{d^2 v_{Comp}}{dt^2} + \frac{1}{r_C}\frac{dv_{Comp}}{dt} + \frac{1}{L_f} v_{Comp} = \frac{V_{DC}}{L_f} m + \frac{di_S}{dt} \tag{4.18}$$

This model is then used in the developing strategy for the converter's controller as in the following section.

4.4.2 Sliding-mode Controller

The controller's outer-loop is composed of two parallel section based on a Notch filter harmonics extraction technique. The first part is dedicated to compensate for load's voltage and added to a second part which compensates for source current harmonics. The controller demonstrated in the diagram of Figure 4.6, restores a stable voltage at the load PCC terminals, while compensating for current harmonics and reactive power. In the source current regulation block, the notch filter extracts magnitude of the fundamental and its phase shift, leaving harmonics and the reactive component. The control gain *G* representing the impedance of the source for current harmonics, should be enough to clean the grid from current harmonics fed through the non-linear load. For a more precise compensation of current harmonics, the source and load voltage harmonics should also be considered in the algorithm.

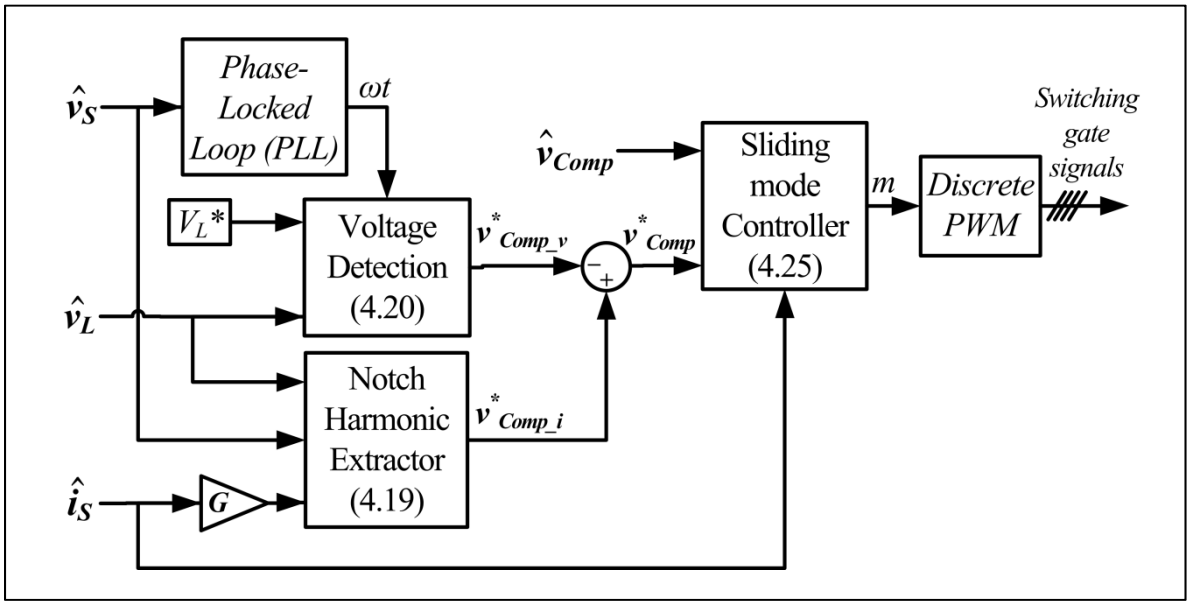

Figure 4.6 Control system architecture scheme

The source and load voltages together with the source current are considered as system input signals. The Single-phase discrete phase-locked loop (PLL) was used to obtain the reference angular frequency synchronized with the source utility voltage (ω_s). Furthermore, the v_{compi}

contains a fundamental component synchronized with the source voltage in order to compensate for the reactive power. The gain *G* representing the resistance for harmonics converts compensating current into a relative voltage. The generated reference voltage v_{Comp_i} required to clean source current from harmonics.

$$v_{comp_i} = +Gi_{Sh} - v_{Lh} + v_{Sh} \tag{4.19}$$

Hereby, as voltage distortion at the load terminals is not desired, the voltage sag and swell should also be investigated to indirectly maintain the voltage magnitude at load side equal to the reference V_L* defined by the operator.

$$v_{comp_v} = \left[k_p\left(V_L^* - \hat{V}_L\right) + k_i \int \left(V_L^* - \hat{V}_L\right) \cdot d_t\right] \sin(\omega_L t) \tag{4.20}$$

Where k_p and k_i are respectively the proportional and integrator gains of the PI regulator and $\hat{V}_L$ is the magnitude of $\hat{v}_L$. The final compensating voltage reference is reached by combination of the stated components related to current issues and voltage issues.

$$v_{comp}^* = -v_{comp_v} + v_{comp_i} \tag{4.21}$$

The inner-loop is made with the sliding mode control (SMC) approach to generate duty cycle required by IGBTs to fire and produce desired compensating voltage. Indeed, the sliding mode control (SMC) is a nonlinear and robust type control method that alters the dynamics of a nonlinear system by applying discontinuous control signal that forces the system to slides along a sliding surface. The state-feedback control law is not a continuous function of time while this variable structure control method can switch from one continuous structure to another one based on the current position in the state space plan. The controller is designed in a way that the trajectories of the state controlled variables always lean toward an adjacent and limited bandwidth region and thus it slides along the boundaries of the control structures. A switching function σ represents the distance that the states variable is away from the

sliding surface. During which if the state is outside of the sliding surface it has a nonzero value, while during the time the state is in the sliding surface it is equal to a constant zero.

The system is under control if there exists, a controller to move the trajectory closer to the sliding mode's one. Then, once the sliding mode is achieved Eqn. 4.22 equal to zero and the system remains on the sliding mode surface. Besides sliding mode trajectories σ is kept constant, so that its derivation remain equal to zero as of Eqn 4.24. Thus the system will be stable with respect previous assumptions remains true and the system will slide along the desired surface to achieve this equilibrium.

$$\sigma = \left(\frac{d}{dt} + \lambda\right) \cdot e \tag{4.22}$$

Where the error is

$$e = \left(v_{Comp} - v^*_{Comp}\right) \tag{4.23}$$

$$\dot{\sigma} = \left(\frac{d^2 e}{dt^2} + \lambda \frac{de}{dt}\right) = 0 \tag{4.24}$$

The equivalent duty cycle m_{eq} using the compensator's developed model Eqn 4.18 is found as follow.

$$m_{eq} = \frac{C_f L_f}{V_{DC}}\left[L_f \frac{d^2 v^*_{Comp}}{dt^2} + \lambda \frac{d v^*_{Comp}}{dt} + \left(\frac{1}{r_C C_f} - \lambda\right)\frac{d \hat{v}_{Comp}}{dt} + \frac{1}{L_f C_f}\hat{v}_{Comp} - \frac{1}{C_f}\frac{di_S}{dt}\right] \tag{4.25}$$

The control law described generating the duty cycle for the upper switch sent to the PWM could be then defined as follow.

$$m = m_{eq} - K_1 \cdot Sgn\,(\sigma) \tag{4.26}$$

This control law is then implemented for simulations and laboratory experiments. The entire control scheme for the THSeAF presented in Figure 4.6 was implemented in MATLAB/Simulink for real-time simulations and calculation of the compensating voltage. For laboratory experiments, same controller is implemented on the dSPACE module and executed on the dsp1103 control board.

To ensure stability of the sliding mode over the entire state space of the system, and therefore ensure that the system converges to the sliding surface. Let choose a Lyapunov function as Eqn 4.27.

$$V = \frac{1}{2}\sigma.\sigma^T \tag{4.27}$$

One must show that a Lyapunov function is strictly positive definite, if its derivative is negative definite.

$$\dot{V} = \sigma\dot{\sigma} = \sigma\left[\left(\frac{d^2e}{dt^2} + \lambda\frac{de}{dt}\right)\right] \tag{4.28}$$

Considering previously developed relations, one can obtain:

$$\frac{d^2e}{dt^2} = \frac{d^2v_{Comp}}{dt^2} - \frac{d^2v^*_{Comp}}{dt^2} \tag{4.29}$$

$$= \frac{1}{r_C C_f}\left(-\frac{dv_{Cmp}}{dt} + r_C\left(\frac{di_f}{dt} + \frac{di_S}{dt}\right)\right) - \frac{d^2v^*_{Comp}}{dt^2}$$

Using Eqn 4.12,

$$\frac{d^2e}{dt^2} = \frac{1}{r_C C_f}\left(-\frac{dv_{Comp}}{dt} + r_C\frac{di_S}{dt} + \frac{r_C}{L_f}\left(mV_{DC} - v_{Comp}\right)\right) - \frac{d^2v^*_{Comp}}{dt^2} \tag{4.30}$$

Introducing Eqn 4.26 in Eqn4.30, and then the result in Eqn 4.28 the following is reached:

$$\dot{V} = \sigma\left[\left(\frac{1}{r_C C_f}\left(-\frac{dv_{Comp}}{dt} + r_C\frac{di_S}{dt} + \frac{r_C}{L_f}\left(\left(m_{eq} - K_1 \cdot Sgn\,(\sigma)\right)V_{DC} - v_{Comp}\right)\right) - \frac{d^2 v^*_{Comp}}{dt^2} + \lambda\frac{de}{dt}\right)\right] \tag{4.31}$$

By performing mathematical simplifications, the following relation is derived:

$$\dot{V} = \sigma\left[\left(-\frac{V_{DC}}{L_f C_f}K_1 \cdot Sgn\,(\sigma) + \underbrace{\frac{d^2 v_{Comp}}{dt^2} - \frac{d^2 v^*_{Comp}}{dt^2}}_{\frac{d^2 e}{dt^2}} + \lambda\frac{de}{dt}\right)\right] \tag{4.32}$$

Hence substituting by Eqn 4.24 in Eqn 4.32:

$$\dot{V} = \sigma\left[\left(-\frac{V_{DC}}{L_f C_f}K_1 \cdot Sgn\,(\sigma) + \frac{d^2 e}{dt^2} + \lambda\frac{de}{dt}\right)\right] = -\frac{V_{DC}}{L_f C_f}K_1 \cdot \sigma \cdot Sgn\,(\sigma) \tag{4.33}$$

Using the inequality: $\sigma \cdot Sgn\,(\sigma) \leq |\sigma|$, the derivative of the Lyapunov should satisfy the following relation:

$$\dot{V} = -\frac{V_{DC}}{L_f C_f}K_1 \cdot \sigma \cdot Sgn\,(\sigma) \leq -\frac{V_{DC}}{L_f C_f}K_1|\sigma| \tag{4.34}$$

This inequality (Eqn 4.34) will be satisfied by appropriately selecting the sliding mode parameter K_1>0. The convergence rate of the state variables will depend on this selection.

4.5 Simulations and Experimental Results

This subsection presents results of the Transformerless-HSeAF configuration in MATLAB/Simulink using a time steps of T_s = 10µs. Then for experimental implementation the controller is loaded on the dSPACE/dsp1103 for fast control prototyping. To achieve reliable and error-free implementation, the complete control loop was executed every 40µs.

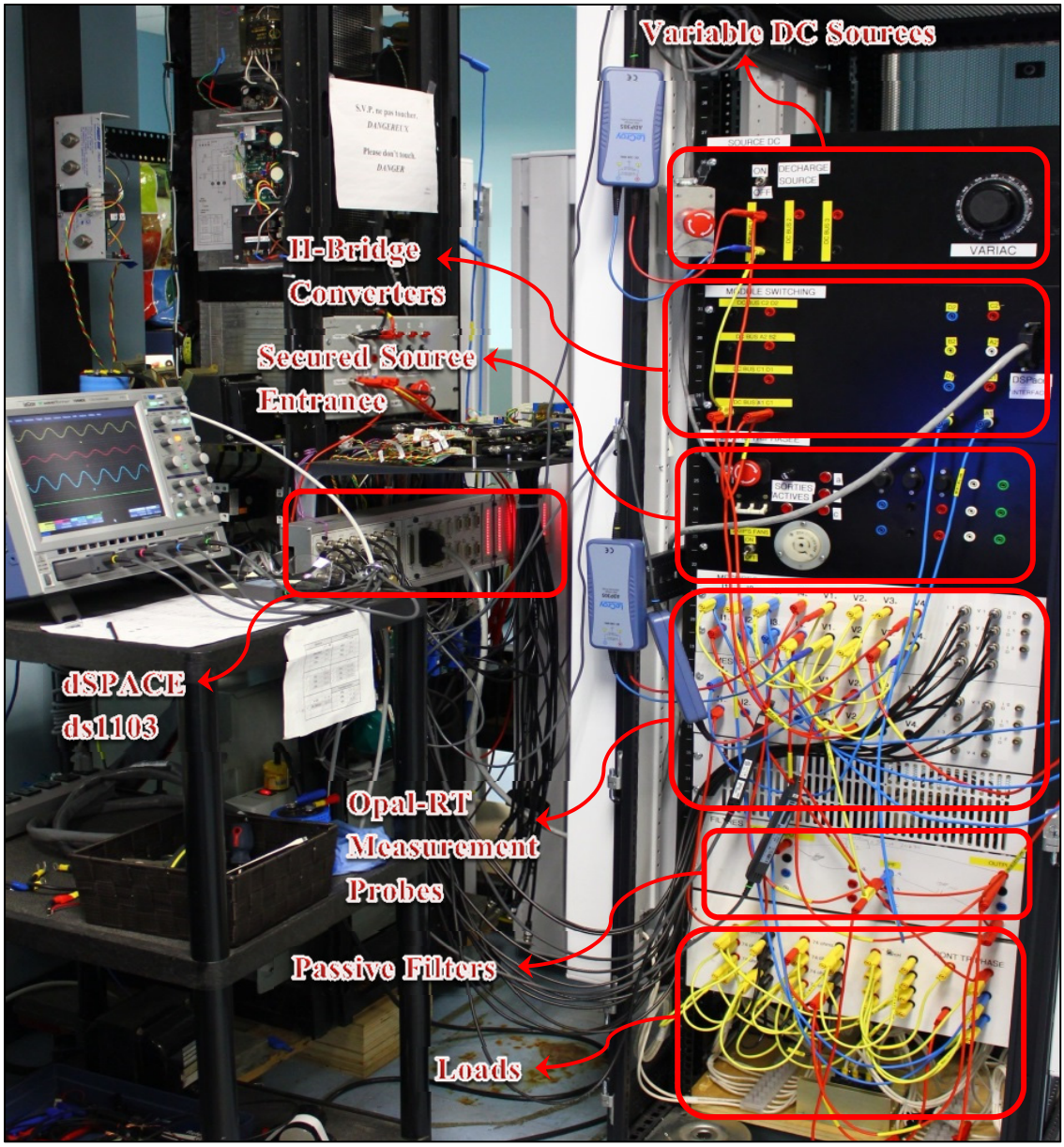

Figure 4.7 Laboratory setup used for the THSeAF experimental tests (front view)

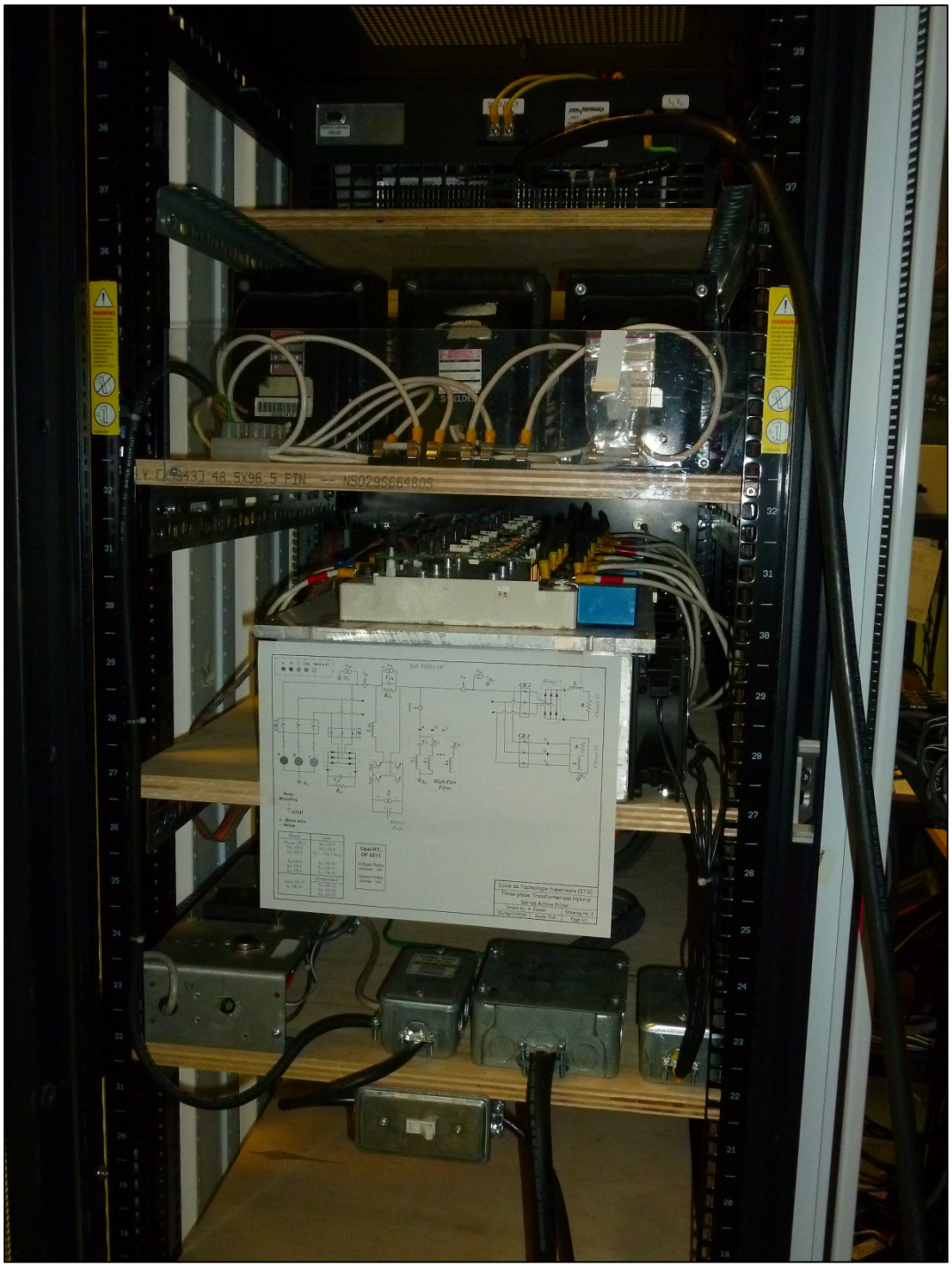

Figure 4.8 Laboratory setup of the THSeAF (back sight)

Table 4.1 Experimental configuration parameters

Symbol	Definition	Value
v_s	Line phase-to-neutral voltage	120 Vrms
f	System frequency	60 Hz
L_S	Supply equivalent inductance	150 μH*
R_{NL}	Non-linear Load resistance	40 Ω
C_{NL}	Non-linear Load capacitance	1000 μF
S_L	Linear load power	864 VA
PF	Linear load power factor	70 %
L_f	Switching ripple filter inductance	5 mH
C_f	Switching ripple filter capacitance	2 μF
r_C	Switching ripple damping resistor	50 Ω
F_5	Fifth order shunt passive filter	150μF, 2.5mH
F_7	Seventh order passive filter	50μF, 2.5mH
F_{HPF}	High-pass filter	2μF
T_S	dSPACE Synchronous sampling time	40 μs
f_{PWM}	PWM frequency	10 kHz
G	Control gain for harmonics current	3 Ω
V_{DC}	dc auxiliary power supply voltage	130 V

* Adopted value for the offline simulations

The combination of a single-phase non-linear load and a linear load with a total rated power of 1.6 kVA with a 0.8 lagging power factor is used for laboratory experiments and simulations. The compensator connected in series to the system compensates the current and voltage related issues instantaneously as demonstrated in the simulation results in Figure 4.9.

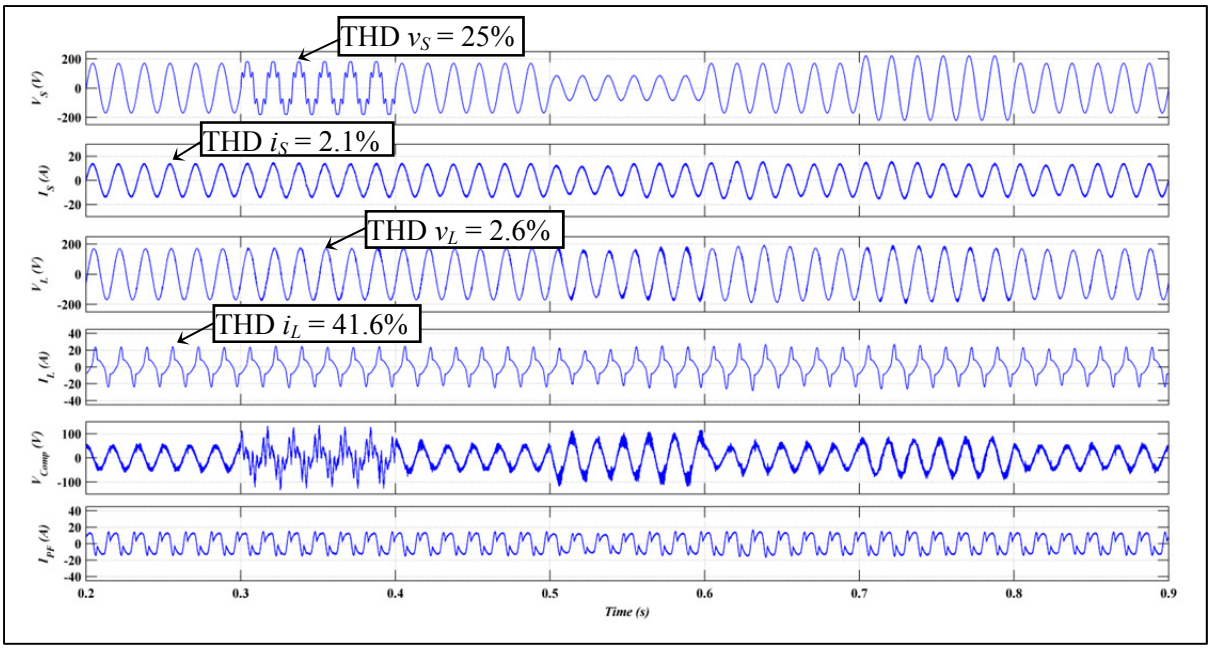

Figure 4.9 Simulation results of the THSeAF compensating current harmonics and performing a voltage restoration on the load. (a) Source voltage v_S, (b) source current i_S, (c) load voltage v_L, (d) load current i_L, (e) Active-filter voltage V_{Comp}, (f) Harmonics current of the passive filter i_{PF}

The THSeAF is preventing load currents distortions with a high THD to flow into the utility while correcting the power factor. As demonstrated in this simulation during a distortion initiated from 0.3s to 0.4s, by the grid, the compensator delivers a clean and harmonic-free supply at the load terminals. During a Grid sags from 0.5s to 0.6s and swells from 0.7s to 0.8s, the compensator delivers a regulated voltage supply with a constant voltage magnitude at the residential entrance.

The complete experimental setup is demonstrated in Figure 4.7. The results of various scenarios similar to those conducted in the simulation are illustrated in figures 4.10 through 4.15. The Figure 4.10 shows the compensator during steady state operating with parameters described in Table 4.1 which indicates the parameters of the system used for simulation and for experimental setup.

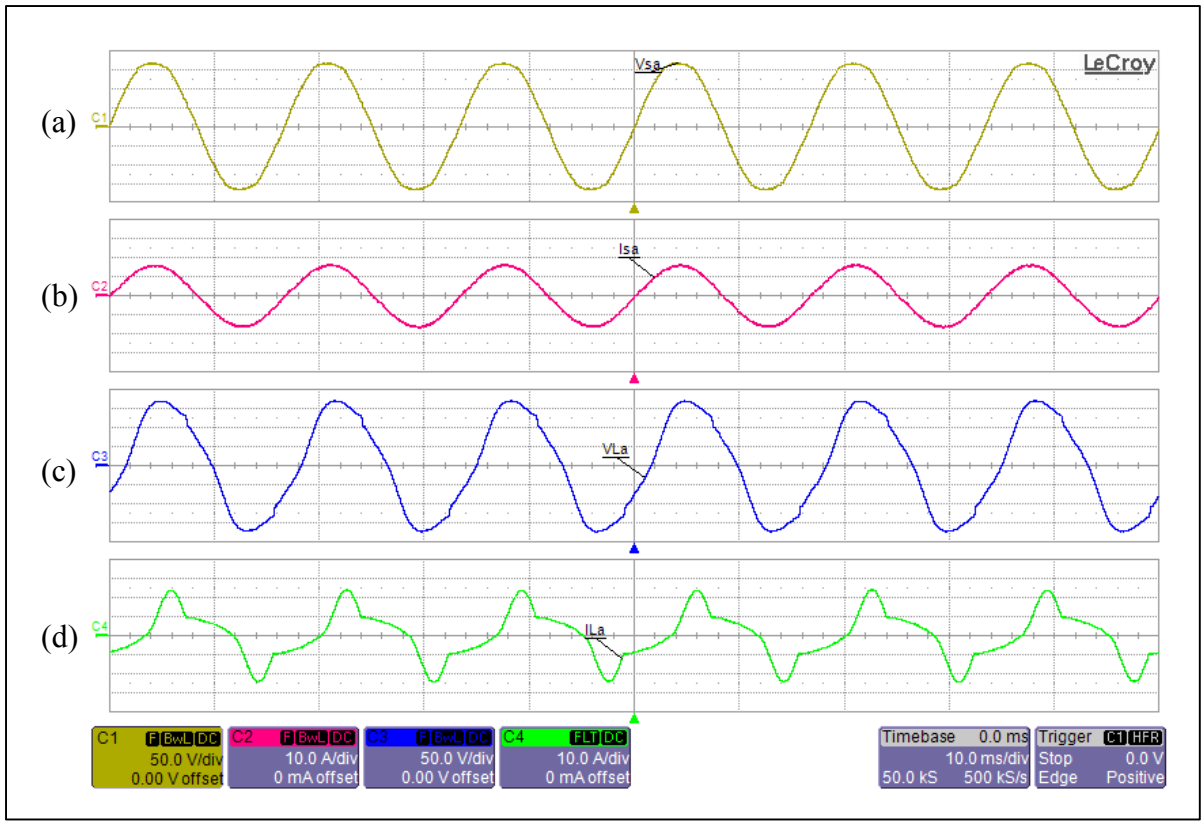

Figure 4.10 Steady state waveforms of the THSeAF compensating load current (a) Source voltage v_S [50V/div], (b) source current i_S [10A/div], (c) load PCC voltage v_L [50V/div], (d) load current i_L [10A/div]

The compensation during steady state depicted in the Figure 4.10, shows the highly polluted load harmonics isolated from the utility. The compensator maintains the load's voltage regulated with constant amplitude and free of all kinds of distortions independently of the grid condition. The load's voltage THD could be reduced to the desired value by performing a fine tuning of the shunt passive filter which indirectly contributes to the voltages quality as explained in previous section. This is a one-time tuning independent of other parameters of the system. The harmonic content and THD factor of source and load voltage and current for the Figure 4.10 are presented in Figure 4.11.

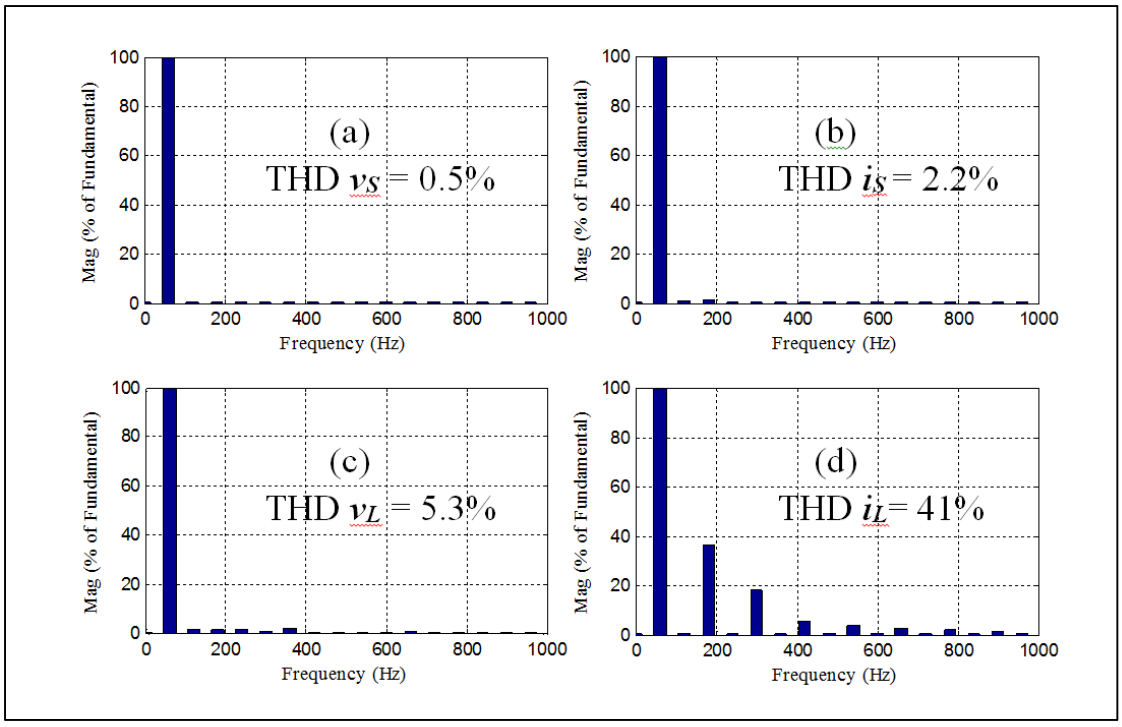

Figure 4.11 Harmonic contents in percentage of fundamental when THSeAF in operation (a, b) Source voltage and current, (c, d) Load voltage and current

The Figure 4.12 shows worst circumstance in which the utility's voltage becomes distorted with THD of 13.8%. The compensator should prevent these voltage distortions initiated by the grid from appearing at the loads terminals while cleaning the grid's current from the harmonic pollution of the load.

The line current shows dramatic improvements in its THD while the THSeAF is operating in a hybrid approach. A gain G of 3 Ω equivalent to 0.4 p.u. was used to control current harmonics. As mentioned earlier, the capability of operating with reduced dc voltage is considered as one of advantage of the proposed configuration. For these experiments the dc voltage is maintained at 130 VDC. The grid is cleaned of current harmonics with a near unity power factor operation and the THD is reduced to less than 2.2% in normal operation and less than 4% during grid's voltage perturbations. While the series controlled source cleans the current of harmonic components, the source current is forced to be almost in phase with the source voltage.

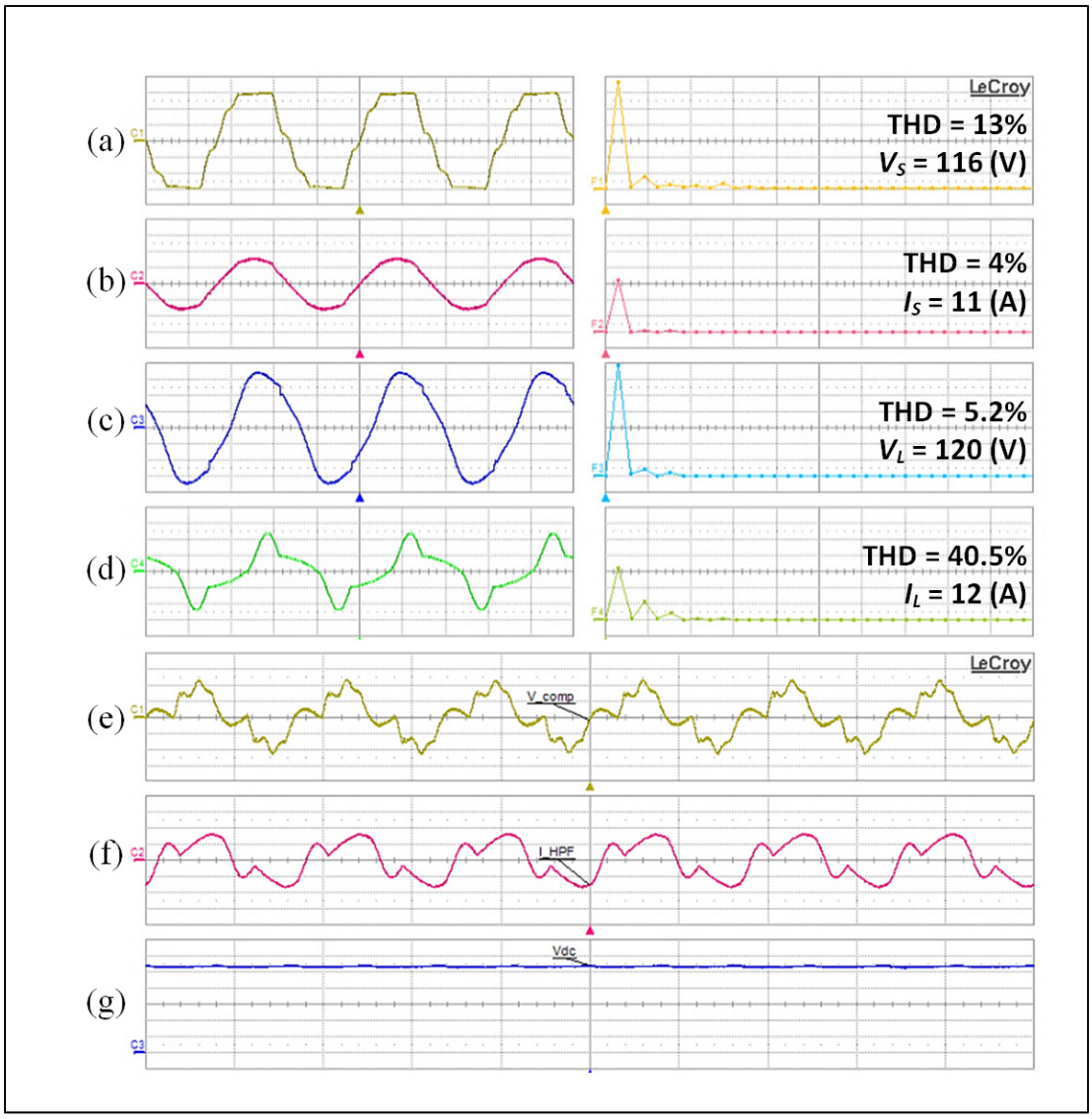

Figure 4.12 Experimental waveforms and harmonic spectrum under non-sinusoidal grid voltage. (a) Source voltage v_S [50V/div], (b) source current i_S [10A/div], (c) load terminal voltage v_L [50V/div], (d) load current i_L [10A/div], (e) THSeAF voltage v_{Comp} [20V/div], (f) passive filter current i_{PF} [10A/div], (g) DC voltage v_{DC} [50V/div]

The series compensator has the ability to slide the load voltage in order for the power factor to reach unity. Likewise FACTS devices, the series compensator could control the power flow between two buses and allowing a control on the load flow instantaneously by a third party operator as required for a Smart grid system. Prior to the compensation the grid was providing 1.573 kVA with a PF of 0.8 to the polluting load which in return was producing a

highly distorted current causing failure of other devices on the PCC and associated voltage distortion. Subsequently, when the THSeAF starts operating, the utility will supply 1.252 kVA at a PF equal to 0.99, while the load consumes 1.428 kVA with a PF of 0.8.

The compensator shows high efficiency in normal operation where the total compensator losses including switching, inductors resistances and damping resistances could be neglected. The compensator is absorbing 88 W and exchange 537 VAR. This amount of active power is stocked in the bidirectional DC source. The power flow and THD of measured values are summarized in Table 4.2 for case demonstrated in Figure 4.12 using the AEMC 8230-PowerPad Power Quality Meter.

Table 4.2 Laboratory measured value and power flow analysis

	Load PCC		**Grid Utility (Source)**	
Measures	Voltage, V_L (V)	Current, I_L (A)	Voltage, V_S (V)	Current, I_S (A)
THD (%)	5.2	40.5	13	4
Fund. (rms)	120	11.9	116	10.8
Active power, P (W)	1155		1243	
Reactive power, Q (var)	617		80	
Power, S (VA)	1428		1252	
Power Factor, PF (%)	80		99	
Compensator, THSeAF	S_{Comp}= + 88W – j537var			

Experimented results illustrate high fidelity towards simulations. During a grid's voltage sags, the compensator regulates the load voltage magnitude, compensates current harmonics and corrects the power factor as shown in Figure 4.13.

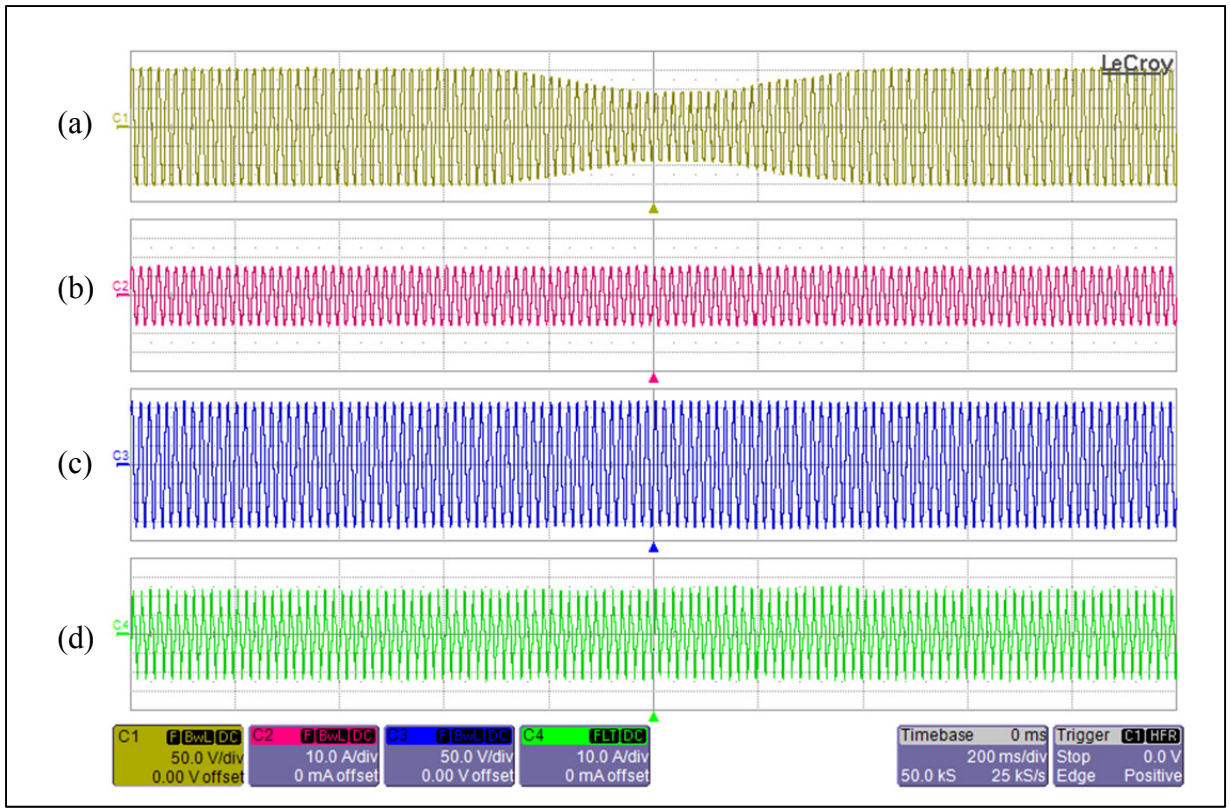

Figure 4.13 Waveforms during a variation of the source voltage
(a) Source voltage v_S [50V/div], (b) source current i_S [10A/div],
(c) load PCC voltage v_L [50V/div], (d) load current i_L [10A/div]

The presented waveforms in Figure 4.13 show extreme possible cases in which the THSeAF could face during the worst scenario requiring compensation of voltage harmonics. While cleaning the source current from harmonics and correcting the power factor the compensator regulates the load terminal voltage. As mentioned previously, the auxiliary source provides necessary amount of power to maintain the supply at the load terminals despite variation in the utility's voltage magnitude.

The behavior of the proposed compensator during dynamic load variation could be depicted from the oscilloscope's snapshots in Figure 4.14 and Figure 4.15, where the loads are suddenly changed. Under these tests the system is subjected to 44% of variation in the load power and consequently in the load's current magnitude. The THSeAF reacts instantly to this variation and do not interfere its operation functionality. It is usual to observe source voltage

variation due to the grid impedance, while the load's voltage is kept constant after a short transient voltage variation depending on the momentum of the load disengagement or connection.

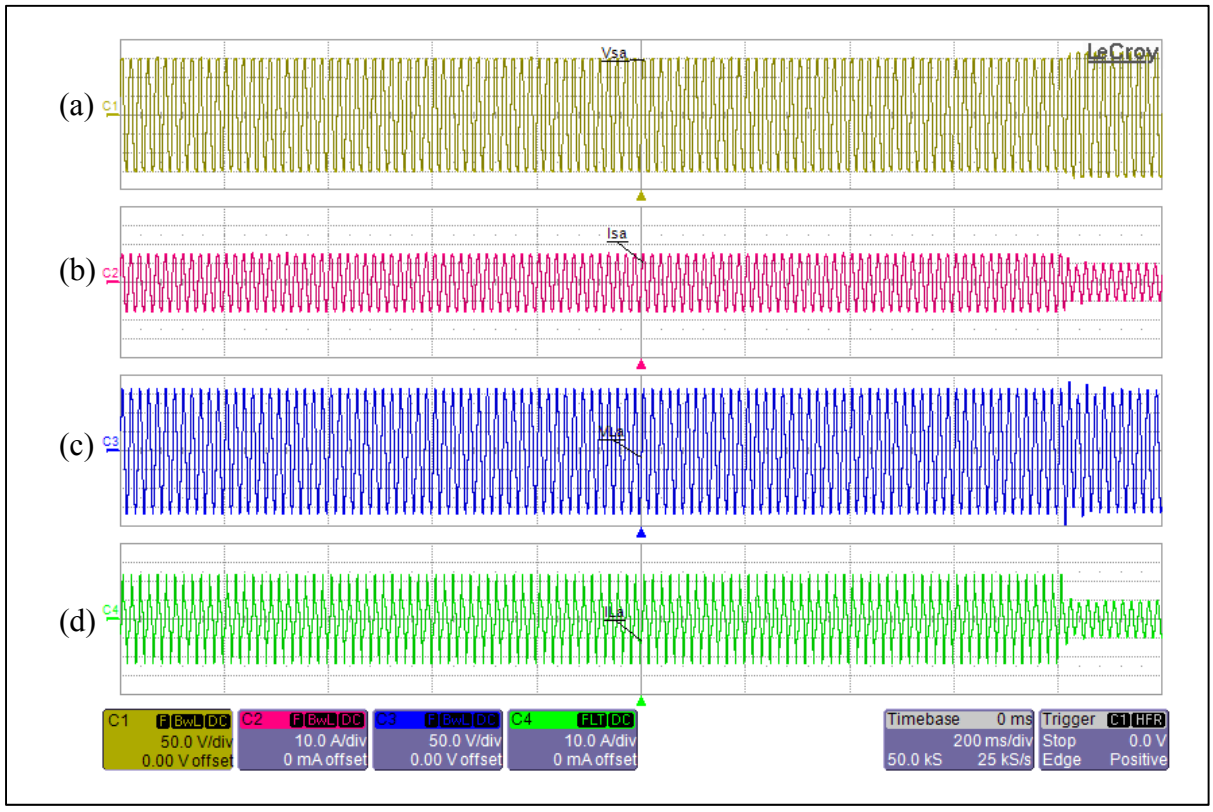

Figure 4.14 Waveforms during a dynamic decrease in the load under Grid perturbation (a) Source voltage v_S [50V/div], (b) source current i_S [10A/div], (c) load PCC voltage v_L [50V/div], (d) load current i_L [10A/div]

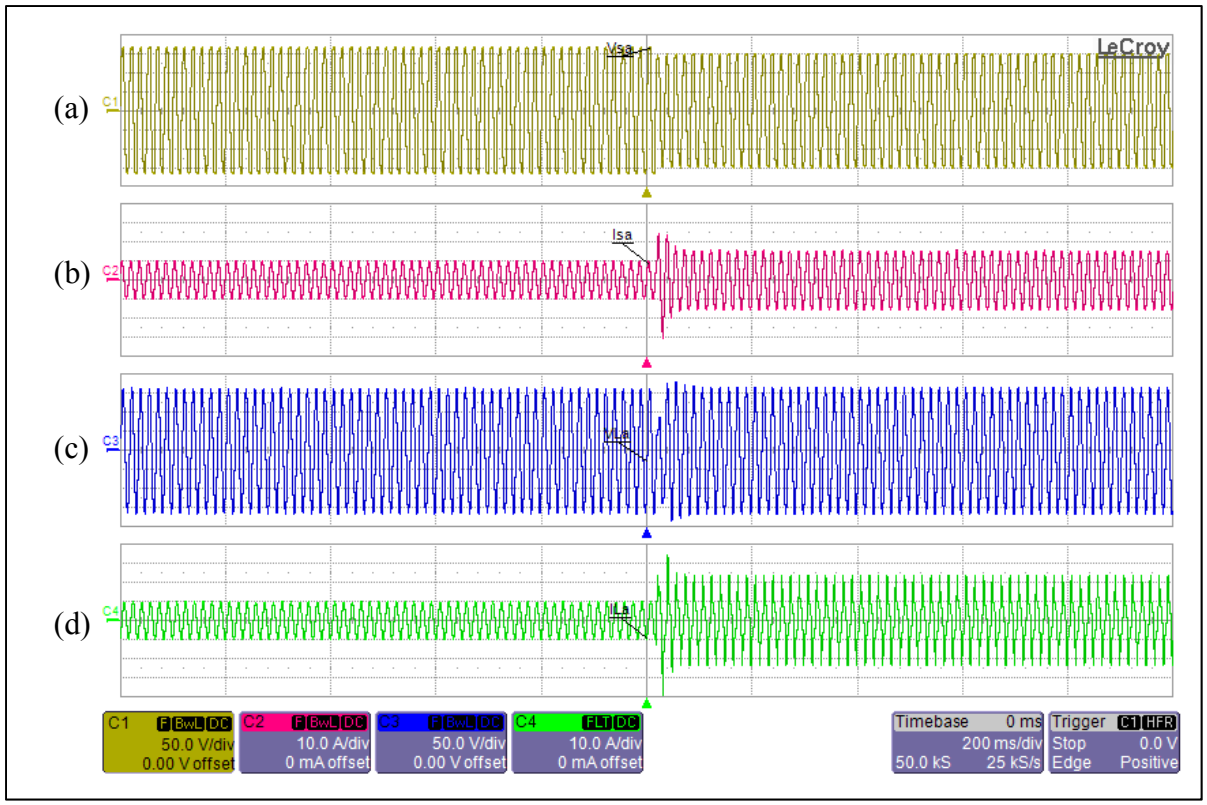

Figure 4.15 Waveforms during a dynamic increase in the load during grid's voltage distortion. (a) Source voltage v_S [50V/div], (b) source current i_S [10A/div], (c) load PCC voltage v_L [50V/div], (d) load current i_L [10A/div]

The THSeAF prevent existing perturbation on the grid's voltage to propagate on the load PCC protecting sensitive loads by maintaining a sinusoidal and regulated voltage. Moreover, in a worst possible scenario presented in Figure 4.13, the already distorted utility's voltage is subjected to voltage magnitude variation. The compensator should inject power to maintain the load PCC voltage regulated at the desired level. During voltage sag the auxiliary source supplies the difference of power to maintain the magnitude of the load side voltage regulated. The harmonic content and THD factor of the source utility and load PCC presented shows dramatic improvements in THD while the load draw polluted current waveforms. Furthermore, although the grid's voltage is polluted the compensator in a hybrid approach regulates and maintains a harmonics-free load's voltage.

4.6 Multilevel type of converter used as THSeAF with a PR controller

In this section a Multilevel compensator based on an NPC 3 level converter with a PR controller onboard is presented as a solution to enhance the power quality of typical households as shown in Figure 4.16. With the support of an NPC multilevel converter (Cipriano Dos Santos et al., 2015) and a Proportional plus Resonant (PR) controller, this Multilevel Transformerless Hybrid Series Active Filter (Multilevel-THSeAF) is improving power quality issues regardless of voltage and other limitations (Lin et al., 2015). This configuration will help reducing passive component sizing and improve the overall compensator design, the reason why the NPC configuration faces a wide range of applications (Rivera et al., 2015).

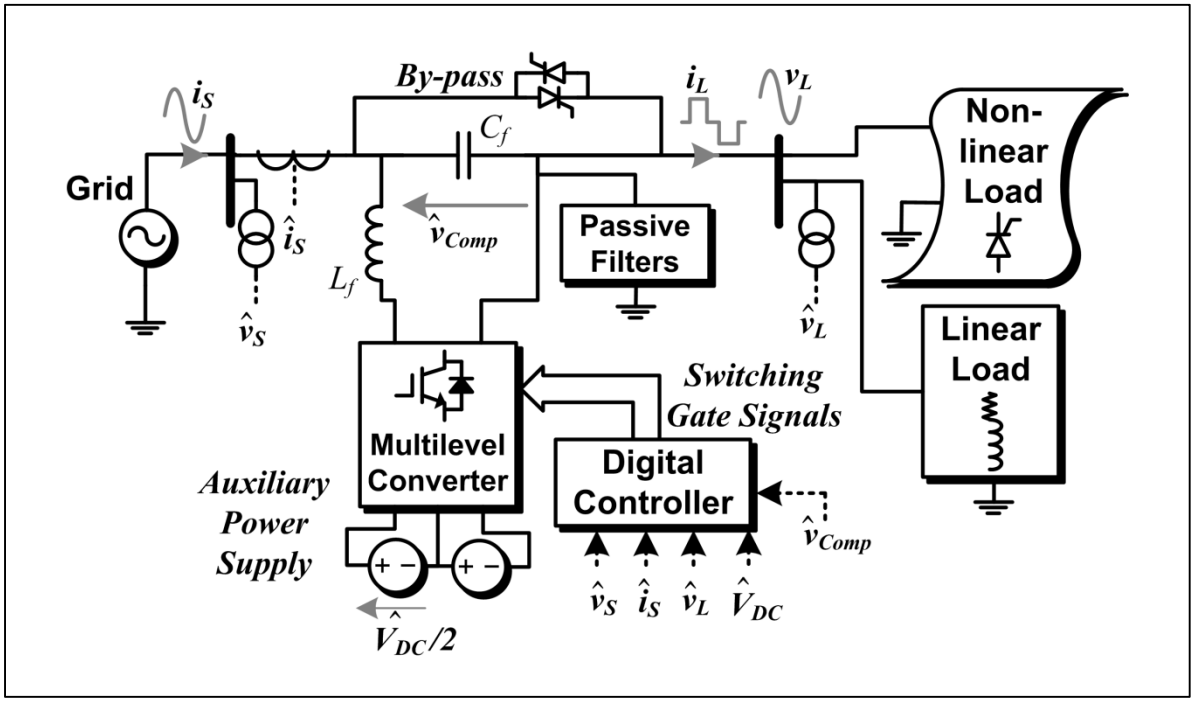

Figure 4.16 Electrical circuit connection with the Multilevel-THSeAF

The trends toward a future Smart Grid, and growth in evolution of electronic polluting components, such as electric vehicle charging station, cloud servers, PCs, and smart TVs power supplies have drastically created a concern on power quality of current and future

power systems (Liserre, Sauter et Hung, 2010). The increase in electronics devices associated with fast charging devices and combined with external energy sources require early investigation on harmonic and non-active power compensation (Guerrero et al., 2013). This widespread harmonic polluting devices not only reduces the system's efficiency, but also has detrimental impacts on grid voltage distortion levels (Zhikang et al., 2014). Likewise, distorted current waveform creates additional heating losses, and causes failure in sensitive electrical devices. Several references could be found in the literature addressing specified (Akagi et Isozaki, 2012b) or common case dealt with power quality issues either related to voltage distortions or current harmonics (Marques et al., 2012). This research work proposes an efficient and affordable solution using a multilevel configuration as demonstrated in Figure 4.17 to reduce dc side voltage for low level distribution system.

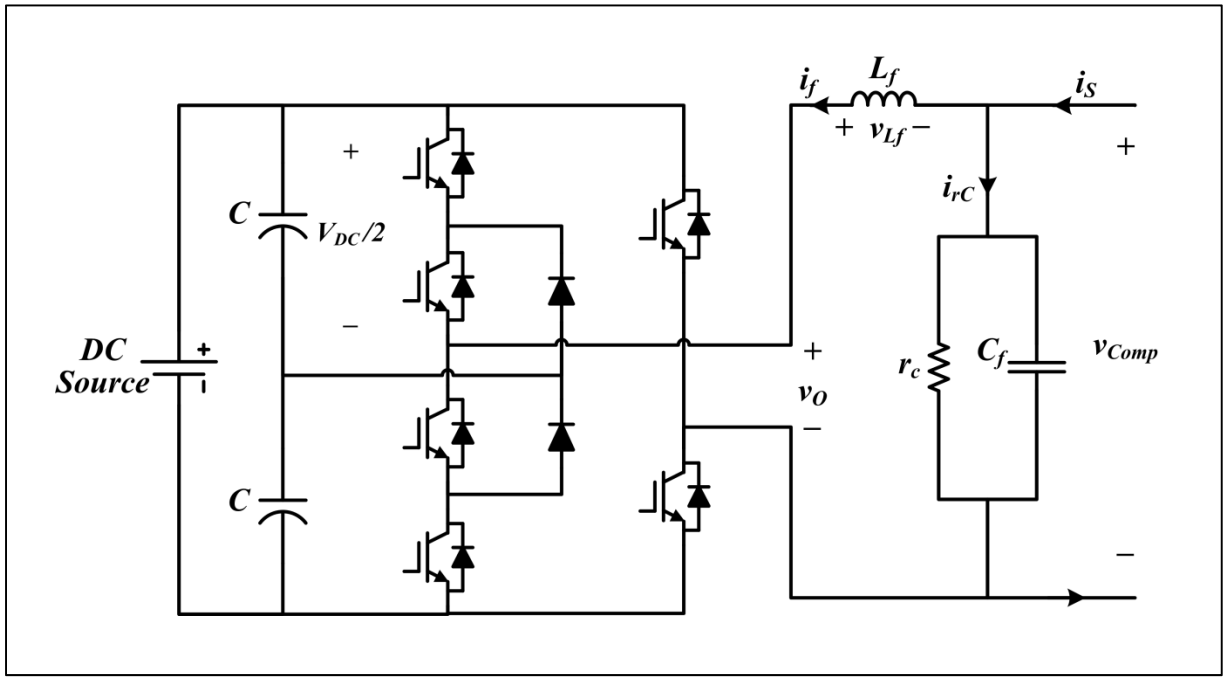

Figure 4.17 Hybrid converter topology for the proposed series compensator

The main objective of this section is to propose an efficient device capable to rectify current related issues in smart grids which also provides sustainable and reliable voltage supply at entrance of residential and commercial buildings. The use of this device will facilitate the

integration of energy storage systems and renewables for modern households (Qinglai et al., 2014). The proposed low cost configuration take advantages of the NPC structure (Hagiwara, Maeda et Akagi, 2012), and it is noteworthy that ride of the bulky transformer it is an economic key toward power quality improvement of future grids. This compensator cleans the current drawn from the utility and similarly to a Dynamic voltage restorer (DVR) the point of common coupling (PCC) and utility smart meters will be protected from voltage distortions and wrong computation of power and energy balance. This compensator could inject or absorb active power during grid voltage variations to ensure high quality supply along with complete decoupling from polluted loads.

4.6.1 System configuration of the Multilevel-THSeAF

The compensator depicted in Figure 4.16 is composed of a multilevel single-phase converter connected in series between the utility and the house's entrance terminals. A passive filter is connected in shunt as alternative path for load current harmonic. An auxiliary supply is connected on the dc side. To filter high frequency switching harmonics, a passive filter is used at the output of the converter. A bank of tuned passive filters ensures a low impedance path for current harmonics. In this paper the studied system is implemented for a rated power of 1 kVA. To ensure a fast transient response with sufficient stability margins over a wide range of operation, the controller is implemented on an Opal-RT/Wanda real-time simulator. For an accurate real-time measurement the Opal-RT OP8665 probes is taking care of measurements. The system parameters are identified in Table 4.3. A variable source up to 120 Vrms is connected to a 1 kVA non-linear load. The THSeAF is connected in series in order to inject the compensating voltage. On the DC side of the compensator, an auxiliary dc-link energy storage system is installed. Similar parameters are also applied for simulations. A fast electric vehicle charging plug level-2 is as well connected to the load's PCC.

On the DC side of the compensator, auxiliary dc-link energy storage components are installed at a reduced voltage of 100V. The objective of this paper is to propose an efficient

device capable to rectify current related issues in smart grids which also provides sustainable and reliable voltage supply at entrance of residential and commercial buildings.

Table 4.3 Experimental configuration parameters

Symbol	**Definition**	**Value**
V_s	Line phase-to-neutral voltage	110 Vrms
f	System frequency	60 Hz
L_S	Supply equivalent inductance	150 µH*
R, L	Non-linear CSC load	25 Ω, 20mH
L_f	Switching ripple filter inductance	2.5 mH
C_f	Switching ripple filter capacitance	0.2 µF
r_C	Switching ripple damping resistor	60 Ω
T_s	Opal-RT Synchronous sampling time	40 µs
f_{PWM}	PWM frequency	8 kHz
F_5	Fifth order shunt passive filter	56µF, 5mH
F_7	Seventh order passive filter	14µF, 10mH
F_{11}	Eleventh order passive filter	6µF, 10mH
F_{HPF}	High-pass filter	2µF
V_{DC}	dc auxiliary power supply voltage	110 V, 120* V

* Adopted value for the offline simulations

Using the circuit of Figure 4.16, several critical scenarios such as grid distortion, sag or swell are simulated using discrete time steps of T_s = 40µs as shown in Figure 4.18. The Multilevel-THSeAF connected in series injects a compensating voltage which results in a drastic improvement of source current distortions and a cleaned load voltage. While the load current contains a THDI_L of 12%, the source current is cleaned with a THDI_S of 2.1%. When the utility is highly polluted with a THDV_S of 25.5%, the load voltage is regulated and contains a THD of only 1.2%.

4.7 Proportional plus Resonant Controller (P+R)

Based on the average equivalent circuit of the inverter, the small-signal model of the proposed configuration is obtained. Then, this model is implemented in the control approach. The proposed control strategy takes advantages of both a proportional and resonant controller to generate gating signals of the power electronics devices.

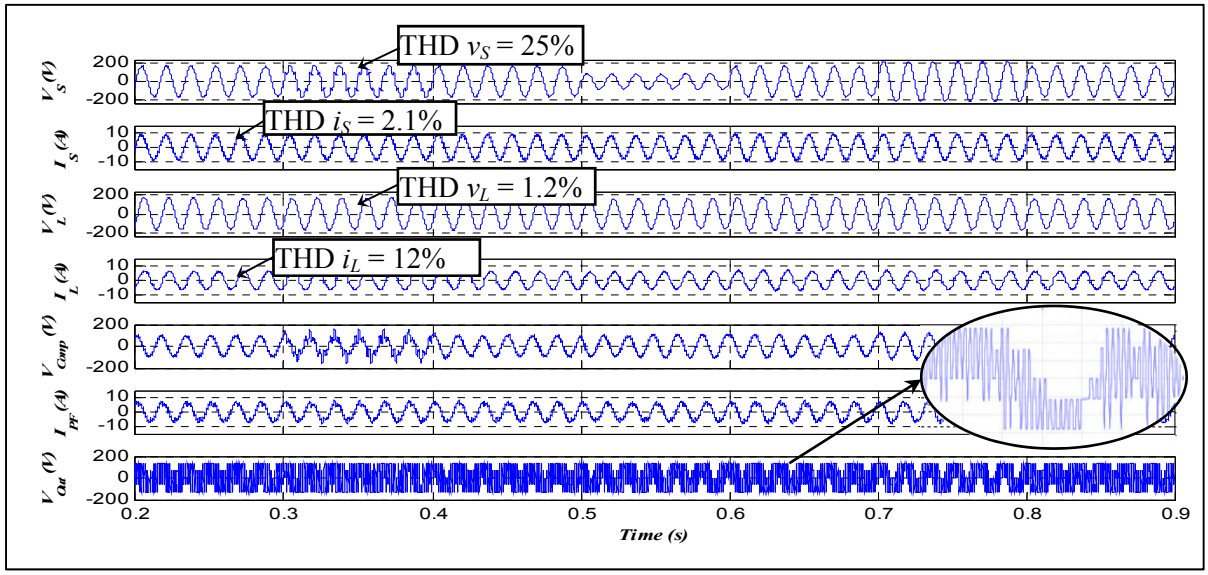

Figure 4.18 Simulation results of the THSeAF compensating current harmonics and performing a voltage restoration on the load. (a) Source voltage v_S, (b) source current i_S, (c) load voltage v_L, (d) load current i_L, (e) Active-filter voltage V_{Comp}, (f) Harmonics current of the passive filter $i_{PF,}$ (g) Converter's output voltage V_{Out}

The controller strategy implemented in this paper is based on a Proportional plus resonant controller to generate IGBT's gate signals. The reference signal applied to the P+R regulator is created by two detection block taking care of the voltage and current issues respectively as presented in the diagram of Figure 4.19.

As the compensating voltage reference is an oscillating signal with several harmonic components, the P+R regulator has numerous advantages over other control approaches. To develop the controller, the average equivalent circuit of the converter is used with the small-signal model of the proposed configuration to analyze the effects of delays on the transient

response of the compensator. The proposed control strategy takes advantages of both a proportional and resonant controller to generate gating signals.

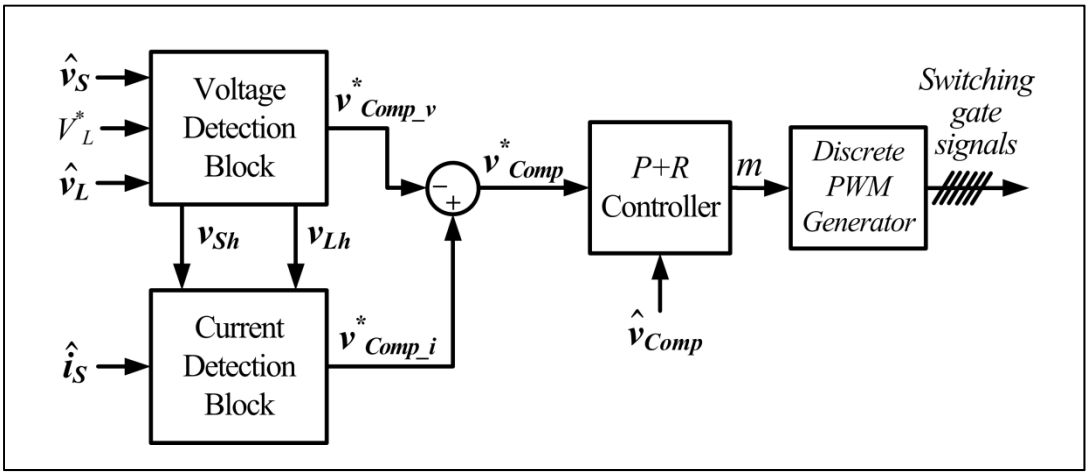

Figure 4.19 Control system architecture scheme for P+R

The transfer function of the controller with a multi-resonant property is given by:

$$G_{P+R}(s) = K_P + \sum_{h=1,3,5,7,\ldots}^{n} \frac{2K_{rh} \cdot \omega_C \cdot s}{s^2 + 2\omega_C \cdot s + (h \cdot \omega)^2} \tag{4.35}$$

Where h is the harmonic order, K_p and K_r are gains, and $h\omega$ is the resonant frequency and ω_C is the cutoff frequency. The frequency responses with a delay time are depicted in Figure 4.20, where the open loop Bode diagram is shown for the system without regulation, with a PI regulator, and the P plus Resonant controller respectively.

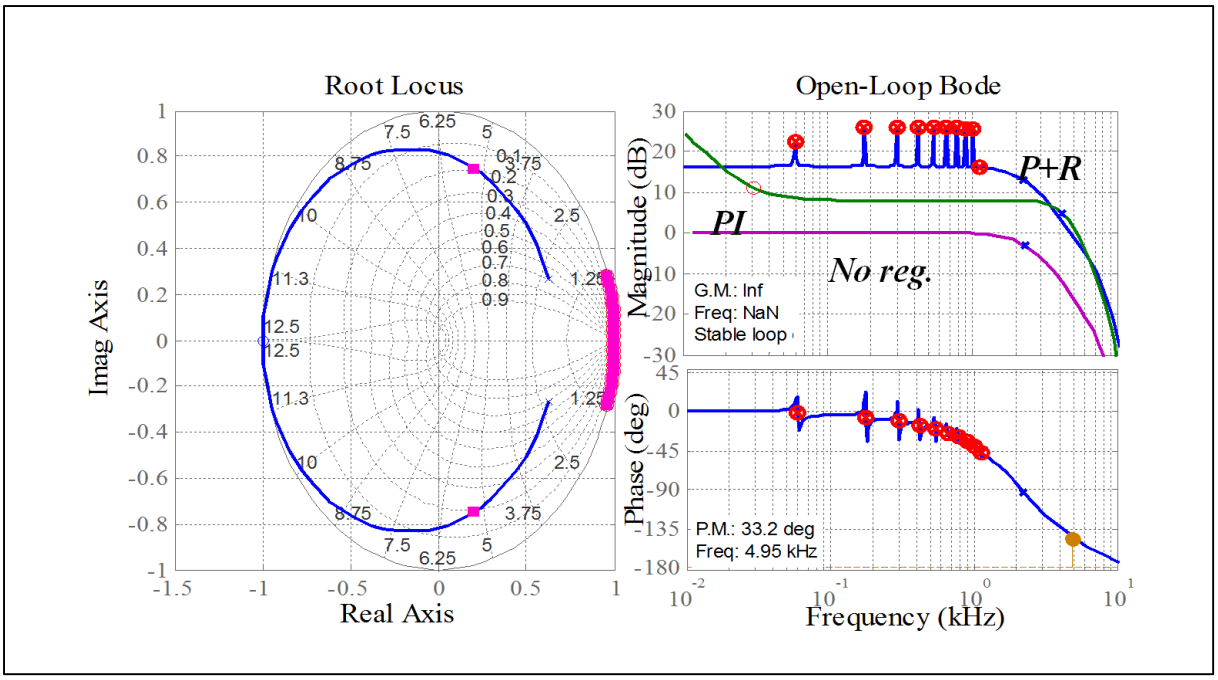

Figure 4.20 Frequency response of the system including a 40 μs delay time
(a) Root Locus diagram, (b) Bode diagram

4.8 Controller Discrete Equivalent

In this section the discrete equivalent of the P+R continuous function needed to simulate a sampled-data system, is presented. In a real life, the controller is discrete while the physical plant is continuous. Thus to design a controller to be implemented on a digital controller which will then interact with a continuous-time plant one may start from directly design a discrete controller or discretizing a continuous *s*-function. In this case the P+R function in Laplace domain will be discretized and the *z*-domain function which is ready to be implemented is derived and the stability of the developed *Z*-function will be analyzed.

4.8.1 Design of discrete equivalent via numerical integration

To obtain the discrete equivalent of a transfer function via numerical integration, one should first write the system differential equation, and then apply one of the three following

numerical integration depending on the sensitivity and stability requirements. The operation can be carried out directly on transfer function in the frequency domain.

The Forward rectangular rule in Laplace domain:

$$s \rightarrow \frac{z-1}{T} \tag{4.36}$$

The Backward rectangular rule:

$$sz \rightarrow \frac{z-1}{T} \tag{4.37}$$

The Trapezoidal rule:

$$\frac{s+sz}{2} \rightarrow \frac{z-1}{T} \tag{4.38}$$

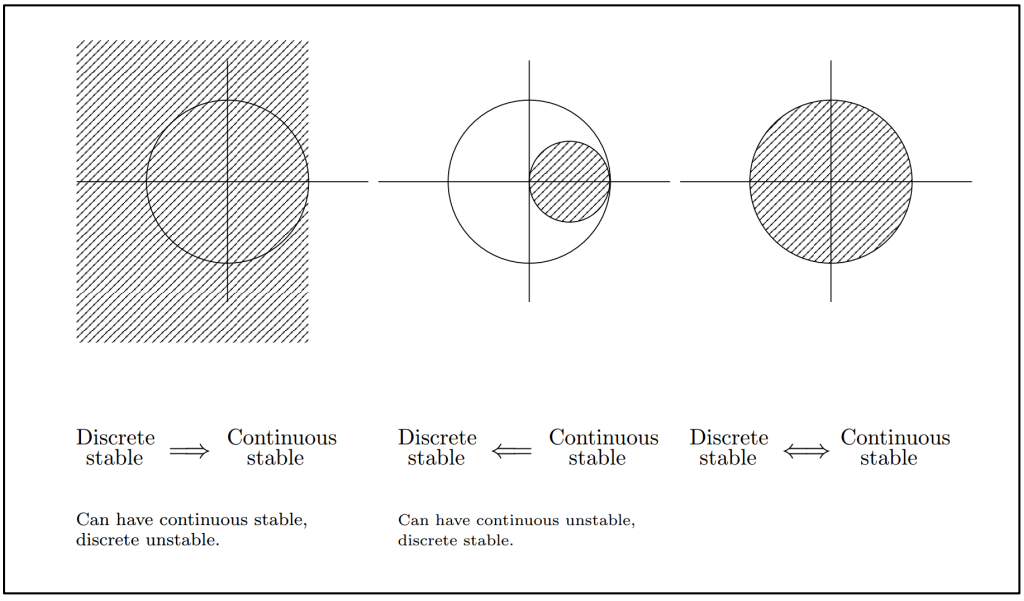

Figure 4.21 Representation of the stable region of *s*-plane under three z-transform approximations; (a) forward rectangular, (b) backward rectangular, and (c) bilinear

As illustrated in the Figure 4.21, under the trapezoid rule, the stable region of *s*-plane is mapped on to the stable region of the *z*-plane stable circle. This and other observations are summarized below. Using this rule, the discrete system is stable if and only if the continuous-time system is stable. For the forward rule, the discrete-time system will be stable only if the continuous system is also stable.

4.8.1.1 Euler approximation

The P+R controller function is calculated using the Forward rectangular rule also called the Euler's approximation. Consequently, in the Laplace function the variable *s* and s^2 are replaced by the following term:

$$s \rightarrow \frac{z-1}{T} \quad , \quad s^2 \rightarrow \frac{(z-1)^2}{T^2} \tag{4.39}$$

Where z is the variable in the *z*-domain and *T* is the sampling time constant also known as step-time T_S in Matlab environment. By performing the Z-transform on the Eqn 4.27, the discrete transfer function is achieved as follow.

$$G_{P+R}(z) = K_P + \sum_{h=1,3,5,7,\ldots}^{n} \frac{2K_{rh} \cdot \omega_C \cdot z - 2K_{rh} \cdot \omega_C}{z^2 + 2(\omega_C T - 1) \cdot z + (1 - 2 \quad {}_C T) + (h \cdot \omega)^2 \cdot T^2} \tag{4.40}$$

4.8.1.2 The Bilinear approximation (Tustin)

The Tustin or bilinear approximation uses the trapezoidal rule. The frequency variable *s* is replaced by the following term.

$$s \rightarrow \frac{2 \cdot (z-1)}{T(z+1)} \quad , \quad s^2 \rightarrow \frac{4(z-1)^2}{T^2(z+1)} \tag{4.41}$$

This results in the following discrete transfer function in the z-domain.

$$G_{P+R}(z) = K_P + \sum_{h=1,3,5,7,\dots}^{n} \frac{2K_{rh} \cdot \omega_C \cdot z^2 \cdot T - K_{rh} \cdot \omega_C \cdot T}{(1 + \omega_C T + (h\omega T)^2)z^2 + \left(\frac{(h\omega T)^2}{2} - 2\right)z + 1 - \omega_C T + \frac{(h\omega T)^2}{4}} \quad (4.42)$$

According to the two developed discrete function one can implement either of them for a real-time simulation or a practical experiments on a digital controller. Meanwhile, the choice of gains is tied with the stability study of the transfer function. The gains should be chosen depending on the sampling time imposed by the digital controller, and the behavior of the system itself. In a general rule; the more the sampling time *T*, is a small value, the more the chance to reach a stable system.

4.9 Simulations and Experimental Results for the Multilevel-THSeAF

To validate he study various scenarios similar to those effectuated in the simulation are performed on a laboratory prototype. Figure 4.22 shows the setup components with parameters described in Table 4.3. The Opal-RT real-time simulator, the NPC converter along with precise probes dedicated for RCP applications are noticeable in the picture.

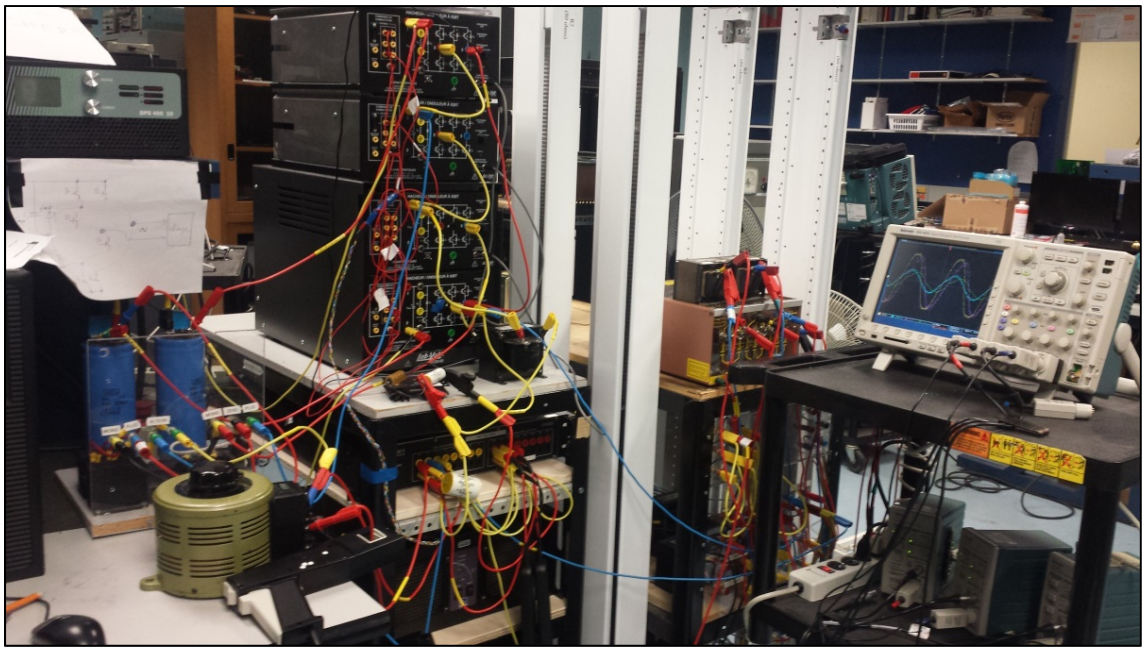

Figure 4.22 Laboratory setup used for experiments

The compensation during steady state depicted in Figure 4.23, shows the polluted load harmonics isolated from the utility. Moreover, the compensator maintains the load's voltage regulated with constant amplitude and free of all kinds of distortions independently of the grid condition. The load's voltage THD could be reduced to the desired value by performing a fine tuning of the shunt passive filter which indirectly contributes to the voltages quality as explained in previous section. This is a one-time tuning independent of other parameters of the system. The harmonic content and THD factor of source and load voltage and current for the Figure 4.23 are presented in Figure 4.24. It is noticed that the reactive power is compensated and a unity power factor is achieved.

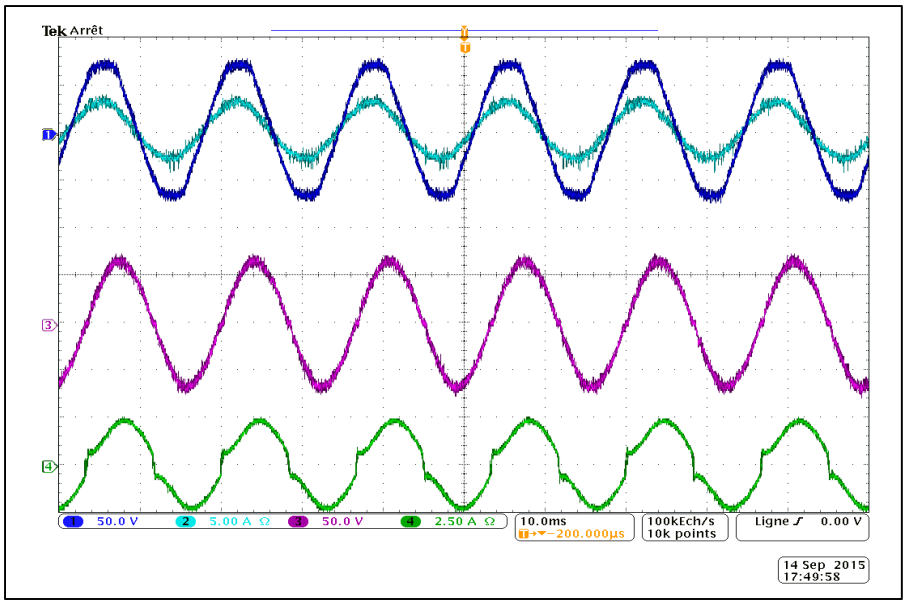

Figure 4.23 Steady state waveforms of the THSeAF compensating load current. (a) Source voltage v_S [50V/div], (b) source current i_S [5A/div], (c) load PCC voltage v_L [50V/div], (d) load current i_L [2.5A/div]

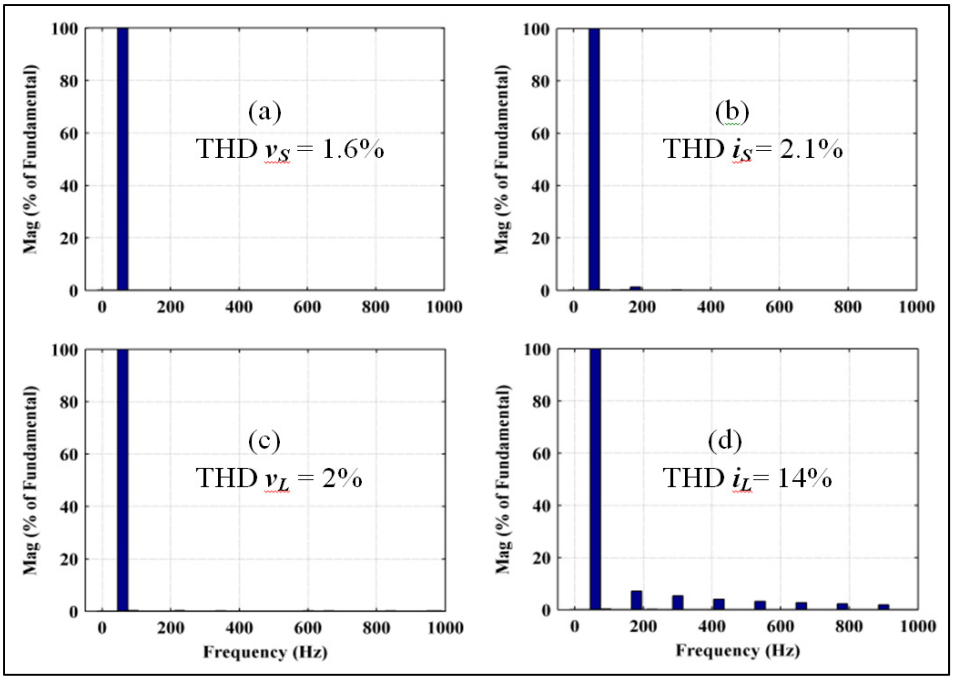

Figure 4.24 Harmonic contents in percentage of fundamental when THSeAF in operation; (a, b) Source voltage and current, (c, d) Load voltage and current

Experimented results illustrate high fidelity towards simulations. During a grid's voltage sags, the compensator regulates the load voltage magnitude, compensates current harmonics and corrects the power factor as shown in Figure 4.25.

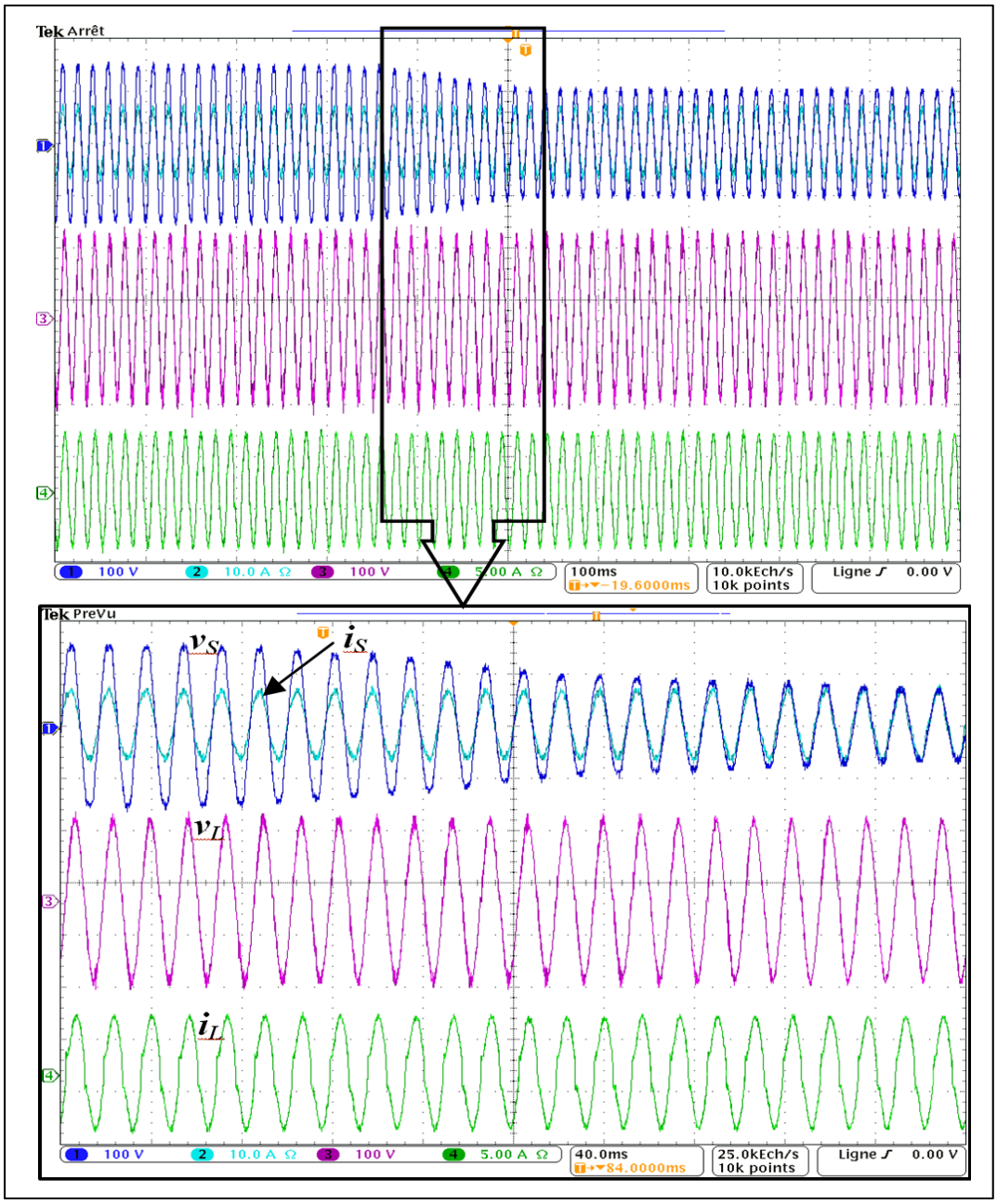

Figure 4.25 Waveforms during a sags; (a) Source voltage v_S [100V/div], (b) source current i_S [10A/div], (c) load PCC voltage v_L [100V/div], (d) load current i_L [5A/div]

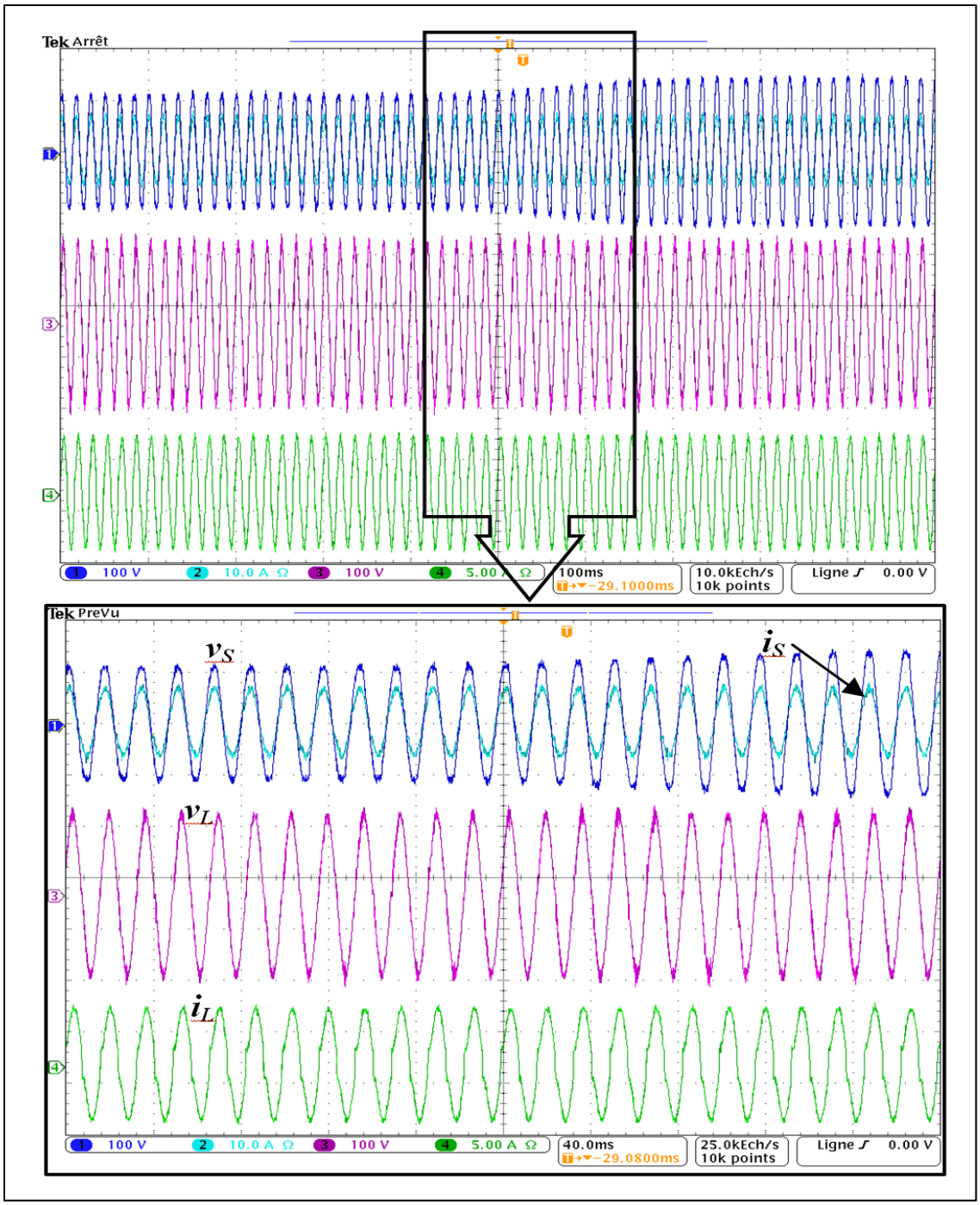

Figure 4.26 Waveforms during a swells; (a) Source voltage v_S [100V/div], (b) source current i_S [10A/div], (c) load PCC voltage v_L [100V/div], (d) load current i_L [5A/div]

The previous figures show possible cases in which the THSeAF could face during the worst scenario requiring regulation of the load voltage, while cleaning the source current from

harmonics and correcting the power factor the compensator regulates the load terminal voltage. The auxiliary source provides necessary amount of power to maintain the supply at the load terminals despite variation in the utility's voltage magnitude. As expected from simulations, during a grid's extended voltage swell, the compensator regulates the load voltage magnitude by injecting active power while compensating current harmonics and correcting the power factor as shown in Figure 4.26.

4.10 Conclusion

In this chapter, first a THSeAF with a sliding mode controller founded on a Notch harmonics detection technique for power quality improvement was developed and tested on a voltage fed non-linear load. The proposed configuration cleans the utility's current and could ensure a desired power factor upon request. With regards to the control approach and taking advantage of the proposed robust structure, it delivered a harmonic free voltage across the residential entrance terminals. The theoretical modeling of the proposed configuration besides the controller mathematical developments were investigated and simulated. Results of the laboratory implementation, have demonstrated that this active compensator responds to sudden abrupt variations in the source voltage by providing a constant and distortion-free supply to the load while eliminating grid current harmonics. Therefore, this THSeAF contributes to the improvement of the grid's power quality.

The chapter is then followed, by an improved Multilevel-THSeAF based on an NPC configuration. A remarkable controller is developed and therefore implemented to face power quality issues of a single-phase residential building. The P+R controller was adapted for the Multilevel-THSeAF configuration and a discrete model was established for real-time simulations and practical laboratory implementations were demonstrated for validation. The M-THSeAF can regulate and improve load voltage terminals and when connected to a renewable auxiliary source, the topology is able to counteract actively to the power flow in the system. Having a constant and distortion-free supply at load PCC, it was denoted that the active compensator responds well to source voltage variations. Furthermore, the compensator

eliminates source harmonic currents and improves grid power quality with no need to use typical bulky series transformers. While, having a more precise and higher quality produced compensating voltage, this multilevel configuration allows considerably reducing passive components used in the compensator. Even if the P+R controller is relatively complex, especially for practical applications, regarding the highly oscillating shape of the compensating voltage reference, it shows a higher performance compared to the conventional PI or the Sliding mode controllers.

CHAPTER 5

A THREE-PHASE THSEAF TO IMPROVE POWER QUALITY OF WEAK DISTRIBUTION SYSTEMS

5.1 Introduction

In this chapter the power quality of three-phase system is treated. A three-phase series compensator is proposed to overcome power quality of three-phase systems at low voltage distribution systems. Similar to single-phase SeAF, the proposed series active power filter adapted for the three-phase system with four-wire system is able to clean the grid's current from harmonics, unbalance and correct the power factor. Moreover, it would have the capability of cleaning the load side voltage problems and ensuring a stable and perturbation-free supply. In this chapter first an advanced comprehensive control approach for Hybrid series active power filters is demonstrated. To illustrate the efficiency of the approach the control strategy is applied to a configuration which consists of a Hybrid series active filter (HSeAF) with isolating transformer. The proposed control strategy, make this topology capable of compensating current distortions at the source utility and voltage harmonics and related issues from the load point of common coupling (PCC). The controller compels the HSeAF to perform similar to a Unified power quality conditioner (UPQC). The control algorithm is using the synchronous reference frame SRF and the *p-q* theory to create an approach treating a multitude of problems. It makes the HSeAF able to treat diverse power quality issues related to current and voltage simultaneously. With a fast and accurate response, it makes the PCC more reliable, cleans the load's current, and corrects the power factor.

In a second stage the chapter assesses the deployment of the previous proposed detection approach to a novel transformerless configuration. The section is dedicated to propose a novel configuration of Series hybrid active filters ridded of the bulky transformer. The proposed configuration could be connected to the grid without requiring a costly series isolating transformer. This topology is capable of compensating current harmonics at the

source and voltage distortion at the point of common coupling. Furthermore, an appropriate controller similar to the one developed in the first stage of this chapter could compel the Transformerless hybrid series active filter (THSeAF) to perform similar or superior characteristics than a conventional HSeAF while operating like a Unified power quality conditioner (UPQC) with quasi-similar behavior. The transformerless configuration is more cost-effective than any other series compensators based on a transformer to inject the desired compensating voltages. It could be operated as a dynamic voltage regulator, in which it will compensate unwanted harmonics, unbalances, sags, and swells at terminals of a sensitive load. When performing as a series hybrid active filter, it cleans the power system from current distortions together with harmonics and unbalances, similar to a shunt active filter. The detailed operation of the proposed topology is presented and analyzed in detail. Modeling and controller design are given and validated by simulations of the system dynamic for different load and supply conditions.

In the third section a novel three-phase Transformerless Hybrid Series Active Filter (THSeAF) based on voltage fed converters to address major power quality issues related to residential and commercial buildings is presented. This device presents an affordable solution to overcome current related issues as well as integrating renewables to ensure a sustainable supply. The controller based on a novel combination of Synchronous Reference Frame (SRF) and *p-q* theory to extract voltage and current harmonics and unbalances is developed. This controller is an improved version of the one presented in the first section of this chapter. To produce gate switching signals for the three-phase THSeAF a conventional Proportional-Integral controller (PI) is used to produce reference waveforms produced earlier to rectify harmonic currents initiated from typical non-linear loads. The device ensures a reliable and dynamically restored power supply on the load's point of common coupling (PCC) by means of three auxiliary DC supplies. This section describes mitigation of power quality related issues into a micro-grid system. Finally, a combination of simulation results and analysis are carried out for validation.

5.2 Control Algorithm for a 3P4W Hybrid Series Active Filter

With the increasing of three-phase loads, the future grids should provide an efficient and sustainable power supply implicating renewable sources. To do so, the series active power compensators are competent players in addressing power quality issues while integrating renewable energies into the system. Hence, both single-phase and three-phase loads will be protected from voltage distortions. On the other hand, the current harmonic pollution arises from nonlinear loads, which affect equipment in the polluting plant requires to be corrected. This section aims to contribute to the integration of series active filters as a powerful compensator in Smart power grids environment. The use of active filters as an affordable solution for power quality is indispensable to increase simultaneously the efficiency and sustainability of modern power systems.

5.2.1 The 3P4W System Configuration

The concept of a series active compensation was initially introduced to act as a voltage regulator. It insures a sinusoidal balanced voltage on the load side despite the presence of perturbations such as unbalance, harmonic distortion, sags and swells in the grid supply. Instead, the Shunt AFs where cleaning load current by injecting equal but opposite harmonic compensating currents. Various attractive approaches have been proposed to combine the shunt and series active filter, leading to UPQC type of topology. They were introduced to take the advantages of both mentioned active power filters. The series connected filter compensate voltage harmonics and related issues, and the shunt connected across the load eliminate current distortions (Khadkikar, 2012). However, the complexity and elevated price of this configuration put it as the last technical resort.

Alike to single-phase case studied in this thesis, an alternative in three-phase is also to combine a passive filter with a series active filter. This three-phase configuration of the series active part operating in conjunction with the shunt passive filter will compensate load current harmonics. Taking advantage of the passive branch, the HSeAF with the appropriate control

approach will be able to compensate disturbances in the current load such as unbalances and distortions by higher-order harmonics. To do so, the series active filter is forced to inject an appropriate voltage to the line through a series connected transformer as shown in the Figure 5.1.

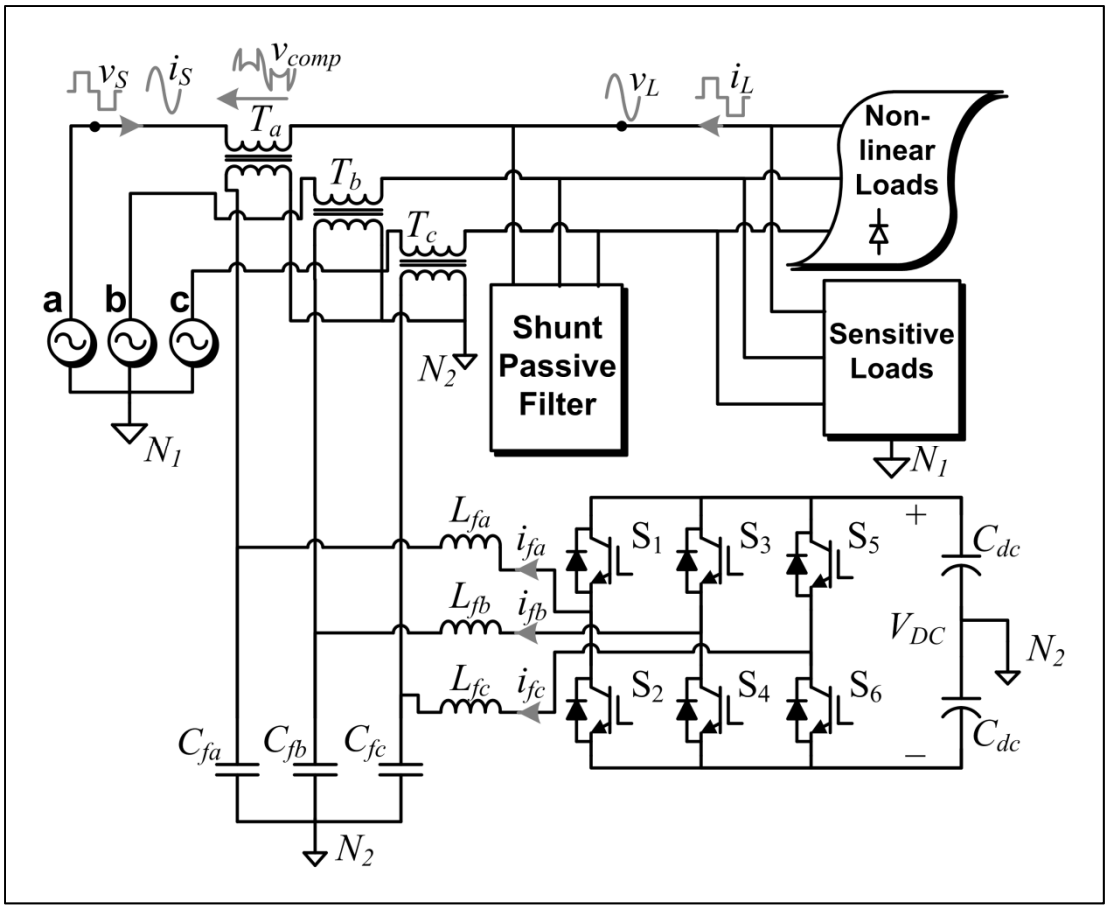

Figure 5.1 Connection schematic of the hybrid series active filter with the distribution power system

This widely used topology in the scientific word (Fujita et Akagi, 1991a; Peng, Akagi et Nabae, 1990) could be rated lower compared to shunt AF, making its industrial applications more economic than UPQC or a hybrid shunt filter. With an appropriate control algorithm, this configuration could be a competent device to overcome power quality issues.

5.2.2 Proposed Harmonic Detection Strategy for a Three-phase System

Many theories for the three-phase system have been developed to control active filters and then performing compensation of unwanted harmonics, unbalances, swells, and sags. In this section the controller term refers to the detection section of the entire digital controller, in which the reference signal is produced and then an outer controller (PI, sliding mode, P+R, etc.) will take care to generate the duty cycle for the PWM modulator. The control detection algorithms employed for series active filters differ depending on the compensation objectives. They are classified in three principal categories as follow;

5.2.2.1 Current control based approach

Controllers based on this strategy compensate the current harmonics of the non-linear load (Hamadi, Rahmani et Al-Haddad, 2007). In this application, the series active filter operates similar to a shunt active power filter. A shunt passive filter is required, which remains open circuit for the fundamental and closed circuit for the harmonics. Moreover, in closed-loop iteration, this strategy will reduce voltage harmonics at the load terminals. Regarding the fact that any voltage harmonics across the passive filter will produce a current harmonic with the same order, while the SeAF will try to compensate theses current harmonics resulted from these voltage distortions. Hence, it indirectly compensates the voltage harmonics created by the distribution system (Singh, Al-Haddad et Chandra, 1998).

5.2.2.2 Voltage control based approach

The second category is dedicated to applications where the SeAF compensates the voltage issues; voltage harmonic distortions, unbalances, sag, and swells. In these applications, the SAF is considered as a Dynamic voltage regulator (DVR) to ensure a sinusoidal and balanced voltage for sensitive loads in presence of any perturbation in the distribution system.

5.2.2.3 Proposed Combined compensation approach

The last category corresponds to the approaches applied for the Hybrid series active filter (HSeAF) as UPQC. In this way, the control algorithm should increase the abilities of the HSeAF to compensate the current issues as well as potential voltage distortions and likewise UPQC it should isolate the load from the distribution system. This three-phase approach aims to reduce the compromise between the two mentioned compensation objectives. The proposed approach is able to make the HSeAF operates as a DVR or Hybrid mode independently based on the user's choice. This approach is constituted of two sections presented hereafter. To operate as a voltage compensator only the primary control of Figure 5.2 will operate. It is based on the synchronous reference frame detection to extract the fundamental, and compensating the remaining unwanted voltages harmonics.

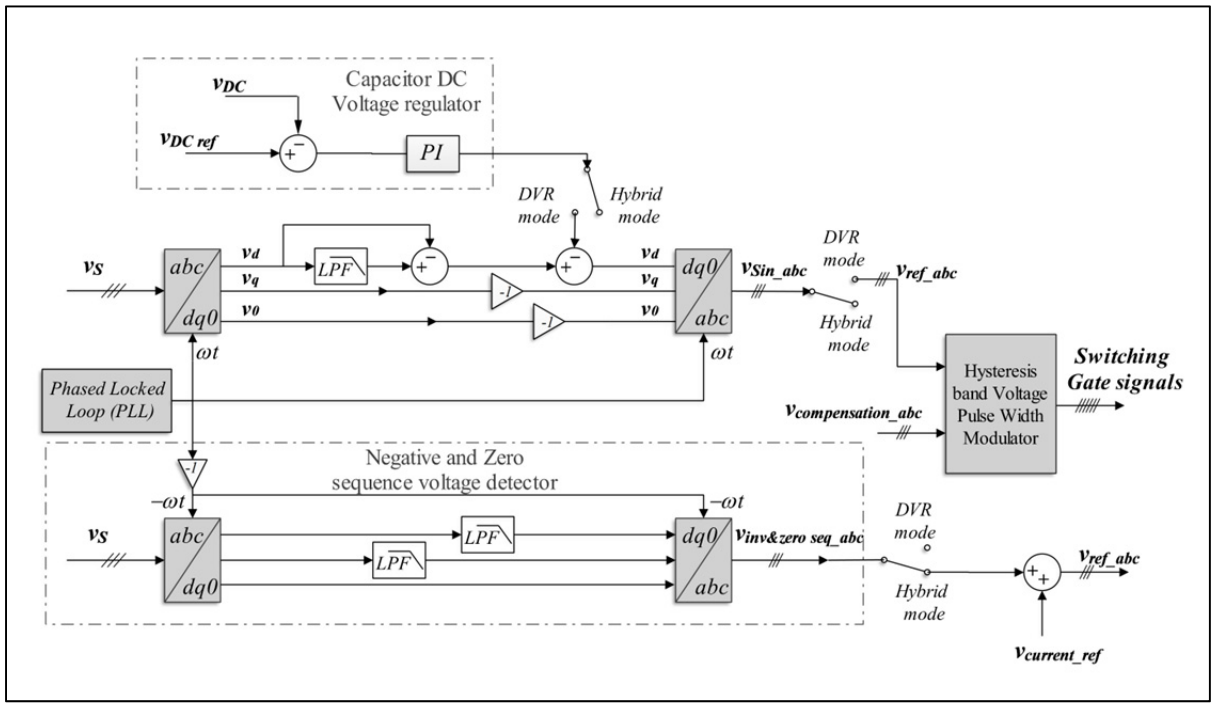

Figure 5.2 Functional block diagram for a three-phase load voltage controller, and a three-phase fundamental voltage generator

Based on this Park's transformation, it is possible to create a control strategy to compensate voltage issues at load terminals of a sensitive load. By compensating the oscillating part of the direct voltage and the whole quadrature voltage, it became possible to obtain the compensation voltage in two-phase. Then a reverse Park's transformation is required to obtain the three-phase compensation voltage references. The three signals are then sent to a Hysteresis pulse width modulator to generate the gate signals for the converter.

$$v_{dq0} = \underbrace{\sqrt{\frac{2}{3}}\begin{bmatrix} \cos(\omega t) & \cos\left(\omega t - \frac{2\pi}{3}\right) & \cos\left(\omega t + \frac{2\pi}{3}\right) \\ \sin(\omega t) & \sin\left(\omega t - \frac{2\pi}{3}\right) & \sin\left(\omega t + \frac{2\pi}{3}\right) \\ 1/\sqrt{2} & 1/\sqrt{2} & 1/\sqrt{2} \end{bmatrix}}_{T} \begin{bmatrix} v_a \\ v_b \\ v_c \end{bmatrix} \tag{5.1}$$

A low-pass filter (LPF) is used to extract the oscillating portion of the direct components and obtain the compensating voltage in *dq0* coordinates.

$$v_{comp}(dq0) = \begin{bmatrix} -\tilde{v}_d + V_{DCreg} \\ -v_q \\ -v_0 \end{bmatrix} \tag{5.2}$$

$$v_{ref}(abc) = T^{-1} \times \begin{bmatrix} -\tilde{v}_d \\ -v_q \\ -v_0 \end{bmatrix} = T^{-1} \times v_{comp}(dq0) \tag{5.3}$$

This compensation strategy is capable of compensating the zero sequence voltage as well as unbalance leaving only the fundamental to the point of common coupling. To maintain a constant regulated DC bus voltage across the capacitors, a PI controller is therefore used. The required voltage (V_{DCreg}) is then added to the oscillating direct voltage.

Compensating the oscillating part of the direct voltage, the quadrature portion of voltage, and the zero-sequence voltage allow extracting the fundamental direct component. This could be directly used for voltage compensation as a DVR or given to the current controller as will be

explained. When the strategy plans to compensate in the hybrid mode, the current distortions, the second controller is therefore activated, as presented in Figure 5.3. The primary part is to extract the fundamental of the voltage used in the second section and generating the compensating current. This current is then transformed to a regulated compensating voltage. To calculate the compensating current the *p-q* theory could be used (Javadi, Olivier et Sirois, 2010).

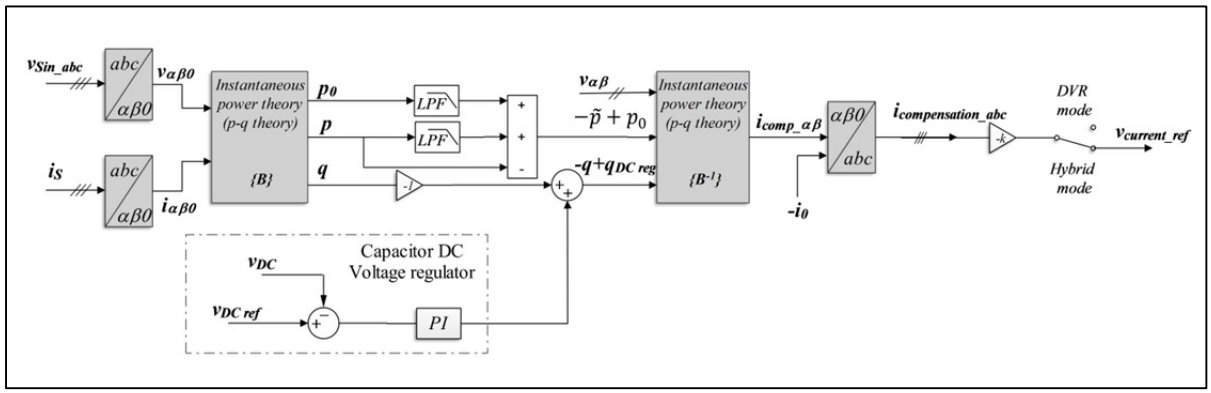

Figure 5.3 Control block diagram compensating load current harmonics and performing power factor correction

In a three-phase system, with three or four wires, instantaneous voltages and currents are described as instantaneous space vectors ***v*** and ***i***. Related vectors in *αβ0* coordinate are then obtained using Clarke's transformation.

$$i_{\alpha\beta0} = \begin{bmatrix} i_\alpha \\ i_\beta \\ i_0 \end{bmatrix} = \underbrace{\sqrt{\frac{2}{3}} \begin{bmatrix} 1 & -1/2 & -1/2 \\ 0 & \sqrt{3}/2 & -\sqrt{3}/2 \\ 1/\sqrt{2} & 1/\sqrt{2} & 1/\sqrt{2} \end{bmatrix}}_{C} \times \begin{bmatrix} i_a \\ i_b \\ i_c \end{bmatrix} \tag{5.4}$$

$$v_{\alpha\beta0} = \begin{bmatrix} v_\alpha \\ v_\beta \\ v_0 \end{bmatrix} = C \times \begin{bmatrix} v_{an} \\ v_{bn} \\ v_{cn} \end{bmatrix} \tag{5.5}$$

Instantaneous powers are defined as follow:

$$\begin{bmatrix} p \\ q \\ p_0 \end{bmatrix} = \underbrace{\begin{bmatrix} v_\alpha & v_\beta & 0 \\ v_\beta & -v_\alpha & 0 \\ 0 & 0 & v_0 \end{bmatrix}}_{B} \begin{bmatrix} i_\alpha \\ i_\beta \\ i_0 \end{bmatrix} \tag{5.6}$$

Instantaneous three-phase active power is then equal to the sum of real power p and the zero-sequence power p_0. In the case of a three-phase three-wire balanced system, p_0 does not exist and $p_{3\varphi}$ is equal to p.

$$p_{3\varphi} = \vec{\boldsymbol{v}} \cdot \vec{\boldsymbol{\imath}} = v_{an} i_a + v_{bn} i_b + v_{cn} i_c = v_\alpha i_\alpha + v_\beta i_\beta + v_0 i_0 = p + p_0 \tag{5.7}$$

With reference to $\alpha\beta 0$ coordinate, obtained currents from the power expressions are decomposed into active and reactive parts. They were then used for current compensation. In order to obtain the instantaneous active currents ($i_{\alpha p}$, $i_{\beta p}$) and instantaneous reactive currents ($i_{\alpha q}$, $i_{\beta q}$), these orthogonal currents (i_α and i_β) can be decomposed into their active (i_p) and reactive (i_q) parts.

$$\begin{bmatrix} i_\alpha \\ i_\beta \end{bmatrix} \triangleq \overbrace{\begin{bmatrix} i_{\alpha p} \\ i_{\beta p} \end{bmatrix}}^{i_p} + \overbrace{\begin{bmatrix} i_{\alpha q} \\ i_{\beta q} \end{bmatrix}}^{i_q} = \tag{5.8}$$

$$= \frac{1}{{v_\alpha}^2 + {v_\beta}^2} \begin{bmatrix} v_\alpha & v_\beta \\ v_\beta & -v_\alpha \end{bmatrix} \begin{bmatrix} p \\ 0 \end{bmatrix} + \frac{1}{{v_\alpha}^2 + {v_\beta}^2} \begin{bmatrix} v_\alpha & v_\beta \\ v_\beta & -v_\alpha \end{bmatrix} \begin{bmatrix} 0 \\ q \end{bmatrix}$$

Both active and reactive powers can be divided into a constant amplitude component and an oscillating component:

$$\begin{cases} p = \bar{p} + \tilde{p} \\ q = \bar{q} + \tilde{q} \end{cases} \tag{5.9}$$

By compensating the reactive portion of current, a conventional unity power factor ($cos\theta \approx 1$) will be achieved, so it will be possible to observe that no phase shifting exist between the

voltage waveform and the current. Due to the presence of both zero-sequence currents and voltages in a four wire system, p_0 must also be considered.

$$\boldsymbol{B}^{-1} = \begin{bmatrix} \frac{v_\alpha}{{v_\alpha}^2 + {v_\beta}^2} & \frac{v_\beta}{{v_\alpha}^2 + {v_\beta}^2} & 0 \\ \frac{v_\beta}{{v_\alpha}^2 + {v_\beta}^2} & \frac{-v_\alpha}{{v_\alpha}^2 + {v_\beta}^2} & 0 \\ 0 & 0 & \frac{1}{v_0} \end{bmatrix} = \frac{1}{{v_0}^2\left({v_\alpha}^2 + {v_\beta}^2\right)} \begin{bmatrix} {v_0}^2 v_\alpha & {v_0}^2 v_\beta & 0 \\ {v_0}^2 v_\beta & -{v_0}^2 v_\alpha & 0 \\ 0 & 0 & v_0\left({v_\alpha}^2 + {v_\beta}^2\right) \end{bmatrix} \tag{5.10}$$

The oscillating portion of the active power and the zero sequence power, if this latter exists, are compensated in this strategy. In order to maintain a constant regulated DC voltage across the capacitors, a *PI* controller is used. The required power to maintain the DC voltage constant is considered to be reactive and could be added to the amount of reactive compensating power resulting in the compensating currents.

The compensating instantaneous active current:

$$\boldsymbol{i}_p(\alpha\beta 0) = \boldsymbol{B}^{-1} \times \begin{bmatrix} \tilde{p} \\ 0 \\ -p_0 \end{bmatrix} \tag{5.11}$$

The compensating instantaneous reactive current:

$$\boldsymbol{i}_q(\alpha\beta 0) = \boldsymbol{B}^{-1} \times \begin{bmatrix} 0 \\ q - q_{DC} \\ 0 \end{bmatrix} \tag{5.12}$$

The current is then transformed to a relative three-phase voltage ($\boldsymbol{v}_{current\_ref}$) using the gain *G*.

$$\boldsymbol{v}_{current_{ref}} = -G \times \left(\boldsymbol{C}^{-1} \times \begin{bmatrix} -\boldsymbol{i}_p(\alpha\beta 0) \\ -\boldsymbol{i}_q(\alpha\beta 0) \\ -\boldsymbol{i}_0 \end{bmatrix} \right) \tag{5.13}$$

The three-phase voltage reference generated compensates the harmonic currents generated by a non-linear load. In order for the series hybrid active filter to function as UPQC, the $\boldsymbol{v}_{current\_ref}$ and the voltage required to compensate the unbalance component of the source voltage, should be added.

The interesting spot line to implement the current compensator is that this strategy compensates the voltage harmonics as they generate current harmonics. Hence, the second section of the controller will compensate the total current issues and the voltage harmonics at the load terminals. To behave as a UPQC, unbalance including the negative and zero-sequence component of the voltage should be compensated. The first section of the controller accomplishes this task.

$$\boldsymbol{v}_{ref}(abc) = -\left(\overbrace{\widetilde{G\boldsymbol{i}_h}}^{include\ v_h} + \boldsymbol{v}_0 + \boldsymbol{v}_{inv} \right) \tag{5.14}$$

The three-phase compensating $\boldsymbol{v}_{ref}$ and the voltage across the series transformer are then given to a hysteresis band pulse width modulator to generate the switching gate signals. Upon implementation of this controller, the series hybrid active filter will have similar functionality as a UPQC. Hereafter simulations are presented using the developed controller.

5.2.3 Detection Strategy Verification

The parameters used for these case studies are as follow. A three-phase 120/208 V programmable voltage source is connected to a 3 kW non-linear load and a 3.19 kVA linear load with a 0.75 power factor. The shunt passive filter constituted of a three-phase high-pass filter is made of a 570 μF capacitor in parallel with an inductance of 12.5 mH. The resonance

frequency is tuned at 60 Hz, and it will damp any higher current harmonic frequencies. A transformer rated at 1 kVA with a ratio of 2 is connected in series to the radial system in order to inject the compensating voltage of the 3 kVA HSeAF.

Results are classified under two categories; the compensator compensates only the voltage harmonics and voltage related issues from the point of common coupling. Thereafter, the compensator will be acting in a hybrid approach by taking into account the compensation of source current harmonics as well.

5.2.3.1 Source voltage harmonic compensation (DVR operation)

In this compensation mode, the controller compensates voltage harmonics, unbalances, swells and sags from the sensitive load terminal. The load is constituted of a non-linear and a linear load. These loads draw a distorted current of 20 A (max) with a total harmonic distortion (THD) of 15.7%. Figure 5.4 illustrates the system without the compensator. The source became highly distorted between 0.18s and 0.22s with a fifth and seventh order harmonics with 20 and 15 percent of fundamental respectively (THD V_S = 25.1%). Thereafter, at 0.26s up to 0.3s a faulty unbalances occurred on one phase and its corresponding magnitude decrease to 0.6 pu. This unbalance contains a zero-sequence and negative component. To study the transient behavior with a dynamic load, the linear load is disconnected at 0.34s to 0.38s (THDI_S =28.8%).

When the HSeAF is inserted, it will try to compensate voltage harmonics and related issues at the PCC when performing as a DVR. The compensator is able to deliver a purely sinusoidal and balanced three-phase voltage at the PCC despite the presence of any distortion and unbalance in the distribution system. Figure 5.5 demonstrates the phase voltage and current of the source, before the series compensator is connected. According to this figure, the compensator has no effect on the source current when performs voltage compensation function.

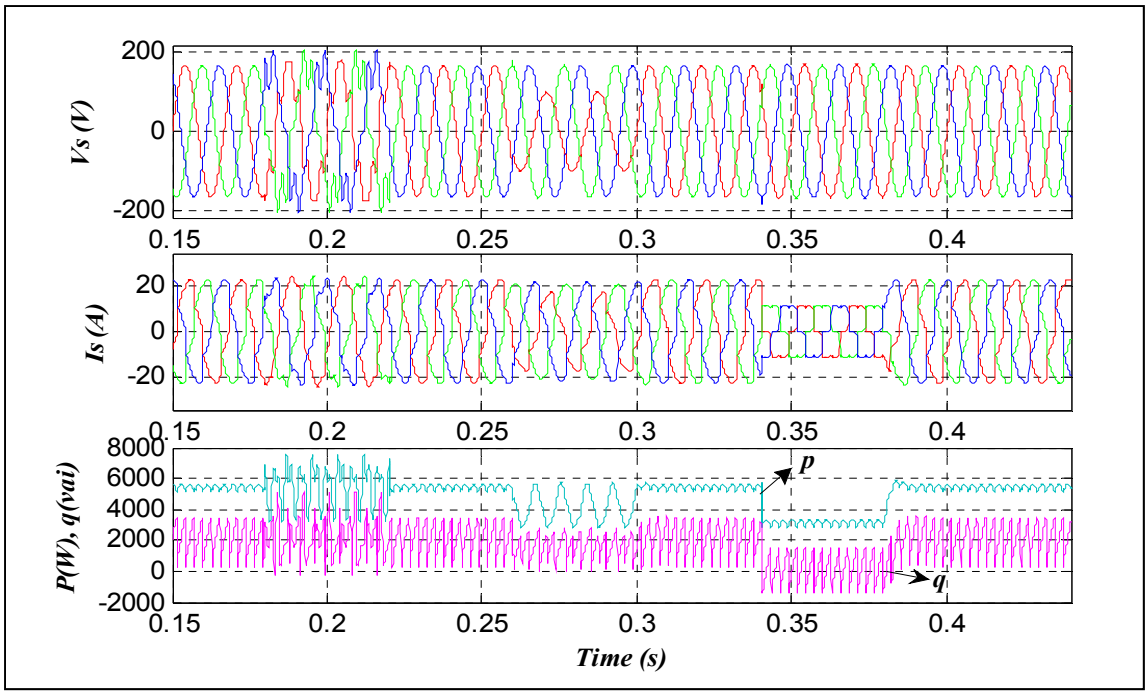

Figure 5.4 System behavior during distortion and load changes without compensation; a) three-phase voltage V_S, b) three-phase distorted current I_S, c) instantaneous active and reactive powers

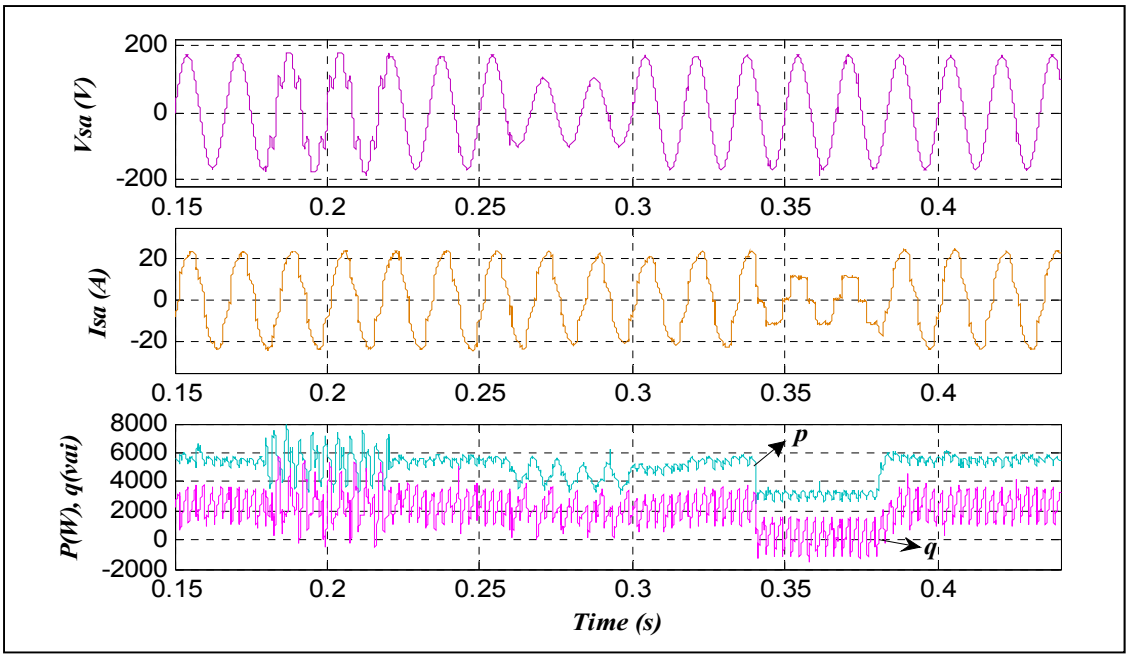

Figure 5.5 a) Source voltage, b) source distorted current, c) instantaneous load active and reactive powers, while the HSeAF in operation

Figure 5.6 confirms expected results with the series compensator connected to the PCC. It compensates voltage harmonics (from 0.18s to 0.22s) and unbalance (from 0.26s to 0.3s) while consuming small amount of active power. The THD is reduced to 8% during distortions on the distribution system. The higher order harmonics around the switching frequency could be eliminated by means of a small tuned passive filter.

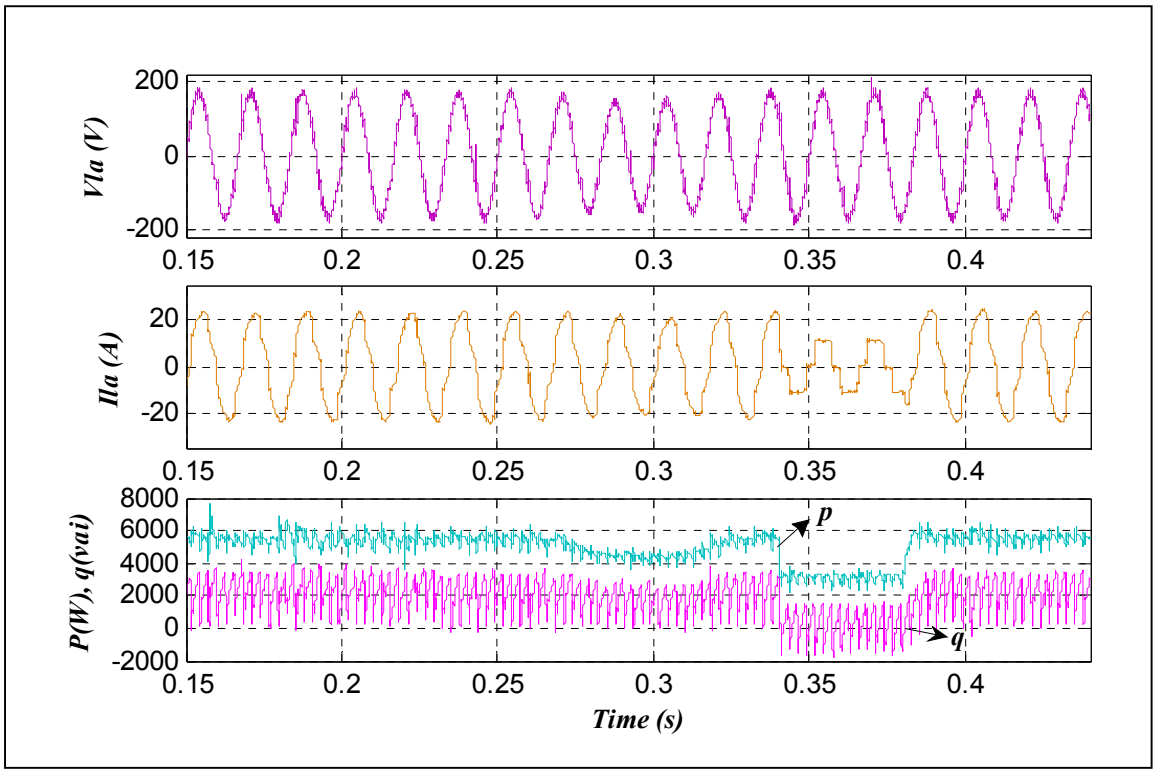

Figure 5.6 a) Load PCC voltage, b) dynamic load distorted current,
c) load's instantaneous active and reactive powers

It is possible to replace the DC source with two capacitors of 3100 µF. The PI controller connected to the voltage regulator assumes a constant voltage at the capacitor's terminals. Result of this configuration is shown in Figure 5.7, where the PCC voltage THD is reduced. The transient response of the capacitor's voltage regulation depends on the PI controller. The gains should be adjusted in such a way to reduce the impact on the compensation performances. The DC voltage is regulated at 80 volts for each of the capacitors as shown in Figure 5.8. These tests illustrate the in a DVR operation to regulate for the load voltage.

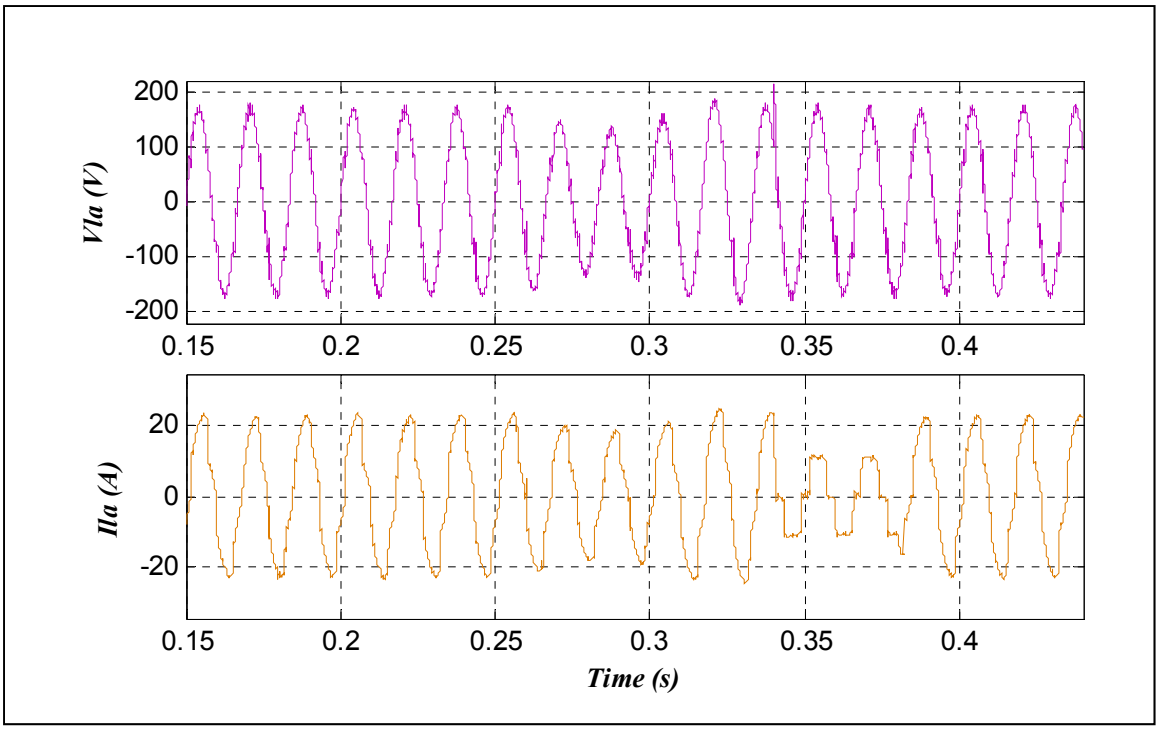

Figure 5.7 a) Load PCC voltage, b) dynamic load distorted current

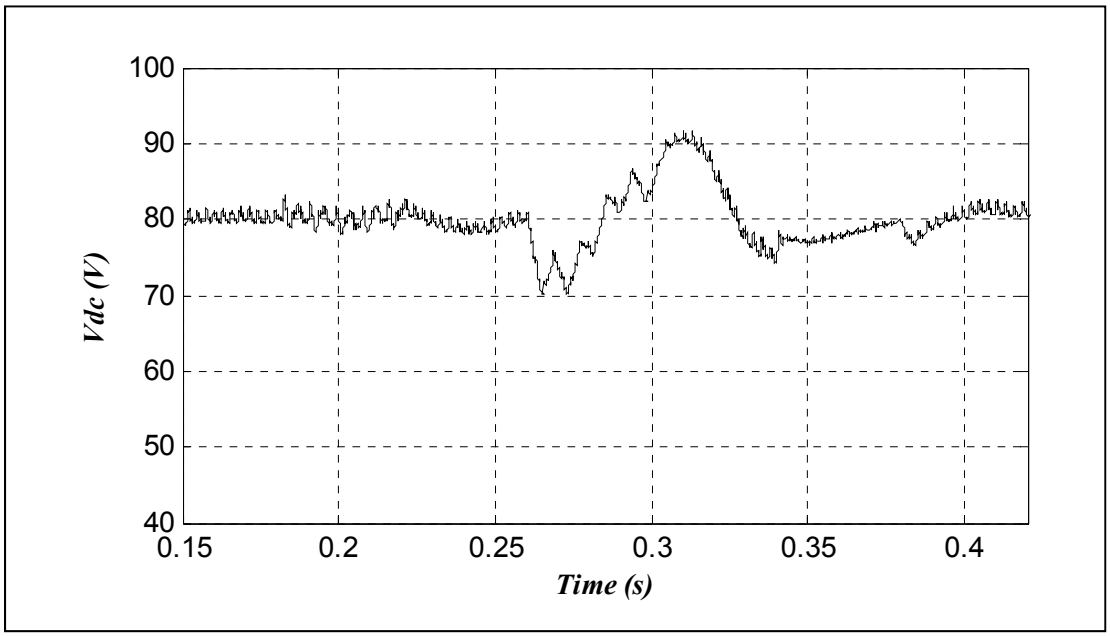

Figure 5.8 DC regulated capacitor's voltage

5.2.3.2 Voltage and current combined compensation

This strategy, considers both voltage and current related problems for compensation such as distortions, unbalance, and power factor correction. In the following results, the proposed algorithm is implemented on the Hybrid series active filter. Figure 5.9 and Figure 5.10 illustrate the HSeAF compensating voltage harmonics and unbalances coming from the power system. In a widespread compensation, the HSeAF attempts also to compensate the voltage issues at the load PCC and clean the distribution system from any current distortion and correct the power factor. The power required to maintain the capacitor's voltage constant is added to the instantaneous reactive power. The HSeAF isolates the load PCC from the distribution system where it is connected and cleans the impact of the non-linear load on the source. The current distortion is compensated at the source, and a unity power factor is achieved. During normal operation the current THD is reduced from 15.7% at the load PCC to 4.9% at the distribution system. While the grid supply became distorted at 1.2s, the source impedance distorts the current as seen in Figure 5.9. As explained the controller has to make a compromise between the correction of the current and voltage. Hence, in this difficult condition the priority is to have a reliable and harmonic free voltage at the PCC. This could be adjusted by performing a fine tuning on the shunt passive filter.

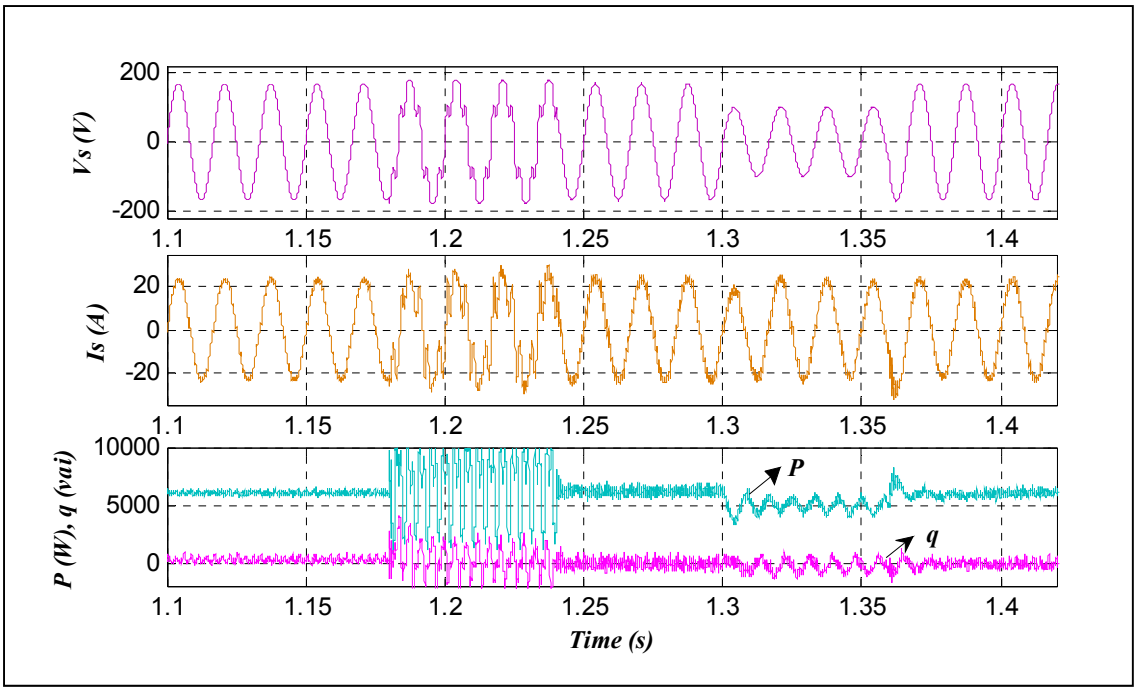

Figure 5.9 a) Phase to neutral source voltage, b) source current, c) instantaneous source active and reactive powers

Voltage at the PCC has a balanced and sinusoidal waveform despite presence of distortion and unbalance at the utility supply shown in Figure 5.10 where THD V_L = 5.3%.

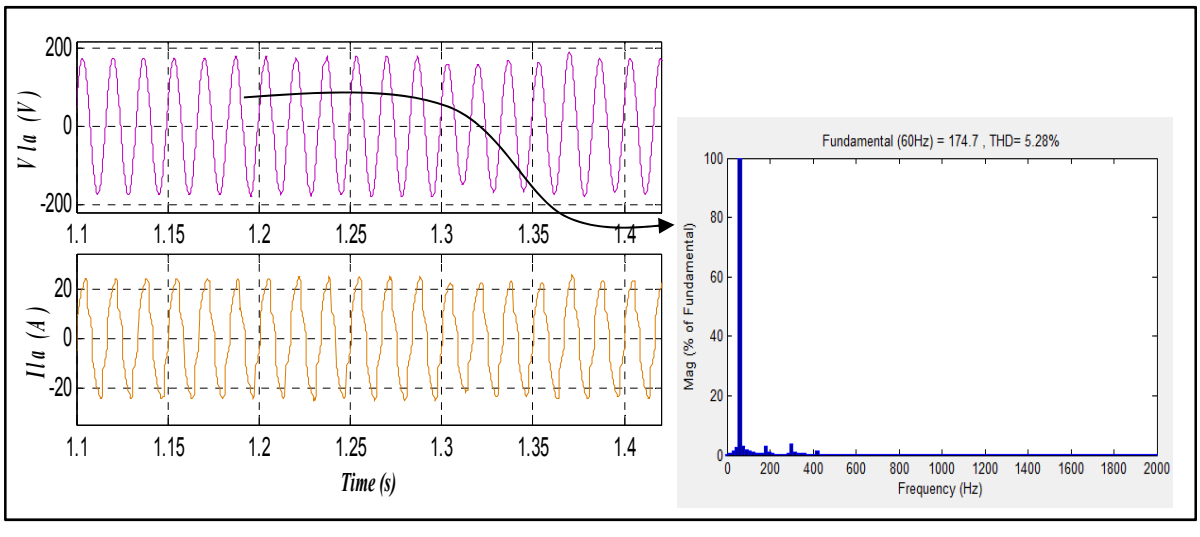

Figure 5.10 a) Load PCC voltage, b) load distorted current

To study the behavior of the proposed algorithm on a dynamic load, the linear load is disconnected at 1.8s. The non-linear load draws a highly distorted current with a THD I_L equal to 28.8%. However, as shown in Figure 5.11, the current at the source is less polluted (THD I_S = 7.4%) even during dynamic load change and the HSeAF follows the load variation instantaneously.

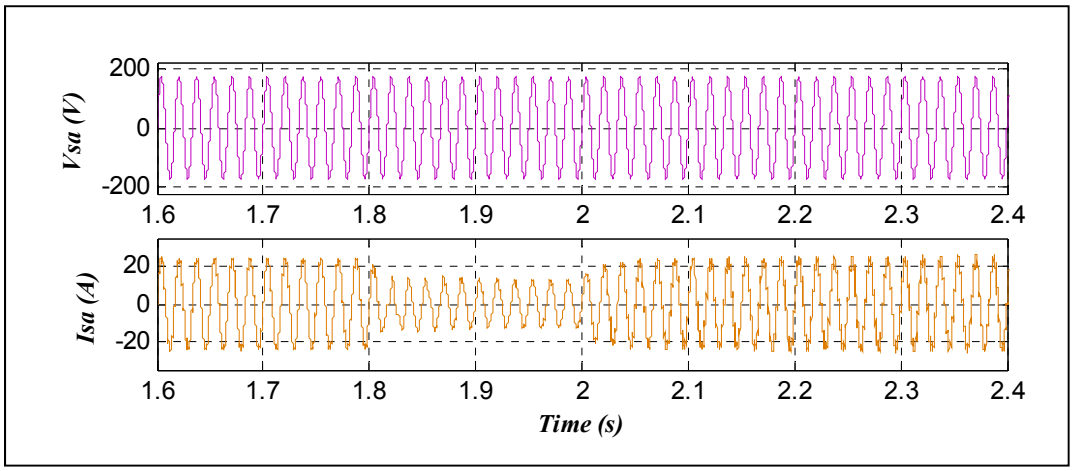

Figure 5.11 Source side voltage and current

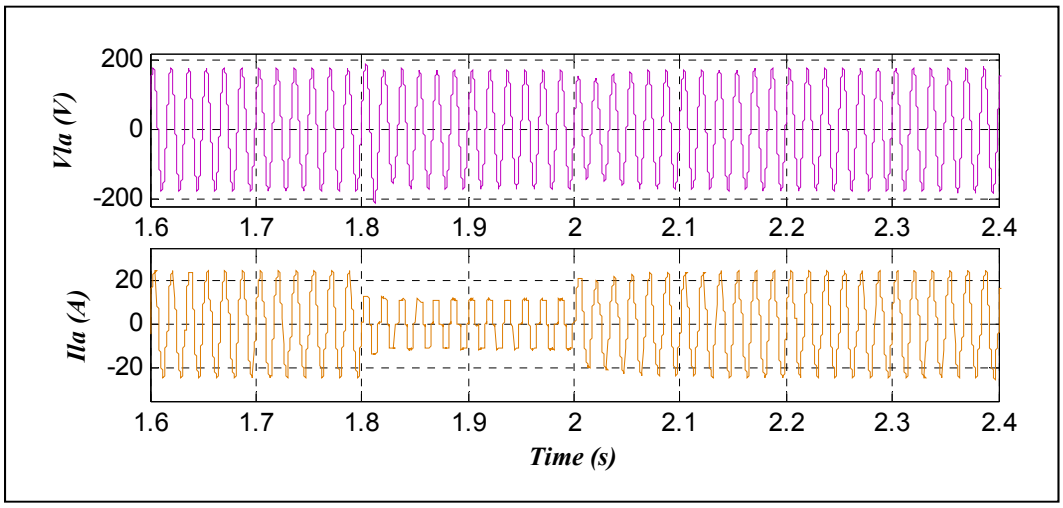

Figure 5.12 Load PCC voltage and the load's distorted current

The proposed algorithm applied to the Hybrid series active filter has abolished current harmonics, unbalance and corrected the power factor from the distribution system. Figure

5.12 shows that the current THD was reduced from 15.7% at the load terminals to 4.9% at the distribution system. Moreover, perturbation such as voltage harmonics (THD V_S= 25.1%), disappeared from the load PCC (THD V_L= 5.6 %).

5.3 A Novel Three-phase Transformerless Hybrid Series Active Power Filter using Current Fed Converters

To increase the efficiency and sustainability of Smart grids and help higher penetration of renewable fluctuating power into the network different approaches were proposed from DVRs to Shunt active power filters who were introduced to compensate voltage and current problems respectively (Chi-Seng, Man-Chung et Ying-Duo, 2008). Regardless of recent attempts, due to the complexity of series active compensators comparing with commercially available shunt active power filters; they are still not much deployed (Varschavsky et al., 2010). Hence, this section intends to introduce a new viable three-phase topology to perform compensation of both voltage and current issues at distribution level. Hybrid series active filters are widely studied configurations (Fujita et Akagi, 1991b; Peng, Akagi et Nabae, 1993) but this section proposes a new active power filter, the three-phase Transformerless HSeAF for Smart grid applications to make the PCC more reliable. The proposed configuration will uses the control algorithm proposed earlier in this chapter to compensate for voltage distortions, eliminate current harmonics of a nonlinear load and preventing their propagation through the power system, and correcting the power factor (Akagi et Kondo, 2010; Bingsen et Venkataramanan, 2009). The proposed topology will isolate harmonic flow of nonlinear loads and compensate its current distortions at lower cost as compared to UPQC (Choi, Li et Vilathgamuwa, 2000).

5.3.1 Proposed Three-phase Transformerless Topology

This subsection explains in detail the architecture developed for a transformerless hybrid series active filter (THSeAF). The transformer issued to generate the compensating voltage and creating an electrical isolation between the converter, and the power system is bulky and could be replaced. This injection transformer is responsible for the extra cost of series active

filters. It increases the complexity and losses in the system. Different approaches were proposed to replace the series transformer (Li, Choi et Vilathgamuwa, 2002).

The configuration proposed in this section is constituted of a shunt passive filter tuned at 60Hz and a transformerless series active filter using current auxiliary source. To do so, three inline capacitors are connected to three full-bridge single phase converters as shown in Figure 5.13. This configuration is intended to compensate current distortion and correcting load power factor in addition to ensure a stable and hassle-free delivered supply to the loads.

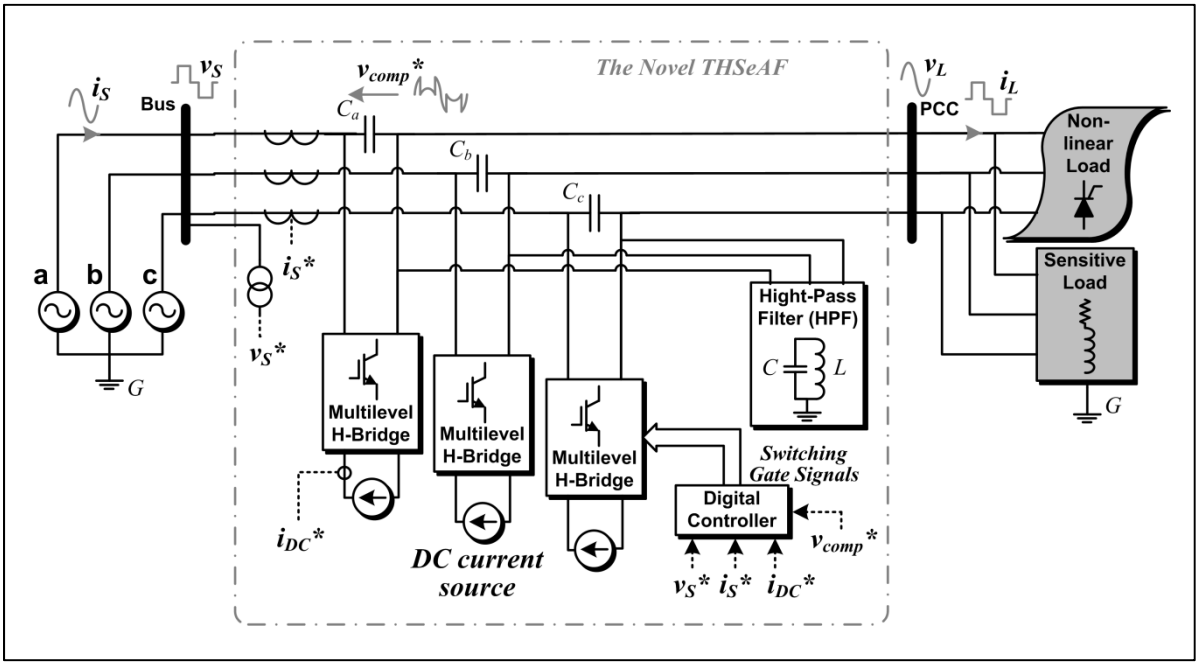

Figure 5.13 Schematic of the Transformerless hybrid series active filter (THSeAF) connected to the grid

According to Figure 5.14, if the supply voltage magnitude is taken as reference (V_S), then Figure 5.14(b) represents the voltage at the load PCC without compensator.

$$V_{PCC} = V_S - R_S I - jX_S I + jX_C I \tag{5.15}$$

$$C = \frac{3I^2}{2\pi.60.Q_{comp}} \tag{5.16}$$

where R_S and X_S are the real and imaginary parts of the grid impedance. In addition based on equation 5.17, replacing the series transformer with a series capacitor not only reduces expenses and increases the voltage at the PCC, but also increases the capacity to transfer more power from the transmission line. There exist inline capacitors already installed in power systems to compensate the reactive power of the load and correct the power factor and reducing the voltage drops at the end of power transmission lanes. Meanwhile, the installed capacitors in this application are relatively much less than those installed for the mentioned application.

$$P_{max} = \frac{V_S V_{PCC}}{X_S - X_C} \sin\delta \tag{5.17}$$

$$P_{\max}(without\ compensator) \leq P_{\max\ (with\ capacitor)} \tag{5.18}$$

A lower outlay for the capacitor compared to same rating transformer is a noticeable advantage of this configuration. As mentioned in-line capacitors are already widely used for reactive power compensations, and voltage regulation at the end of transmission lines. A tradeoff is done in the proposed configuration; the numbers of IGBTs arms are doubled compared to the conventional topology using a three-phase bridge. This configuration proposes a current source supply to feed the dc side of the converters. Depending on the application, this source could be replaced by an inductance or a renewable-distributed-energy supply (e.g. Photovoltaic source). The other advantage of such topology compared to the traditional configuration is the exclusion of the series inductances and shunt capacitors at output terminals of the converter. Therefore, voltage harmonics, unbalances, sags, and swells at the PCC could be eliminated. It also cleans the source from undesirable current harmonics, unbalances, and corrects the power factor.

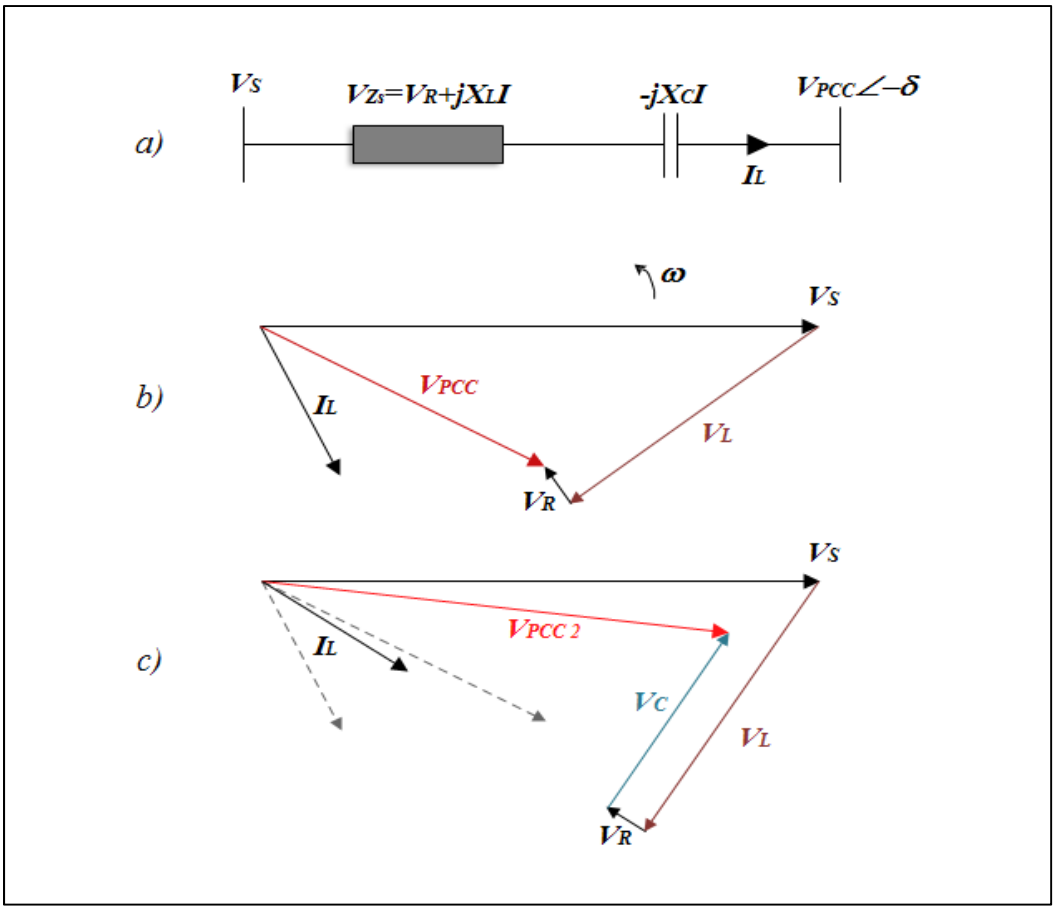

Figure 5.14 a) Single-line diagram of a distribution system with series compensator, b) phasor diagram without series capacitor, c) voltage representation with a series capacitor

Employing the passive filter is required to compensate current harmonics. The mandatory passive filter acts as open circuit for the fundamental and closed circuit for the harmonics. Moreover, this strategy also compensates voltage harmonics at the load terminals. Any voltage harmonics across the passive filter will produce a current harmonic with the same order in the shunt passive filter. The THSeAF will try to compensate the current harmonics resulted from these voltage distortions. Hence, it indirectly compensates the voltage harmonics created by the distribution system at the load PCC (Javadi et Al-Haddad, 3-5 Oct. 2011; Singh, Al-Haddad et Chandra, 1999).

5.3.2 Current Fed Three-phase THSeAF Configuration

The control algorithm for the active part is the one proposed in Figure 5.2 and Figure 5.3. The controller operates under three distinct objectives; to compensate voltage harmonics and related issues similar to a DVR, to compensate load current similar to a shunt active filter, and finally opting to compensate for both voltage and current issues. The control strategy to compensate voltage issues at the sensitive load terminals is based on the Park's transformation. The *dq0* transformation is applied to source voltage, then by compensating the oscillating portion of the direct voltage and the whole quadrature voltage; it is possible to obtain the compensation voltage in two-phase. A reverse Park's transformation is then required to obtain the three-phase reference voltage. The three signals are then sent to a Hysteresis pulse width modulator to generate twelve gate signals for the IGBT converters. The configuration of Figure 5.13 is composed of a three-phase programmable voltage source (120/208V) connected to a 3kW non-linear load and a 3.2kVA linear load with a 0.75 power factor. The shunt passive filter constituted of a three-phase high-pass filter composed of a 570μF capacitor in parallel with an inductance of 12.5mH. The resonance frequency is tuned at 60Hz, and it will assist to damp any higher current harmonic frequencies. For the Hybrid series active filter (HSeAF) a transformer rated at 1.5kVA with a ratio of 2 is connected in series to the radial system in order to inject the compensating voltage. For the proposed THSeAF, the transformer is replaced by a 1061μF capacitor. Hence, the 1.5mH series inductance and the 10μF shunt capacitor are not required in the proposed configuration.

5.3.3 Simulation Results

To properly compare a conventional series active filter with the proposed transformerless configuration, simulations are classified in three operating conditions; the active compensator compensates only the voltage issues at the load terminals, then they will compensate current issues from the source system, and finally they operate similar to a UPQC by taking care of both voltage and current related issues. The radial system presented in Figure 5.13 constituted of a non-linear and a linear load drawing a total distorted current of 20A with a

THD of 15.7%, is used for compensation purpose. As illustrated in Figure 5.15 the grid became highly polluted during 0.18s and 0.22s. Then, at 0.26s an unbalance containing zero-sequence and negative component, occurred on one phase and its corresponding magnitude decreases to 0.6pu. Finally to evaluate the transient performance of the compensator upon a dynamic load, one of the loads is disconnected at 0.34s.

5.3.3.1 Source voltage distortion compensation

In this compensation mode (DVR), the compensators attempt to regulate voltage harmonics, unbalance and related load voltage issues. The compensators ensure a sinusoidal and balanced load voltage in presence of any perturbation in the distribution system.

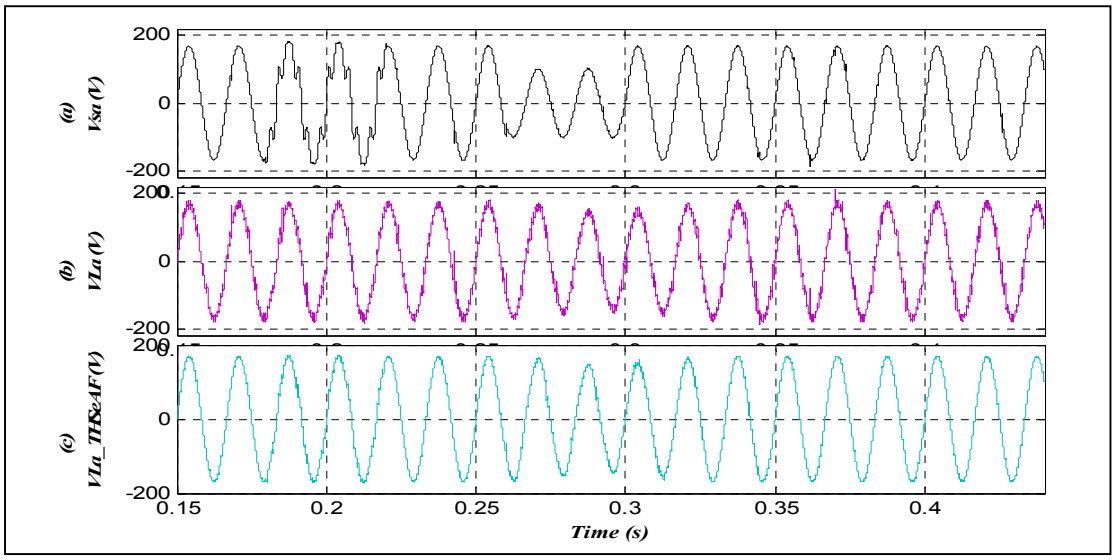

Figure 5.15 Voltage distortion compensation: a) Source voltage, b) load PCC voltage with conventional compensator HSeAF, c) load PCC voltage with THSeAF

The waveforms of Figure 5.15 confirm expected result with the compensator connected in series with the radial system. They compensate voltage harmonics and unbalance at the PCC without consuming a significant amount of power. During grid perturbation (0.18s to0.22s) where THDV_S = 25%, the conventional HSeAF reduces load voltage THD to 8%, while the

proposed topology (THSeAF) reaches a THD of 5%. Thus, in the DVR mode, the proposed configuration demonstrates a better performance over the conventional topology.

5.3.3.2 Source current compensation

In this operating mode, the filters compensate the current harmonics of the non-linear load. This strategy compensates also voltage harmonics at the load terminals. Figure 5.16 demonstrates both of compensators (HSeAF and THSeAF) eliminating current harmonics and correcting the power factor. The conventional HSeAF reduces the source current distortion (THD I_S = 7%), while the transformerless topology practically eliminates them (THD I_{S_THSeAF} = 1.1%) with the same control technique and same operating conditions.

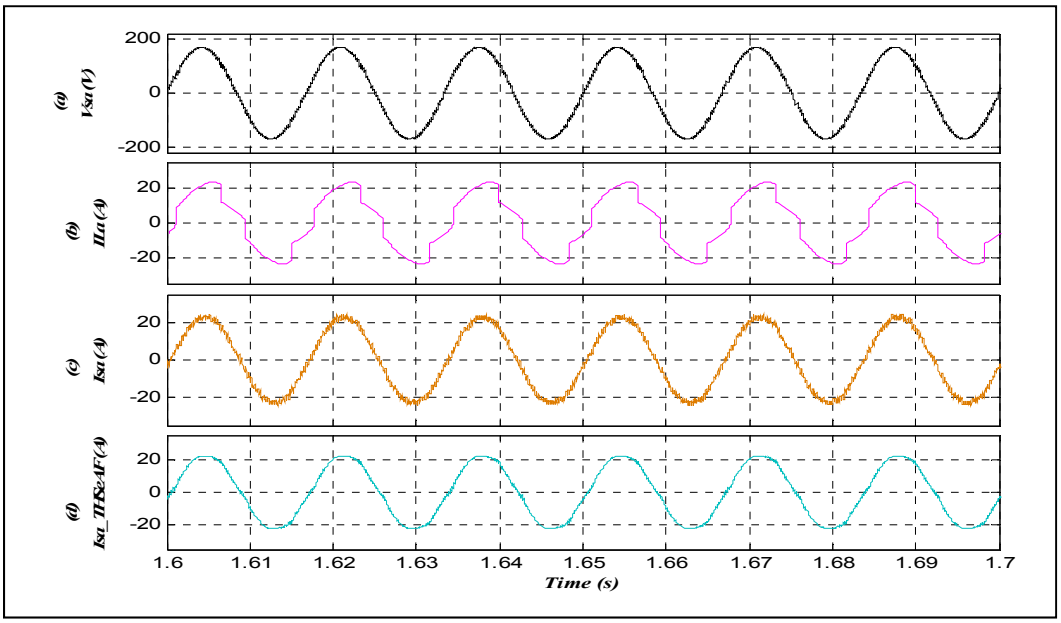

Figure 5.16 Source current harmonics compensation: a) Source voltage, b) load distorted current, c) source current with conventional HSeAF, d) source current with THSeAF

The Figure 5.17 illustrates the behavior of both compensators toward a dynamic load. As explained earlier, the voltage at the load terminal will be cleaned of harmonics as well, while

the voltage unbalance is present (THD V_L = 3.3%). The results indicate a proper operation of the Transformerless hybrid active filter.

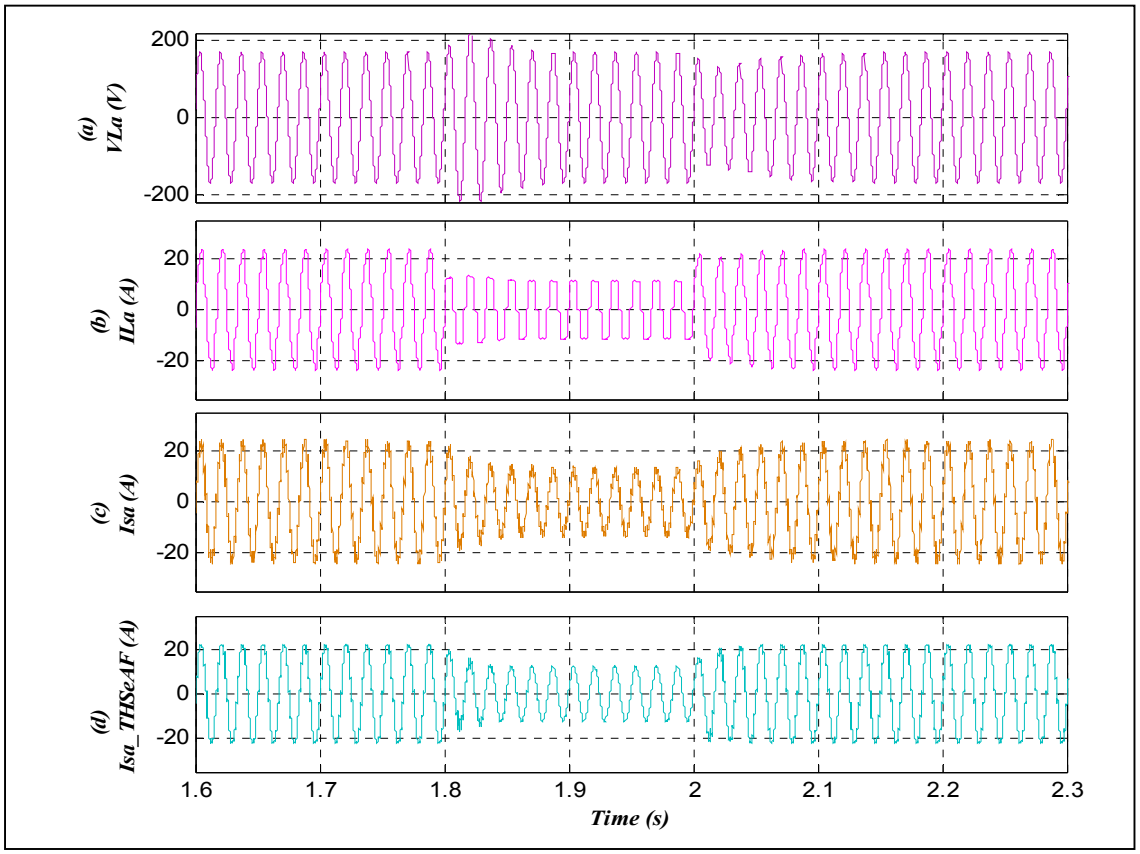

Figure 5.17 Compensation during load variation: a) Load PCC voltage, b) dynamic load distorted current, c) source current with conventional compensator, d) source current with THSeAF

5.4 A Three-phase THSeAF Based on Voltage-Fed Type of Converter for Weak Systems Based on SRF and *p-q* Controllers

Electric vehicles market shows a considerable growth, therefore it became crucial to monitor and evaluates their behavior when charging and the associated current waveforms (Qinglai et al., 2014; Yilmaz et Krein, 2013). In some existing North American charging stations, the cars are connected between two phases of the 3P4W system, creating heavy unbalances. On the other hand, pushed by social efforts, governments start to investigate more on implementation of renewable energy sources, creating research and developments in this field (Yanzhi, Xue et Pedram, 2014). This work proposes an efficient three-phase Transformerless Hybrid Series Active Filter (THSeAF) capable to rectify current related issues in the smart micro-grids which also provides sustainable and reliable voltage supply at the PCC where residential and commercial buildings are connected with nonlinear time varying load side demand. The use of this device will facilitate the integration of energy storage systems and renewables for modern systems. The compensator is connected at distribution level to prevent harmonic currents of a load to flow into the grid while protecting the loads from voltage perturbations coming from the utility.

This proposed low cost configuration ride of the common bulky series transformer is an economic key toward power quality improvement of Smart grids development. This compensator cleans the current drawn from the utility and similarly to a DVR, the point of common coupling (PCC) and utility smart meters will be protected from voltage distortions and wrong computation of power and energy balance. This compensator could inject or absorb active power during grid voltage variations to ensure high quality supply along with complete decoupling the grid from polluted loads.

5.4.1 Proposed System Architecture

Conventional series Hybrid active filters have a common configuration as shown earlier in the first section with a three-phase converter and three isolating transformers, while the proposed configuration do not contain series transformers.

5.4.1.1 Three-Phase THSeAF system configuration based on VSC converters

The transformerless hybrid series active power filter shown in Figure 5.18 is composed of a two-level H-bridge converter connected in series between the grid and the PCC, where the presented configuration allows an independent control on each individual phase regardless of the others. A bank of tuned passive filters ensures a low impedance path for current harmonics. A DC bidirectional source could be connected to inject power during voltage sags and absorbs it during overvoltage. The simulation case study system is rated for 8 kVA.

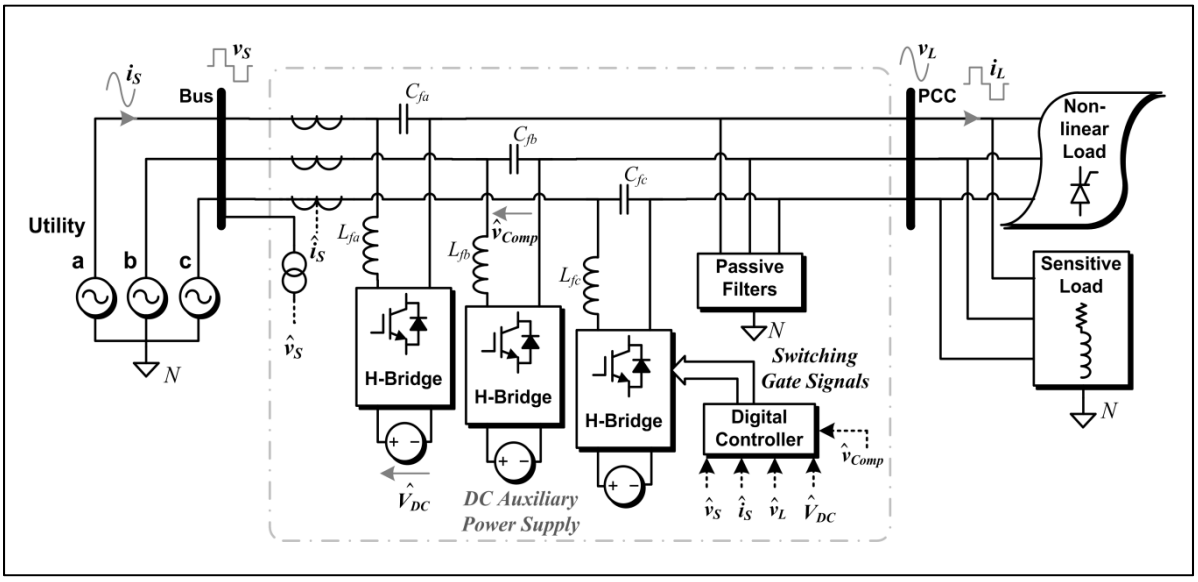

Figure 5.18 The proposed three-phase THSeAF connected ahead of load's PCC

The studied loads consume 7.6kW and exchange 2.3kVAR with the network, resulting in a lagging power factor of 95 percent as shown in Figure 5.19. A programmable source 120/208-V is simulating several critical scenarios such as grid distortion, sag or swell. The THSeAF is connected in series in order to inject the compensating voltage. On the DC side of the compensator, auxiliary dc-link energy storage components are installed. The shunt passive filter constituted of a multiple tuned filters is composed of capacitor in series with an inductance with values tuned at desired frequency. Active filters are often keen to compensate current distortions, thus this is one of the priorities of the compensator.

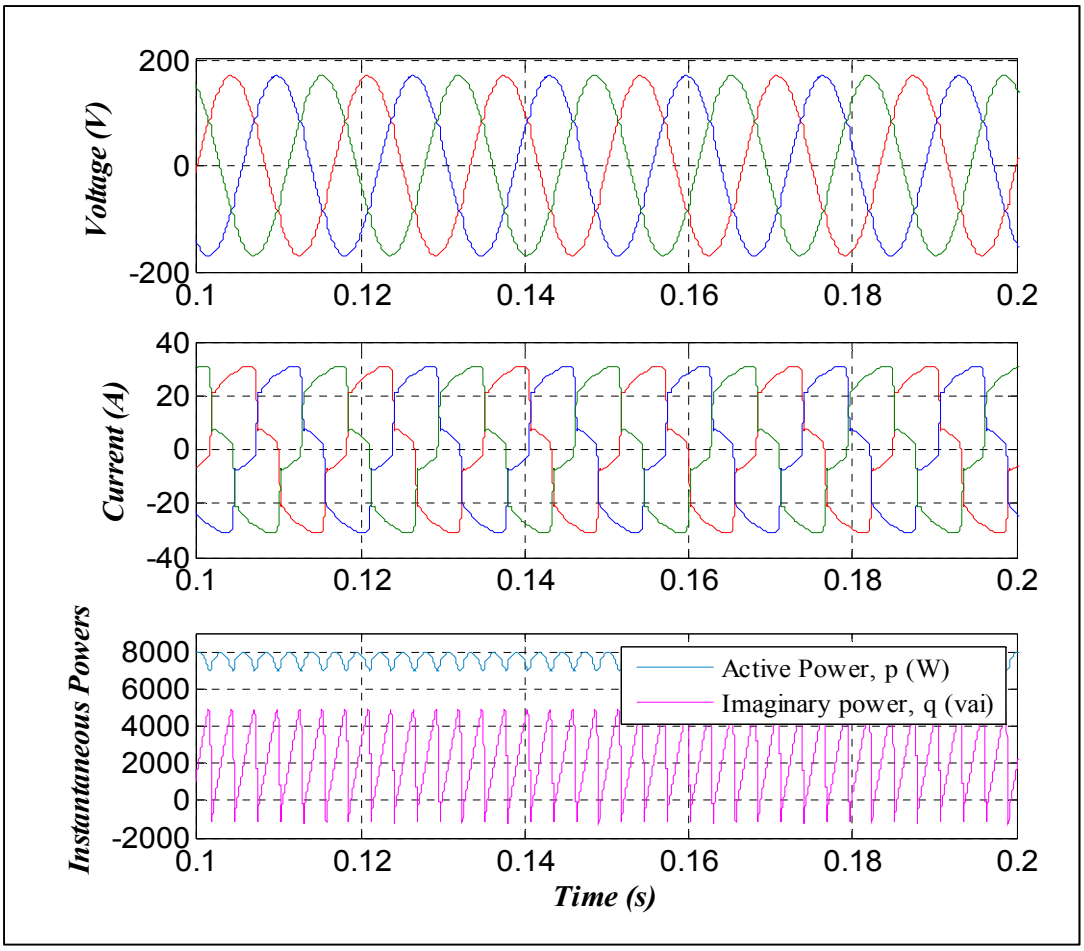

Figure 5.19 Steady state operation of the system without compensation;
a) three-phase voltage v_S, b) three-phase distorted current i_S,
c) instantaneous active and reactive powers

The distorted current and voltage waveforms of the non-linear load joint with a linear load are depicted in Figure 5.19, where the THSeAF is bypassed and current harmonics flow directly into the grid with parameters described in Table 5.1. As obviously distinguished, the current harmonics of the load produces voltage distortions when passing through the line and system impedances. Thus, to address such power quality issues, the proposed topology will be connected to the grid without the use of the bulky series injection transformer. This configuration will be able of compensating source current harmonics and voltage distortion at the point of common coupling.

Table 5.1 Simulation parameters

Symbol	Definition	Value
V_s	Line-to-line voltage	208 Vrms
f	System frequency	60 Hz
$R1, L1$	Linear Load	12.5 Ω, 40mH
R, L	Non-linear Load	12.5 Ω, 20mH
L_f	Switching ripple filter inductance	5 mH
C_f	Switching ripple filter capacitance	0.5 μF
r_C	Switching ripple damping resistor	50 Ω
f_{PWM}	PWM frequency	8 kHz
V_{DC}	dc auxiliary power supply voltage	100~150 V

5.4.1.2 Principle of the hybrid control approach

The Series active filter represents a controlled voltage source Inverter (VSI). In order to prevent current harmonics to drift into the power system, this series source should have a high impedance characteristic for all harmonic components. The principle of such modeling is well documented in (Fujita et Akagi, 1991b). The use of a passive filter becomes mandatory to compensate current issues while maintaining a constant voltage free of distortions at the load terminals.

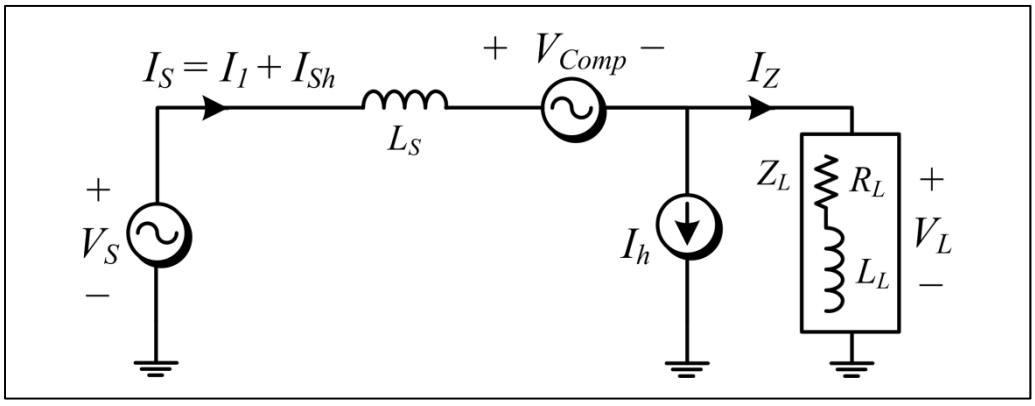

Figure 5.20 Single-phase equivalent circuit for current harmonics

The behavior of the series active filter (SeAF) for a current control approach is evaluated from the phasor's equivalent circuit described in Figure 5.20. The non-linear load is modeled by an impedance Z_L representing the power consumed and a current source generating current harmonics. The Series active filter, whose output voltage V_{Comp} is considered as an ideal controlled voltage source. The control approach is based on the detecting source current with a gain (G) proportional to the current harmonics (I_{sh}) flowing to the grid, the load voltage, as well as the source voltage harmonics. This approach gives results which are less sensitive to the value of the gain G to achieve low level of current harmonic distortions.

$$V_{Comp} = +GI_{Sh} - V_{Lh} + V_{Sh} \tag{5.19}$$

By substituting Eqn. 5.19 in the system equations, the two following variables are found.

$$I_{Sh} = \frac{(Z_L I_h + V_{Lh})}{(Z_S + Z_L + G)} \tag{5.20}$$

$$V_{Lh} = Z_L(I_{Sh} - I_h) \tag{5.21}$$

By introducing Eqn 5.21 into Eqn 5.20, it became obvious that source current harmonics are completely eliminated independent of the value of the gain G.

$$I_{Sh} = \frac{+Z_L I_h - Z_L I_h}{Z_S + Z_L + G} = 0 \tag{5.22}$$

Consequently in this approach even in presence of source voltage distortions the source current is always clean of any harmonic component. An additional component is then added to regulate the load voltage terminals which will be described in the next section. This extra component assists the THSeAF to operate similar to a Dynamic voltage restorer (DVR) and maintain the load voltage regulated despite variation in the utility's voltage supply.

5.4.2 Control Algorithm Implemented for the Three-phase THSeAF

A THSeAF configuration based on a VSC type of converter is considered in this section in order to avoid current harmonic pollution to flow into the grid. The control strategy to compensate for current and voltage issues are based on the Park's transformation. The inclusive diagram of the controller is illustrated in Figure 5.21. The Controller is mainly composed of three distinct parts; the voltage detection, current detection, and the PI regulator. The task attributed to each set of block is depicted in the present section.

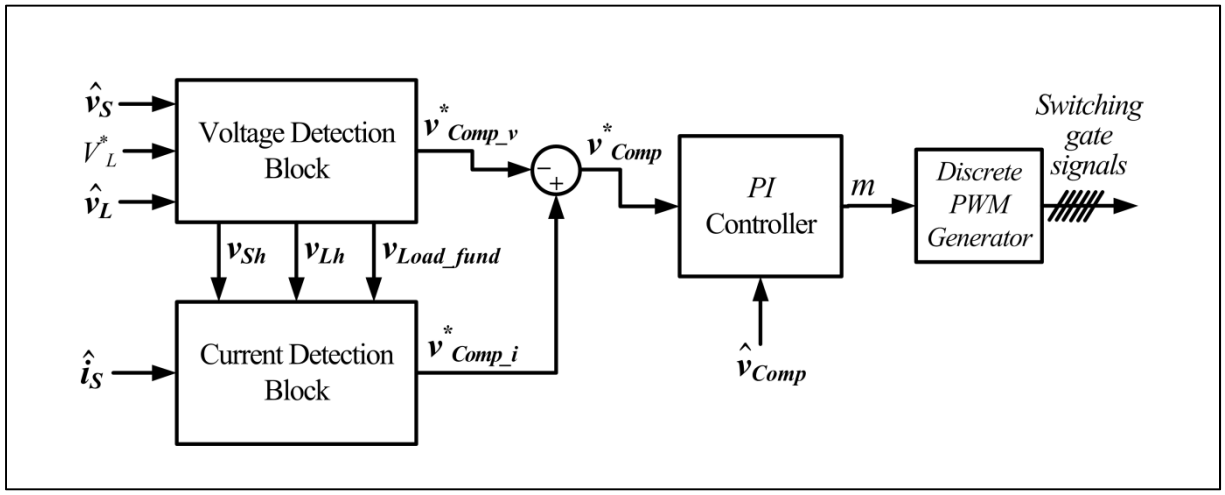

Figure 5.21 Controller architecture scheme

Since in this research dissertation the objective is to focus on the topology and the detection principle of the compensation, the regulator itself became less significant. Thus a conventional PI regulator is implemented at this stage to demonstrate the effectiveness of the proposed configuration. The transfer function is

$$PI(s) = K_{pDC} + \frac{K_{iDC}}{s} \tag{5.23}$$

Where, K_p is the proportional gain and K_i the integration gain of the controller. The output of the regulator is the gate firing signals for the IGBTs. In the previous stage of the controller as

depicted in Figure 5.21, after the voltage and currents are measured on a discrete sampling basis, the task to extract components which should be eliminated is underway. Ahead of other block sets, the voltage detector using the synchronous reference frame (SRF) principle extract first the fundamental component of the load voltage as depicted in Figure 5.22.

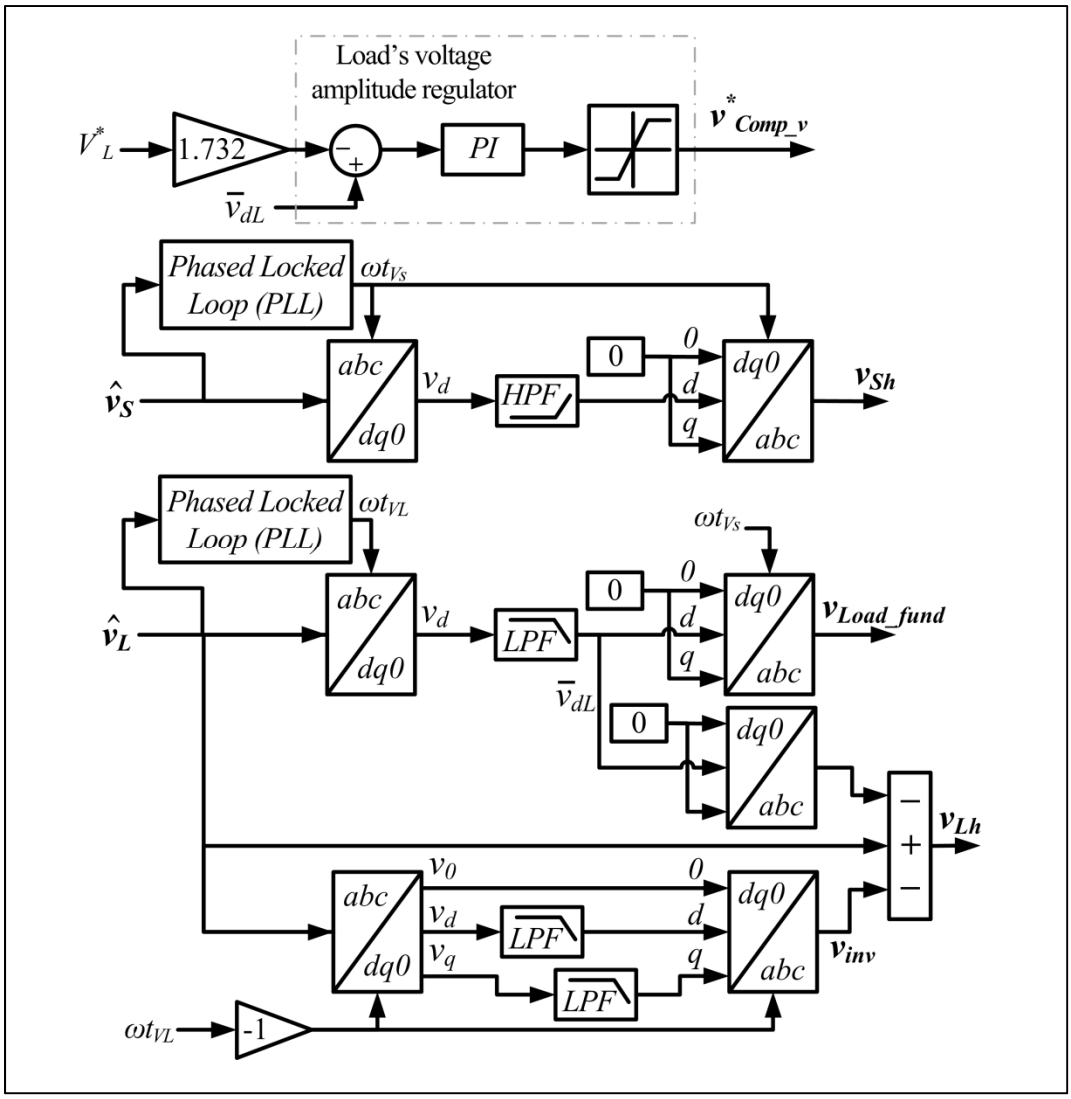

Figure 5.22 The voltage detection control pattern

The *dq0* transformation is applied to produce each of the components. To produces the v_{Sh}, it is applied to the source voltage, where by extracting high frequency oscillating portion of the direct component, the resultant source harmonics are obtained. Likewise introduced, other

components are produced by manipulating and extracting adequate components of direct and/or quadrature voltage. A reverse Park's transformation is required to obtain the three-phase compensation voltage. The three signals are then sent and summed and sent to a PWM.

$$\boldsymbol{T} = \sqrt{\frac{2}{3}}\begin{bmatrix} \cos(\omega t) & \cos\left(\omega t - \frac{2\pi}{3}\right) & \cos\left(\omega t + \frac{2\pi}{3}\right) \\ \sin(\omega t) & \sin\left(\omega t - \frac{2\pi}{3}\right) & \sin\left(\omega t + \frac{2\pi}{3}\right) \\ 1/\sqrt{2} & 1/\sqrt{2} & 1/\sqrt{2} \end{bmatrix} \tag{5.24}$$

$$\boldsymbol{v}_{dq0} = \begin{bmatrix} v_d \\ v_q \\ v_0 \end{bmatrix} = \boldsymbol{T} \cdot \begin{bmatrix} v_a \\ v_b \\ v_c \end{bmatrix}$$

To extract the load voltage harmonics during unbalance circumstances, the SRF is used to extract the inverse and zero-sequence component. By employing and inverted load's angular frequency and a tuned Low-pass filter (*LPF*) to extract the oscillating portions, it is made possible to obtain the $\boldsymbol{v}_{inv}$ in *dq0* coordinate and then in *abc* frame as follow.

$$\boldsymbol{v}_{inv}(dq0) = \begin{bmatrix} -\tilde{v}_d \\ -\tilde{v}_q \\ -v_0 \end{bmatrix} \tag{5.25}$$

$$\boldsymbol{v}_{inv}(abc) = \boldsymbol{T}^{-1}(-\omega t_{VL}) \times \boldsymbol{v}_{inv}(dq0) \tag{5.26}$$

To regulate and restore the load voltage, a term is added which consisted of comparing the direct value of the load side to a constant reference. A PI is then regulating this error during sag, swell, and unbalance. The auxiliary DC supplies the amount of power required to establish a regulated load voltage. To compensate current distortions the current detection block is operating as detailed in Figure 5.23. The *p-q theory* is used for the task of extracting the harmonics, unbalance and other current related issues. The instantaneous voltage and current space vectors $\boldsymbol{v}$ and $\boldsymbol{i}$ in *αβ0* coordinate are obtained using Clarke's transformation.

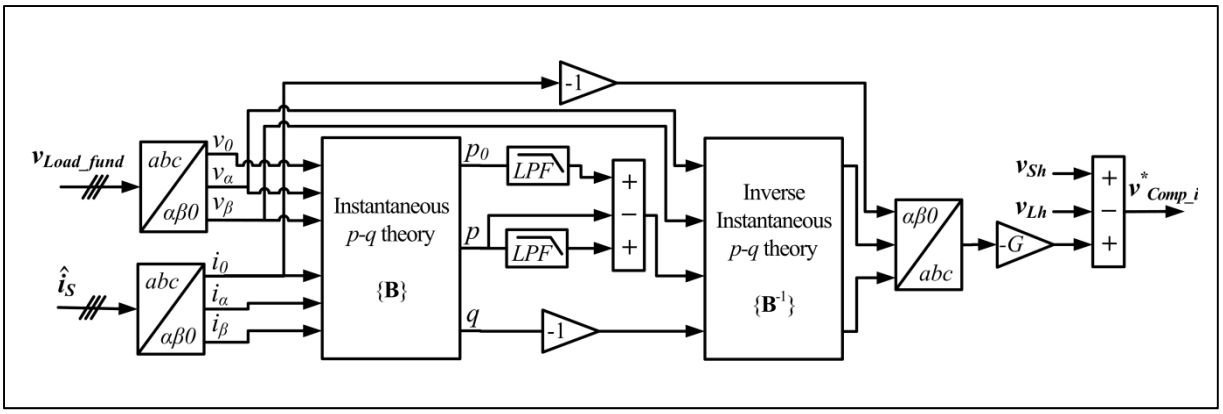

Figure 5.23 The diagram of the current detection part of the controller

$$\boldsymbol{C} = \sqrt{\frac{2}{3}} \begin{bmatrix} 1 & -1/2 & -1/2 \\ 0 & \sqrt{3}/2 & -\sqrt{3}/2 \\ 1/\sqrt{2} & 1/\sqrt{2} & 1/\sqrt{2} \end{bmatrix} \tag{5.27}$$

$$\boldsymbol{i}_{\alpha\beta 0} = \begin{bmatrix} i_\alpha \\ i_\beta \\ i_0 \end{bmatrix} = \boldsymbol{C} \times \begin{bmatrix} i_a \\ i_b \\ i_c \end{bmatrix}, \quad \boldsymbol{v}_{\alpha\beta 0} = \begin{bmatrix} v_\alpha \\ v_\beta \\ v_0 \end{bmatrix} = \boldsymbol{C} \times \begin{bmatrix} v_{an} \\ v_{bn} \\ v_{cn} \end{bmatrix}$$

Thereafter the instantaneous powers are defined.

$$\begin{bmatrix} p \\ q \\ p_0 \end{bmatrix} = \underbrace{\begin{bmatrix} v_\alpha & v_\beta & 0 \\ v_\beta & -_\alpha & 0 \\ 0 & 0 & v_0 \end{bmatrix}}_{\hat{B}} \begin{bmatrix} i_\alpha \\ i_\beta \\ i_0 \end{bmatrix} \tag{5.28}$$

With reference to *αβ0* coordinate, the powers are produced with the load's fundamental component but in phase with the source voltage. Obtained currents from the power expressions are decomposed into active and reactive parts. They were then used for current compensation purposes.

$$\begin{bmatrix} i_\alpha \\ i_\beta \end{bmatrix} \triangleq \overbrace{\begin{bmatrix} i_{\alpha p} \\ i_{\beta p} \end{bmatrix}}^{i_p} + \overbrace{\begin{bmatrix} i_{\alpha q} \\ i_{\beta q} \end{bmatrix}}^{i_q} = \frac{1}{{v_\alpha}^2 + {v_\beta}^2} \begin{bmatrix} v_\alpha & v_\beta \\ v_\beta & -v_\alpha \end{bmatrix} \begin{bmatrix} p \\ 0 \end{bmatrix} + \frac{1}{{v_\alpha}^2 + {v_\beta}^2} \begin{bmatrix} v_\alpha & v_\beta \\ v_\beta & -v_\alpha \end{bmatrix} \begin{bmatrix} 0 \\ q \end{bmatrix} \tag{5.29}$$

Where ($i_{\alpha p}$, $i_{\beta p}$) are instantaneous active currents and ($i_{\alpha q}$, $i_{\beta q}$) are instantaneous reactive currents. Both active and reactive powers can be divided into a constant amplitude component and an oscillating component. By compensating the reactive portion of current, a conventional unity power factor is achieved. Due to the presence of both zero-sequence currents and voltages in a four wire system, p_0 must also be considered. The oscillating portion of the active power and the zero sequence power, if this latter exists, are compensated in this strategy.

$$\boldsymbol{B}^{-1} = \frac{1}{{v_0}^2\left({v_\alpha}^2 + {v_\beta}^2\right)} \begin{bmatrix} {v_0}^2 v_\alpha & {v_0}^2 v_\beta & 0 \\ {v_0}^2 v_\beta & -{v_0}^2 v_\alpha & 0 \\ 0 & 0 & v_0\left({v_\alpha}^2 + {v_\beta}^2\right) \end{bmatrix} \tag{5.30}$$

Compensating instantaneous active and reactive currents are obtained as follows:

$$\boldsymbol{i}_p(\alpha\beta 0) = \boldsymbol{B}^{-1} \times \begin{bmatrix} -\tilde{p} \\ 0 \\ p_0 \end{bmatrix} \quad , \quad \boldsymbol{i}_q(\alpha\beta 0) = \boldsymbol{B}^{-1} \times \begin{bmatrix} 0 \\ -q \\ 0 \end{bmatrix} \tag{5.31}$$

The current is then transformed to a relative three-phase voltage using a gain (G).

$$\boldsymbol{v}_{ih}(abc) = -G \times \left(\boldsymbol{C}^{-1} \times \begin{bmatrix} \boldsymbol{i}_p(\alpha\beta 0) \\ \boldsymbol{i}_q(\alpha\beta 0) \\ -\boldsymbol{i}_0 \end{bmatrix} \right) \tag{5.32}$$

Where $\boldsymbol{C}^{-1}$ is the Clarke's reverse transform matrix. The three-phase voltage reference compensates the current harmonics produced by a non-linear load. The interesting spot line to implement the current compensator is that it compensates the voltage harmonics as they generate current harmonics consequently. In order for the THSeAF to operate in optimal

conditions, as defined in the earlier section, two extra terms are required to make a perfect compensation of current harmonics with low gain *G* under grid perturbations.

$$\boldsymbol{v}^{*}_{Comp_i}(abc) = -(G\boldsymbol{i}_{Sh} + \boldsymbol{v}_{Lh} - \boldsymbol{v}_{Sh}) \tag{5.33}$$

To conclude, the generic compensating voltage reference is reached by combination of the stated components related to current issues and voltage issues together.

$$\boldsymbol{v}^{*}_{comp} = -\boldsymbol{v}_{comp_v} + \boldsymbol{v}_{comp_i} \tag{5.34}$$

This reference is then compared with the measure output voltage of the compensator and by passing through the PI regulator; the duty cycle $\boldsymbol{m}$ is produced. The duty cycle is a matrix of three components, each for a phase of the system.

5.4.3 Results of the 3φ THSeAF Improving Power Quality

To analyze the behavior of the proposed topology to eradicate power quality issues, the system of Figure 5.18 is implemented in Matlab/SPS by applying a fixed discrete time step of T_S = 10μs, which allows a reliable results comparable to an experimental implementation. In the simulation result shown in Figure 5.24, the compensator starts operating at 0.05s. It can be clearly observed that the major part of the source current harmonics are instantly compensated reaching a current's total harmonic distortion (THD) of 0.7%, whereas the load's current is highly polluted with a THD of 21%. The PI regulator is forcing within three cycles the converter to follow the reference to produce the exact compensating voltage. The voltage generated by the compensator will force the nonlinear loads to draw a sinusoidal current in phase with the corresponding source voltage to achieve a unity power factor. The shunt passive filter in the configuration is essential to prevent current harmonics to flow into the grid.

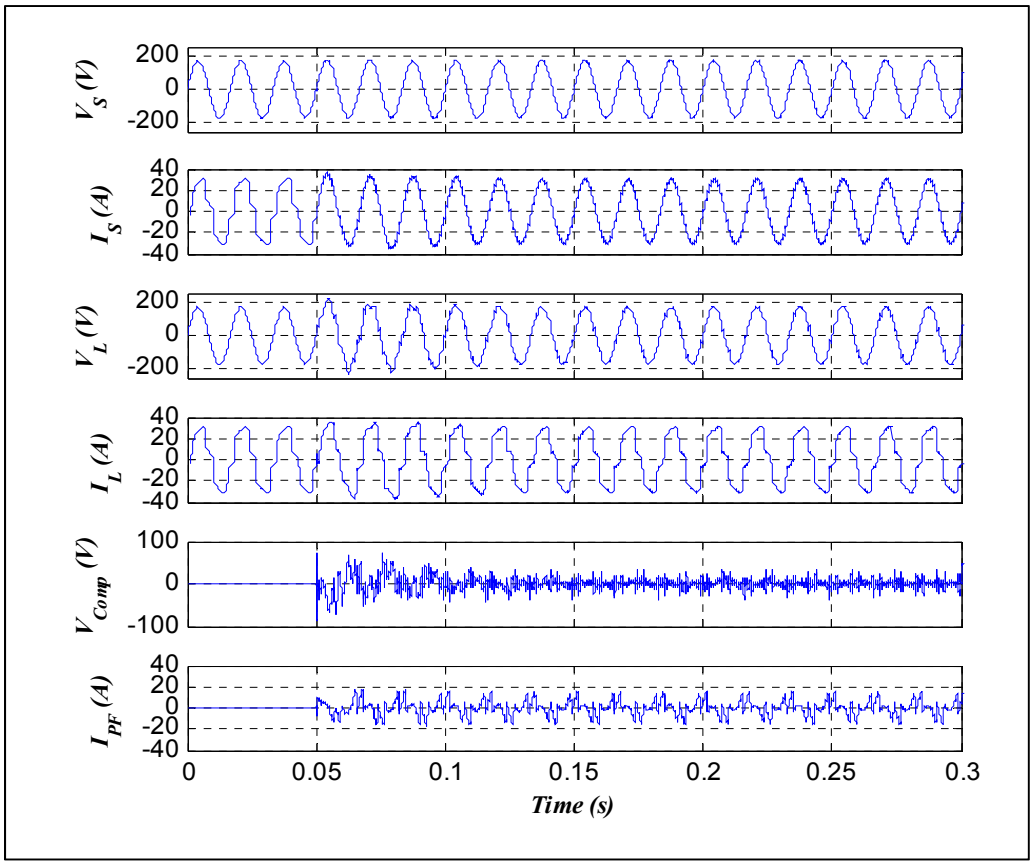

Figure 5.24 Transformerless-HSeAF compensating current harmonics;
(a) Source voltage v_S, (b) source current i_S, (c) Load voltage v_L,
(d) load current i_L, (e) Active-filter voltage v_{Comp},
(f) Harmonics current of the HPF i_{HPF}

The Figure 5.25 demonstrates how the compensator compensates the reactive power of the load leaving the source supplying only the active part. The diagram shows the measured average three-phase active power (P) and reactive power (Q) associated with a set of three-phase voltages and currents within one to two cycles calculating their mean values. The compensator do not interfere the active power flow, meanwhile it has the ability to control the power flow by lagging or leading the current.

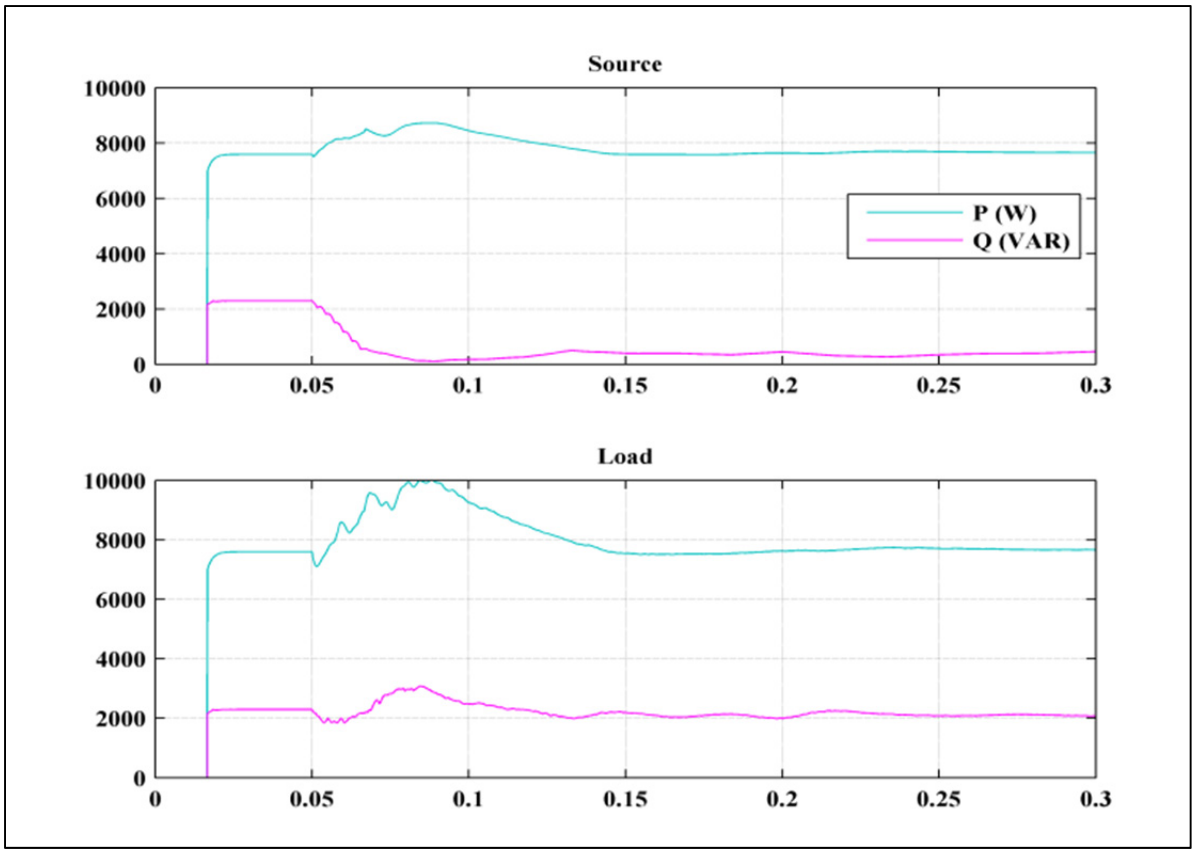

Figure 5.25 Three-phase calculated powers of the system; a) Source delivered power, b) load consumption

During voltage pollution, the compensator maintains an appropriate harmonic-free and regulated voltage at the load terminals. Figure 5.26 demonstrates the behavior of the system when the utility's voltage is highly polluted with a fifth and seventh order harmonics of 20 and 15 percent of the fundamental respectively resulting in a three-phase supply ($\boldsymbol{v}_S$) containing a THD of 25%. The proposed compensator continues to clean the grid's current from harmonics and corrects the power factor while the load's voltage THD is kept under the 5% limitation imposed by standards and regulations.

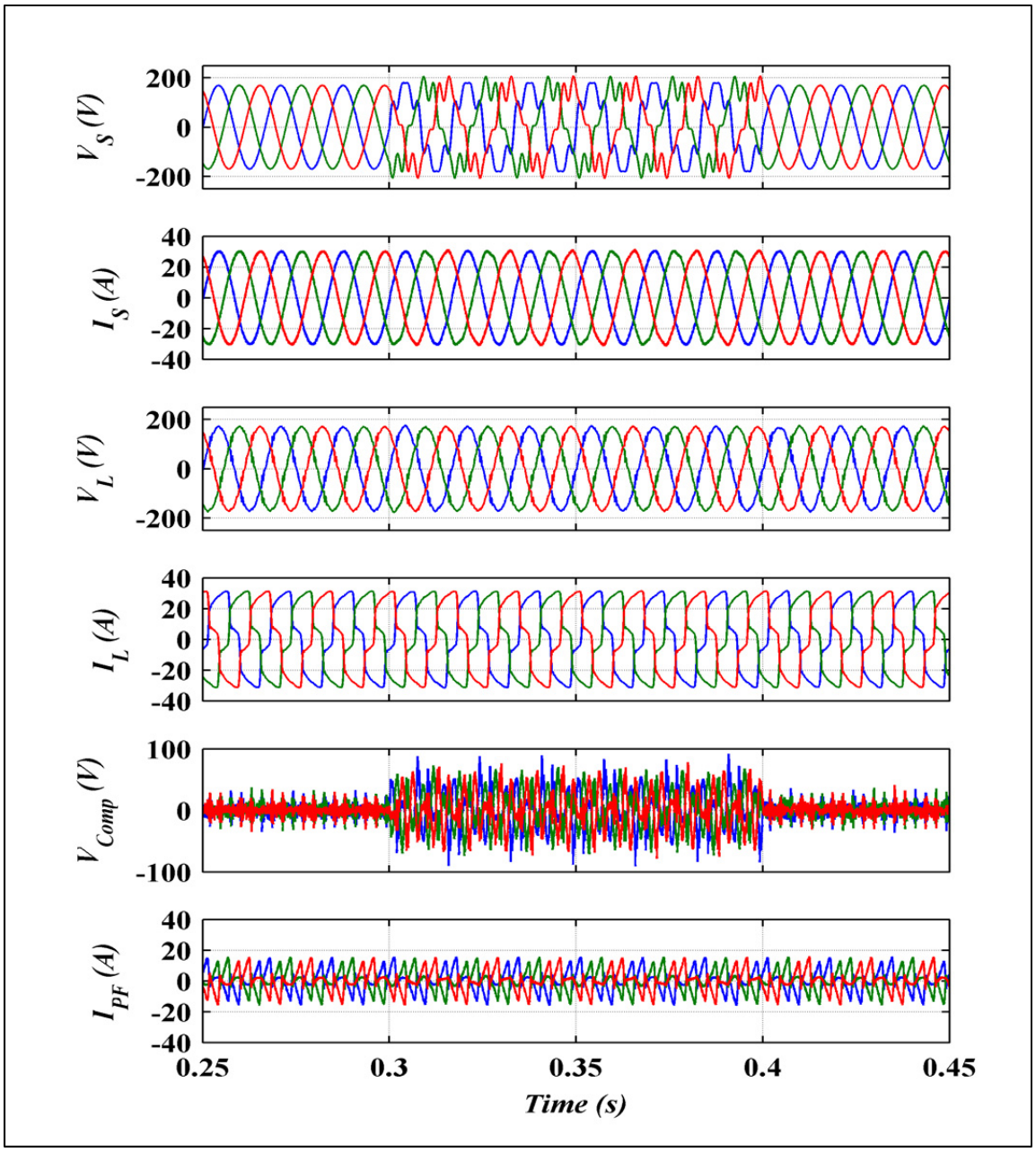

Figure 5.26 Three-phase waveforms during grid's perturbation while the THSeAF is enhancing the power quality

Figure 5.27 illustrates the response of the system during source voltage unbalance (from 0.5s to 0.6s and 0.7s to 0.8s) while the filter regulates the load terminal voltage. This active power compensator is able to follow variation in the load consumption while preventing current harmonics to flow into the grid side. Furthermore, it maintains a sinusoidal and regulated

voltage across the point of common coupling of loads. The response of the system during a load variation is demonstrated in Figure 5.28, where the compensator follows this variation while performing the power quality improvement.

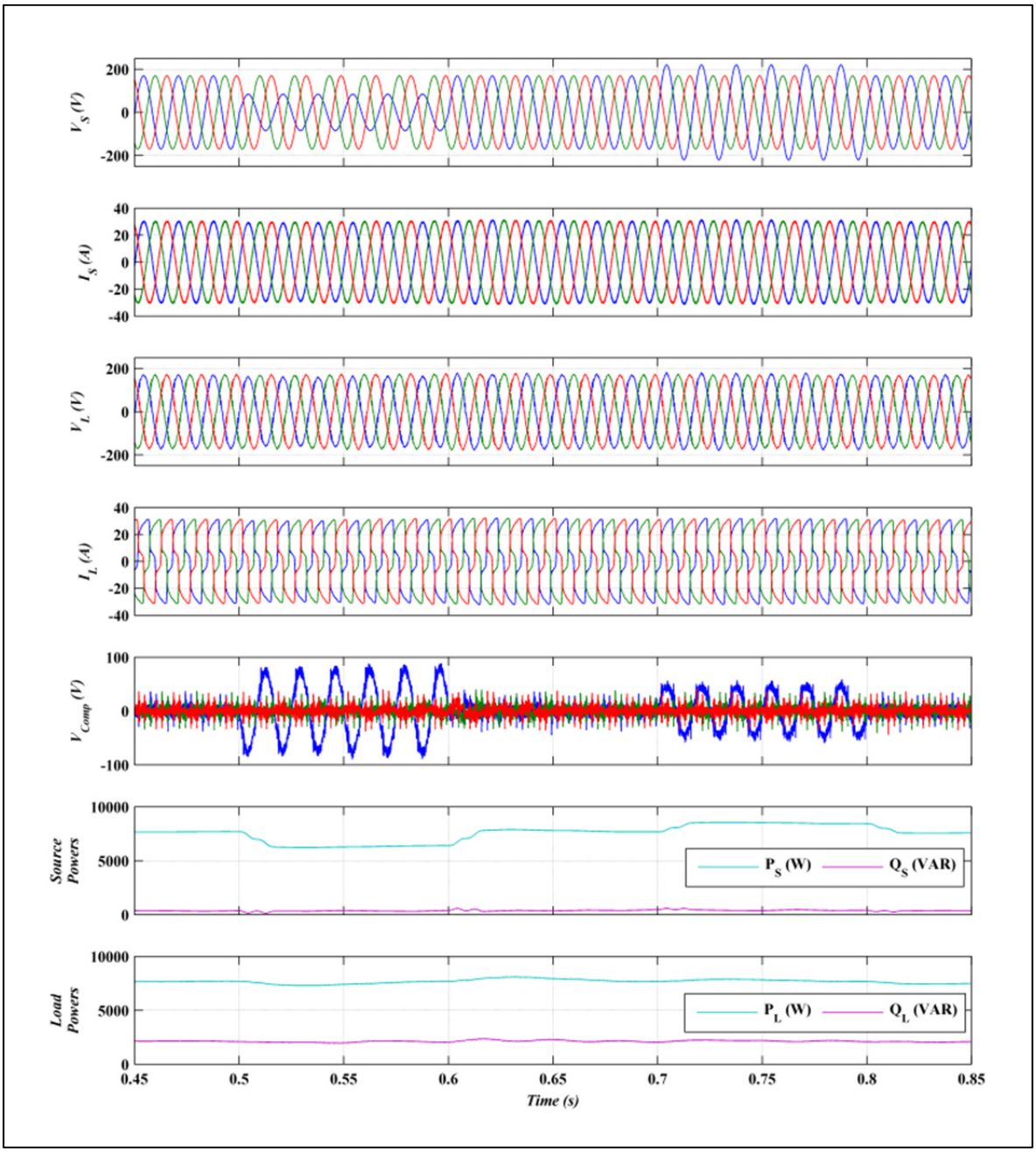

Figure 5.27 Three-phase waveforms during voltage unbalance while the THSeAF deliver a regulated and balanced supply to the loads

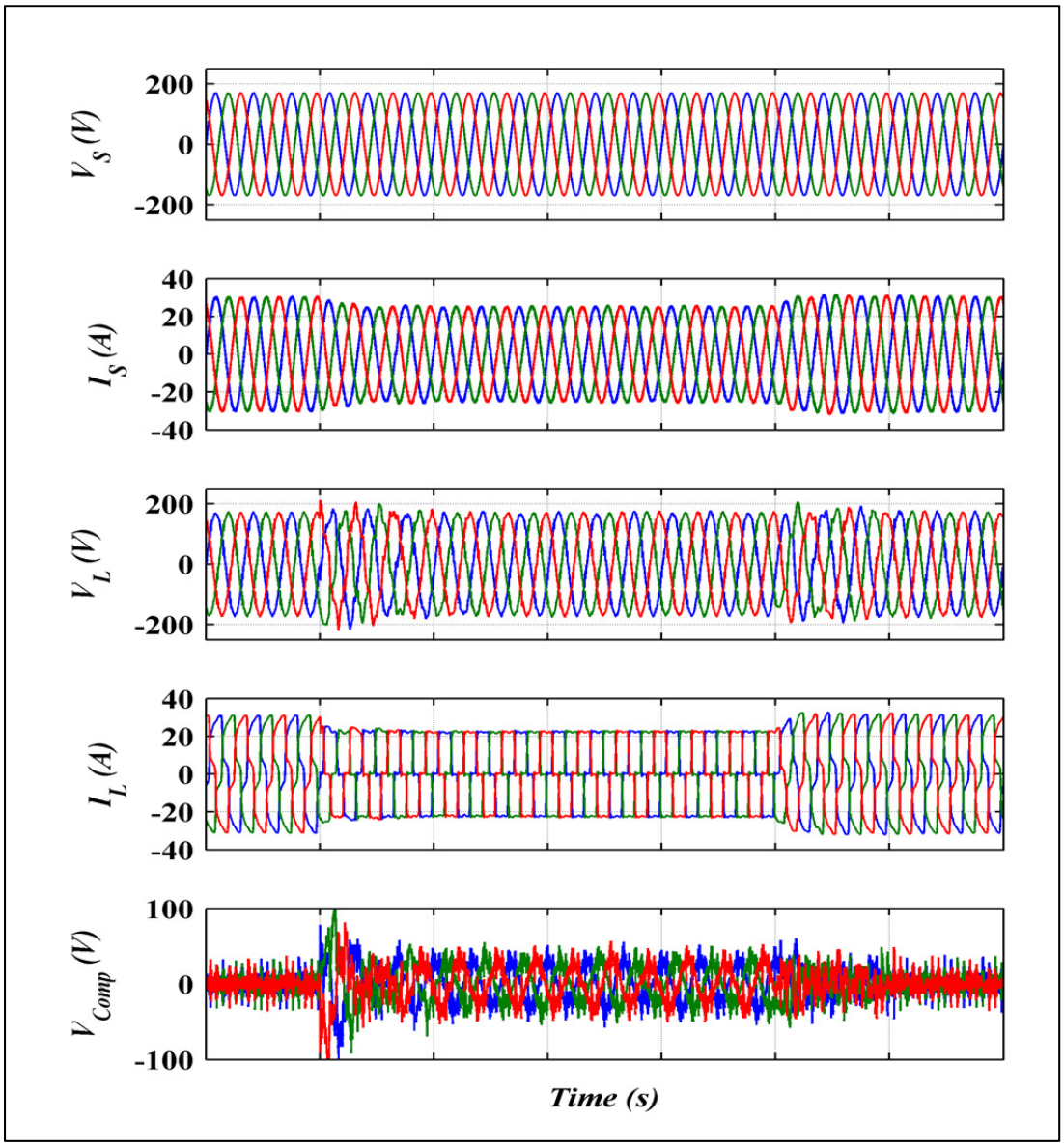

Figure 5.28 System response to load dynamic variation

5.5 Experimental results

The study is validated through the three-phase laboratory prototype realized according to the electric schema of Figure 5.18 without the linear load. The RCP setup illustrated in the Appendix II, was realized to demonstrate efficiency and behavior of the proposed transformerless configuration. The THSeAF is subjected to two kind of compensation; within the first test the compensator acting as an active filter, cleans the source current, while during the second series of test the compensator operates in a hybrid approach as explained in previous sections regulating also the load's voltage in addition to the current harmonic compensation. The setup's parameters are tabulated as shows Table 5.2, where some parameters are subjected to variation upon requested during the tests.

Table 5.2 Three-phase THSeAF experimental configuration parameters

Symbol	**Definition**	**Value**
v_s	Line-to-line voltage	190~208 Vrms
f	System frequency	60 Hz
R	Non-linear load resistance	25 Ω
L	Non-linear load inductance	20 mH
S	Load power rating	2.6~3.1 kVA
L_f	Switching ripple filter inductance	5 mH
C_f	Switching ripple filter capacitance	2 μF
r_C	Switching ripple damping resistor	50 Ω
T_S	dSPACE Synchronous sampling time	42 μs
f_{PWM}	PWM frequency	8 kHz
V_{DC}	dc auxiliary power supply voltage	100~150 V

The following results show the system without compensator installed. The PowerPad 3945-B of AEMC Instruments is used for power analysis. As illustrated in Figure 5.29, the load current is polluted with a THD of 26.7% which necessitate a harmonic cleaning.

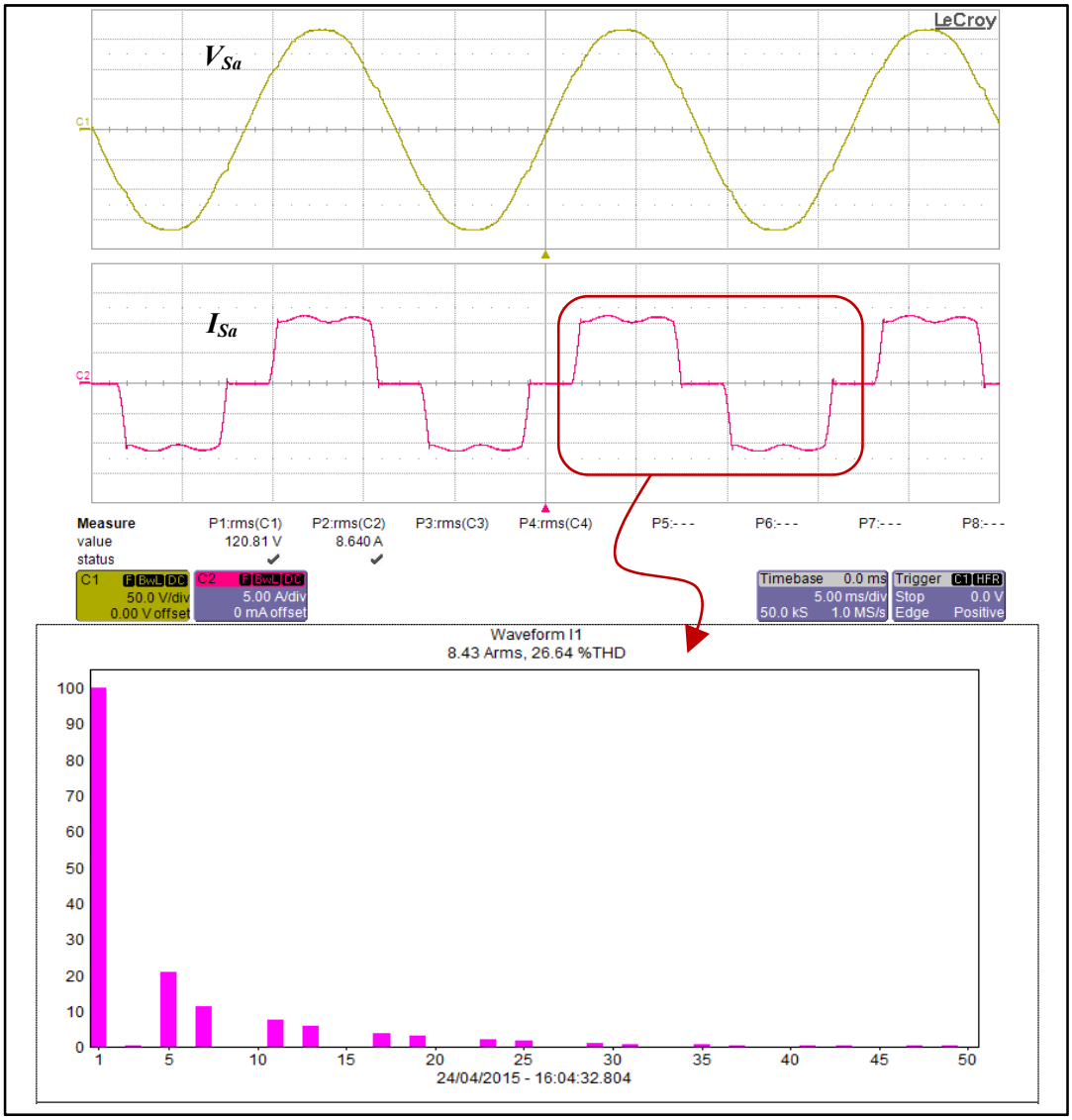

Figure 5.29 Voltage and current of the 3φ non-linear load without compensation

5.5.1 Load Current Harmonic Compensation

5.5.1.1 The TSeAF operation without the shunt passive filter branches

In this section only the Active part is connected to operate as harmonic isolator and the shunt passive filter is not yet connected. In this test, the non-linear load is connected solely to the

PCC to have a higher degree of pollution. The Transformerless series active filter (TSeAF) active's part is generating a voltage to force the load to draw a sinusoidal waveform current. To point out the importance of the compensation strategy developed in the Chapter 2.6, the following tests are prepared with the non-linear load (THDi = 26.7%) connected to the PCC. Thus, in the first results shown in Figure 5.30, the controller algorithm which generates the compensating voltage reference (Figure 5.21), the two components related to voltage harmonics are absent. Consequently, even with a relatively high harmonic gain G equal to 45, the load current still contain important amount of harmonics (THDi = 17.6%). Even though, this result could be improved by performing a fine tuning of the converter's output filter as well as by increasing the dc voltage, the components and the dc voltage are kept constant to help a comparative study with other results demonstrated in this thesis.

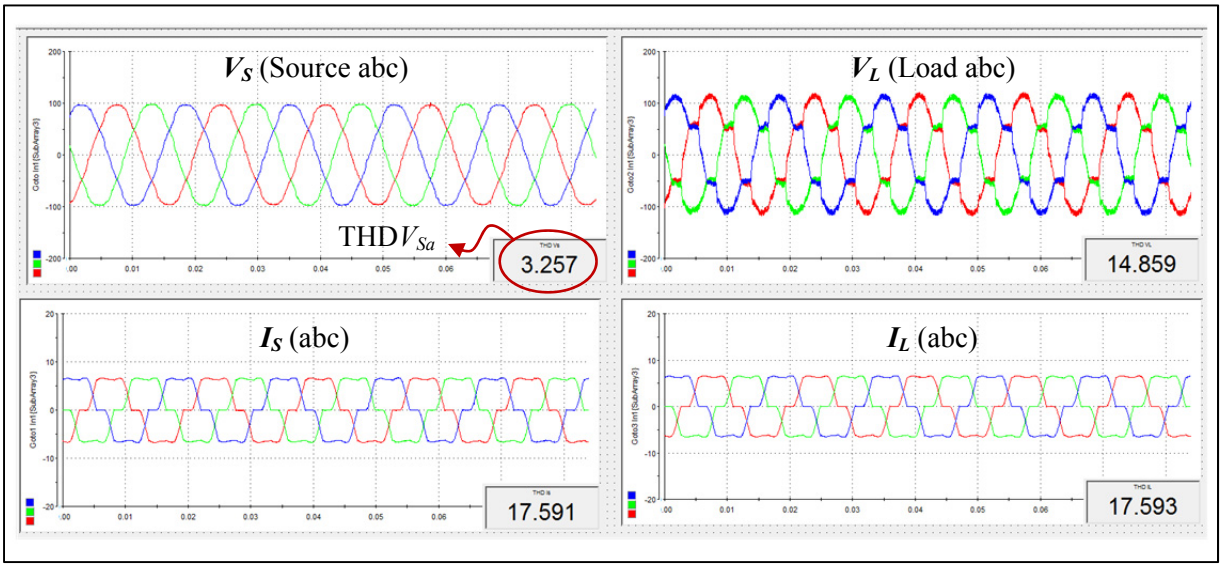

Figure 5.30 The source current harmonic compensation with v_{Comp}= +Gi_{Sh}

As endorsed previously, by including the voltage harmonics into the control law better results are achieved. The Figure 5.31 demonstrates the results when the $\boldsymbol{v}_{Comp}$= +$\boldsymbol{Gi}_{Sh}$-$\boldsymbol{v}_{Lh}$+$\boldsymbol{v}_{Sh}$. The fact to have these components implicated in the control process allows reducing considerably the harmonic gain G and obtaining fairly enhanced results. With intact output converter's

filter, the harmonic distortion is reduced to 8.6%, with a small gain *G* of 3.7 compared with 45 in the previous test.

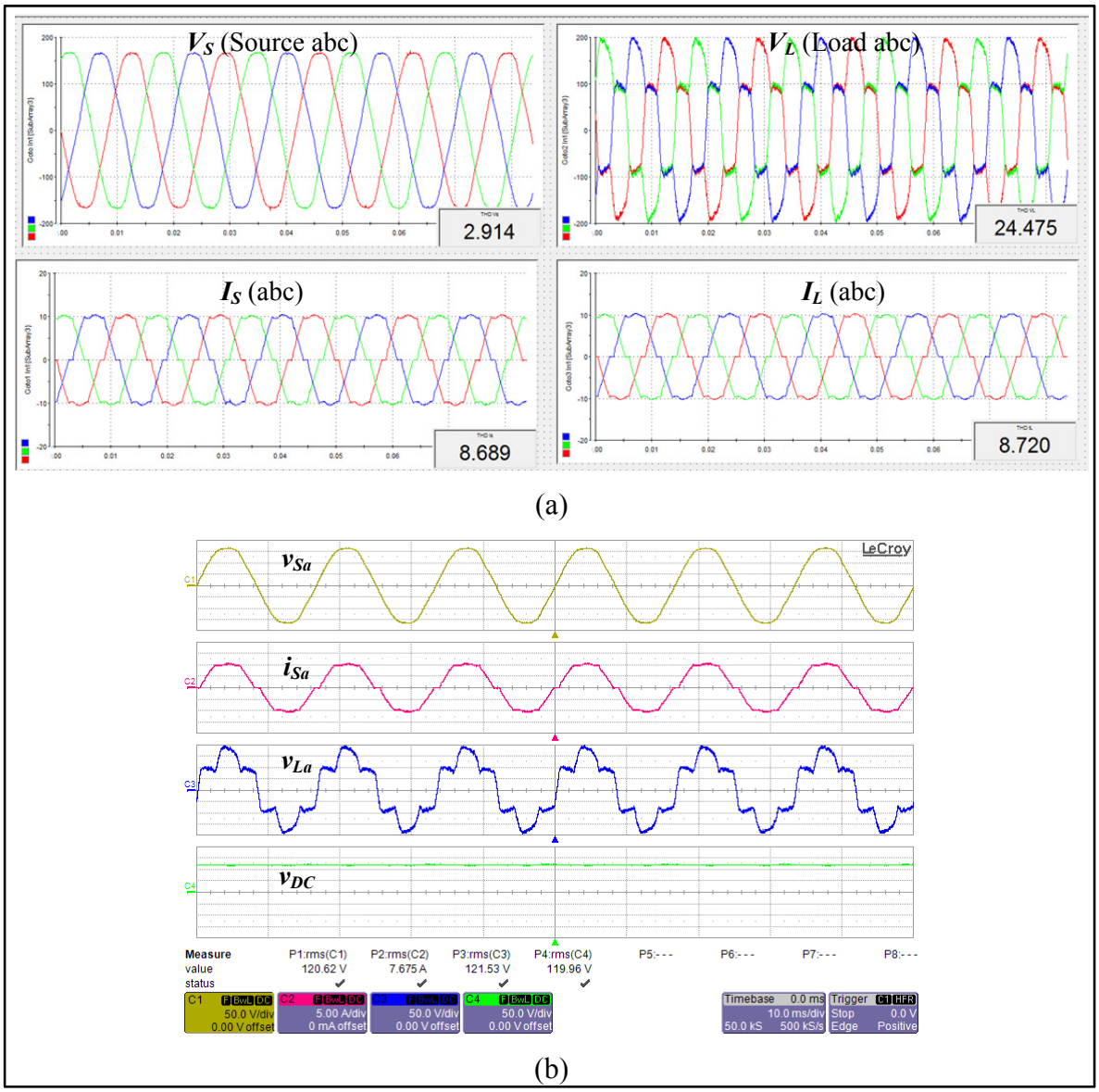

Figure 5.31 The TSeAF compensating load current harmonics;
(a) 3φ dSPACE snapshot during operation of the real-time system,
(b) Oscilloscope's measurement of one phase

5.5.1.2 The THSeAF operation with the shunt passive filter branches

In the following tests the shunt passive filter branches are connected to help improving the load's voltage and creating a low impedance pathway for current harmonics coming from the load. The nominal voltage is reduced to 110 Vrms ph-N and consequently the rating of the system is reduced to 2.6 kVA. This assist the active part to perform more reliable as it requires lower compensating voltage and less stiffness to achieve desired result. Related waveforms captured from the experimental prototype are summarized in Figure 5.32. The results are obtained at reduced DC voltage 100Vdc.

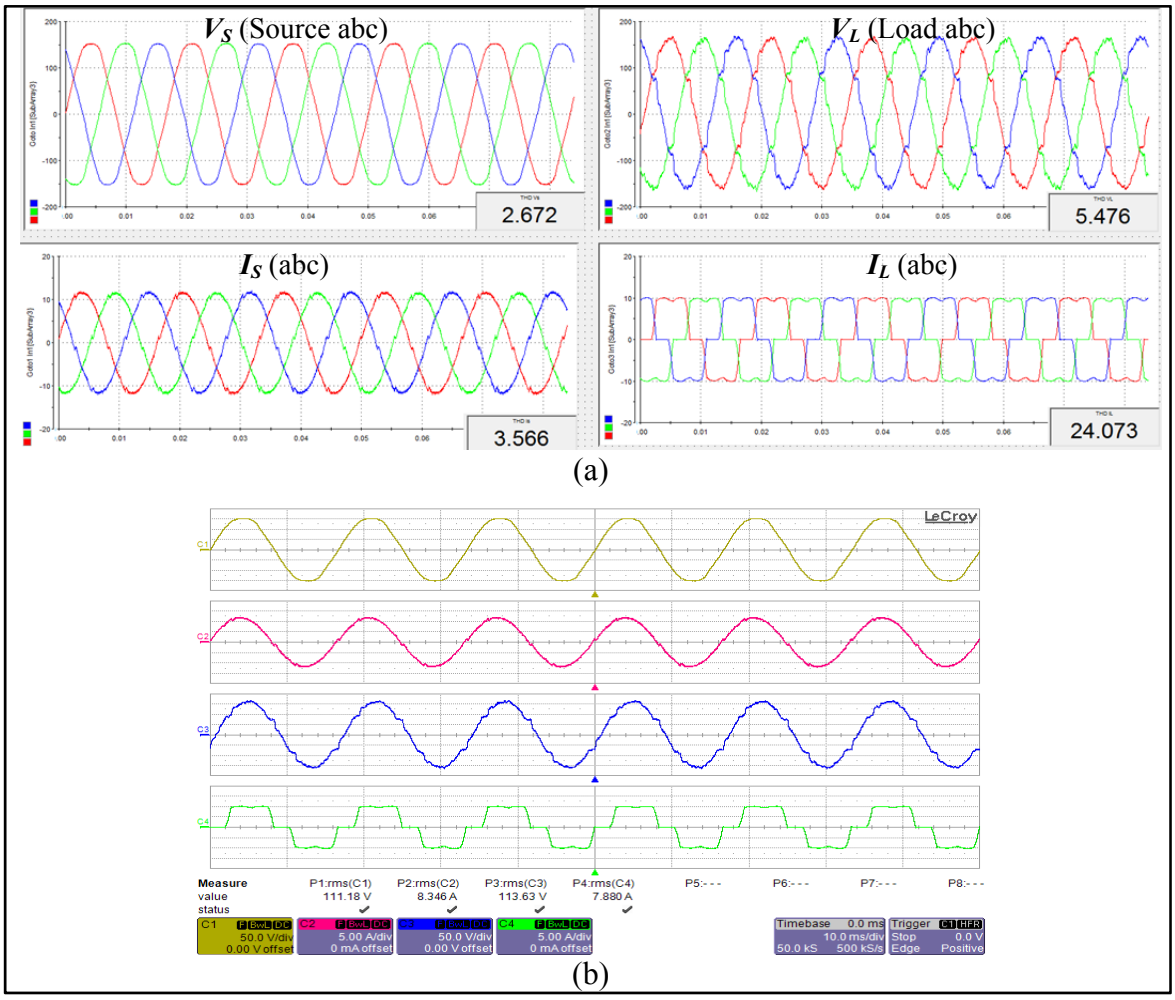

Figure 5.32 The THSeAF compensating load current harmonics; (a) dSPACE snapshot during operation of the real-time system; (b) Oscilloscope's measurement on phase-A

The Table 5.3 shows the non-linear load current harmonic components before compensation where the THD reach 25%.

Table 5.3 Load current harmonic decomposition

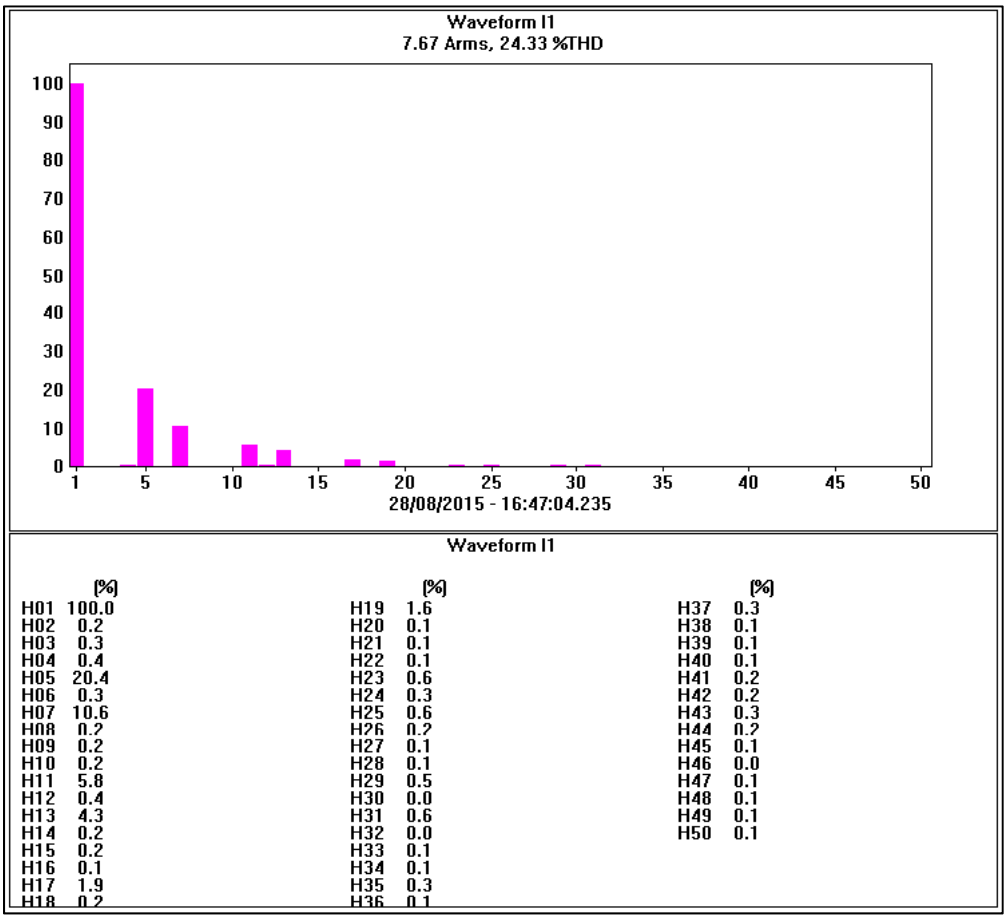

After compensation as illustrated in Table 5.4, the THSeAF forces the current harmonics to circulate into the shunt passive filter and cleans the source current from undesired harmonics. The following table illustrates clearly that the current flowing into the grid is now ridded of bulk of harmonics and the THD of i_S achieves 3.5%.

Table 5.4 Source current harmonic content after compensation by the THSeAF

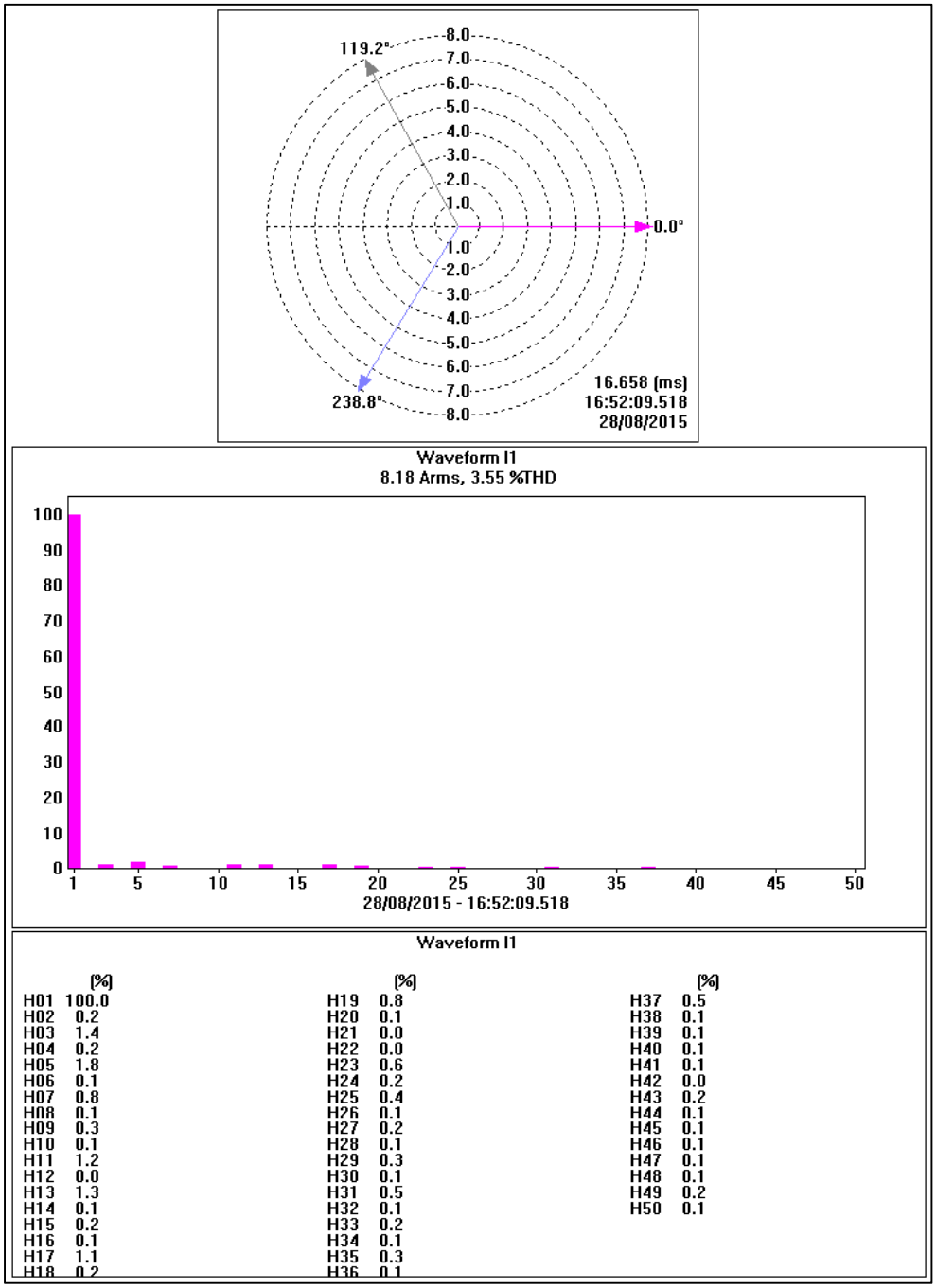

5.5.2 THSeAF in Hybrid Compensation of Current and Voltage Issues

The THSeAF is aimed to compensate bulk issues related to voltage and current simultaneously. To achieve this objective the controller developed earlier in Chapter 5.4.2 is implemented to regulate the load voltage in addition to source current compensation. The compensator will operate similar to a DVR to restore the load voltage despite perturbation in the grid's supply. In this experiment two tests are performed; the supply voltage unbalance and the Sags and Swells. In both essays it is noticed that the load voltage remains regulated.

5.5.2.1 Supply Voltage Unbalance

The report shows the grid's line-to-line voltage subjected to a tough unbalance. The load voltage is regulated to 110 Vrms phase-to-ground equivalent to 190 Vrms line-to-line. The line voltages show distortion and unbalance that should be compensated by the THSeAF to ensure a balanced and sinusoidal waveform at the load side. As described in the Table 5.5, the supply voltage is unbalanced and contains, zero and negative sequence components. The phasor representation of voltage vectors confirms the presence of these two undesired components in addition to the positive sequence component.

Table 5.5 Unbalanced utility voltage

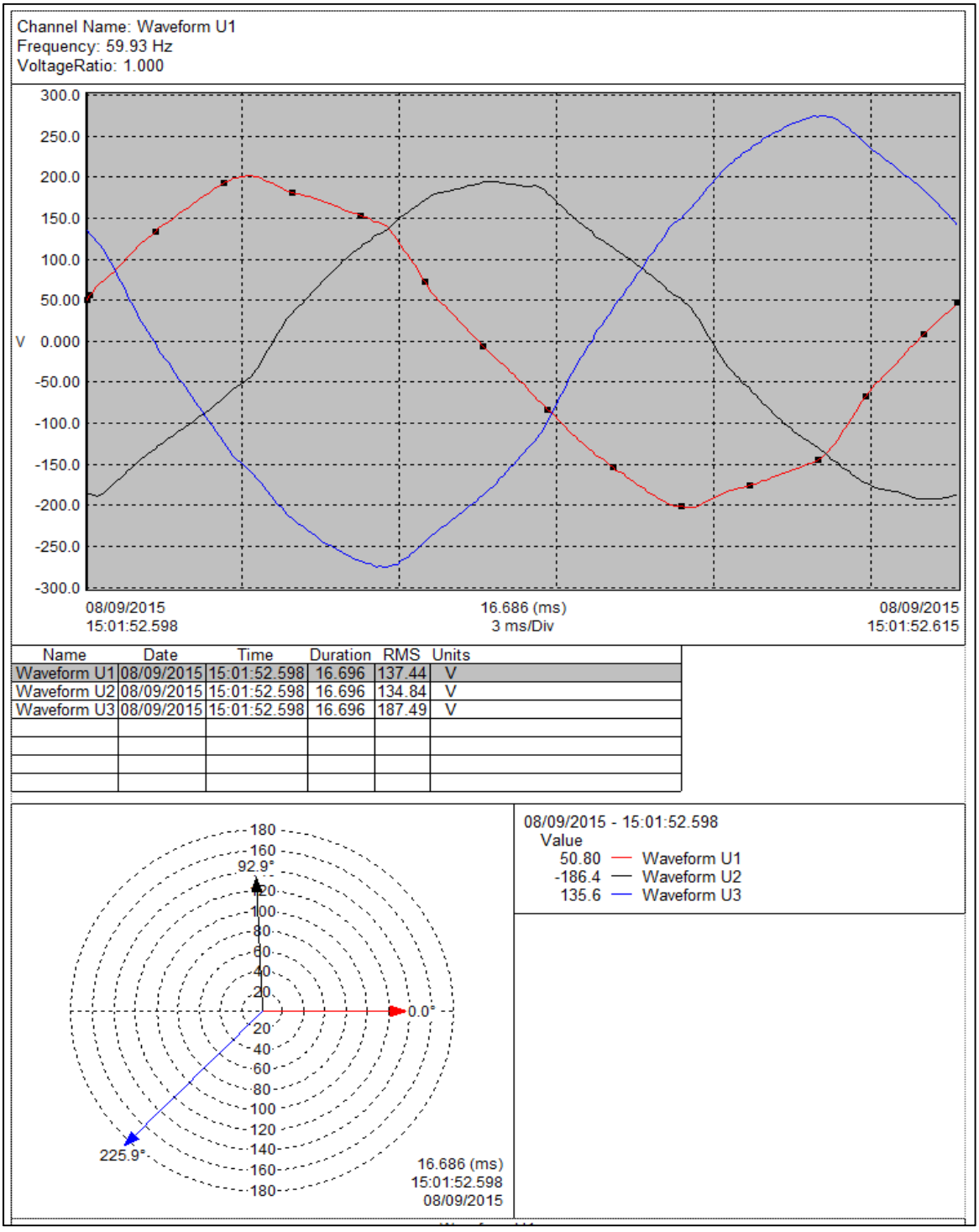

The Figure 5.33 is demonstrating experimental results for the three-phase system. The compensator is operating compensation by performing a restoration of a balanced three-phase voltage while compensating load current simultaneously. The three auxiliary DC supplies for each phase are maintained at 110 Vdc. The load voltage is regulated at the nominal value of 110 Vrms Ph-N.

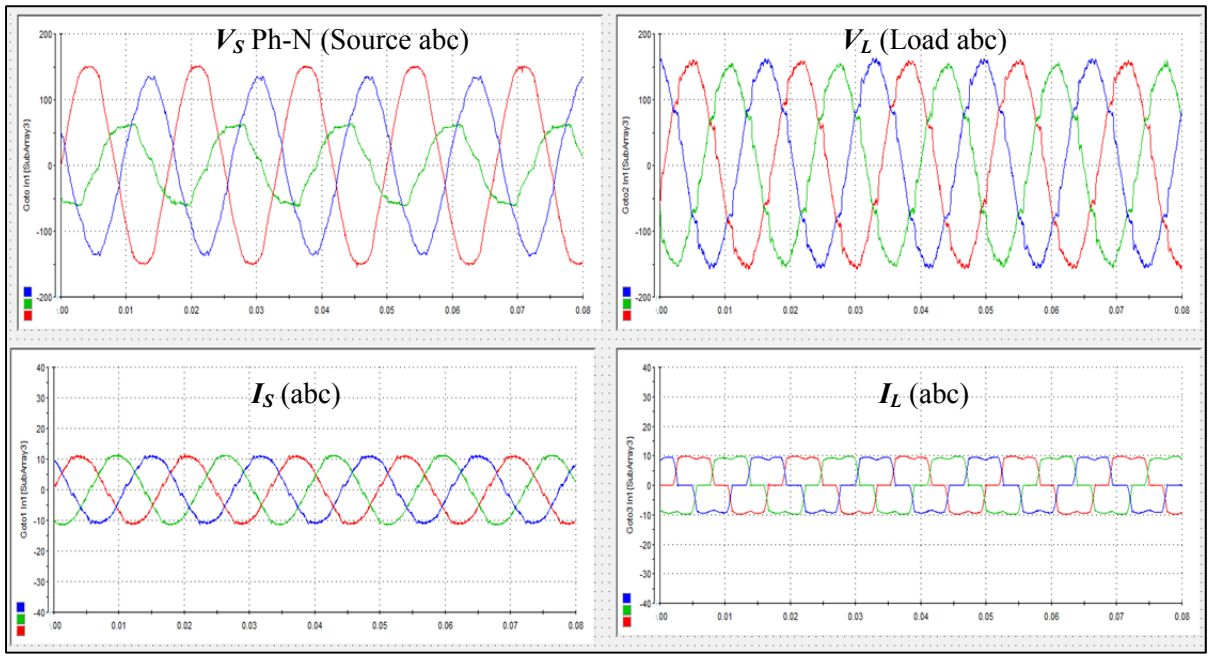

Figure 5.33 THSeAF compensating load current harmonics and performing voltage restoration, dSPACE snapshot during real-time operation

5.5.2.2 Supply Voltage Sags and Swells

The Series hybrid active filter is advantageous when the voltage is subjected to sags and swells as shown in Figure 5.34. In such circumstances, the three-phase source (grid) voltage amplitude is reduced for few cycles. The compensator will absorbs or inject required amount of active power to maintain the load voltage amplitude at a constant value.

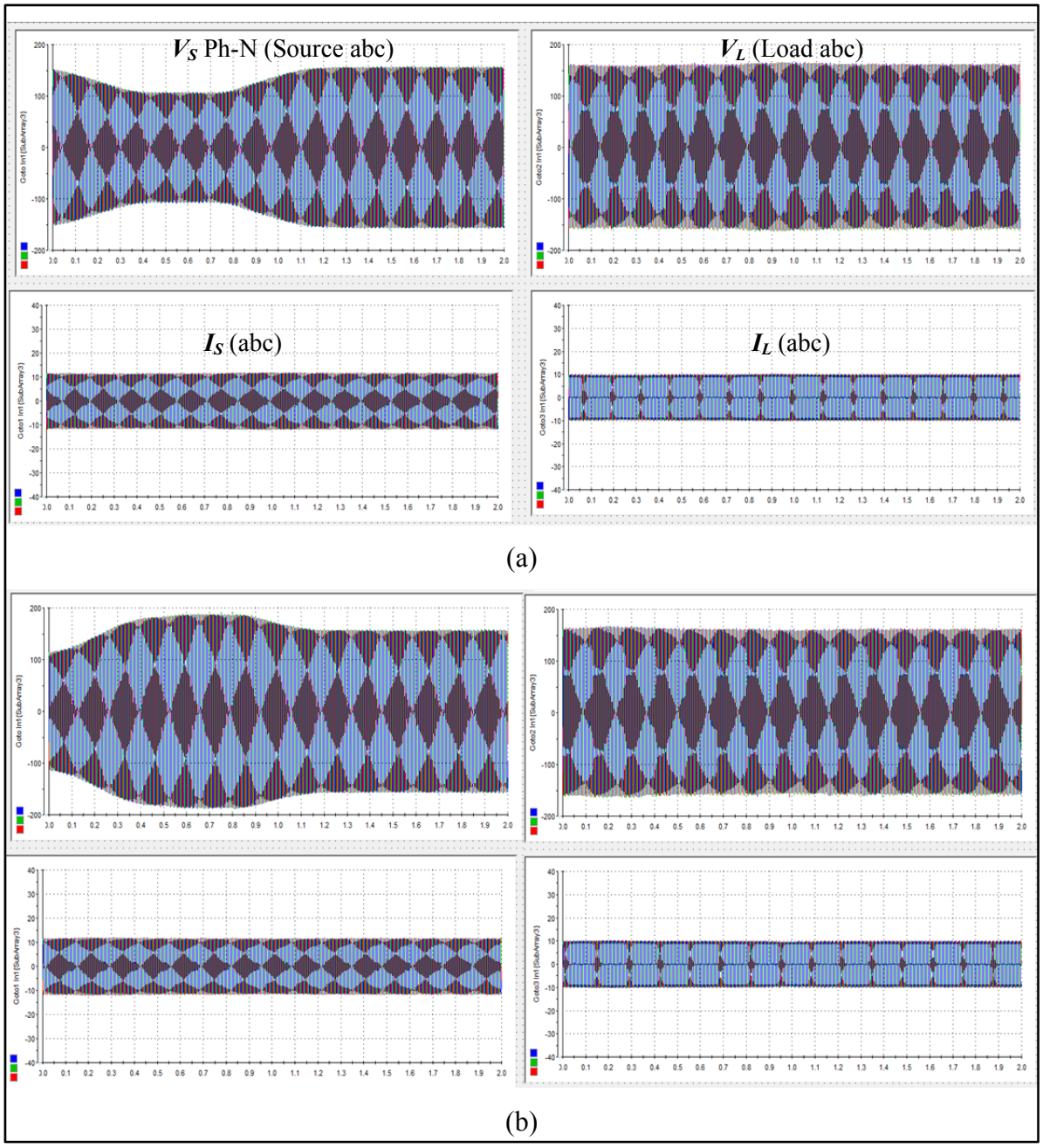

Figure 5.34 The three-phase THSeAF prototype compensating in real-time the load current harmonics and performing voltage regulation during;
(a) three-phase Sags, (b) three-phase Swells

5.6 Conclusion

Using the series active power filter is advantageous in terms of reducing harmonics without active power consumption while improving the efficiency of the electrical system. To compensate current issues a hybrid series active filter could be an attractive alternative solution to UPQCs. Consequently, the control algorithm employed in the series active filter is important. In the first section of this chapter, a comprehensive control strategy has been proposed and analyzed. The proposed control algorithm made the HSeAF able to operate as a DVR and compensate voltage distortion and unbalance at the point of common coupling where sensitive loads are installed. Furthermore, it was as well behaving similar to a shunt active filter by correcting the power factor and compensating current harmonics produced by a non-linear load. The advantage of the proposed controller was that it could combine the two functionalities and force the active power filter operating similar to a UPQC.

In the second stage of this chapter a novel topology has been proposed to replace conventional HSeAF. It has been demonstrated that the proposed Transformerless-HSeAF is advantageous in terms of distortions reduction and voltage regulation at the point of common coupling. By eliminating current harmonics from the distribution system the proposed configuration improves the efficiency of the power system. This THSeAF configuration is obviously more cost-effective and less complex than those based on a transformer to inject compensating voltage to the system. It could be an attractive alternative solution to UPQCs and shunt active filters. Moreover, results have demonstrated an improved behavior compared to the conventional HSeAF. It compensates voltage distortions and unbalances at the point of common coupling where sensitive loads are installed. Furthermore, it corrects the power factor and compensates load current from the power system.

In the last section of the chapter a three-phase THSeAF based on VSC type of converter was introduced to address power quality issues related to residential and commercial buildings. The proposed control algorithm consisting of the SRF and the *p-q* theory was developed to extract voltage and current harmonics as well as unbalance, sags, and swells. Simulation

results carried out on a typical non-linear load, illustrates success of the compensator and the controller in rectifying harmonic currents and the reactive power. A sustainable and reliable supply was restored on the load's PCC. It has been demonstrated that this active compensator responds seamlessly to variations in the source voltage and load power. Furthermore, by eliminating source harmonic currents and unbalances, it was demonstrated that the global grid power quality will be assessed.

CONCLUSION

This thesis presents a comprehensive research work to enhance the power quality of distribution and low-level power systems utilizing the Series active power filter. It addresses the topology, control, and real-time implementation of Series compensator for possible industrial applications. The thesis has carried out a study on series compensators and developed a smart power electronic compensator to enhance the static and dynamic behavior of electrical network carrying high percentage of fluctuating renewable energy sources. Several new concepts are introduced, supported by thorough analytical studies and approved by means of offline simulations and validated through real-time experimental implementations. Furthermore, the scope of the presented thesis covers, single-phase, bi-phase, and three-phase with three or four wire SeAF based systems.

The most significant conclusions of this research work are briefly summarized as follow:

- A thorough literature review of the past and the most recent research works in the development of Smart Grids and the area of power quality compensation using Series active filter was conducted. Reported literatures on these topics are briefly discussed. The concepts on the power quality and application of active power filtering in smart grids were also evaluated. Various type of nonlinear loads based on the power quality compensation objective were presented and analyzed. A brief review on conventional harmonic compensation technique such as passive compensators was conducted. A shorten briefing on the active power filtering principles and the state of the art in active compensation was presented. Furthermore, basics of power quality including key concepts and theoretical backgrounds were explained;

- Extended reviews along with the feasibility of the series active power compensator to improve power quality of a week system were investigated. A comprehensive state of the art on Series compensator history, configurations, control strategies, and related involvements in this field was conducted to provide a perspective of Series active

compensator's technology to researchers dealing with power quality issues. The design factors and ratings of passive components to realize a controlled voltage source by means of power electronics semiconductors were provided and analyzed using off-line simulations. Furthermore, a new control approach was proposed and analyzed to improve series harmonic compensation performances. Some complementary studies on the stability of the system were carried out along with validation using experimental results;

- A novel configuration called the single-phase Transformerless Hybrid Series Active Filter (THSeAF) was introduced to enhance power quality of an electrified transportation system consisted of single-phase current fed type of non-linear load. A new type of control strategy was proposed to prevent current harmonic distortions of a CSC type of non-linear loads to flow into the utility and correcting the power factor of this later. The proposed active power compensator ride of the bulky transformer has protected a sensitive load from voltage disturbances, sags, and swells initiated by the power system. The detailed designing and rating of components to realize the THSeAF for a practical implementation were also presented. Simulations and experimental results were presented to validate the proposed concept. The presented experimental results which were carried out on a laboratory prototype demonstrated the effectiveness of the proposed topology for the single-phase system when subjected to several critical scenarios;

- To improve power quality of Single-phase distribution systems feeding voltage-fed type of nonlinear loads, a Transformerless active power compensator using a sliding mode control algorithm and a Notch harmonic detection technique were proposed. It has been demonstrated that the newly developed device provides compensation for current harmonics coming from a VSC type of nonlinear load such as an electric vehicle charging station. The proposed active configuration controlled by an adapted control strategy was able to enhance the power quality while cleaning the point of common coupling (PCC) from possible voltage distortions and corrects the reactive

power of a residential consumer. Furthermore, to overcome drawbacks of real-time control an accurate compensation method was proposed. Offline simulations allow preliminary studies of the system while the developed laboratory benchmark has allowed validation over experimental results. Furthermore, an advance promoting Multilevel THSeAF with a PR controller onboard was presented to improve power quality by means of an NPC multilevel converter and the Proportional plus Resonant (PR) controller. Different aspects of the harmonic compensation strategy, the influence of the controller's choice, and the impacts of the delay time during a real-time implementation were meticulously investigated;

- The three-phase system with poor power quality has been thoroughly studied. A three-phase Series active power compensator was proposed to overcome the power quality of a low-level distribution system. Similar to the single-phase SeAF, the proposed series active power filter adapted for the three-phase system with or without the fourth wire system is able to clean the grid's current from harmonics, unbalance and correct the power factor. It has been demonstrated that the active filter had the capability of cleaning the load side voltage problems and ensuring a stable supply without perturbation to the load PCC. An advanced comprehensive control approach for three-phase Hybrid series active power filters with high efficiency response was also proposed and evaluated by simulation. The developed inner-loop of the controller was taking advantage of a combination of Synchronous Reference Frame (SRF) and the *p-q* theory to produce the compensating voltage reference. The controller's outer-loop producing gate switching signals for the three-phase THSeAF uses a proportional-integral controller;

- A novel three-phase transformerless configuration based on auxiliary current sources was presented. The proposed topology ride of the bulky transformer was capable of compensating current harmonics at the source and voltage distortion at the load terminals. Using the previously developed controller the proposed three-phase active filter (THSeAF) was performing superior to a conventional HSeAF while operating

similar to a Unified power quality conditioner (UPQC). Regarding the fact that voltage source converters are more common in industrial applications, a second three-phase Transformerless Hybrid Series Active Filter (THSeAF) based on voltage fed converters to address major power quality issues related to residential and commercial buildings was developed. To demonstrate the efficiency of each developed section numerous simulations were conducted which results illustrate the performance of the proposed techniques. To complete and validate the study a three-phase prototype was realized in the laboratory and experimental results were demonstrated to show the fidelity of the practical implementation towards real-time and offline simulations.

In summary, this thesis dissertation puts forward a novel topology and newly developed adapted control strategies for Hybrid series active power filters which not only contributes in the scientific and technical development of active power filtering for power quality improvement of future Smart Grids, but also reduces the overall system cost. It also proves that with a meticulously adapted controller and a proper dispatch of available resources, significant advantages can be achieved. The research work reported in this thesis along with experimentally validated results would certainly be considered as a remarkable development in the field of Smart technologies and power quality enhancement utilizing Series active power compensators.

RECOMMENDATIONS

This thesis work provides the comprehensive aspects of the design and implementation of a hybrid series compensator for smart grids to enhance the quality of power at the distribution level. This section presents some guidelines to extend the research work as it stands now. A brief discussion on the directions for possible future works is also outlined.

Recommendations for Thesis Work Extension

- A Series active power filter is realized for single and three-phase systems. The work presented in this thesis utilizes the single-, two-, and three-phase systems configuration. All developed concepts (DVR, SeAF, HSeAF, THSeAF) may be applied to aforementioned systems. However, applying these concepts successfully to improve power quality requires modifications. This is mainly due to the way the compensating voltage is produced through the active filter. In the single-phase the control strategy is similar for all configurations as they could compensate load current harmonics and reactive power, and regulates load voltage. While for the two- and three-phase systems depending on the presence of the isolating transformer the configuration differ from the transformerless configuration. On the other hand, the presence of the neutral wire for the three-phase system influences the controller algorithm;

- In the current practice, as the work emphasis the transformerless configuration, the transformer leakage impedance is not taken into account in transient calculations. Thus, the key components of the active filter contributing in producing a series compensating voltage which follow with high precision the reference, are the output RLC filter. Additionally, the switching frequency and the DC voltage are the parameters to consider when designing the passive filter. Moreover, a possible solution to reduce the damping resistor is the active damping technique which requires some study of its efficiency for series compensation. Additionally, a comparative evaluation, for different approaches, with various passive combinations can be carried out;

- As mentioned already, the power factor correction and the DC voltage regulation is one of the most important limitations that the Series active power filter needs to consider. Based on this thesis work, two approaches, the DC regulation, and power factor compensation (CHAPTER 2) are introduced to tackle the transfer of power to make the series compensator operating. A systematic comparative study can be done to evaluate above mentioned approaches with regards to the necessity of a DC voltage to make the VSI function as a controlled voltage source. The connection of an auxiliary source assist the power transfer as well as it ensures a constant DC bus voltage. The study can focus on the connection of renewable sources and the way it regulate the DC voltage. Such a kind of study could be of significant importance for the integration of renewable energy sources. It could acts as a comprehensive guide to make non predictive energy sources to have energy storage component and perform as a UPS during grid's sags, swells, and interruptions.

Possible Direction for Future Works

Photovoltaic and wind energies are emerging power sources. Although the solar PV is seen as a clean and sustainable energy source drawing upon the most widely distributed renewable energy source, the unpredictability of a constant energy source is its greatest constraint. Meanwhile, as studied briefly in this thesis work they could be used as the auxiliary DC source of the THSeAF. In such case, the series compensator could interface these renewables to the grid while improving the power quality of the system. The compensator could manage and regulate these distributed generation (DG) power to supply partially or in total the loads connected to the PCC in addition to manage the transfer of power between the grid and the load.

During normal operation, the series active power filter can store active power in a battery pack connected to the DC bus, and supply it to the consumers during grid's perturbation or interruptions. Moreover, the battery stores the renewable energy power and uses it as backup to provide an uninterruptible power supply to the load. Now, the research should be directed

towards applications in which the renewable sources not only provide electric power but at the same time, improve the quality of power (voltage and current) and increase the stability and reliability of smart grids. One remarkable and powerful solution, the THSeAF, is presented in this work. However, the integration of series active power compensator and renewable source may play a significant role in future distribution systems to simultaneously overcome power managements, and enhance the power quality in various aspects.

It is as well essential to study and elaborate the behavior of the compensator during transients and faulty condition. Various scenarios including different type of faults occurred both in the grid or load side should be analyzed for both single and three phase systems. Moreover, possible action of the compensator toward each scenario and the impact of the later on the system operation should also be evaluated.

APPENDIX I

FREQUENCY DOMAIN TRANSFORMATION BETWEEN THE STATIONARY *abc* AND ROTATING *dq0* FRAMES

Depending on the issues the control algorithm employed in series active filters differ. An adaptive controller for the series active filter which guarantees a sinusoidal balanced voltage on the load side despite the presence of perturbations in the source voltage uses frequently the SRF algorithm. As a further development by substituting Eqn A I-1, Eqn 2.52, and Eqn 2.53 into Eqn 2.49 gives the general form of the transfer function ***M(s)*** in *s*-plane, where the frequency domain equation of each term is derived using the Laplace transform.

$$LPF(s) = K_p + \frac{K_i \omega_c}{s + \omega_c} \tag{A I-1}$$

Similarly,

$$M_{11}(s) = L\left\{\frac{2}{3} LPF(t).\cos^2(\omega t) - 1\right\} \tag{A I-2}$$

$$= \frac{2}{3}\left(\left(\left(K_p + \frac{K_i \omega_c}{s + \omega_c}\right) \otimes \frac{s}{s^2 + \omega^2}\right) \otimes \frac{s}{s^2 + \omega^2}\right) - \frac{1}{s}$$

$$= \frac{1}{6}\big(LPF(s + j2\omega) + 2LPF(s) + LPF(s - j2\omega)\big) - \frac{1}{s}$$

$$= \frac{2k_p s^4 + \big(-3 + 2k_i w_c + 6k_p w_c\big)s^3 + \big(-9w_c + 8k_p w^2 + 4k_i {w_c}^2 + 6k_p {w_c}^2\big)s^2}{3s(s + w_c)(s^2 + 2w_c s + 4w^2 + {w_c}^2)}$$

$$+ \frac{\big(-12w^2 - 9{w_c}^2 + 2k_i {w_c}^3 + 2k_p {w_c}^3 + 4k_i w^2 w_c + 8k_p w^2 w_c\big)s - 12w^2 w_c - 3w_c}{3s(s + w_c)(s^2 + 2w_c s + 4w^2 + {w_c}^2)}$$

and

$$M_{12}(s) \qquad \text{(A I-3)}$$

$$= -\frac{k_p s^3 + \left(k_i w_c + 3k_p w_c\right)s^2 + \left(4k_p w^2 + 2k_i {w_c}^2 + 3k_p {w_c}^2 - \sqrt{3}k_i w w_c\right)s}{3(s + w_c)(s^2 + 2w_c s + 4w^2 + {w_c}^2)}$$

$$+ \frac{2k_i w^2 w_c + 4k_p w^2 w_c - \sqrt{3}k_i w {w_c}^2 + k_i {w_c}^3 + k_p {w_c}^3}{3(s + w_c)(s^2 + 2w_c s + 4w^2 + {w_c}^2)}$$

$$M_{13}(s)$$

$$= -\frac{k_p s^3 + \left(4k_p w^2 + 2k_i {w_c}^2 + 3k_p {w_c}^2 + \sqrt{3}k_i w w_c\right)s + \left(k_i w_c + 3k_p w_c\right)s^2}{3(s + w_c)(s^2 + 2s w_c + 4w^2 + {w_c}^2)}$$

$$+ \frac{2k_i w^2 w_c + 4k_p w^2 w_c + \sqrt{3}k_i w {w_c}^2 + k_i {w_c}^3 + k_p {w_c}^3}{3(s + w_c)(s^2 + 2s w_c + 4w^2 + {w_c}^2)}$$

$$M_{21}(s)$$

$$= -\frac{k_p s^3 + \left(k_i w_c + 3k_p w_c\right)s^2 + \left(4k_p w^2 + 2k_i {w_c}^2 + 3k_p {w_c}^2 - \sqrt{3}k_i w w_c\right)s}{3(s + w_c)(s^2 + 2w_c s + 4w^2 + {w_c}^2)}$$

$$+ \frac{2k_i w^2 w_c + 4k_p w^2 w_c - \sqrt{3}k_i w {w_c}^2 + k_i {w_c}^3 + k_p {w_c}^3}{3(s + w_c)(s^2 + 2w_c s + 4w^2 + {w_c}^2)}$$

$$M_{22}(s)$$

$$= \frac{k_p s^4 + \left(-6 + k_i w_c + 3k_p w_c\right)s^3 +}{6s(s + w_c)(s^2 + 2s w_c + 4w^2 + {w_c}^2)}$$

$$+ \frac{\left(-18w_c + 4k_p w^2 + 2k_i {w_c}^2 + 3k_p {w_c}^2 - 2\sqrt{3}k_i w w_c\right)s^2}{6s(s + w_c)(s^2 + 2s w_c + 4w^2 + {w_c}^2)}$$

$$+ \frac{\left(-24w^2 - 18{w_c}^2 + k_i {w_c}^3 + k_p {w_c}^3 + 8k_i w^2 w_c + 4k_p w^2 w_c - 2\sqrt{3}k_i w {w_c}^2\right)s}{6s(s + w_c)(s^2 + 2s w_c + 4w^2 + {w_c}^2)}$$

$$+ \frac{-24w^2 w_c - 6{w_c}^3}{6s(s + w_c)(s^2 + 2s w_c + 4w^2 + {w_c}^2)}$$

$$M_{23}(s) = \frac{k_p s^3 + \left(k_i w_c + 3k_p w_c\right)s^2 + \left(4k_p w^2 + 2k_i {w_c}^2 + 3k_p {w_c}^2\right)s}{6(s + w_c)(s^2 + 2s w_c + 4w^2 + {w_c}^2)}$$

$$+ \frac{k_i {w_c}^3 + k_p {w_c}^3 - 4k_i w^2 w_c + 4k_p w^2 w_c}{6(s + w_c)(s^2 + 2s w_c + 4w^2 + {w_c}^2)}$$

$$M_{31}(s)$$

$$= -\frac{k_p s^3 + \left(4k_p w^2 + 2k_i {w_c}^2 + 3k_p {w_c}^2 + \sqrt{3}k_i w w_c\right)s + \left(k_i w_c + 3k_p w_c\right)s^2}{3(s + w_c)(s^2 + 2s w_c + 4w^2 + {w_c}^2)}$$

$$+ \frac{2k_i w^2 w_c + 4k_p w^2 w_c + \sqrt{3}k_i w {w_c}^2 + k_i {w_c}^3 + k_p {w_c}^3}{3(s + w_c)(s^2 + 2s w_c + 4w^2 + {w_c}^2)}$$

$$M_{32}(s) = \frac{k_p s^3 + \left(k_i w_c + 3k_p w_c\right)s^2 + \left(4k_p w^2 + 2k_i {w_c}^2 + 3k_p {w_c}^2\right)s}{6(s + w_c)(s^2 + 2s w_c + 4w^2 + {w_c}^2)}$$

$$+ \frac{+k_i {w_c}^3 + k_p {w_c}^3 - 4k_i w^2 w_c + 4k_p w^2 w_c}{6(s + w_c)(s^2 + 2s w_c + 4w^2 + {w_c}^2)}$$

$$M_{33}(s)$$

$$= \frac{k_p s^4 + \left(-6 + k_i w_c + 3k_p w_c\right)s^3}{6s(s + w_c)(s^2 + 2s w_c + 4w^2 + {w_c}^2)}$$

$$+ \frac{\left(-18w_c + 4k_p w^2 + 2k_i \quad {}_c{}^2 + 3k_p {w_c}^2 + 2\sqrt{3}k_i w w_c\right)s^2}{6s(s + w_c)(s^2 + 2s w_c + 4w^2 + {w_c}^2)}$$

$$+ \frac{\left(-18{w_c}^2 - 24w^2 + k_i {w_c}^3 + k_p {w_c}^3 + 8k_i w^2 w_c + 4k_p w^2 w_c + 2\sqrt{3}k_i w {w_c}^2\right)s}{6s(s + w_c)(s^2 + 2s w_c + 4w^2 + {w_c}^2)}$$

$$+ \frac{-24w^2 w_c - 6{w_c}^3}{6s(s + w_c)(s^2 + 2s w_c + 4w^2 + {w_c}^2)}$$

APPENDIX II

THE "HSEAF" LABORATORY SETUP #1

The Electrical footprint for the 3P4W Hybrid Series AF laboratory setup is as follow.

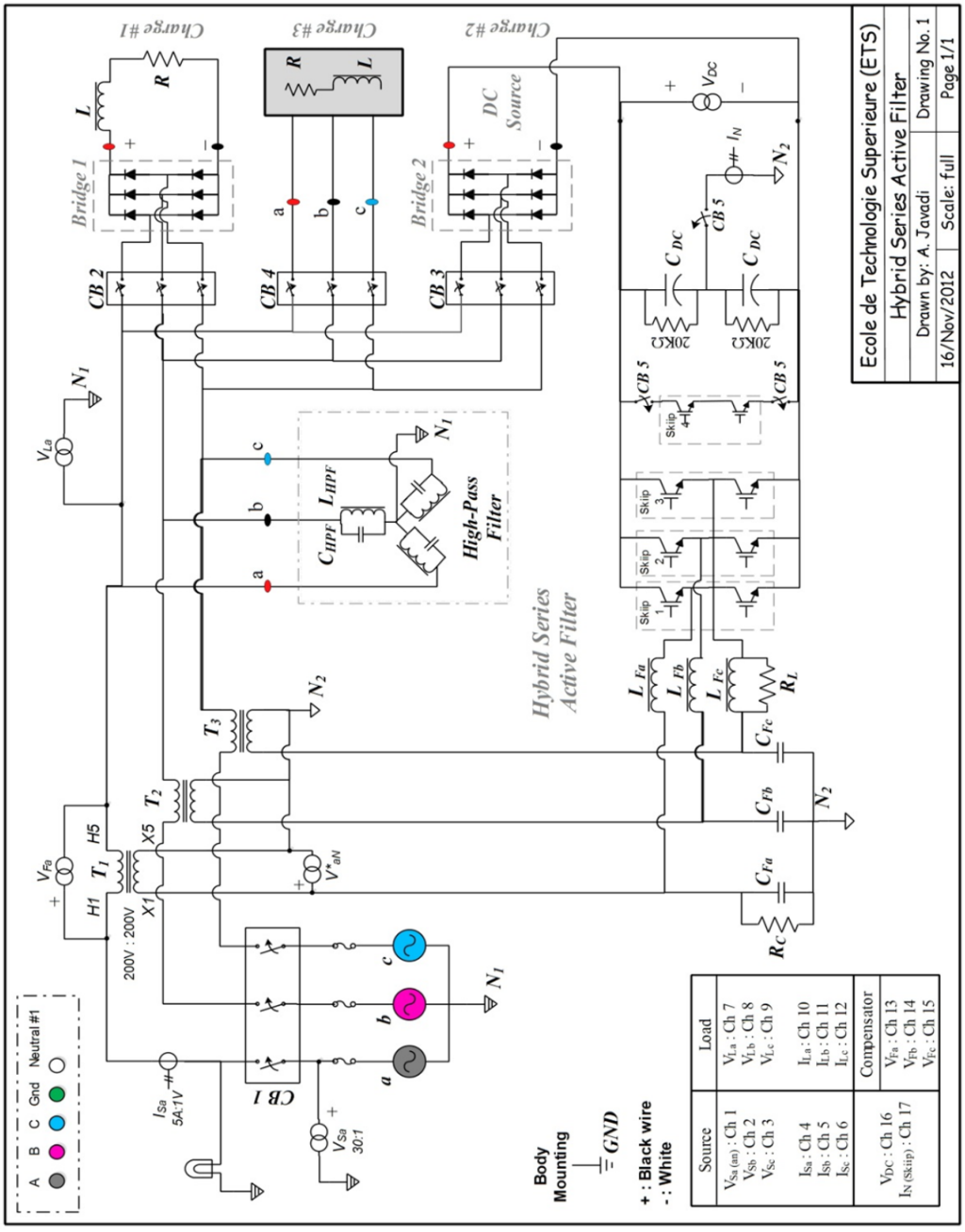

Figure-A II-1 HSeAF laboratory setup circuit schematic

The prototype for the Hybrid Series Active Power Filter (HSeAF) system was designed, developed, and implemented in the laboratory of GREPCI. In this Appendix the essential hardware prototype components are briefly discussed. Some of the important problems and limitations that arose during the experimental implementation and the steps toward overcoming those issues are also highlighted.

It is noticed that the realized test in this research work could be classified under the RCP category. A Rapid Control Prototyping (RCP) means different control techniques and various algorithms could be implemented on the dSPCAE real-time module to test them on the realized experimental setup. It could be consider the duality of a Power-Hardware-In-The-Loop (PHIL) in which the external controller under test is connected to the real-time module in which the power hardware components are simulated inside the real-time simulator.

The major components of this setup consist of:

i) Voltage Source Converters: Two voltage source converters are realized using IGBT switches. The structure of each module illustrated in the following picture consists of four physically separate arms containing two switches in each arm. Meanwhile, one driver controls these Hal-bridge SEMIKRON/ SkiipPack (1242GB120-407CTV). As results they operate like a single arm with 1200V and 1200A of power capacity.

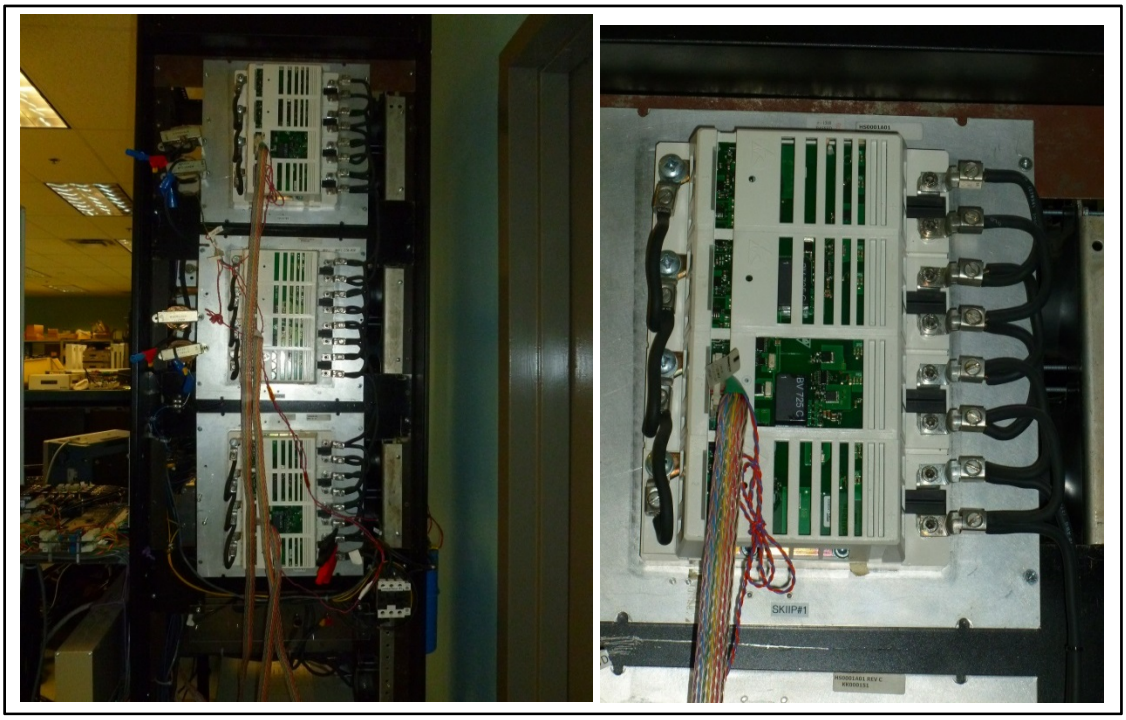

Figure-A II-2 Half-Bridge power Skiip 1.5MW converters used in the HSeAF prototype

back zurück

SEMIKRON

SKiiP 1242 GB 120 - 407 CTV

Absolute Maximum Ratings

Symbol	Conditions [9]	Values	Units
V_{isol} [4]	AC, 1min	3000	V
T_{op} ,T_{stg}	Operating / stor. temperature	-25...+85	°C
IGBT and Inverse Diode			
V_{CES}		1200	V
V_{CC} [6]	Operating DC link voltage	900	V
I_C	IGBT	1200	A
T_j [3]	IGBT + Diode	-40...+150	°C
I_F	Diode	1200	A
I_{FM}	Diode, t_p < 1 ms	2400	A
I_{FSM}	Diode, T_j = 150 °C, 10ms; sin	8640	A
I^2t (Diode)	Diode, T_j = 150 °C, 10ms	373	kA^2
Driver			
V_{S1}	Stabilized Power Supply	18	V
V_{S2}	Non-stabilized Power Supply	30	V
f_{smax}	Switching frequency	14	kHz
dV/dt	Primary to secondary side	75	kV/µs

Characteristics

Symbol	Conditions [1]		min.	typ.	max.	Units
IGBT [11]						
$V_{(BR)CES}$	Driver without supply		≥V_{CES}	–	–	V
I_{CES}	V_{GE} = 0,	T_j = 25 °C	–	–	1,8	mA
	V_{CE} = V_{CES}	T_j = 125 °C	–	60	–	mA
V_{TO}	T_j = 125 °C		–	–	1,38	V
r_T	T_j = 125 °C		–	–	1,8	mΩ
V_{CEsat}	I_C = 1000A,	T_j = 125 °C	–	–	3,2	V
V_{CEsat}	I_C = 1000A,	T_j = 25 °C	–	–	3,05	V
E_{on} + E_{off}	V_{CC}=600/900V,I_C=1200A T_j = 125 °C		–	–	360/586	mJ
C_{CHC}	per Phase, AC side		–	5,6	–	nF
L_{CE}	Top, Bottom		–	4	–	nH
Inverse Diode [2]						
V_F = V_{EC}	I_F= 1000A;	T_j = 125 °C	–	–	2,43	V
V_F= V_{EC}	I_F= 1000A;	T_j = 25 °C	–	–	2,55	V
E_{on} + E_{off}	I_F= 1200A;	T_j = 125 °C	–	–	48	mJ
V_{TO}	T_j = 125 °C		–	–	0,91	V
r_T	T_j = 125 °C		–	–	1,0	mΩ
Thermal Characteristics						
$R_{th(j-c)}$ [10]	per IGBT		–	–	0,023	K/W
$R_{th(j-c)D}$ [10]	per Diode		–	–	0,063	K/W
$R_{th(c-s)}$ [10]	P16 heatsink; see case S4		–	–	33	K/KW
Driver						
I_{S1}	Supply current 15V-supply			290+580*f_s/f_{fmax}+1,3*I_{AC}/A		mA
I_{S2}	Supply current 24V-supply			220+420*f_s/f_{fmax}+1,0*I_{AC}/A		mA
$t_{Interlock-driver}$	Interlock-time			3,3		µs
SKiiPPACK protection						
I_{TRIPSC}	Short circuit protection			1500		A
I_{TRIPLG}	Ground fault protection			–		A
T_{TRIP}	Over-temp. protection			115		°C
U_{DCTRIP} [9]	U_{DC}-protection			920		V
Mechanical Data						
M1	DC terminals, SI Units		4	–	6	Nm
M2	AC terminals, SI Units		8	–	10	Nm

SKiiPPACK®

SK integrated intelligent Power PACK halfbridge SKiiP

1242 GB 120 - 407 CTV [7,9]

Preliminary Data

Case S4

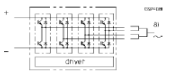

Features

- Short circuit protection, due to evaluation of current sensor signals
- Isolated power supply
- Low thermal impedance
- Optimal thermal management with integrated heatsink
- Pressure contact technology with increased power cycling capability, compact design
- Low stray inductance
- High power, small losses
- Over-temperature protection

1) $T_{heatsink}$ = 25 °C, unless otherwise specified
2) CAL = Controlled Axial Lifetime Technology (soft and fast) without driver
3) Driver input to DC link / AC output to DC link / AC output to heatsink with Semikron-DC link (low inductance) other heatsinks on request
4) C - Integrated current sensors T - Temperature protection V - 15 V or 24 V power supply
5) AC connection busbars must be connected by the user; copper busbars available on request options available for driver: U - DC link voltage sense F – Fiber optic connector
6) "z" referenced to temperature sensor
7) NPT-technology with homogenous current-distribution

PIN-array - halfbridge driver SKiiPPACK 4-fold type "GB"

X1:

Pin	signal	remark
1	shield	connected to GND, when shielded cable is used
2	BOT IN[2]	positive 15V CMOS logic; 10 kΩ impedance, don't connect when using fiber optic
3	ERROR OUT[1]	LOW = NO ERROR; open Collector Output; max. 30 V / 15 mA don't connect when using fiber optic, propagation delay 1 µs min. pulsewidth error-memory-reset 8 µs
4	TOP IN[2]	positive 15V CMOS logic; 10 kΩ impedance don't connect when using fiber optic
5	Overtemp. OUT[1]	LOW = NO ERROR = ϑ_{DCB} < 115 ± 5°C open collector Output; max. 30 V / 15 mA „low" output voltage < 0,8 V „high" output voltage max. 30 V
6	+ 24 V_{DC} IN	24 V_{DC} (20 - 30 V)
7	+ 24 V_{DC} IN	don't supply with 24 V, when using + 15 V_{DCIN} supply voltage monitoring threshold 19,5 V
8	+ 15 V_{DC} IN	15 V_{DC} ± 4 %
9	+ 15 V_{DC} IN	don't supply with 15 V, when using + 24 V_{DCIN} supply voltage monitoring threshold 13 V
10	GND	GND for power supply and
11	GND	GND for digital signals
12	Temp. analog OUT or U_{DC} analog OUT[2]	U_{DC} when using option "U" actual DC-link voltage, 9 V refer to U_{DCmax} max. output current 5 mA; overvoltage trip level 9 V
13	GNU aux[3]	GNU for analog signals
14	I analog OUT	current actual value, 8,0 V refer to I_C @ 25 °C overcurrent trip level 10 V ⇔ 125 % I_C @ 25 °C current value > 0 ⇔ SKiiP is source current value < 0 ⇔ SKiiP is sink

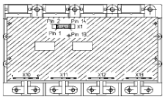

X10: halfbridge 1 (HB1) OUT

Pin	Signal
1	
2	
8	Collector TOP (HB1)
11	Gate TOP (HB1)
12	Emitter TOP (HB1)
13	Collector BOT (HB1)
16	Gate BOT (HB1)
17	Emitter BOT (HB1)

X11: halfbridge 2 (HB2) OUT

Pin	Signal
1	Temp.-Sensor (HB2)1
2	Temp.-Sensor (HB2)2
8	Collector TOP (HB2)
11	Gate TOP (HB2)
12	Emitter TOP (HB2)
13	Collector BOT (HB2)
16	Gate BOT (HB2)
17	Emitter BOT (HB2)

X12: halfbridge 3 (HB3) OUT

Pin	Signal
1	
2	
8	Collector TOP (HB3)
11	Gate TOP (HB3)
12	Emitter TOP (HB3)
13	Collector BOT (HB3)
16	Gate BOT (HB3)
17	Emitter BOT (HB3)

X13: halfbridge 4 (HB4) OUT

Pin	Signal
1	
2	
8	Collector TOP (HB4)
11	Gate TOP (HB4)
12	Emitter TOP (HB4)
13	Collector BOT (HB4)
16	Gate BOT (HB4)
17	Emitter BOT (HB4)

type "GAL"
as type "GB" except
- PIN X1-4: connect this pin to GND
- TOP switch does not exist

type "GAR"
as type "GB" except
- PIN X1-2: connect this pin to GND
- BOTTOM switch does not exist

1) Open collector output, external pull up resistor necessary
2) When using option "U" the analog temperature signal is not available
3) GND aux = reference for analog output signals
4) „high" (min) 11,2 V „low" (max) 5,4 V

Figure-A II-3 SEMIKRON datasheet for the original Skiips

To realize the three-phase configuration three modules are required. The whole converters will be operating as a three-phase converter in which the dSPCE is performing the RCP application.

ii) Transformers: Three single phase transformers are required to realize the Hybrid series power filter. These 5kVA Hammond dry type of transformers shown in the following pictogram are employed for the experimental setup. To have a unity ratio (1:1), the input connection (H1-H5) is used along with the (X1-X5) terminals. With such configuration each transformer could have a nominal power up to 4 kW.

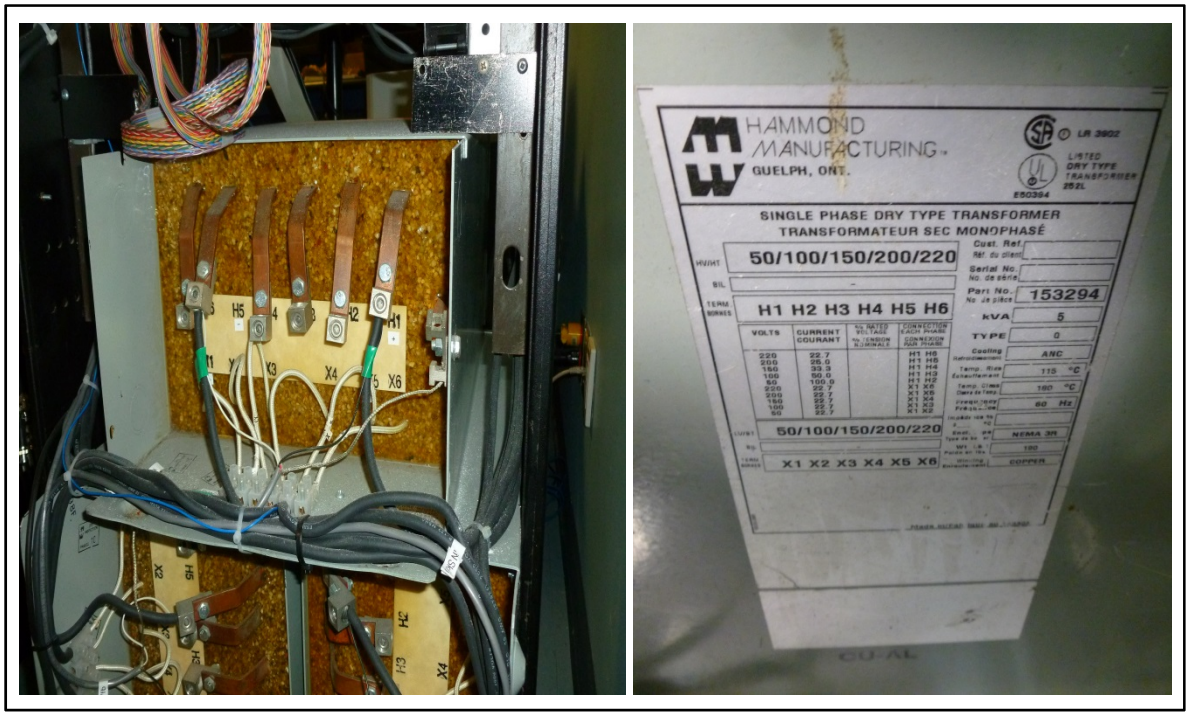

Figure-A II-4 Single-phase Hammond manuf. Dry transformer and the transformer's nameplate

iii) The measurement sensors: To realize the RCP setup, the necessary voltages and currents should be sensed and adapted to be sent to the dSPACE Analog inputs. The current sensor block diagram and voltage probes are illustrated. These homemade cards require fine tuning and calibration with a precise Oscilloscope (in our case the "LeCroy 104MXi") before tests to ensure a precise measurement.

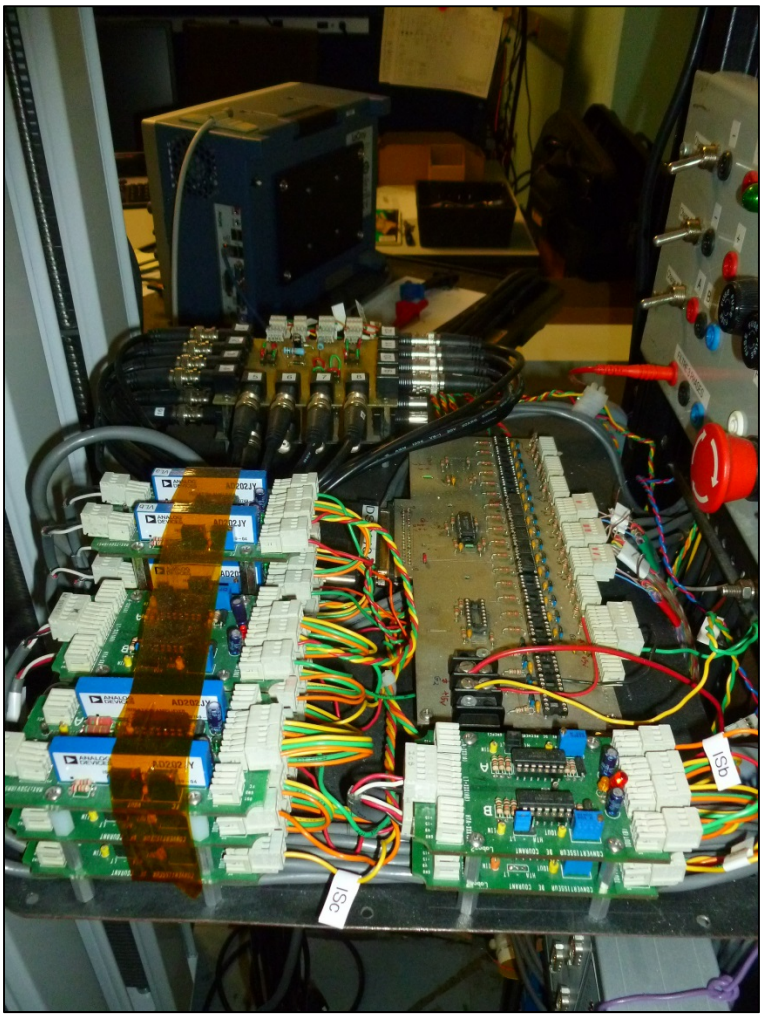

Figure-A II-5 The measurement probes, sensors protections, and IGBT firing drivers with their protections

The current probes transform the input current waveform with a magnitude of 5 Amperes to a voltage type of signal with a magnitude of 1Volts, thus the ratio of transformation to consider in the controller is “5:1”. The dc offset should also be equal to zero.

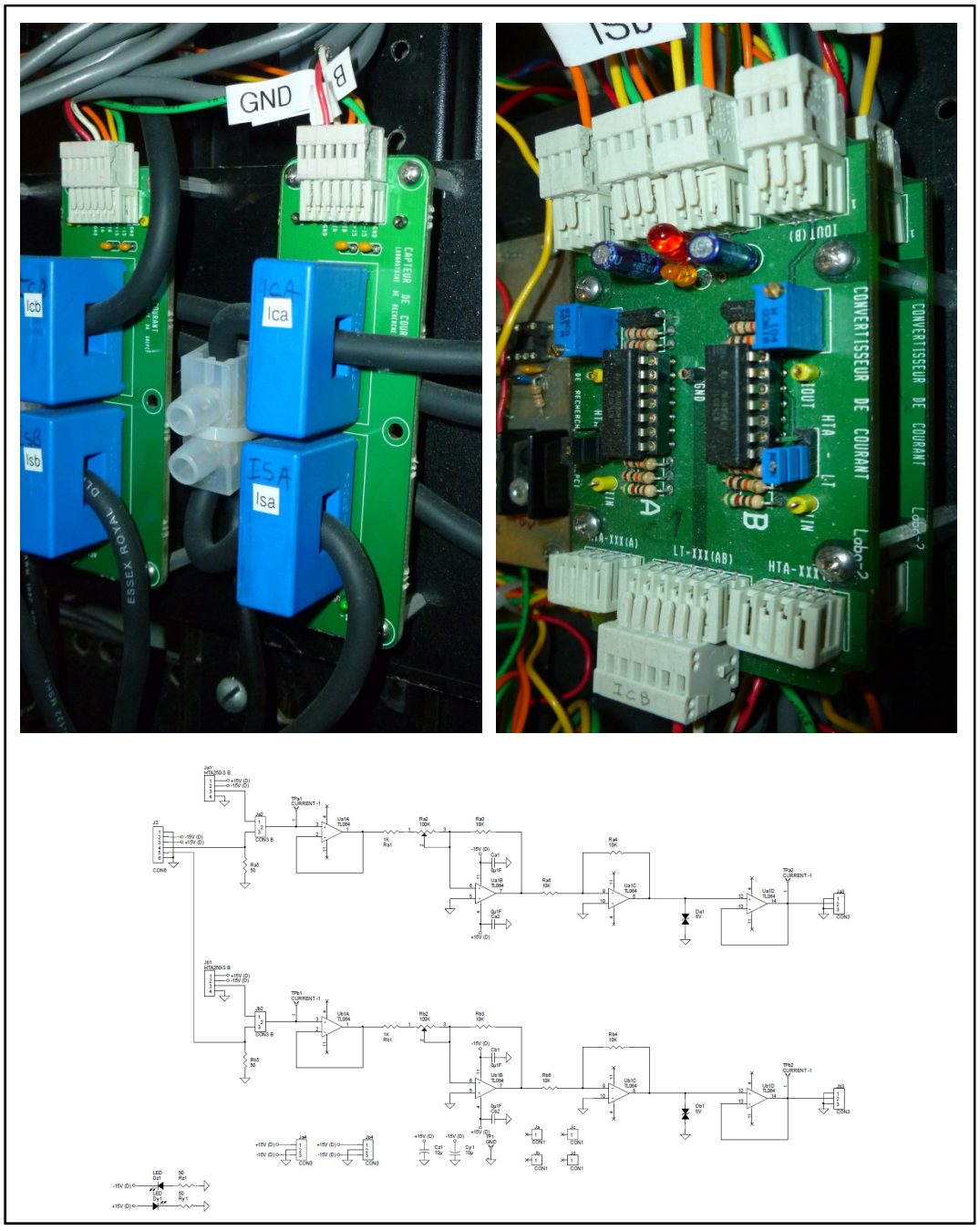

Figure-A II-6 Current probe sensing circuit

The voltage measurement probes transform voltage waveform of 100 volts to a signal with a magnitude of 6.7 volts with a ratio of “1:0.67”.

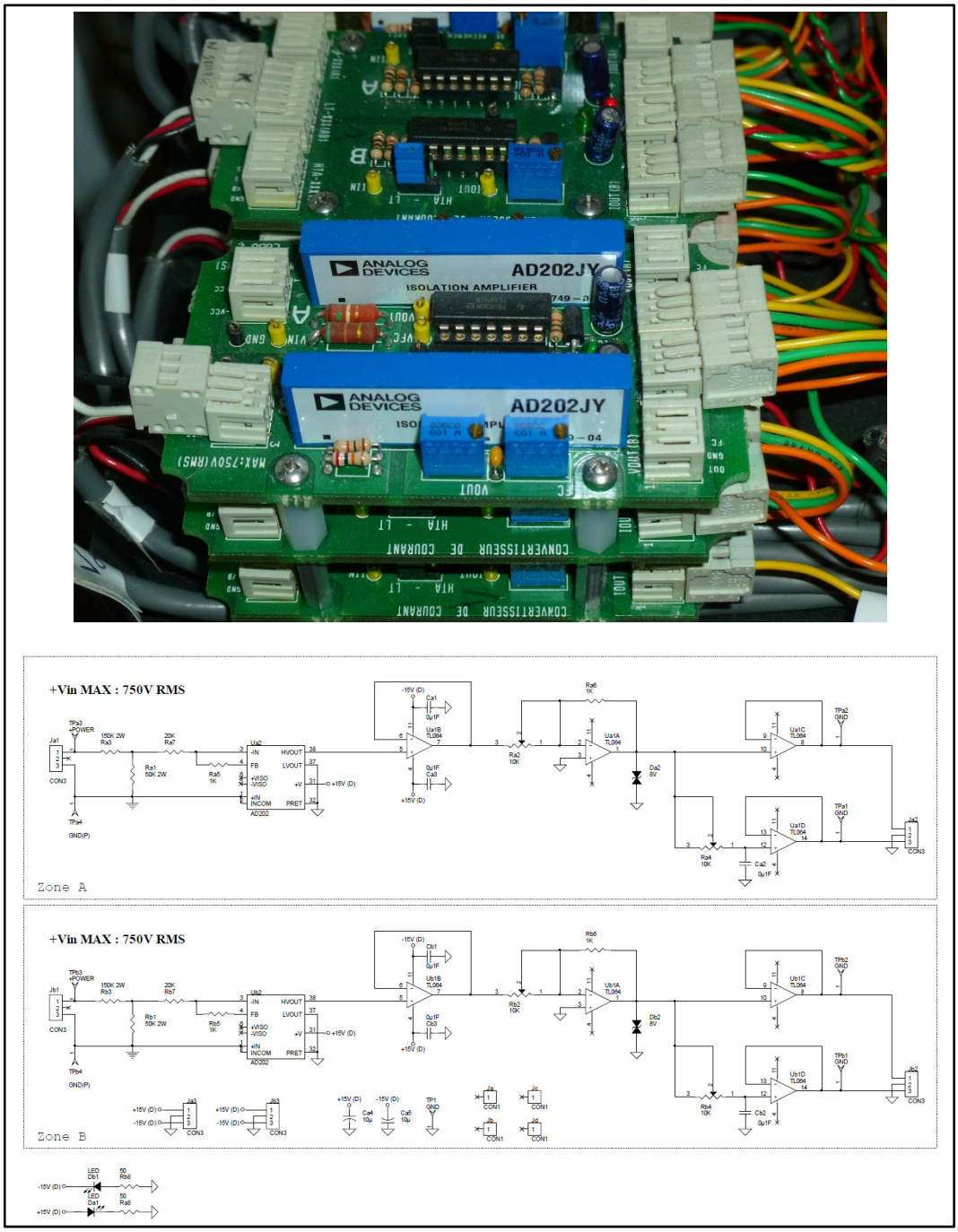

Figure-A II-7 Voltage probes

iv) The real-time Simulator: The real-time simulator used in this application to realize the RCP setup was a dSPACE module. For a real-time control of the three-phase inverter a DS1103 is used mainly because the simulation studies were carried out using the MATLAB/ SPS. Since the Simulink block sets support the dSPACE, it became easy to implement the control algorithms in real-time. The DS1103 board is built on PowerPC-604e microprocessor and its I/O interfaces make the board ideally suited for developing controllers.

The pins of the homemade Cable illustrated in the following figure are twisted in a way to use the generated PWM signals and their complementary been adapted for an H-bridge converter application.

Figure-A II-8 The dSPACE interface with Analog and Digital I/Os

The DS1103 board revision has a total of 16 Analog inputs called A/D converters (ADCH1…ADCH16). They have the following characteristics:

- 16-bit resolution;
- ±10 V input voltage range;
- ± 5 mV offset error;
- ± 0.25% gain error.

The slave DSP on the DS1103 provides a separate timing I/O unit that you can use to generate and measure pulse-width modulated (PWM) and square-wave signals. The slave DSP provides output channels for a 3-phase PWM signal generation or four single-phase PWM signals in the frequency range of 1.25Hz up to 5MHz.

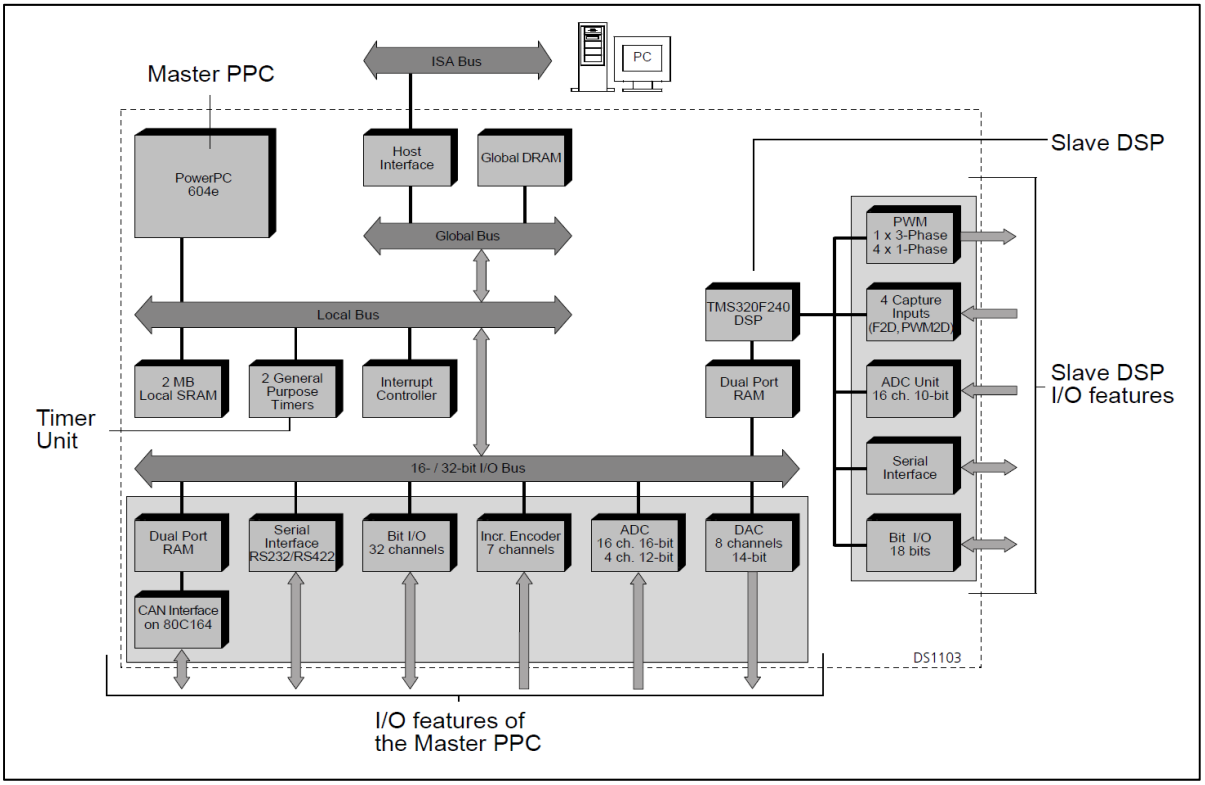

Figure-A II-9 An overview of the architecture of the functional units of the DS1103 (PowerPC 604e)

APPENDIX III

THE "THSEAF" LABORATORY SETUP #2

To realize the scopes of this research work, a second experimental setup was built. In this regards the previously presented Semikron's module where modified in the GREPCI in order to have four independently controlled arms (2 semiconductors per arm). The developed Gate drivers card where produced and tested in the laboratory, before been used in the second setup. The newly developed Semikron modules (4 arms per module) are as well been used by other researchers in the laboratory.

Figure-A III-1 The Transformerless Hybrid Series Power Active filter setup

The major components of this setup consist of:

i) Voltage Source Converters: The following figure illustrates the semiconductor bridges used in this experimental setup. Each module contains 4 arms (8 switches) creating two H-bridge converters controlled separately. The setup has consumed two modules in order to been able to produce the three-phase system as shown in the following picture.

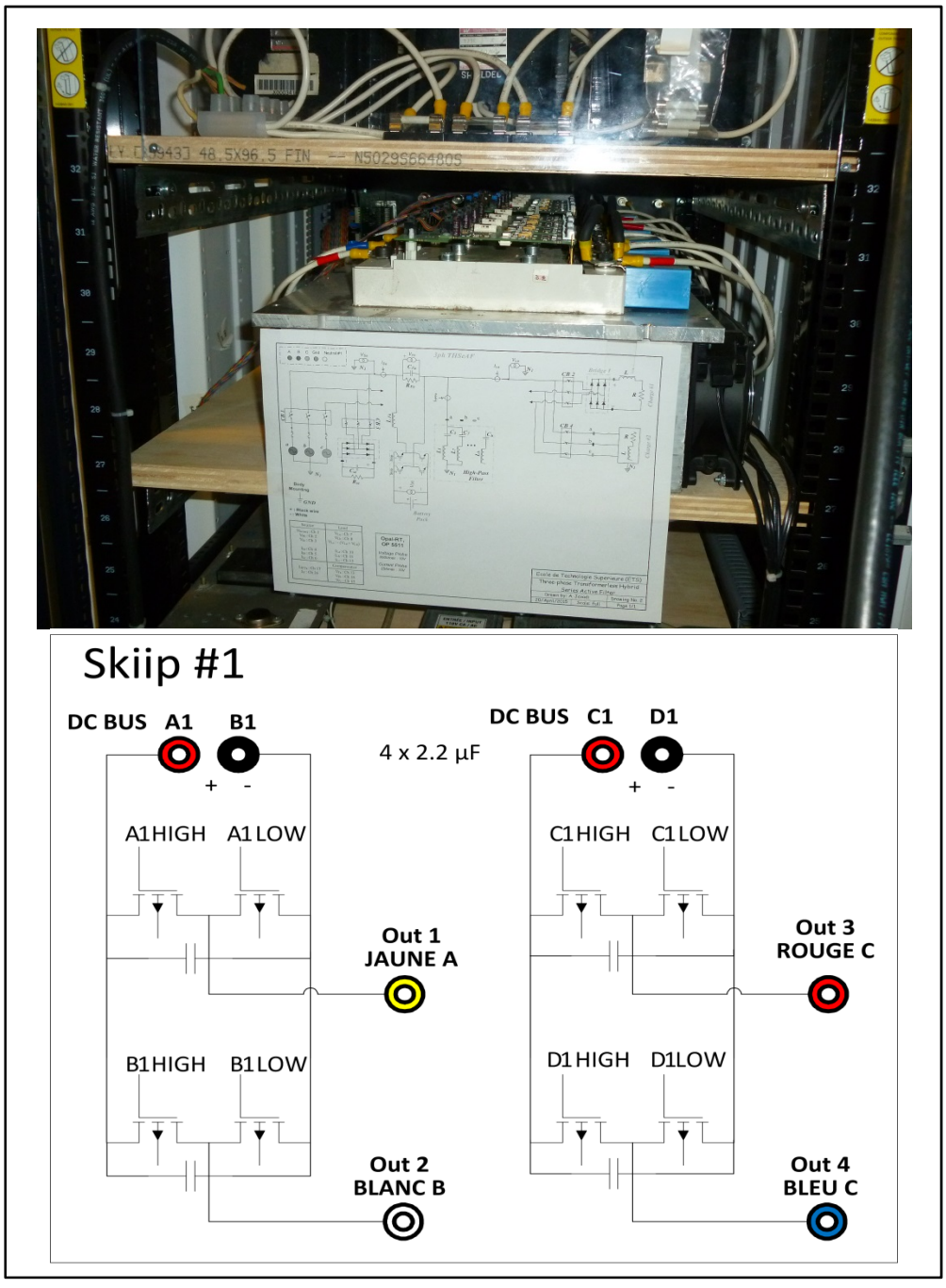

Figure-A III-2 The developed H-bridge converters with Semikron IGBTs

The developed Gate driver cards are shown in the following pictures. These cards are powered by a 5V external DC supply and consume around 1.1 Amperes. The 15V supply required to change the state of semiconductors is produced using printed transformer in which at the same time the low voltage part of the PCB is electrically isolated from the power section. In conclusion, each arm could operate at 1200 V and support a nominal current up to 300 A.

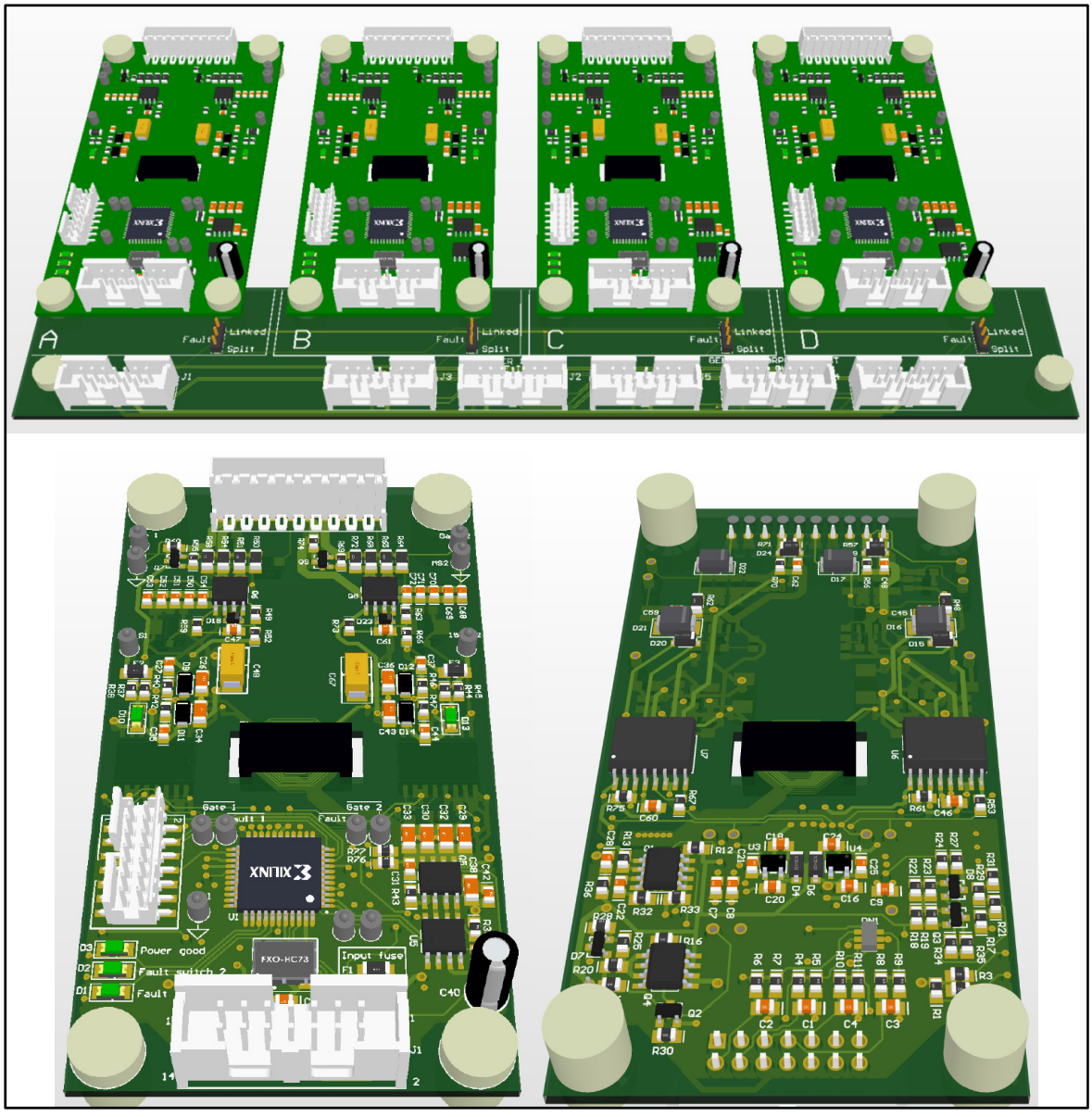

Figure-A III-3 The IGBTs driver cards 3D overview

ii) Fast Isolation card: To isolate the DS1103 connection outputs from the Gate drivers a fast isolation card was developed based on the recent chipset *Si-8440-BB*. The isolation card could operate easily for PWM signals having a frequency up to 1 Mbps and 1 kV of isolation between its primary and secondary.

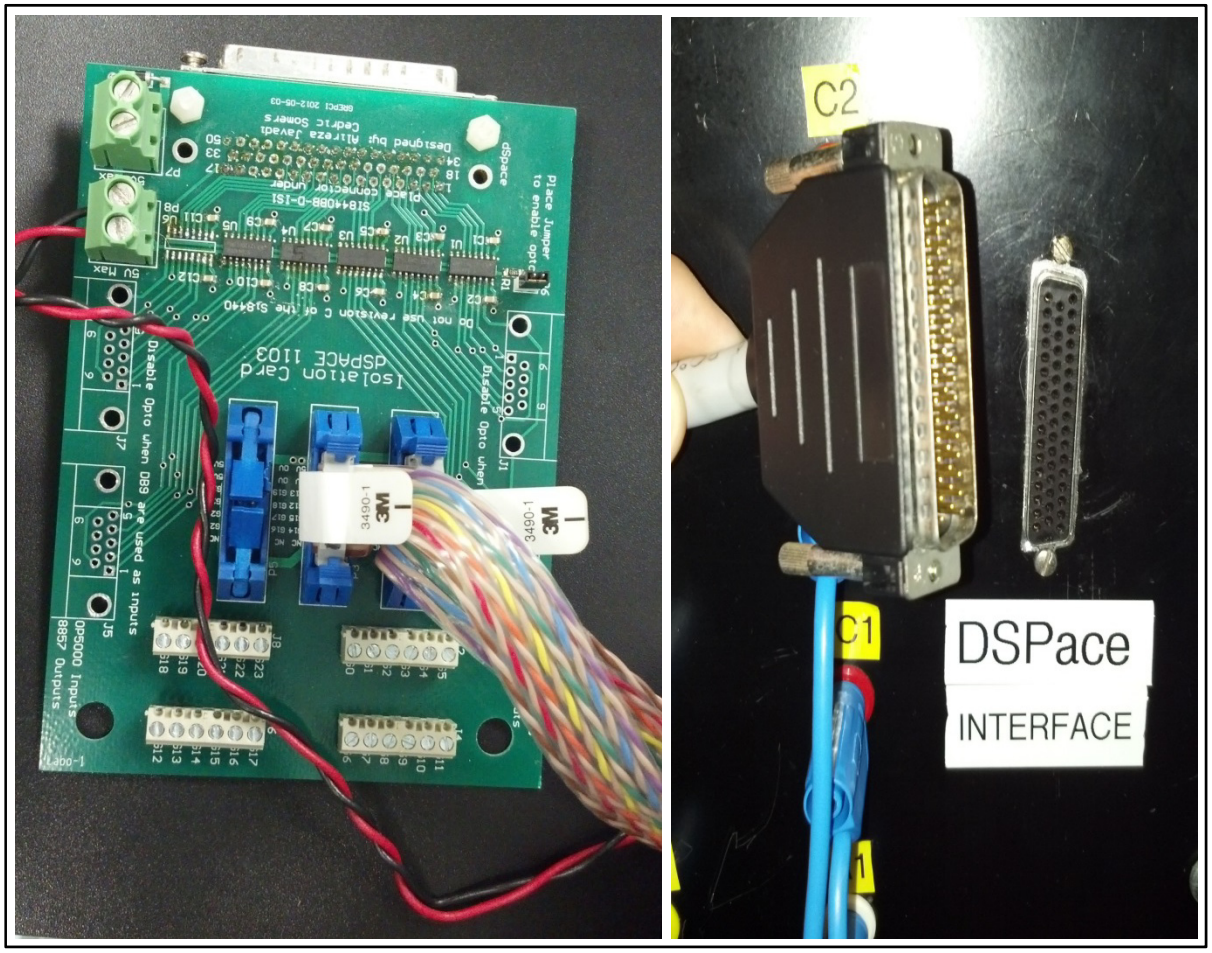

Figure-A III-4 Gate isolation card between dSPACE-GateDrive, and homemade cable DB-37 to DB-50

The electrical pathway for the twisted connection cable which adapts the db-37 pins to the db-50 pins used by the isolation card for an H-bridge converter is illustrated in the following figure.

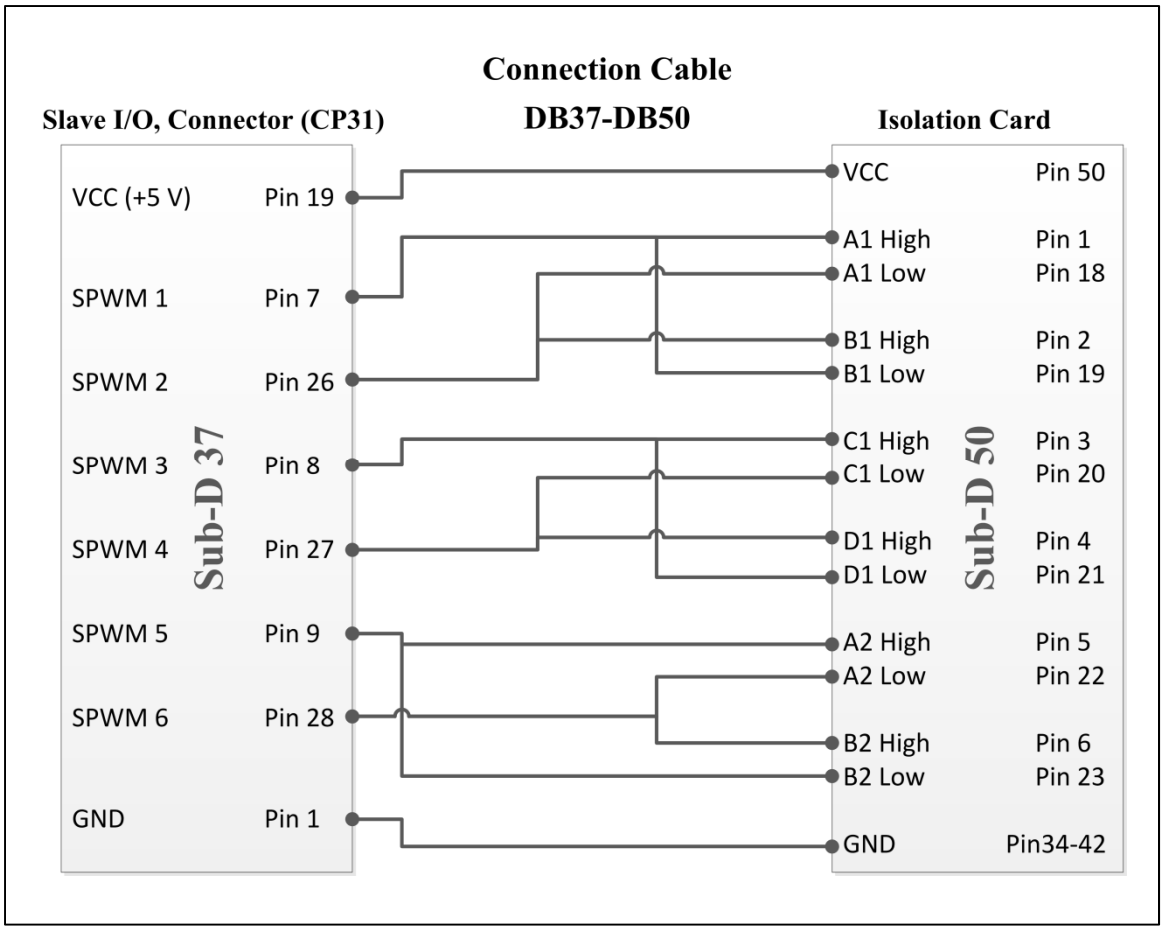

Figure-A III-5 The connection dSPACE-IsoCard cable

iii) The DC auxiliary sources: The dc auxiliary sources were realized with three relatively small single-phase transformers. The nominal rating of each transformer is 500VA, designed around 30% of the load's power rating.

For protection purposes, a discharge circuit was realized using a 500Ω resistance to discharge the dc capacitors in 6.25s. The discharge switch is available on the dashboard panel in order the operator could proceed at the end of laboratory essays. The power loss in the discharging resistors if capacitors were charged at 170V is equal to 55 W.

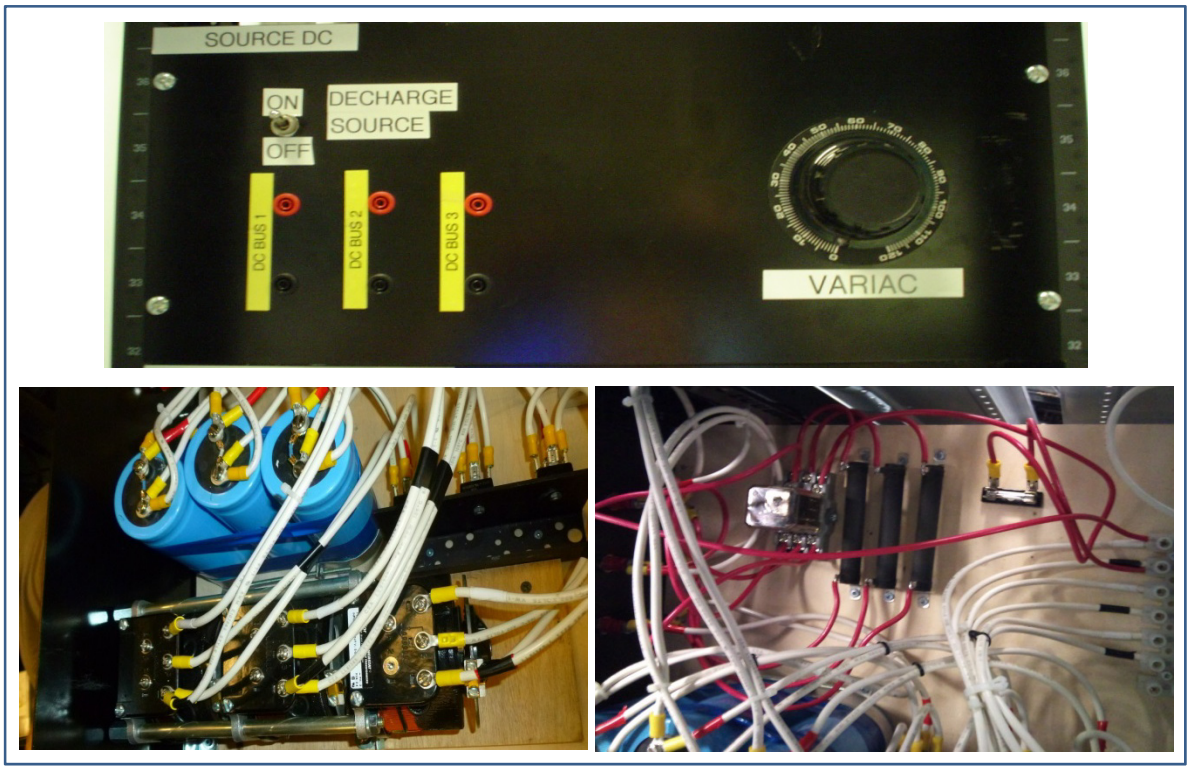

Figure-A III-6 The isolated DC sources and the discharging compartment

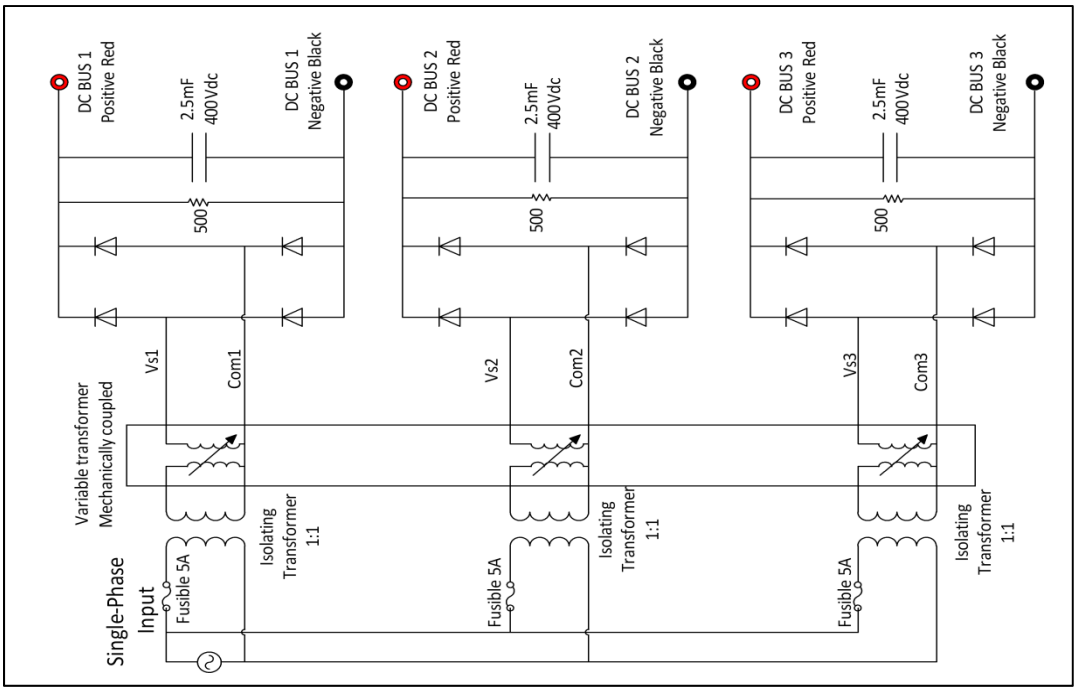

Figure-A III-7 The dc sources circuit diagram

BIBLIOGRAPHY

Abdel-Rahman, O., J. A. Abu-Qahouq, L. Huang et I. Batarseh. 2008. « Analysis and Design of Voltage Regulator With Adaptive FET Modulation Scheme and Improved Efficiency ». *Power Electronics, IEEE Transactions on,* vol. 23, n° 2, p. 896-906.

Abu-Rub, Haithem, Mariusz Malinowski et Kamal Al-Haddad. 2014. *Power electronics for renewable energy systems, transportation, and industrial applications* (2014). Chichester, West Sussex, United Kingdom: Wiley InterScience, 1 ressource en ligne (xxx. 795 pages) p.

Ajaei, F. B., S. Afsharnia, A. Kahrobaeian et S. Farhangi. 2011. « A Fast and Effective Control Scheme for the Dynamic Voltage Restorer ». *Power Delivery, IEEE Transactions on,* vol. 26, n° 4, p. 2398-2406.

Akagi, H. 2005. « Active Harmonic Filters ». *Proceedings of the IEEE,* vol. 93, n° 12, p. 2128-2141.

Akagi, H., et K. Isozaki. 2012a. « A Hybrid Active Filter for a Three-Phase 12-Pulse Diode Rectifier Used as the Front End of a Medium-Voltage Motor Drive ». *IEEE Transaction on Power Delivery,* vol. 27, n° 1, p. 69-77.

Akagi, H., et K. Isozaki. 2012b. « A Hybrid Active Filter for a Three-Phase 12-Pulse Diode Rectifier Used as the Front End of a Medium-Voltage Motor Drive ». *IEEE Trans. on Power Electron.,* vol. 27, n° 1, p. 69-77.

Akagi, H., et R. Kondo. 2010. « A Transformerless Hybrid Active Filter Using a Three-Level Pulsewidth Modulation (PWM) Converter for a Medium-Voltage Motor Drive ». *Power Electronics, IEEE Transactions on,* vol. 25, n° 6, p. 1365-1374.

Akagi, H., Y. Tsukamoto et A. Nabae. 1990. « Analysis and design of an active power filter using quad-series voltage source PWM converters ». *IEEE Transactions on Industry Applications,* vol. 26, n° 1, p. 93-98.

Akagi, Hirofumi, Edson Hirokazu Watanabe et Mauricio Aredes. 2007. *Instantaneous power theory and applications to power conditioning*, 1. Coll. « Power Engineering ». Psicataway, NJ: Wiley- Interscience, 379 p.

Al-Hadidi, H. K., A. M. Gole et D. A. Jacobson. 2008. « A Novel Configuration for a Cascade Inverter-Based Dynamic Voltage Restorer With Reduced Energy Storage Requirements ». *Power Delivery, IEEE Transactions on,* vol. 23, n° 2, p. 881-888.

Amjadi, Z., et S. S. Williamson. 2011. « Modeling, Simulation, and Control of an Advanced Luo Converter for Plug-In Hybrid Electric Vehicle Energy-Storage System ». *IEEE Trans. Vehicular Tech.,* vol. 60, n° 1, p. 64-75.

Arcuri, S., M. Liserre, D. Ricchiuto, T. Kerekes et F. Blaabjerg. 2011. « Stability analysis of grid inverter LCL-filter resonance in wind or photovoltaic parks ». In *IECON 2011 - 37th Annual Conference on IEEE Industrial Electronics Society*. (7-10 Nov. 2011), p. 2499-2504.

Babaei, E., et M. F. Kangarlu. 2011. « Voltage quality improvement by a dynamic voltage restorer based on a direct three-phase converter with fictitious DC link ». *Generation, Transmission & Distribution, IET,* vol. 5, n° 8, p. 814-823.

Babaei, E., M. F. Kangarlu et M. Sabahi. 2010. « Mitigation of Voltage Disturbances Using Dynamic Voltage Restorer Based on Direct Converters ». *Power Delivery, IEEE Transactions on,* vol. 25, n° 4, p. 2676-2683.

Barbosa, P. G., J. A. Santisteban et E. H. Watanabe. 1998. « Shunt-series active power filter for rectifiers AC and DC sides ». *Electric Power Applications, IEE Proceedings -,* vol. 145, n° 6, p. 577-584.

Barros, J. D., et J. F. Silva. 2010. « Multilevel Optimal Predictive Dynamic Voltage Restorer ». *IEEE Trans. Ind. Electron.,* vol. 57, n° 8, p. 2747-2760.

Basu, M., S. P. Das et G. K. Dubey. 2008. « Investigation on the performance of UPQC-Q for voltage sag mitigation and power quality improvement at a critical load point ». *Generation, Transmission & Distribution, IET,* vol. 2, n° 3, p. 414-423.

Bingsen, Wang, et G. Venkataramanan. 2009. « Dynamic Voltage Restorer Utilizing a Matrix Converter and Flywheel Energy Storage ». *Industry Applications, IEEE Transactions on,* vol. 45, n° 1, p. 222-231.

Brenna, M., R. Faranda et E. Tironi. 2009. « A New Proposal for Power Quality and Custom Power Improvement: OPEN UPQC ». *Power Delivery, IEEE Transactions on,* vol. 24, n° 4, p. 2107-2116.

Chern-Lin, Chen, Lee Che-Ming, Tu Rong-Jie et Horng Guo-Kiang. 1999. « A novel simplified space-vector-modulated control scheme for three-phase switch-mode rectifier ». *IEEE Transactions on Industrial Electronics,* vol. 46, n° 3, p. 512-516.

Chi-Seng, Lam, Wong Man-Chung et Han Ying-Duo. 2008. « Voltage Swell and Overvoltage Compensation With Unidirectional Power Flow Controlled Dynamic Voltage Restorer ». *Power Delivery, IEEE Transactions on,* vol. 23, n° 4, p. 2513-2521.

Choi, S. S., B. H. Li et D. M. Vilathgamuwa. 2000. « Dynamic voltage restoration with minimum energy injection ». *Power Systems, IEEE Transactions on,* vol. 15, n° 1, p. 51-57.

Chudamani, R., K. Vasudevan et C. S. Ramalingam. 2009. « Non-linear least-squares-based harmonic estimation algorithm for a shunt active power filter ». *Power Electronics, IET,* vol. 2, n° 2, p. 134-146.

Cipriano Dos Santos, E., J. H. Gonzaga Muniz, E. R. Cabral da Silva et C. B. Jacobina. 2015. « Nested Multilevel Topologies ». *Power Electronics, IEEE Transactions on,* vol. 30, n° 8, p. 4058-4068.

Dannehl, J., M. Liserre et F. W. Fuchs. 2011. « Filter-Based Active Damping of Voltage Source Converters With LCL Filter ». *IEEE Transactions on Industrial Electronics,* vol. 58, n° 8, p. 3623-3633.

Dixon, J. W., G. Venegas et L. A. Moran. 1997. « A series active power filter based on a sinusoidal current-controlled voltage-source inverter ». *Industrial Electronics, IEEE Transactions on,* vol. 44, n° 5, p. 612-620.

El Badsi, B., B. Bouzidi et A. Masmoudi. 2013. « Bus-Clamping-Based DTC: An Attempt to Reduce Harmonic Distortion and Switching Losses ». *IEEE Transactions on Industrial Electronics,* vol. 60, n° 3, p. 873-884.

Emanuel, Alexander Eigeles. 2004. « Summary of IEEE standard 1459: Definitions for the measurement of electric power quantities under sinusoidal, nonsinusoidal, balanced, or unbalanced conditions ». *IEEE Transactions on Industry Applications,* vol. 40, n° 3, p. 869-876.

Figueres, E., G. Garcera, J. Sandia, F. Gonzalez-Espin et J. C. Rubio. 2009. « Sensitivity Study of the Dynamics of Three-Phase Photovoltaic Inverters With an LCL Grid Filter ». *Industrial Electronics, IEEE Transactions on,* vol. 56, n° 3, p. 706-717.

Fujita, H., et H. Akagi. 1991a. « Design strategy for the combined system of shunt passive and series active filters ». In *Industry Applications Society Annual Meeting, 1991., Conference Record of the 1991 IEEE*. (Sept. 28 1991-Oct. 4 1991), p. 898-903 vol.1.

Fujita, H., et H. Akagi. 1991b. « A practical approach to harmonic compensation in power systems-series connection of passive and active filters ». *IEEE Transactions on Industry Applications,* vol. 27, n° 6, p. 1020-1025.

Fujita, H., et H. Akagi. 1991c. « A practical approach to harmonic compensation in power systems-series connection of passive and active filters ». *IEEE Trans. Industry Applications,* vol. 27, n° 6, p. 1020-1025.

Fujita, H., et H. Akagi. 1996. « An approach to harmonic-free AC/DC power conversion for large industrial loads: the integration of a series active filter with a double-series diode rectifier ». In *Industry Applications Conference, 1996. Thirty-First IAS Annual Meeting, IAS '96., Conference Record of the 1996 IEEE*. (6-10 Oct 1996) Vol. 2, p. 1040-1047 vol.2.

Fujita, H., et H. Akagi. 1998. « The unified power quality conditioner: the integration of series and shunt-active filters ». *IEEE Transactions on Power Electronics,* vol. 13, n° 2, p. 315-322.

Fukuda, S., et T. Endoh. 1995. « Control method for a combined active filter system employing a current source converter and a high pass filter ». *IEEE Transactions on Industry Applications,* vol. 31, n° 3, p. 590-597.

Ganguly, S. 2014. « Impact of Unified Power-Quality Conditioner Allocation on Line Loading, Losses, and Voltage Stability of Radial Distribution Systems ». *Power Delivery, IEEE Transactions on,* vol. 29, n° 4, p. 1859-1867.

Ghosh, A., A. K. Jindal et A. Joshi. 2004. « Design of a capacitor-supported dynamic voltage restorer (DVR) for unbalanced and distorted loads ». *Power Delivery, IEEE Transactions on,* vol. 19, n° 1, p. 405-413.

Goharrizi, A. Y., S. H. Hosseini, M. Sabahi et G. B. Gharehpetian. 2012. « Three-Phase HFL-DVR With Independently Controlled Phases ». *IEEE Trans. Power Electron.,* vol. 27, n° 4, p. 1706-1718.

Guerrero, J. M., Loh Poh Chiang, Lee Tzung-Lin et M. Chandorkar. 2013. « Advanced Control Architectures for Intelligent Microgrids, Part II: Power Quality, Energy Storage, and AC/DC Microgrids ». *IEEE Trans. on Ind. Electron.,* vol. 60, n° 4, p. 1263-1270.

Gupta, R., A. Ghosh et A. Joshi. 2011. « Performance Comparison of VSC-Based Shunt and Series Compensators Used for Load Voltage Control in Distribution Systems ». *Power Delivery, IEEE Transactions on,* vol. 26, n° 1, p. 268-278.

Gyugyi, Laszlo. 1979. « Reactive Power Generation and Control by Thyristor Circuits ». *IEEE Transactions on Industry Applications,* vol. IA-15, n° 5, p. 521-532.

Hagiwara, M., R. Maeda et H. Akagi. 2012. « Negative-Sequence Reactive-Power Control by a PWM STATCOM Based on a Modular Multilevel Cascade Converter (MMCC-SDBC) ». *IEEE Trans. on Industry App.,* vol. 48, n° 2, p. 720-729.

Hamad, M. S., M. I. Masoud et B. W. Williams. 2014. « Medium-Voltage 12-Pulse Converter: Output Voltage Harmonic Compensation Using a Series APF ». *IEEE Trans. Ind. Electron.,* vol. 61, n° 1, p. 43-52.

Hamadi, A., S. Rahmani et K. Al-Haddad. 2007. « A Novel Hybrid Series Active Filter for Power Quality Compensation ». In *Power Electronics Specialists Conference, 2007. PESC 2007. IEEE*. (17-21 June 2007), p. 1099-1104.

Hamadi, A., S. Rahmani et K. Al-Haddad. 2010. « A Hybrid Passive Filter Configuration for VAR Control and Harmonic Compensation ». *Industrial Electronics, IEEE Transactions on,* vol. 57, n° 7, p. 2419-2434.

Han, B., B. Bae, S. Baek et G. Jang. 2006. « New configuration of UPQC for medium-voltage application ». *Power Delivery, IEEE Transactions on,* vol. 21, n° 3, p. 1438-1444.

Holtz, J. 1992. « Pulsewidth modulation-a survey ». *IEEE Transactions on Industrial Electronics,* vol. 39, n° 5, p. 410-420.

Huayun, Yang, et Ren Shiyan. 2008. « A Practical Series-Shunt Hybrid Active Power Filter Based on Fundamental Magnetic Potential Self-Balance ». *Power Delivery, IEEE Transactions on,* vol. 23, n° 4, p. 2089-2096.

IEEE Guide for Application and Specification of Harmonic Filters. 2003. « ». *IEEE Std 1531-2003*, p. 0_1-60.

IEEE Guide for Application of Power Electronics for Power Quality Improvement on Distribution Systems Rated 1 kV Through 38 kV. 2012. « ». *IEEE Std 1409-2012*, p. 1-90.

IEEE Recommended Practice for Monitoring Electric Power Quality. 1995. « ». *IEEE Std 1159-1995*, p. i.

Veuillez sélectionner un type de document autre que « Generic » afin de faire afficher la référence bibliographique.

IEEE Standard American National Standard Canadian Standard Graphic Symbols for Electrical and Electronics Diagrams (Including Reference Designation Letters). 1993. « ». *IEEE Std 315-1975 (Reaffirmed 1993)*, p. i-244.

IEEE Standard Definitions for the Measurement of Electric Power Quantities Under Sinusoidal, Nonsinusoidal, Balanced, or Unbalanced Conditions. 2010. « ». *IEEE Std 1459-2010 (Revision of IEEE Std 1459-2000)*, p. 1-50.

Veuillez sélectionner un type de document autre que « Generic » afin de faire afficher la référence bibliographique.

International Energy Agency (IEA). 2010. « Modelling Load Shifting Using Electric Vehicles in a Smart Grid Environment ». *OECD/IEA*.

Iyer, G., et P. Agrawal. 2010. « Smart power grids ». In *2010 42nd Southeastern Symposium on System Theory (SSST)*. (7-9 March 2010), p. 152-155.

Javadi, A., et K. Al-Haddad. 3-5 Oct. 2011. « Unfunctionality of the instantaneous p-q theory for the control of series active filters ». In *2011 IEEE Electrical Power and Energy Conference (EPEC)*. p. 386-391.

Javadi, A., et K. Al-Haddad. 2011. « Unfunctionality of the instantaneous p-q theory for the control of series active filters ». In *2011 IEEE Electrical Power and Energy Conference (EPEC)*. (Winnipeg, Canada, 3-5 Oct. 2011), p. 386-391.

Javadi, A., et K. Al-Haddad. 2014. « A single-phase transformerless active filter with reduced DC-link voltage ». In *2014 IEEE 23rd International Symposium on Industrial Electronics (ISIE)*. (Istanbul, Turkey, 1-4 June 2014), p. 2143-2148. IEEE.

Javadi, A., et K. Al-Haddad. 2015. « A Single-Phase Active Device for Power Quality Improvement of Electrified Transportation ». *IEEE Transactions on Industrial Electronics,* vol. 62, n° 5, p. 3033-3041.

Javadi, A., H. Fortin Blanchette et K. Al-Haddad. 2012a. « An advanced control algorithm for Series hybrid active filter adopting UPQC behavior ». In *IECON 2012 - 38th Annual Conference on IEEE Ind. Electron. Society*. (Montreal, Canada, 25-28 Oct. 2012), p. 5318-5323. IEEE.

Javadi, A., H. Fortin Blanchette et K. Al-Haddad. 2012b. « A novel transformerless hybrid series active filter ». In *IECON 2012 - 38th Annual Conference on IEEE Ind. Electron. Society*. (Montreal, 25-28 Oct. 2012), p. 5312-5317. IEEE.

Javadi, A., N. Geiss, H. F. Blanchette et K. Al-Haddad. 2012. « Series active conditionners for reliable Smart grid: A comprehensive review ». In *IECON 2012 - 38th Annual Conference on IEEE Industrial Electronics Society*. (Montreal, 25-28 Oct. 2012), p. 6320-6327.

Javadi, A., A. Hamadi et K. Al-Hadda. 2015. « Power Quality Enhancement of Smart Households using a Multilevel THSeAF with a PR controller onboard ». *Submitted for a possible publication in IEEE Transactions on Smart Grid (Accepted)*.

Javadi, A., A. Hamadi et K. Al-Haddad. 2014. « Stability analysis and effects of dampers on Series active compensator ». In *2014 IEEE 23rd International Symposium on Industrial Electronics (ISIE)*. (Istanbul, Turkey, 1-4 June 2014), p. 2173-2179. IEEE.

Javadi, A., Ab Hamadi et K. Al-Haddad. 2015. « Experimental Investigation on a THSeAF to Improve Power Quality of Typical Households ». *Submitted for a possible publication in IEEE Transactions on Industrial Electronics (Under review)*.

Javadi, Alireza. 2009. « Modeling, Simulation and Real-time Control of an Active filter ». Montreal, École Polytechnique de Montréal, 130 p.

Javadi, Alireza, Abdelhamid Hamadi, Mohamed Haddad, Salem Rahmani et Kamal Al-Haddad. 2015. « A novel hybrid detection approach for series compensation under grid perturbation ». In *2015 IEEE International Conference on Industrial Technology (ICIT)*. (Seville, Spain, 17-19 March 2015), p. 2565-2570. IEEE.

Javadi, Alireza, Guy Olivier et Frederic Sirois. 2010. « A real-time power Hardware-in-the-Loop implementation of an active filter ». *PRZEGLĄD ELEKTROTECHNICZNY (Electrical Review),* vol. 86/11a, p. 7-13.

Jimichi, T., H. Fujita et H. Akagi. 2011. « A Dynamic Voltage Restorer Equipped With a High-Frequency Isolated DC Converter ». *Industry Applications, IEEE Transactions on,* vol. 47, n° 1, p. 169-175.

Jing, Shi, Tang Yuejin, Yang Kai, Chen Lei, Ren Li, Li Jingdong et Cheng Shijie. 2010. « SMES Based Dynamic Voltage Restorer for Voltage Fluctuations Compensation ». *Applied Superconductivity, IEEE Transactions on,* vol. 20, n° 3, p. 1360-1364.

Jun-Young, Lee, et Chae Hyung-Jun. 2014. « 6.6-kW Onboard Charger Design Using DCM PFC Converter With Harmonic Modulation Technique and Two-Stage DC/DC Converter ». *IEEE Trans. Ind. Electron.,* vol. 61, n° 3, p. 1243-1252.

Jurado, F. 2004. « Neural network control for dynamic voltage restorer ». *Industrial Electronics, IEEE Transactions on,* vol. 51, n° 3, p. 727-729.

Kamwa, I., S. R. Samantaray et G. Joos. 2010. « Catastrophe Predictors From Ensemble Decision-Tree Learning of Wide-Area Severity Indices ». *IEEE Transactions on Smart Grid,* vol. 1, n° 2, p. 144-158.

Kazmierkowski, Marian P., Ramu Krishnan et Frede Blaabjerg. 2002. *Control in power electronics : selected problems*, 1. Amsterdam : Academic Press 518 p.

Keliang, Zhou, et Wang Danwei. 2002. « Relationship between space-vector modulation and three-phase carrier-based PWM: a comprehensive analysis [three-phase inverters] ». *IEEE Transactions on Industrial Electronics,* vol. 49, n° 1, p. 186-196.

Kesler, M., et E. Ozdemir. 2011. « Synchronous-Reference-Frame-Based Control Method for UPQC Under Unbalanced and Distorted Load Conditions ». *Industrial Electronics, IEEE Transactions on,* vol. 58, n° 9, p. 3967-3975.

Keyhani, A., et A. Chatterjee. 2012. « Automatic Generation Control Structure for Smart Power Grids ». *IEEE Transactions on Smart Grid,* vol. 3, n° 3, p. 1310-1316.

Khadkikar, V. 2012. « Enhancing Electric Power Quality Using UPQC: A Comprehensive Overview ». *Power Electronics, IEEE Transactions on,* vol. 27, n° 5, p. 2284-2297.

Khadkikar, V., et A. Chandra. 2008. « A New Control Philosophy for a Unified Power Quality Conditioner (UPQC) to Coordinate Load-Reactive Power Demand Between Shunt and Series Inverters ». *Power Delivery, IEEE Transactions on,* vol. 23, n° 4, p. 2522-2534.

Khadkikar, V., et A. Chandra. 2009. « A Novel Structure for Three-Phase Four-Wire Distribution System Utilizing Unified Power Quality Conditioner (UPQC) ». *Industry Applications, IEEE Transactions on,* vol. 45, n° 5, p. 1897-1902.

Khadkikar, V., et A. Chandra. 2011. « UPQC-S: A Novel Concept of Simultaneous Voltage Sag/Swell and Load Reactive Power Compensations Utilizing Series Inverter of UPQC ». *Power Electronics, IEEE Transactions on,* vol. 26, n° 9, p. 2414-2425.

Kuperman, A., U. Levy, J. Goren, A. Zafransky et A. Savernin. 2013. « Battery Charger for Electric Vehicle Traction Battery Switch Station ». *IEEE Trans. Ind. Electron.,* vol. 60, n° 12, p. 5391-5399.

Kurohane, K., et T. Funabashi. 2010. « A Hybrid Smart AC/DC Power System ». *IEEE Transactions on Smart Grid,* vol. 1, n° 2, p. 199-204.

le Roux, A. D., H. Mouton et H. Akagi. 2009. « DFT-Based Repetitive Control of a Series Active Filter Integrated With a 12-Pulse Diode Rectifier ». *Power Electronics, IEEE Transactions on,* vol. 24, n° 6, p. 1515-1521.

Lee, G. M., Lee Dong-Choon et Seok Jul-Ki. 2004. « Control of series active power filters compensating for source voltage unbalance and current harmonics ». *Industrial Electronics, IEEE Transactions on,* vol. 51, n° 1, p. 132-139.

Li, B. H., S. S. Choi et D. M. Vilathgamuwa. 2002. « Transformerless dynamic voltage restorer ». *Generation, Transmission and Distribution, IEE Proceedings-,* vol. 149, n° 3, p. 263-273.

Lin, Ma, T. Kerekes, P. Rodriguez, Jin Xinmin, R. Teodorescu et M. Liserre. 2015. « A New PWM Strategy for Grid-Connected Half-Bridge Active NPC Converters With Losses Distribution Balancing Mechanism ». *Power Electronics, IEEE Transactions on,* vol. 30, n° 9, p. 5331-5340.

Liqun, He, Xiong Jian, Ouyang Hui, Zhang Pengju et Zhang Kai. 2014. « High-Performance Indirect Current Control Scheme for Railway Traction Four-Quadrant Converters ». *IEEE Trans. Ind. Electron.,* vol. 61, n° 12, p. 6645-6654.

Liserre, M., T. Sauter et J. Y. Hung. 2010. « Future Energy Systems: Integrating Renewable Energy Sources into the Smart Power Grid Through Industrial Electronics ». *IEEE Industrial Electronics Magazine,* vol. 4, n° 1, p. 18-37.

Liu, Jianben, Shaojun Dai, Qiaofu Chen et Kun Tao. 2013. « Modelling and industrial application of series hybrid active power filter ». *IET Power Electron.,* vol. 6, n° 8, p. 1707-1714.

Malesani, L., et P. Tenti. 1990. « A novel hysteresis control method for current-controlled voltage-source PWM inverters with constant modulation frequency ». *IEEE Transactions on Industry Applications,* vol. 26, n° 1, p. 88-92.

Marques, C. A. G., M. V. Ribeiro, C. A. Duque, P. F. Ribeiro et E. A. B. da Silva. 2012. « A Controlled Filtering Method for Estimating Harmonics of Off-Nominal Frequencies ». *IEEE Trans. on Smart Grid,* vol. 3, n° 1, p. 38-49.

Massoud, A. M., S. Ahmed, P. N. Enjeti et B. W. Williams. 2010. « Evaluation of a Multilevel Cascaded-Type Dynamic Voltage Restorer Employing Discontinuous Space Vector Modulation ». *Industrial Electronics, IEEE Transactions on,* vol. 57, n° 7, p. 2398-2410.

Mehrizi-Sani, A., et S. Filizadeh. 2009. « An Optimized Space Vector Modulation Sequence for Improved Harmonic Performance ». *IEEE Transactions on Industrial Electronics,* vol. 56, n° 8, p. 2894-2903.

Mohammadi, H. R., A. Y. Varjani et H. Mokhtari. 2009. « Multiconverter Unified Power-Quality Conditioning System: MC-UPQC ». *Power Delivery, IEEE Transactions on,* vol. 24, n° 3, p. 1679-1686.

Monti, A., et F. Ponci. 2010. « Power Grids of the Future: Why Smart Means Complex ». In *COMPENG '10 Complexity in Engineering*. (22-24 Feb. 2010), p. 7-11.

Munir, S., et Li Yun Wei. 2013. « Residential Distribution System Harmonic Compensation Using PV Interfacing Inverter ». *IEEE Trans. on Smart Grid,* vol. 4, n° 2, p. 816-827.

Nguyen Xuan, Tung, G. Fujita et K. Horikoshi. 2010. « An adapted control strategy for dynamic voltage restorer to work as series active power filter ». In *Power Electronics Conference (IPEC), 2010 International*. (21-24 June 2010), p. 2283-2287.

Nielsen, J. G., et F. Blaabjerg. 2005. « A detailed comparison of system topologies for dynamic voltage restorers ». *Industry Applications, IEEE Transactions on,* vol. 41, n° 5, p. 1272-1280.

Nielsen, J. G., M. Newman, H. Nielsen et F. Blaabjerg. 2004. « Control and testing of a dynamic voltage restorer (DVR) at medium voltage level ». *Power Electronics, IEEE Transactions on,* vol. 19, n° 3, p. 806-813.

Nogueira Santos, W. R., E. R. Cabral da Silva, C. Brandao Jacobina, E. de Moura Fernandes, A. Cunha Oliveira, R. Rocha Matias, D. Franca Guedes Filho, O. M. Almeida et P. Marinho Santos. 2014. « The Transformerless Single-Phase Universal Active Power Filter for Harmonic and Reactive Power Compensation ». *IEEE Trans. Power Electron.,* vol. 29, n° 7, p. 3563-3572.

Peng, F. Z., H. Akagi et A. Nabae. 1990. « A new approach to harmonic compensation in power systems-a combined system of shunt passive and series active filters ». *Industry Applications, IEEE Transactions on,* vol. 26, n° 6, p. 983-990.

Peng, F. Z., H. Akagi et A. Nabae. 1993. « Compensation characteristics of the combined system of shunt passive and series active filters ». *IEEE Transactions on Industry Applications,* vol. 29, n° 1, p. 144-152.

Pinto, J. G., H. Carneiro, B. Exposto, C. Couto et J. L. Afonso. 2011. « Transformerless series active power filter to compensate voltage disturbances ». In *Power Electronics and Applications (EPE 2011), Proceedings of the 2011-14th European Conference on*. (Aug. 30 2011-Sept. 1 2011), p. 1-6.

Podmore, R., et M. R. Robinson. 2010. « The Role of Simulators for Smart Grid Development ». *IEEE Transactions on Smart Grid,* vol. 1, n° 2, p. 205-212.

Qinglai, Guo, Xin Shujun, Sun Hongbin, Li Zhengshuo et Zhang Boming. 2014. « Rapid-Charging Navigation of Electric Vehicles Based on Real-Time Power Systems and Traffic Data ». *IEEE Trans. on Smart Grid,* vol. 5, n° 4, p. 1969-1979.

Quoc-Nam, Trinh, et Lee Hong-Hee. 2014. « Improvement of unified power quality conditioner performance with enhanced resonant control strategy ». *Generation, Transmission & Distribution, IET,* vol. 8, n° 12, p. 2114-2123.

Rahimi, F., et A. Ipakchi. 2010. « Demand Response as a Market Resource Under the Smart Grid Paradigm ». *IEEE Transactions on Smart Grid,* vol. 1, n° 1, p. 82-88.

Rahmani, S., A. Hamadi et K. Al-Haddad. 2012. « A Lyapunov-Function-Based Control for a Three-Phase Shunt Hybrid Active Filter ». *Industrial Electronics, IEEE Transactions on,* vol. 59, n° 3, p. 1418-1429.

Rahmani, S., N. Mendalek et K. Al-Haddad. 2010. « Experimental Design of a Nonlinear Control Technique for Three-Phase Shunt Active Power Filter ». *Industrial Electronics, IEEE Transactions on,* vol. 57, n° 10, p. 3364-3375.

Rahmani, Salem, Kamal Al-Haddad et Hadi Kanaan. 2006. « A comparative study of shunt hybrid and shunt active power filters for single-phase applications: Simulation and experimental validation ». *Journal of Mathematics and Computers in Simulation (IMACS), Elsevier,* vol. 71, n^{o} 4-6, p. 345-359.

Ricchiuto, D., M. Liserre, T. Kerekes, R. Teodorescu et F. Blaabjerg. 2011. « Robustness analysis of active damping methods for an inverter connected to the grid with an LCL-filter ». In *Energy Conversion Congress and Exposition (ECCE), 2011 IEEE*. (17-22 Sept. 2011), p. 2028-2035.

Rivera, S., Wu Bin, S. Kouro, V. Yaramasu et Wang Jiacheng. 2015. « Electric Vehicle Charging Station Using a Neutral Point Clamped Converter With Bipolar DC Bus ». *Industrial Electronics, IEEE Transactions on,* vol. 62, n^{o} 4, p. 1999-2009.

Rodriguez, J., E. Wiechmann, J. Holtz, A. Suarez et M. Sepulveda. 1994. « IGBT inverter with vector modulation ». In *IEEE International Symposium on Industrial Electronics, ISIE 94*. (25-27 May 1994), p. 131-136. < 10.1109/ISIE.1994.333144 >.

Roncero-Sanchez, P., et E. Acha. 2009. « Dynamic Voltage Restorer Based on Flying Capacitor Multilevel Converters Operated by Repetitive Control ». *Power Delivery, IEEE Transactions on,* vol. 24, n^{o} 2, p. 951-960.

Roncero-Sanchez, P., E. Acha, J. E. Ortega-Calderon, V. Feliu et A. Garcia-Cerrada. 2009. « A Versatile Control Scheme for a Dynamic Voltage Restorer for Power-Quality Improvement ». *Power Delivery, IEEE Transactions on,* vol. 24, n^{o} 1, p. 277-284.

Rudnick, H., J. Dixon et L. Moran. 2003. « Delivering clean and pure power ». *IEEE Power and Energy Magazine,* vol. 1, n^{o} 5, p. 32-40.

Salmero, P., et S. P. Litra. 2010. « A Control Strategy for Hybrid Power Filter to Compensate Four-Wires Three-Phase Systems ». *IEEE Trans. Power Electron.,* vol. 25, n^{o} 7, p. 1923-1931.

Salmeron, P., et S. P. Litran. 2010. « Improvement of the Electric Power Quality Using Series Active and Shunt Passive Filters ». *IEEE Trans. Power Delivery,* vol. 25, n^{o} 2, p. 1058-1067.

Senturk, O. S., et A. M. Hava. 2009. « High-Performance Harmonic Isolation and Load Voltage Regulation of the Three-Phase Series Active Filter Utilizing the Waveform Reconstruction Method ». *Industry Applications, IEEE Transactions on,* vol. 45, n^{o} 6, p. 2030-2038.

Senturk, O. S., et A. M. Hava. 2011. « Performance Enhancement of the Single-Phase Series Active Filter by Employing the Load Voltage Waveform Reconstruction and Line

Current Sampling Delay Reduction Methods ». *IEEE Trans. Power Electron.,* vol. 26, n° 8, p. 2210-2220.

Seung-Hee, Ryu, Kim Dong-Hee, Kim Min-Jung, Kim Jong-Soo et Lee Byoung-Kuk. 2014. « Adjustable Frequency Duty-Cycle Hybrid Control Strategy for Full-Bridge Series Resonant Converters in Electric Vehicle Chargers ». *IEEE Trans. on Ind. Electron.,* vol. 61, n° 10, p. 5354-5362.

Shangyang, Xiao, Qiu Weihong, G. Miller, T. X. Wu et I. Batarseh. 2009. « An Active Compensator Scheme for Dynamic Voltage Scaling of Voltage Regulators ». *Power Electronics, IEEE Transactions on,* vol. 24, n° 1, p. 307-311.

Shigenori, Inoue, Shimizu Toshihisa et Wada Keiji. 2007. « Control Methods and Compensation Characteristics of a Series Active Filter for a Neutral Conductor ». *Industrial Electronics, IEEE Transactions on,* vol. 54, n° 1, p. 433-440.

Singh, B., K. Al-Haddad et A. Chandra. 1998. « A new control approach to three-phase active filter for harmonics and reactive power compensation ». *Power Systems, IEEE Transactions on,* vol. 13, n° 1, p. 133-138.

Singh, B., K. Al-Haddad et A. Chandra. 1999. « A review of active filters for power quality improvement ». *IEEE Transactions on Industrial Electronics,* vol. 46, n° 5, p. 960-971.

Singh, B., V. Verma, A. Chandra et K. Al-Haddad. 2005. « Hybrid filters for power quality improvement ». *Generation, Transmission and Distribution, IEE Proceedings-,* vol. 152, n° 3, p. 365-378.

Singh, Bhim, Ambrish Chandra et Kamal Al-Haddad. 2015. *Power quality problems and mitigation techniques* (2015). Chichester, West Sussex, United Kingdom: John Wiley & Sons Inc., pages cm. p.

Sixing, Du, Liu Jinjun et Lin Jiliang. 2013. « Hybrid Cascaded H-bridge Converter for Harmonic Current Compensation ». *IEEE Trans. Power Electron.,* vol. 28, n° 5, p. 2170-2179.

Sng, Eng Kian Kenneth, S. S. Choi et D. M. Vilathgamuwa. 2004. « Analysis of series compensation and DC-link voltage controls of a transformerless self-charging dynamic voltage restorer ». *IEEE Trans. Power Delivery,* vol. 19, n° 3, p. 1511-1518.

Srianthumrong, S., H. Fujita et H. Akagi. 2002. « Stability analysis of a series active filter integrated with a double-series diode rectifier ». *IEEE Trans. Power Electron.,* vol. 17, n° 1, p. 117-124.

Staats, P. T., W. M. Grady, A. Arapostathis et R. S. Thallam. 1998. « A statistical analysis of the effect of electric vehicle battery charging on distribution system harmonic voltages ». *IEEE Trans. Power Delivery,* vol. 13, n° 2, p. 640-646.

Tian, J., Q. Chen et B. Xie. 2012. « Series hybrid active power filter based on controllable harmonic impedance ». *Power Electronics, IET,* vol. 5, n° 1, p. 142-148.

U.S. Energy Information Administration and Federal Energy Regulatory Commission. 2011. « Power Plant Report ».

Van der Broeck, H. W., H. C. Skudelny et G. V. Stanke. 1988. « Analysis and realization of a pulsewidth modulator based on voltage space vectors ». *IEEE Transactions on Industry Applications,* vol. 24, n° 1, p. 142-150.

Varaiya, P., F. Wu et J. W. Bialek. 2011. « Smart Operation of Smart Grid: Risk-Limiting Dispatch ». *Proceedings of the IEEE,* vol. 99, n° 1, p. 40-57.

Varschavsky, A., J. Dixon et M. Rotella. 2010. « Cascaded Nine-Level Inverter for Hybrid-Series Active Power Filter, Using Industrial Controller ». *IEEE Trans. Ind. Electron.,* vol. 57, n° 8, p. 2761-2767.

Varschavsky, A., J. Dixon, M. Rotella, Mora, x et L. n. 2010. « Cascaded Nine-Level Inverter for Hybrid-Series Active Power Filter, Using Industrial Controller ». *IEEE Transactions on Industrial Electronics,* vol. 57, n° 8, p. 2761-2767.

Vilathgamuwa, D. M., H. M. Wijekoon et S. S. Choi. 2006. « A Novel Technique to Compensate Voltage Sags in Multiline Distribution System—The Interline Dynamic Voltage Restorer ». *Industrial Electronics, IEEE Transactions on,* vol. 53, n° 5, p. 1603-1611.

Wang, Zhaoan, Qun Wang, Weizheng Yao et Jinjun Liu. 2001. « A series active power filter adopting hybrid control approach ». *IEEE Transactions on Power Electronics,* vol. 16, n° 3, p. 301-310.

Yanzhi, Wang, Lin Xue et M. Pedram. 2014. « Adaptive Control for Energy Storage Systems in Households With Photovoltaic Modules ». *IEEE Trans. on Smart Grid,* vol. 5, n° 2, p. 992-1001.

Yi, Tang, Loh Poh Chiang, Wang Peng, Choo Fook Hoong, Gao Feng et F. Blaabjerg. 2012. « Generalized Design of High Performance Shunt Active Power Filter With Output LCL Filter ». *Industrial Electronics, IEEE Transactions on,* vol. 59, n° 3, p. 1443-1452.

Yilmaz, M., et P. T. Krein. 2013. « Review of the Impact of Vehicle-to-Grid Technologies on Distribution Systems and Utility Interfaces ». *IEEE Trans. on Power Electron.,* vol. 28, n° 12, p. 5673-5689.

Yun Wei, Li, F. Blaabjerg, D. M. Vilathgamuwa et Loh Poh Chiang. 2007a. « Design and Comparison of High Performance Stationary-Frame Controllers for DVR Implementation ». *Power Electronics, IEEE Transactions on,* vol. 22, n° 2, p. 602-612.

Yun Wei, Li, D. Mahinda Vilathgamuwa, F. Blaabjerg et Loh Poh Chiang. 2007b. « A Robust Control Scheme for Medium-Voltage-Level DVR Implementation ». *Industrial Electronics, IEEE Transactions on,* vol. 54, n° 4, p. 2249-2261.

Yun Wei, Li, Loh Poh Chiang, F. Blaabjerg et D. M. Vilathgamuwa. 2007c. « Investigation and Improvement of Transient Response of DVR at Medium Voltage Level ». *Industry Applications, IEEE Transactions on,* vol. 43, n° 5, p. 1309-1319.

Zhenhua, Jiang, Li Fangxing et Zhang Pei. 2009. « A vision of smart transmission grids ». In *Power & Energy Society General Meeting, 2009. PES '09. IEEE*. (26-30 July 2009), p. 1-10.

Zhikang, Shuai, Luo An, Zhu Wenji, Fan Ruixiang et Zhou Ke. 2009. « Study on a Novel Hybrid Active Power Filter Applied to a High-Voltage Grid ». *Power Delivery, IEEE Transactions on,* vol. 24, n° 4, p. 2344-2352.

Zhikang, Shuai, Liu Dingguo, J. Shen, Tu Chunming, Cheng Ying et Luo An. 2014. « Series and Parallel Resonance Problem of Wideband Frequency Harmonic and Its Elimination Strategy ». *IEEE Trans. on Power Electron.,* vol. 29, n° 4, p. 1941-1952.

Zobaa, A. F. 2014. « Optimal multiobjective design of hybrid active power filters considering a distorted environment ». *IEEE Trans. Ind. Electron.,* vol. 61, n° 1, p. 107-114.